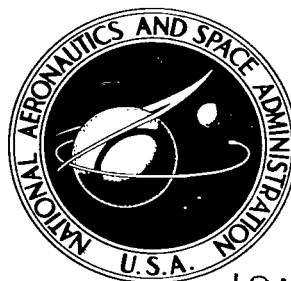


NASA TECHNICAL NOTE



NASA TN D-2351

2.1

LOAN COPY: RETU
AFWL (WLIL-2)
KIRTLAND AFB, N

0154864



TECH LIBRARY KAFB, NM

NASA TN D-2351

ATMOSPHERIC ACOUSTICS AS A FACTOR IN SATURN STATIC TESTING

by Richard N. Tedrick

*George C. Marshall Space Flight Center
Huntsville, Ala.*





0154864

ATMOSPHERIC ACOUSTICS AS A FACTOR
IN SATURN STATIC TESTING

By Richard N. Tedrick

George C. Marshall Space Flight Center
Huntsville, Ala.

NATIONAL AERONAUTICS AND SPACE ADMINISTRATION

For sale by the Office of Technical Services, Department of Commerce,
Washington, D.C. 20230 -- Price \$2.75

TABLE OF CONTENTS

	Page
SUMMARY	1
INTRODUCTION.	1
Description of the Problem	3
Ray Tracing Procedure.	3
Attenuation.	5
General Approaches to the Problem.	6
Example of Pre-Firing Procedures.	9
CONCLUSIONS.	12
APPENDIX.	13
FIGURES	17 - 137

LIST OF ILLUSTRATIONS

Figure	Title	Page
1 - 102	Calculated Acoustic Ray Paths	17-118
103	Sound Pressure Levels Measured During Saturn Test SA-12, March 13, 1963, 1615 CST.	119
104	Measured SPLs From Saturn and Horn, March 13, 1963..	120
105	Mid-frequencies of Octave Bands (cps) Frequency Spectra at Various Ranges From Test	121
A-1 A-5	Virtual Temperature, Wind Speed, and Wind Direction Profiles, Marshall Space Flight Center	122-126
A-6	Time Cross-Section Temperature (Degrees C)	127
A-7	Time Cross-Section Winds, Marshall Space Flight Center.	128
A-8	Time Cross-Section Temperature (Degrees C) , March 13, 1963, Marshall Space Flight Center.	129
A-9	Time Cross-Section Winds, March 13, 1963, Marshall Space Flight Center	130
A-10 — A-16	Surface Weather Map	131-137

TECHNICAL NOTE D-

ATMOSPHERIC ACOUSTICS AS A FACTOR
IN SATURN STATIC TESTING

SUMMARY

The engine noise resulting from the static testing of large space vehicles such as the Saturn S-I is both large in output power level and low in frequency. These characteristics combine to enable the noise to propagate for extremely long ranges. Under some meteorological conditions this energy may be focused by the atmosphere into relatively small areas on the earth's surface. To avoid the problems associated with such focal areas, MSFC has instituted a program of "selective firings" based upon acoustic and atmospheric soundings for the 36 hours prior to the test. The atmospheric and acoustic sounding data are interpreted in the light of the forecasts to anticipate the trends which will govern the meteorological conditions. These findings are then relayed to the responsible project officer who decides whether to fire or reschedule the test. Acoustic measurements are made during the firing to verify the predicted sound pressure levels. This report details the theoretical basis and operational procedures developed at MSFC for the selective firing program. A particular Saturn static test, SA-12 on March 13, 1963, is followed through the forecasting, monitoring, and measuring programs to illustrate the process.

INTRODUCTION

One facet of the static test firing of large space vehicles such as the Saturn S-I has been the generation of large amounts of acoustic energy. Results from field surveys of the noise have shown that the acoustic power radiated has amounted to about one half of 1 per cent of the total mechanical power of the engines. In the case of the Saturn S-I, this means about 40 million watts. Since this energy peaks below one hundred cycles per second, its attenuation due to molecular losses is quite low. Therefore it can be seen that both the high power and the low attenuation associated with large space vehicle testing contributes to a noise problem in the areas surrounding the test tower.

The largest contributing factor to the noise problem is neither of the above factors, however. It is the effect of the atmosphere upon the propagation of sound. Under any condition in which there is a change in the value of the velocity of sound with altitude, there will result refraction (bending) of the path of the sound energy. The sound can, and in fact quite often does, bend back to the earth's surface, thus concentrating additional energy in some area.

Prior to the start of the static testing of large rockets, this refractive focusing was of interest only in rare instances because of the limited signal strengths which it was possible to sustain over appreciable periods. Now, however, it is possible to generate 40 megawatts for several minutes. At Marshall Space Flight Center, the problems of acoustical focusing have been of special interest because of the proximity of the city of Huntsville, Alabama. This city, which is on the north and east boundaries of Redstone Arsenal, is about 5 to 12 miles downwind from the S-I static test tower.

During the winter months, the westerly-southwesterly prevailing wind pattern intensifies and is quite often accompanied by a strong surface temperature inversion. This causes meteorological focusing out the azimuths toward the city. The focal areas do not necessarily occur within the city; they sometimes fall in sparsely-settled mountain areas. However, examination of the past meteorological data (Refs. 1 & 2) shows that such focusing conditions occur during about 50 per cent of the days during certain winter months. These conditions seldom last for more than a few hours at a time, but they need to be taken into consideration during the preparation sequence prior to a static test.

To avoid these problems, the Test Laboratory of MSFC has instituted a program of "selective firings" based upon acoustic and atmospheric soundings for the 36-hour period immediately preceding such a test. This program not only protects the surrounding communities but also allows maximum scheduling flexibility to the test engineer. This report details both the theoretical basis and operational procedures which have been developed and follows the process for illustrative purposes through a particular Saturn static test. It is hoped that this report will present to those faced with a similar problem a complete and self-contained description of the selective firing program.

Description of the Problem

The Saturn S-I with its 40 megawatts of power represents one of the largest steady-state, low-frequency noise sources in the world. This energy is radiated into an atmospheric hemisphere with a very broad directivity (Ref. 3). In effect, a sound source with overall sound power levels of around 206 decibels (referenced to 10^{-13} watts) is created and continues over an operational period of approximately two minutes. Since much of its energy is well below one hundred cycles per second, the resonances of local structures are sometimes affected.

Under certain unfavorable atmospheric conditions, those sound rays emanating from the source at angles with the horizontal up to 20 degrees or more can be refracted such that they return to the earth's surface at considerable distances and focus a seriously high acoustic intensity within a relatively small area. Thus, on occasion, propagated sound from the Saturn tests has produced annoyance and alarm at ranges of 10 miles or more within the city and suburbs of Huntsville.

Actual sound fields which exist in typical out-of-doors situations are almost prohibitively difficult to describe in detail. Since the medium for acoustic transmission is the atmosphere, it is never either homogeneous or quiescent and the boundary conditions are often quite complicated in terms of contour, vegetative covering, and manmade structures. However, it is possible to treat the problem in an approximate way by considering the following principal elements of sound propagation theory: (1) attenuation by spherical divergence, or the spreading out of the wave front; (2) attenuation due to the mechanical properties of the molecular structure of the atmosphere; (3) attenuation due to ground effects along the earth boundary; and (4) attenuation by refraction of sound fronts resulting from spatial variations in air temperature and wind. The most important of the above elements, in terms of the Saturn noise problem, is the refraction effect, which is responsible not only for bending the sound rays back to the earth but often results in focal areas of concentrated sound energy return.

Ray Tracing Procedure

Since the sound velocity in air depends upon temperature, humidity, and wind, it is the variation of these factors with altitude which determines the vertical sound velocity gradient and ultimately the refraction of sound waves. Considering first the effects of temperature and humidity, the sound speed, C , in still, dry air is given by LaPlace's equation

$$C = K \sqrt{T^{\circ K}}, \quad (1)$$

where T^* is the virtual temperature in degrees Kelvin and K is a constant (20.07 for C in meters per second). The virtual temperature is defined as that temperature for the density of a parcel of dry air to equal that of moist air under the same pressure. Virtual temperature is related to the actual temperature, T , by the following expressions:

$$T^* = \frac{T}{1 - 0.377 \frac{e}{p}}, \quad (2)$$

where e is the water vapor pressure and p is the total pressure.

The sound velocity at a fixed point in terrestrial space is a vector quantity made up of two components: (1) a vector whose magnitude is given by C , the sound speed, and whose direction is normal to the wave front at the point; and (2) the vector wind at the point. The vertical component of the wind velocity is customarily neglected. Furthermore, horizontal gradients of temperature and wind are usually assumed to be negligible over the area affected by the sound source.

Conventional analysis of sound refraction depends upon the concept of sound rays, which are defined as a curve such that the tangent at each point is in the direction of the resultant sound velocity. The main transport of sound energy takes place along these rays and the divergence or convergence of rays indicates decreasing or increasing energy concentration.

Following Cox et al. (Ref. 4), the refraction equation for sound rays states that for rays inclined but slightly to the wind

$$C + W_i \cos \theta = A_i \cos \theta, \quad (3)$$

where θ is the inclination of the sound ray from the horizontal; W_i is the component of the wind velocity in a given direction; and A_i , constant for any specific sound ray, is the velocity of the intersection of the wave front with the horizontal. Since the wind velocity seldom exceeds 10 per cent of the sound speed within the first three to four kilometers of the troposphere, the refraction equation may be approximated by introducing a new term, V_i , defined by $V_i = C + W_i$, so that

$$V_i \approx A_i \cos \theta. \quad (4)$$

Toward any chosen azimuth from the sound source, the elevation angle of the sound ray, at altitude h , is related to the starting elevation of the ray, θ_0 , according to the formula

$$V_h \sec \theta_h = V_o \sec \theta_o. \quad (5)$$

When the sound velocity decreases with height, the ray angle increases and the sound ray paths may be represented by a secant function. If the sound velocity increases with height, the ray angles decrease downward. Ray paths can be considered as segments of circles, all having the same curvature $(dV/V) dh$, over altitude intervals where the velocity gradient is constant with altitude. When the value of sound velocity at the earth's surface exceeds all values at higher altitudes, no surface sound return will occur. For a ray to be refracted to the surface from any upper layer, the maximum velocity attained in that layer must exceed the velocity at all points in the medium nearer the surface of the ground.

It should be realized that the usual applications of classical sound ray analysis involve various assumptions which may not be entirely justified aside from simplifying the computational methods. The neglect of vertical velocity can be a serious shortcoming in those cases where natural or artificial convection, or orographic effects produce significant vertical velocity components of the order of 1 meter per second or more. The assumptions of time invariance (over 1 to 2 hours) and of space invariance (over a scale of 10 to 15 miles in a region of hilly terrain) in the sound velocity profiles are perhaps the most serious limitations.

Attenuation

If the attenuation by spherical divergence is considered the loss in decibels of the sound level at point P (at a distance R from the source) relative to that at a reference point P_o (at a distance R_o) from consequence of the inverse first power law,

$$P = A/R, \quad (6)$$

where P is the sound pressure amplitude and A is a constant. In the absence of other effects, such as refractive focusing of sound energy, the sound level will decrease by 20 db for each tenfold increase in R from a chosen reference point. Expressed another way, there is a loss of six decibels each time the range doubles.

The attenuation due to atmospheric absorption is comprised of: (1) "classical" absorption, produced by viscosity, conduction, diffusion, and radiation effects; (2) molecular absorption, which strongly depends upon the humidity; (3) eddy attenuation, due to turbulent fluctuations in the wind structure. The effects of classical absorption are negligible, and at the lower audible frequencies



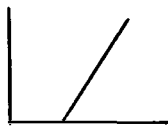
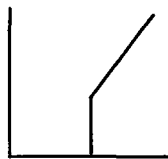
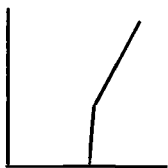
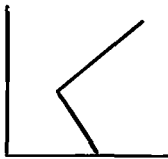
which are of concern in this study, the molecular absorption (which depends upon the second power of the sound frequency) is quite weak. Under typical atmospheric conditions the sound loss due to molecular absorption is approximately 0.5 db per kilometer at 30 cps, and four times as high at 300 cps. The eddy attenuation, which varies with the eddy size and turbulent energy of the wind field, is especially important within the first several hundred feet altitude of the friction layer, where its effect is essentially the same in all directions. The effect of turbulent eddies is to scatter sound into shadow zones and somewhat blur the clear outlines of the classical sound ray patterns. However, few field measurements are available which are directly applicable to the problem. Measurements of wind eddy fluctuations from meteorological towers and captive balloon instruments would be essential in the quantitative determination of sound propagation into and within shadow zones. This is especially true for sound rays whose path are primarily confined to the friction layer.

The ground attenuation can be estimated from a knowledge of the acoustic properties of the surface boundary layer, in addition to the sound frequency, the heights of the source and receiver, and the horizontal components of the source-receiver distance. The general expression for the sound pressure at any point is rather complicated. However, for the special case in which the source and receiver are both very near the ground (the ground is absorbent) and the distance is sufficiently great, the sound pressure level is proportional to the inverse square of the distance (Ref. 5). When the ground absorption coefficient nears unity, the sound loss due to ground attenuation approaches that resulting from spherical divergence.

General Approaches to the Problem

The Test Laboratory of MSFC found it necessary to consider the effects of long range acoustic propagation as described in the previous sections, since, during certain Saturn static tests, focusing and/or intensification of the sound generated during the tests did occur. Because the high frequency portion of the energy generated at the test tower was considerably attenuated by losses to the air, the sound directed into the focal area sounded somewhat like a tornado or sustained thunder. Since much of this energy was in the sub-audible frequency range, the resulting building vibration caused the audible sound outside buildings to seem less than the combined sound levels inside. Thus residents within the focal areas became alarmed, a few even imagining that they were experiencing an earthquake.

TABLE I.
ACOUSTIC VELOCITY PROFILE CATEGORIES

CATEGORY	DESCRIPTION	TYPICAL GRAPHS
0	NO VELOCITY GRADIENT	
1	SINGLE NEGATIVE GRADIENT	
2	SINGLE POSITIVE GRADIENT	
3	ZERO GRADIENT NEAR SURFACE WITH POSITIVE GRADIENT ABOVE	
4	WEAK POSITIVE GRADIENT NEAR SURFACE WITH STRONG POSITIVE GRADIENT ABOVE	
5	NEGATIVE GRADIENT NEAR SURFACE WITH STRONG POSITIVE GRADIENT ABOVE	

To improve public relations with the neighboring communities, Test Laboratory has initiated a policy of "selective firings", i.e., avoiding the testing of the Saturn under atmospheric conditions conducive to high sound pressure levels in the Huntsville area. The first indication of the existence of such conditions may be taken from an appraisal of the acoustic profile (the velocity of sound versus altitude curve) along the azimuths of interest. As stated in Reference 6, it has been found convenient to divide the profiles into six categories (Table I).

The first of these is the "zero" or no-characteristics profile type. This category, while relatively rare in nature, is that which is most often assumed in the theoretical calculation of the effects of large noise sources. Thus, while neither the wind nor temperature may be individually single-layered nor homogeneous, their vector sum occasionally may be. Category one profiles cause the sound to be refracted up and away from the earth's surface. Types two, three, and four give generally similar increases in overall sound pressure level adjacent to or near the test site. Type five, with its negative gradient near the surface with a strong positive gradient above that, results in a shadow zone near the test and a focal area at some distance, usually in the 8 to 40-kilometer range.

To monitor the changing weather conditions and to provide the data for the calculation of the acoustic profiles, an atmospheric sounding station was established at MSFC. The standard government GMD-1B rawinsonde balloon tracking equipment is used. The processing of the data is speeded up somewhat through the use of digital computational techniques. It is planned to have eventually a completely automated data system.

After the rawinsonde data are transmitted to Test Laboratory, they are put on punch cards for input to a digital computer. The computer then uses these meteorological data to calculate the velocity of sound profiles along the azimuths of interest. It also calculates and plots individual acoustic ray paths. These presentations tell the acoustician the location and relative intensities of the focal areas, if any. However, it should be emphasized that thus far no direct relationship has been worked out between the ray path presentations and absolute intensities or sound pressure levels.

At the outset of this program, it was decided to obtain the services of a professional atmospheric forecaster. The Aero-Astrodynamics Laboratory of MSFC has provided this service. A standard procedure has been developed for making 24 to 30-hour forecasts, based upon U.S. Weather Bureau data from all over the North American Continent. These forecasts are of great value in scheduling tentative test days and times. Of significant interest to the forecaster is the

network of meteorological stations which are within a 1000-mile radius of Huntsville. The requisite radiosonde data are available on standard teletype and facsimile circuits. The resulting forecasts are more difficult and exacting to make than those made for most non-quantitative meteorological purposes since it is necessary to forecast temperature, wind direction, and wind velocity for every 250-meter altitude increment from the surface through 3 kilometers.

A third method for predicting the sound pressure levels which will result from a Saturn static test relies upon the use of a high-powered sound source which can be used to approximate the noise from the space vehicle test (Ref. 6). A random siren coupled to an exponential horn is sounded about every one-half hour. The progress of the sound pressure levels upward or downward is compared to that predicted by the forecaster when his predicted winds and temperatures are used in the ray-tracing based upon the current radiosonde data.

Thus it can be seen that the problem has been attacked in three ways: (1) radiosonde measurements of the wind, temperature, and humidity variations with altitude and the calculation of the resulting acoustic velocity profiles; (2) short-range atmospheric predictions or forecasts; and (3) direct measurement of the far-field acoustic propagation characteristics of the atmosphere. As test time approaches, the acoustician and the test engineer have several independent evaluations of what may be the acoustic ramifications of a test which may be held at a specific time and date. This system provides the test engineer the most flexibility in his test scheduling and still allows him to protect the surrounding communities.

Example of Pre-Firing Procedures

The firing of Saturn S-I static test SA-12 on March 13, 1963, gives a fine example of the processes by which acoustic and atmospheric data inputs are generated and used in the static test program. The test, however, should not be considered as representative since such holds and delays due to the atmospheric conditions are actually rare. It is included only to show the total system capability in forestalling acoustic disturbances in the surrounding civilian areas even under the worst of conditions.

The acoustic releases and forecasts are shown in Figures 1 through 102. They are grouped according to azimuth, by date. Thus the entire history toward Huntsville (45°), Triana (222°), or Madison (315°) is kept together. The forecast conditions for 1640 CST (firing time) for each day are placed immediately preceding the data based upon the actual measurements of the meteorological parameters. In this way the reader may observe the accuracy of the forecast procedure. Table II lists all of the meteorological soundings and the corresponding forecasts.

Measured sound pressure levels are also shown on some of the figures from the 45° azimuth. These are the results of horn tests made to verify predictions. The Saturn SPL data are shown in Figure 33.

Saturn static test SA-12 was originally scheduled to fire at 1640 CST on Friday, March 8, 1963. As is the usual procedure, a weather briefing was held the day prior to the scheduled test. These meetings are attended by the Director of Test Laboratory or his representative and by representatives of the Systems Division and Instrumentation Control Division, Aero-Astroynamics Laboratory. The Aero-Astroynamics Laboratory forecast personnel present their atmospheric prognoses at this time and the Test Laboratory acousticians evaluate this forecast in terms of a specific acoustic velocity profile type and the associated rise or fall of sound pressure level.

The forecast was for good weather conditions the next day as far as firing was concerned. No effort is made in the main body of this report to go into detail as far as either specific forecasts or atmospheric conditions are concerned. These are covered in the Appendix. Therefore preparations for the test were continued and the usual second briefing six hours prior to scheduled test was planned. On the morning of March 8, the briefing was held and the general consensus of opinion was that the acoustic and atmospheric conditions were favorable. Preparations went forward until at about X-3 hours when the test was cancelled because of LOX leakages on the vehicle itself. At this time it was decided to attempt to fire on the following day, Saturday, March 9.

Saturday's weather was conducive to acoustic intensification and the horn data that morning showed dangerously high levels in the Huntsville area. As a result, the test was cancelled around noon even though the forecast was for some improvement. The radiosonde released at 1620 CST that afternoon showed the improvement that had been forecast (Fig. 12 and 13).

One balloon release was made at 1600 CST on Sunday, March 10, to provide continuity of data for the forecaster.

On Monday the pre-firing schedule of radiosonde balloon releases, forecasts, and sounding began again to determine the possibility of firing that afternoon. Upon the recommendation of the forecaster the test was again cancelled due to poor weather conditions. The ray tracing toward Huntsville of the meteorological conditions that afternoon (Fig. 20) verified the prediction of poor weather. The test was rescheduled for the following afternoon, but due to flooding on the Arsenal and the resulting power failures, the test was again postponed.

On Tuesday, March 12, the first briefing for Wednesday was held. A focal zone was predicted but it was anticipated that it would fall some 20 to 25 kilometers from the test site out 45° azimuth. This area is an unpopulated zone on the side of Monte Sano mountain away from the city of Huntsville. The prediction was for a shadow zone over Huntsville itself. This prediction (Fig. 31) looked good and the preparations continued for the firing.

The next morning (March 13) the forecast was less optimistic (Fig. 32), but it still indicated only the mountain areas would receive any re-enforced acoustic energies. The acoustic horn was put into use to follow the progress of the sound pressure levels at various points within Huntsville. It showed that while the test would be heard in town, the sound pressure levels which would result would have no deleterious effects. The countdown proceeded and the test was completed successfully. At no point outside the Redstone Arsenal boundary did the sound exceed 107.5 decibels (Fig. 33). While this sound pressure level is somewhat higher than usual, it was several decibels below that which experience has shown to be the threshold of annoyance or damage in Huntsville.

Again it should be emphasized that the firing detailed above for illustration is not typical of most Saturn firings. It is used because it contains nearly all of the possible elements which might affect such static tests: weather, acoustics, component reliability—even a flood.

Figure 103 shows the same acoustical data as Figure 33 but presents it in relation to the city of Huntsville. Figure 104 shows the same data again in a graphical format plotted against range. The slight dip in sound level at thirty-seven thousand feet may be the result of the use of a different type of instrument at that point. (A General Radio Company model 1551-B sound level meter was used instead of the usual frequency-modulated magnetic tape recorder.)

The recorded octave-band sound spectra are presented in Figure 105. The overall sound pressure levels are shown at the left. As might be expected, the spectra show the result of progressive attenuation in the upper octaves. Thus as the range increases the energy in the higher frequency octave bands attenuates faster than that in the octaves below having much of the low frequency energy virtually intact. Beyond ten miles, the peak frequency of the Saturn noise is in the eight cycle per second octave band. This frequency is below the threshold of hearing and so the Saturn test may pass unnoticed except for slight rumblings and the shaking of buildings and windows.

CONCLUSIONS

The engine noise resulting from the static testing of large space vehicles such as the Saturn S-I is both large in output power level and low in frequency. These characteristics combine to enable the noise to propagate for extremely long ranges. The MSFC policy is to use a combination of selected firings, forecasts, atmospheric soundings (measurements), and acoustical measurements using a substitute sound source such as the exponential horn. The use of each of these techniques can be improved to materially raise the accuracy of what is essentially a prediction process. However, even in its present state it is capable of providing the static test engineer the information which he needs to protect the surrounding communities.

APPENDIX

ATMOSPHERIC CONDITIONS DURING THE PERIOD MARCH 8, 1963 to MARCH 13, 1963

Robert R. Schow, Aero-Astroynamics Laboratory, MSFC

A Saturn static test was postponed several times during the period from March 8-13, 1963, due to both apparent mechanical trouble and existing predicted weather conditions which were judged to be conducive for acoustical focusing. The basic tool used in the monitoring of these changing weather conditions was the rawinsonde sounding. The results of these soundings (altitude profiles of the virtual temperature, wind speed, and wind direction) are presented in Figures A-1 through A-5.

Figure A-6 is a time-cross-section for the period March 8-13, 1963, with the temperature at the surface and aloft analyzed for each 5 degrees Celcius. The time cross-section for winds (Fig. A-7) indicates the wind direction (heavy lines) and wind speed (dotted lines) as analyzed from the soundings.

Figures A-8 and A-9 are more detailed time-cross-sections of temperatures and winds for March 13, 1963.

The Weather Maps (Fig. A-10 and A-16) are reproduced from the Daily Weather Maps published by the U. S. Weather Bureau which are valid at midnight CST. Figures A-1 through A-5 are virtual temperature and wind profiles. The virtual temperature is plotted in degree Celcius, while the wind speed is plotted in meters per second. These two parameters use the same scale above zero degrees Celcius. The wind direction is plotted in degrees azimuth.

A description of the weather conditions, with reference to the maps and figures for the period March 8-13, 1963, follows.

At midnight (0001) CST March 8, 1963 (Fig. A-10), a high pressure area covering the eastern portion of the United States was centered over southern Louisiana and Mississippi. Extensions of this high reached into southeastern Wyoming and eastern Virginia. A low pressure center had moved into northern Minnesota with a cold front from the low center southwestward across southern North Dakota and the northeast portion of Montana.

The pressure patterns aloft indicated a very weak trough, across Indiana, superimposed on a ridge which extended from Louisiana into eastern Kansas. A trough was also located off the eastern coast.

Another feature of the chart was the tendency for a low pressure area in northern California. This was associated with a deep low aloft off the northern California and southern Oregon coast. The effects of this low was a major influence in this area on March 11, 1963.

The virtual temperature and wind direction and speed profiles for this day (Fig. A-1) indicated that conditions were becoming non-conducive for acoustical focusing and that few sound rays would return to the earth in Huntsville, Alabama.

The static firing was postponed late in the afternoon, apparently due to a LOX leakage. This test was rescheduled for March 9, 1963.

On March 9, 1963, at midnight (0001) CST (Fig. A-11) the high that had been over southern Louisiana and Mississippi had moved off the eastern coast. A small migratory high had moved into Wisconsin pushing the low from Minnesota to eastern Canada. The front associated with this high was located from the low center in Canada through central Ohio, extreme northern Arkansas, central Kansas and Nebraska to a low center over central North Dakota.

A trough aloft was located from central Missouri to eastern Texas and was associated with this fast moving front. A ridge was moving off the east coast of the United States.

The front and trough aloft passed the Huntsville area in the early morning of March 9, 1963, bringing cooler air and strong southwesterly winds which changed to westerly in the afternoon. This can be seen from Figures A-2, A-6, and A-7. The virtual temperature and wind profile indicate that conditions were conducive for strong acoustical focusing. The static firing was postponed about 1200 CST due to existing and predicted atmospheric conditions. The test was rescheduled for March 11, 1963, due to a prediction of another frontal system affecting this area March 10, 1963.

The low pressure cell over the west coast was moving inland during this time with the system moving more rapidly. At midnight on March 10, 1963 (Fig. A-12), the low over the southwestern United States was centered over central Arizona with a thermal low near El Paso, Texas. The front that was predicted to affect the Huntsville area was located along a line from upper Michigan to northwestern Arkansas to eastern Wyoming and western North Dakota. As the high pressure ridge from Mississippi to Iowa moved to the east, the front became stationary and remained north of the Huntsville area.

A low pressure center was located over the Oklahoma panhandle at midnight (0001) CST March 11, 1963 (Fig. A-13). A frontal system associated with this low extended from Oklahoma City, Oklahoma, to Waco, Texas, and across the Gulf of Mexico and the Florida peninsula. Along and ahead of this front, general rain, thunderstorms and showers were observed. Due to general unstable conditions, very strong winds (in the order of 37 m/sec) were observed from the south throughout the day. The temperature and wind profiles (Fig. A-13) indicated that conditions were conducive to very strong acoustical focusing. Flooding conditions were created during the evening of March 11, 1963, and the early morning of March 12, 1963, when 6.23 inches of rain were recorded. The test was postponed and rescheduled for March 12, 1963.

At midnight (0001) CST (Fig. A-14) the cold front had not passed this area. It was located from near Memphis, Tennessee, to Brownsville, Texas. It was moving more slowly than it had been due to a new low forming over the Oklahoma panhandle, causing the low aloft to slow down. Thunderstorms continued in this area until about 0700 March 12, 1963. The winds did not shift to the west or northwest because of the low in Oklahoma moving to the east. A new cold front was pushing into central South Dakota at this time also. The test was postponed because of power failures and because personnel were not able to come to work after the flooding conditions of the previous night.

The atmospheric conditions as indicated by the temperature and wind profiles (Fig. A-4) were not conducive to strong acoustical focusing, but the conditions appeared marginal.

By midnight March 13, 1963 (Fig. A-15), the cold front in the midwest had joined with the low in Oklahoma and had moved over southern Indiana. The front was located from the low center to Shreveport, Louisiana, and across Texas, New Mexico, and Arizona into central California. The front was becoming weak and diffuse due to high pressure areas building over Georgia and South Dakota. The atmospheric conditions, indicated by the temperature and wind profiles (Fig. A-5) were generally changing and becoming less conducive to acoustical focusing throughout the day, until the front passed between 1400 and 1500 hours (Fig. A-8 and A-9).

TABLE II
SCHEDULE OF METEOROLOGICAL SOUNDINGS AND
FORECASTS FOR TEST SA-12

Date	Sounding	Forecast
Friday, March 8, 1963	0700 CST	
	0945 CST	
	1055 CST	
	1300 CST	
	1455 CST	
	1620 CST	X-1 Day, X-6 Hour
Saturday, March 9, 1963	0700 CST	
	0900 CST	
	1045 CST	
	1620 CST	X-6 Hour
Sunday, March 10, 1963	1600 CST	No Forecast
Monday, March 11, 1963	0700 CST	
	0800 CST	
	1000 CST	
	1335 CST	
	1615 CST	X-6 Hour
Tuesday, March 12, 1963	1000 CST	
	1400 CST	
	1630 CST	No Forecast
Wednesday, March 13, 1963	0700 CST	
	0820 CST	
	1005 CST	
	1055 CST	
	1300 CST	
	1400 CST	
	1500 CST	
	1615 CST	X-1 Day, X-6 Hour
	1700 CST	

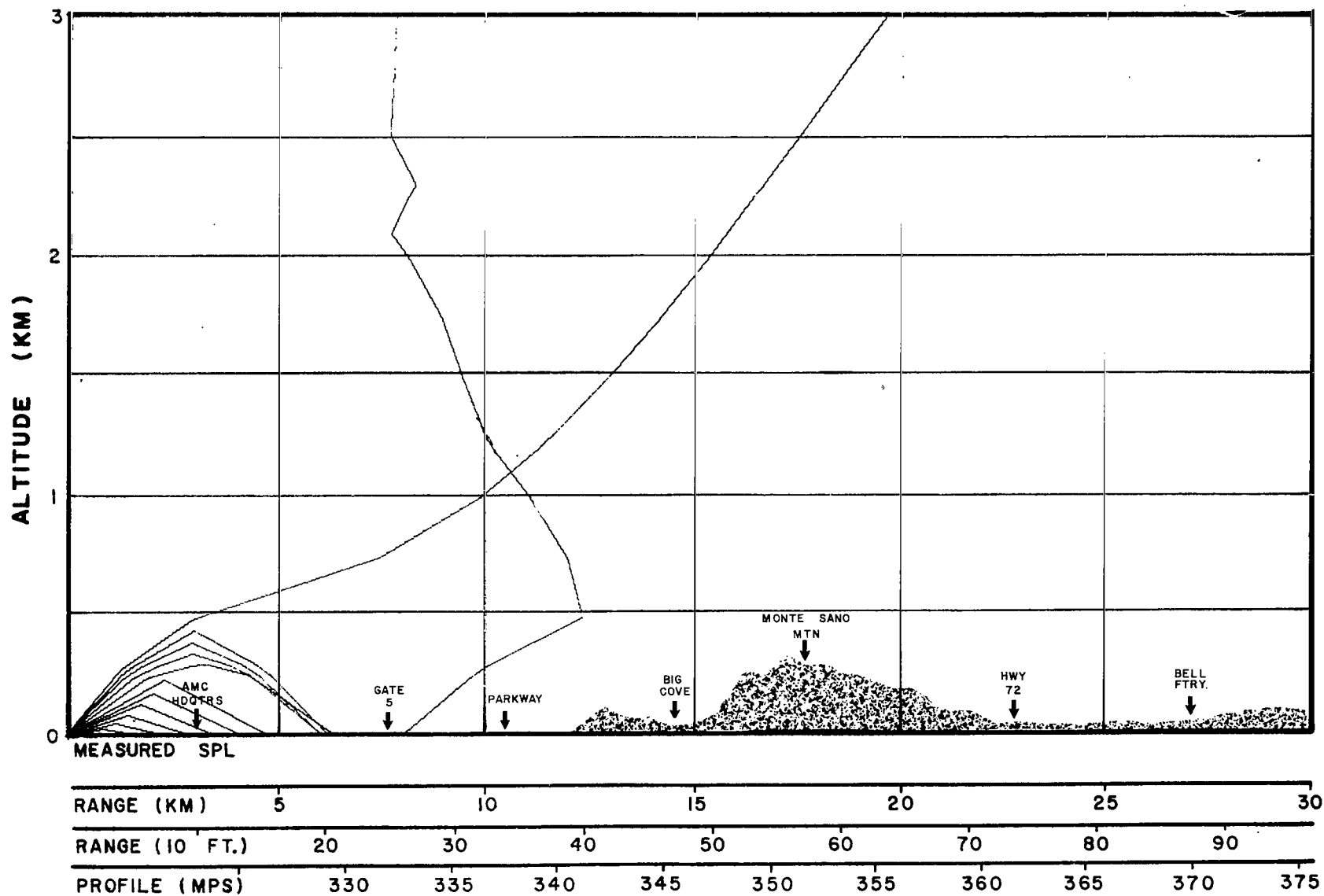


FIG.1 CALCULATED ACOUSTIC RAY PATHS
HUNTSVILLE, ALA., 45° AZIMUTH

DATE 3/8/63
TIME 0700G

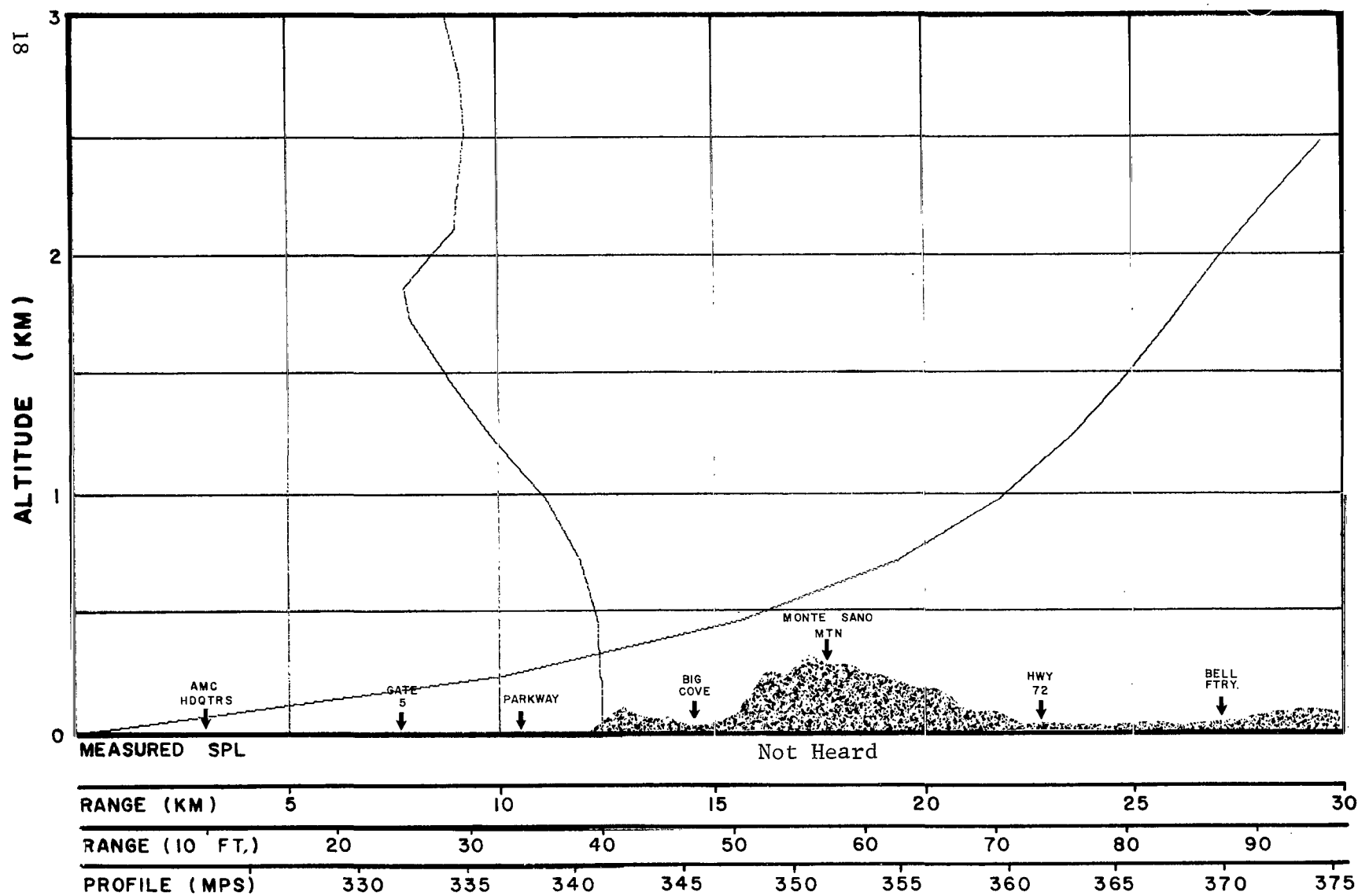


FIG. 2 CALCULATED ACOUSTIC RAY PATHS
HUNTSVILLE, ALA., 45° AZIMUTH

DATE 3/8/63
TIME 0945C

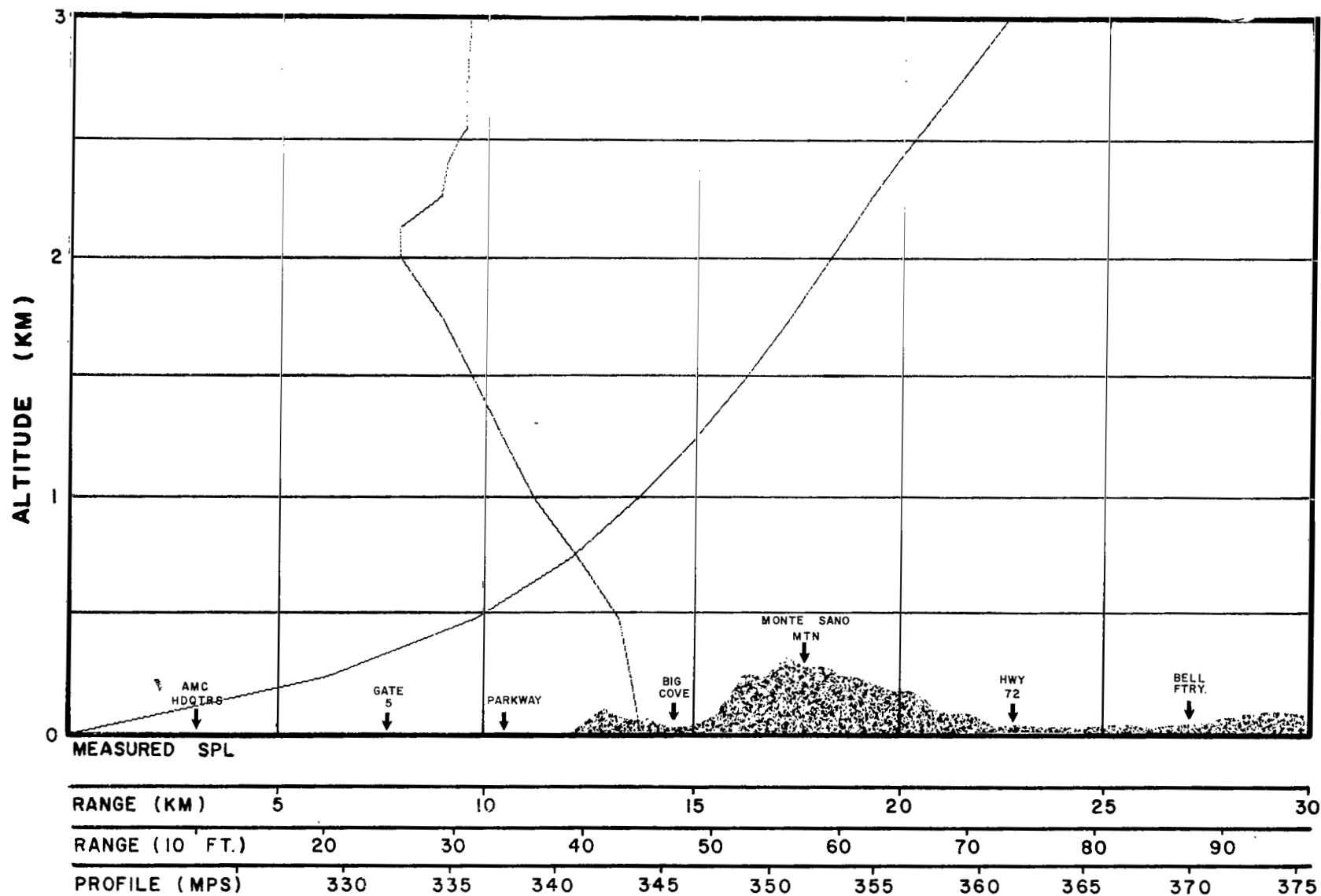


FIG. 3 CALCULATED ACOUSTIC RAY PATHS
HUNTSVILLE, ALA., 45° AZIMUTH

DATE 3/8/63
TIME 1055C

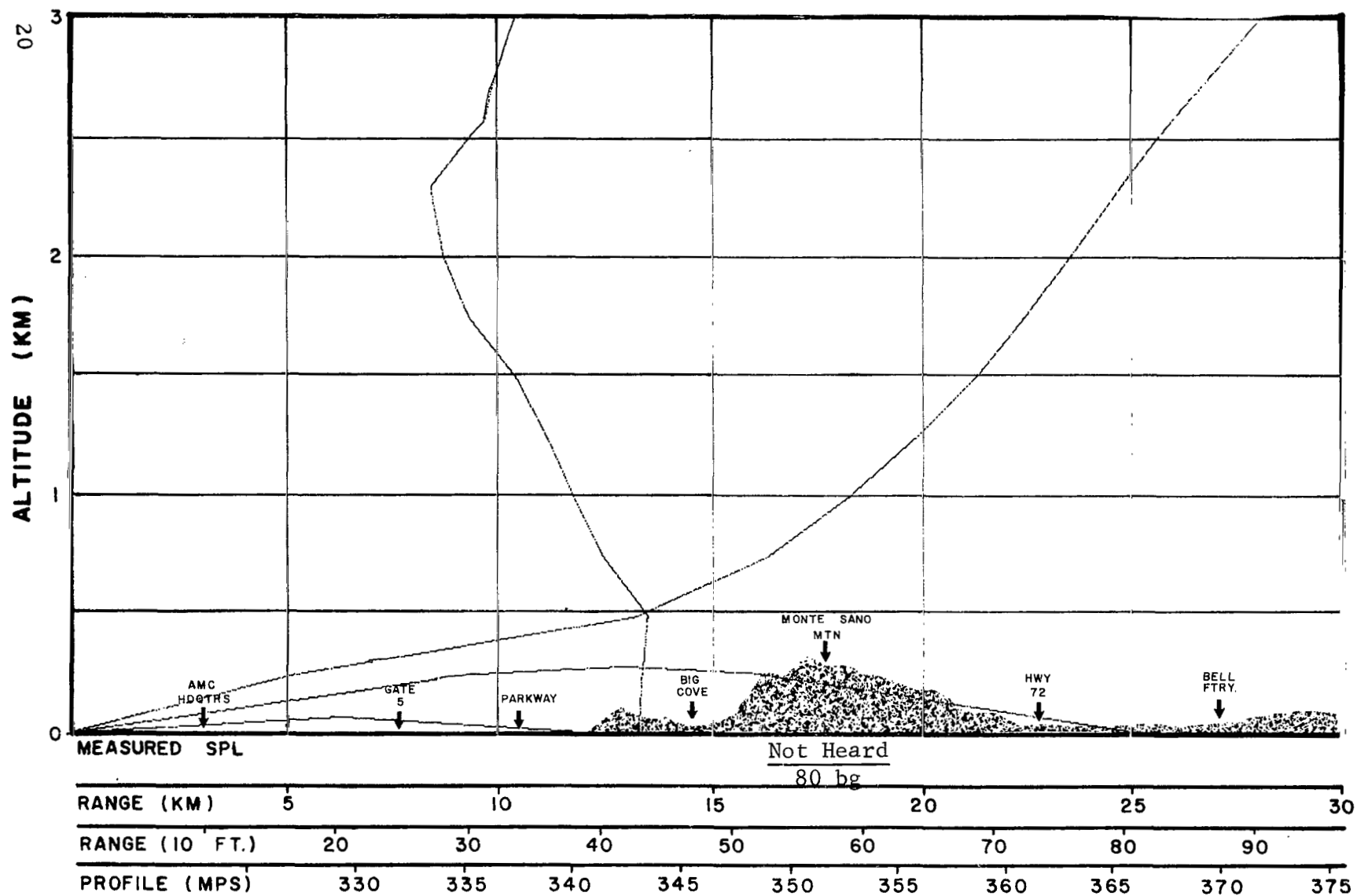


FIG.4 CALCULATED ACOUSTIC RAY PATHS
HUNTSVILLE, ALA., 45° AZIMUTH

DATE 3/8/63
TIME 1300C

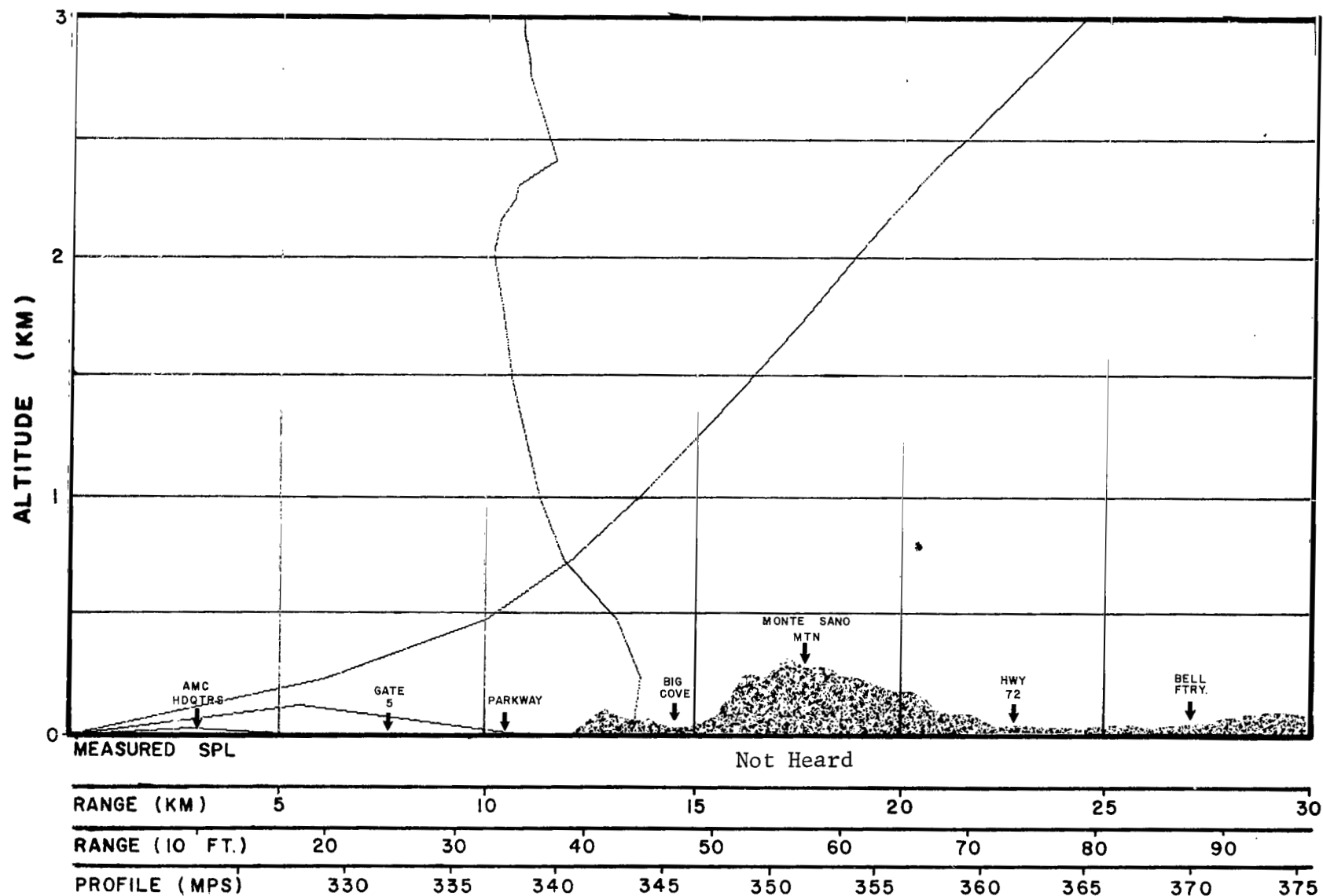


FIG.5 CALCULATED ACOUSTIC RAY PATHS
HUNTSVILLE, ALA., 45° AZIMUTH

DATE 3/8/63
TIME 1455C

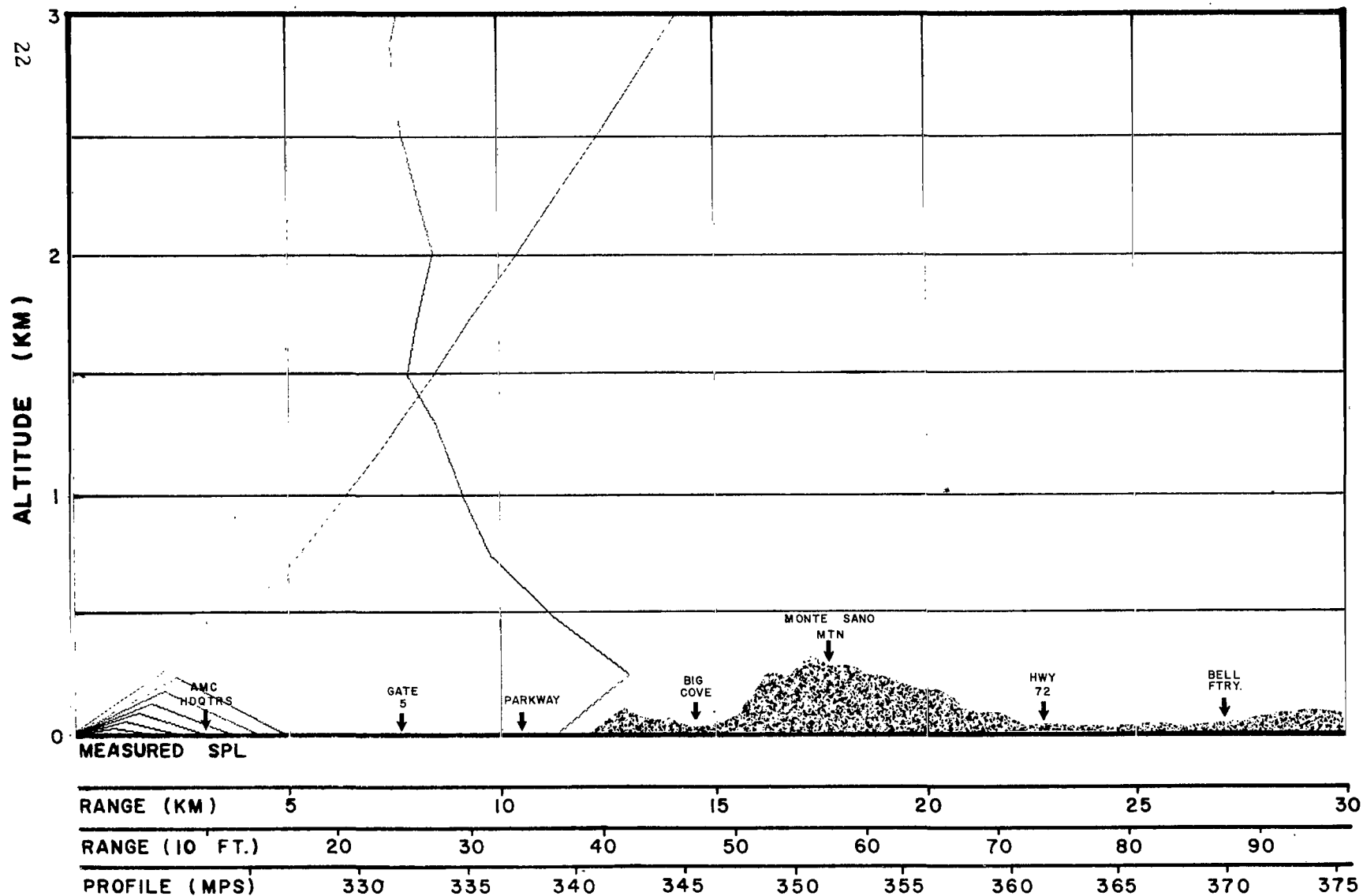


FIG.6 CALCULATED ACOUSTIC RAY PATHS
HUNTSVILLE, ALA., 45° AZIMUTH

DATE 3/7/63
TIME X-1 Day Fore-
cast

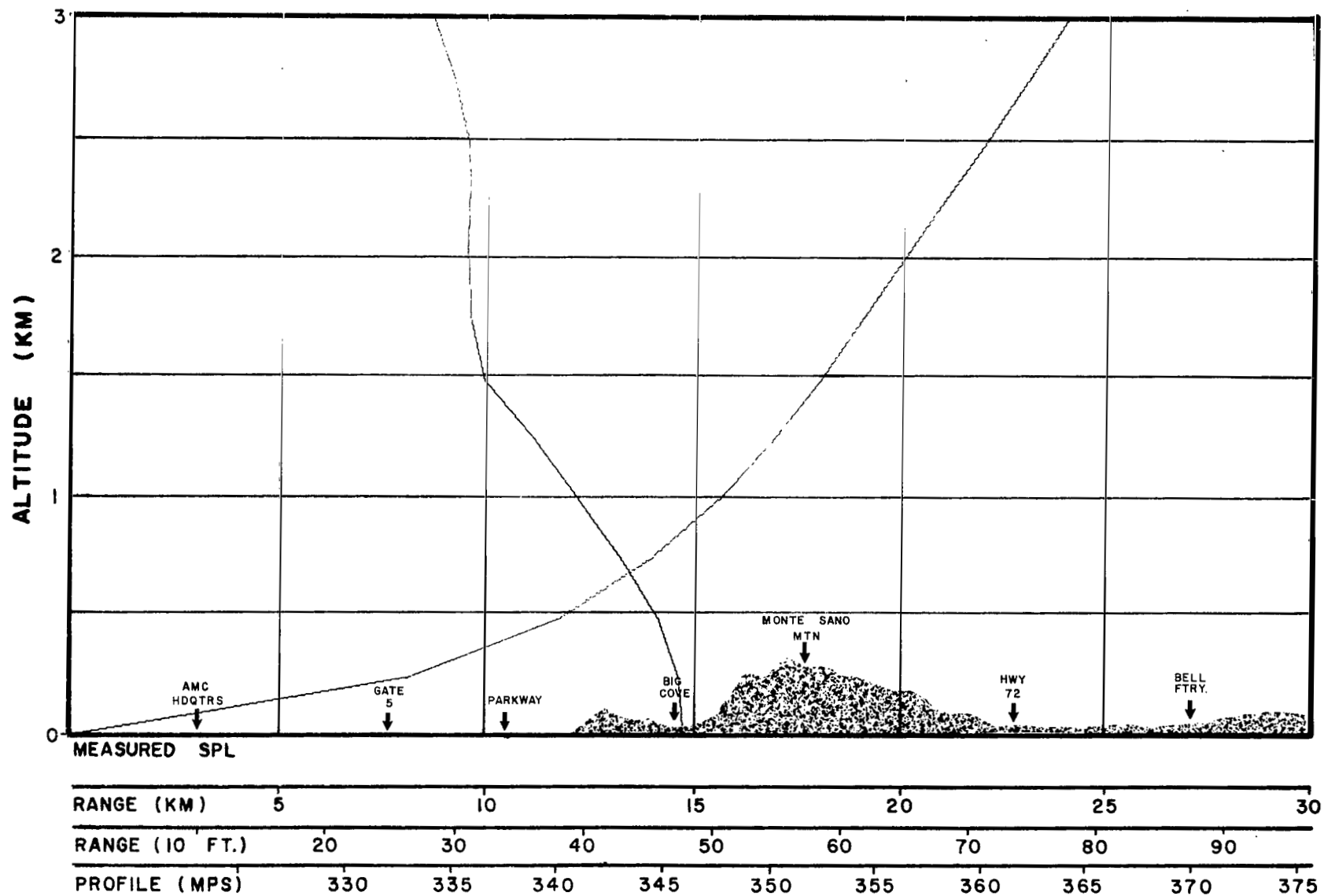


FIG. 7 CALCULATED ACOUSTIC RAY PATHS
HUNTSVILLE, ALA., 45° AZIMUTH

DATE 3/8/63
TIME X-6 Hour Fore-
cast

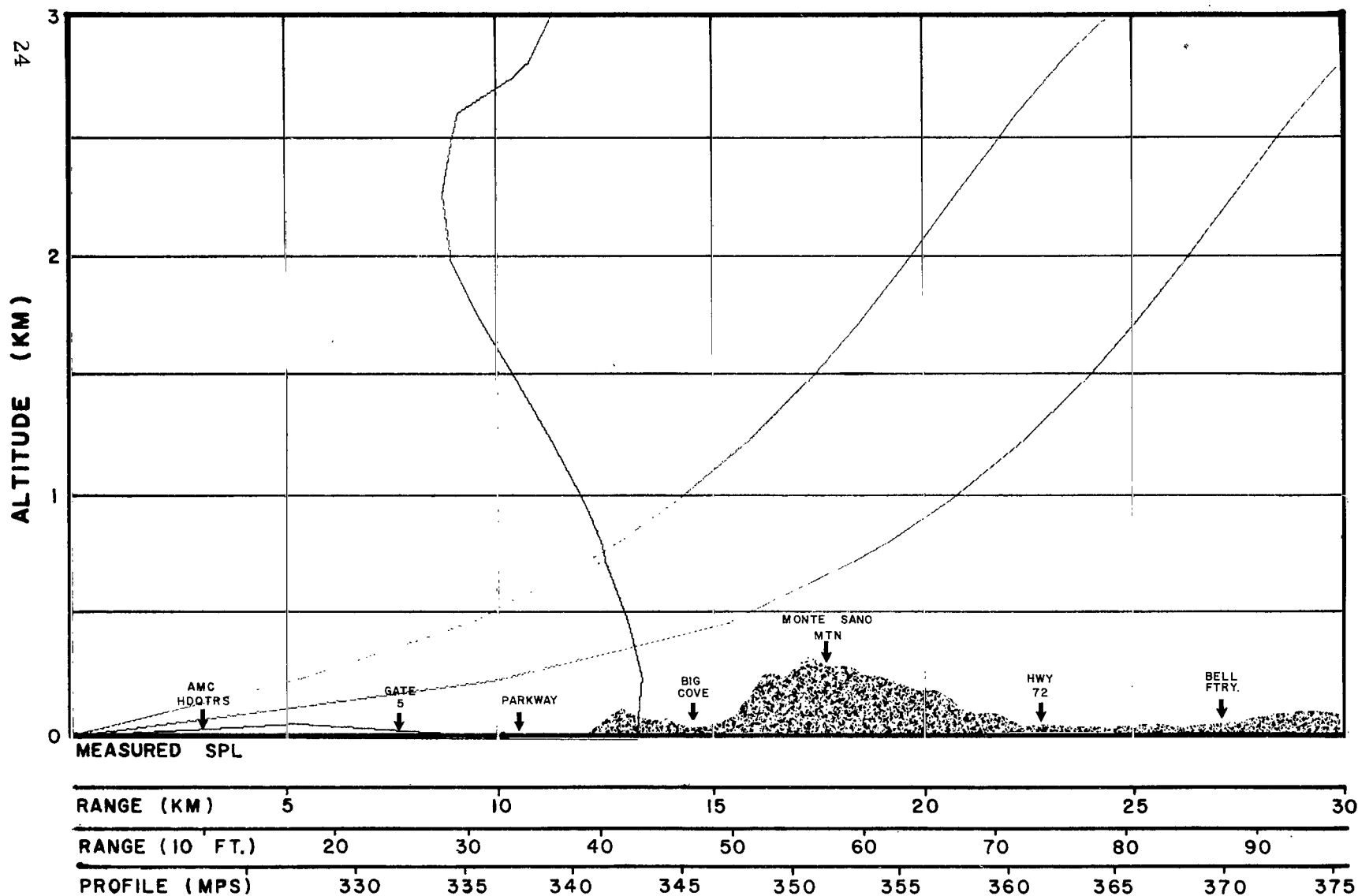


FIG. 8 CALCULATED ACOUSTIC RAY PATHS
HUNTSVILLE, ALA., 45° AZIMUTH

DATE 3/8/63
TIME 1620C

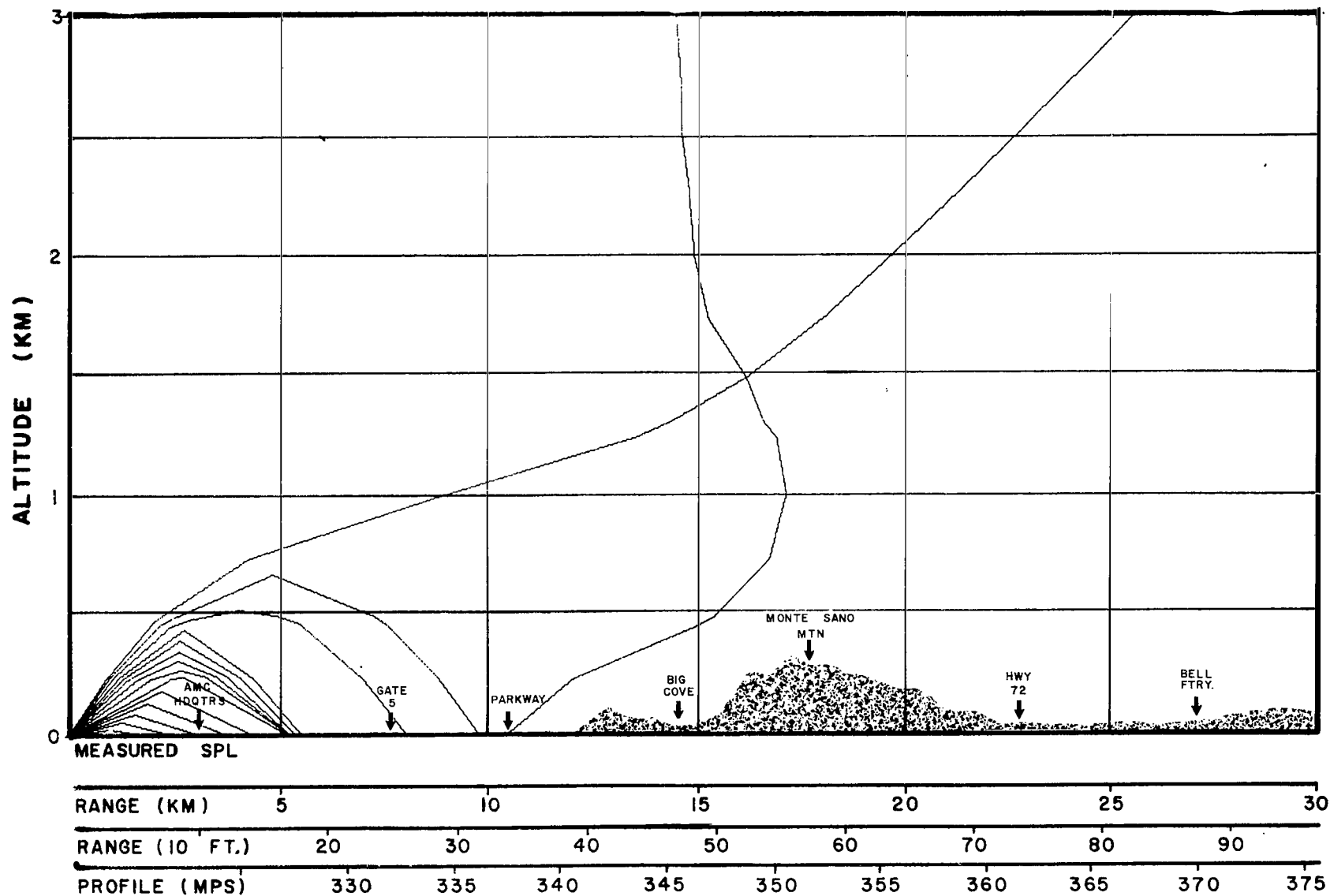


FIG. 9 CALCULATED ACOUSTIC RAY PATHS
HUNTSVILLE, ALA., 45° AZIMUTH

DATE 3/9/63
TIME 0700c

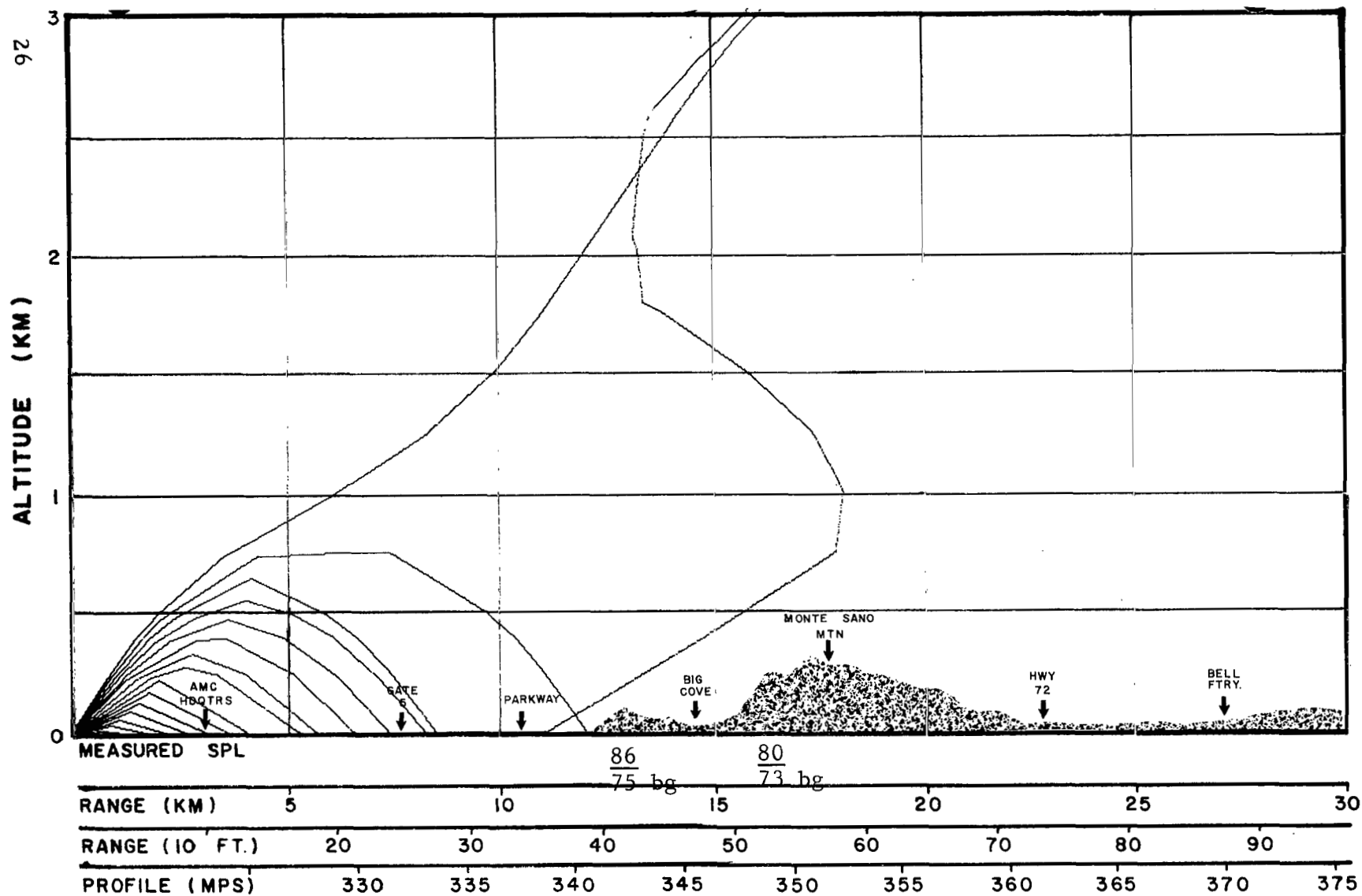


FIG. 10. CALCULATED ACOUSTIC RAY PATHS
HUNTSVILLE, ALA., 45° AZIMUTH

DATE 3/9/63
TIME 0900C

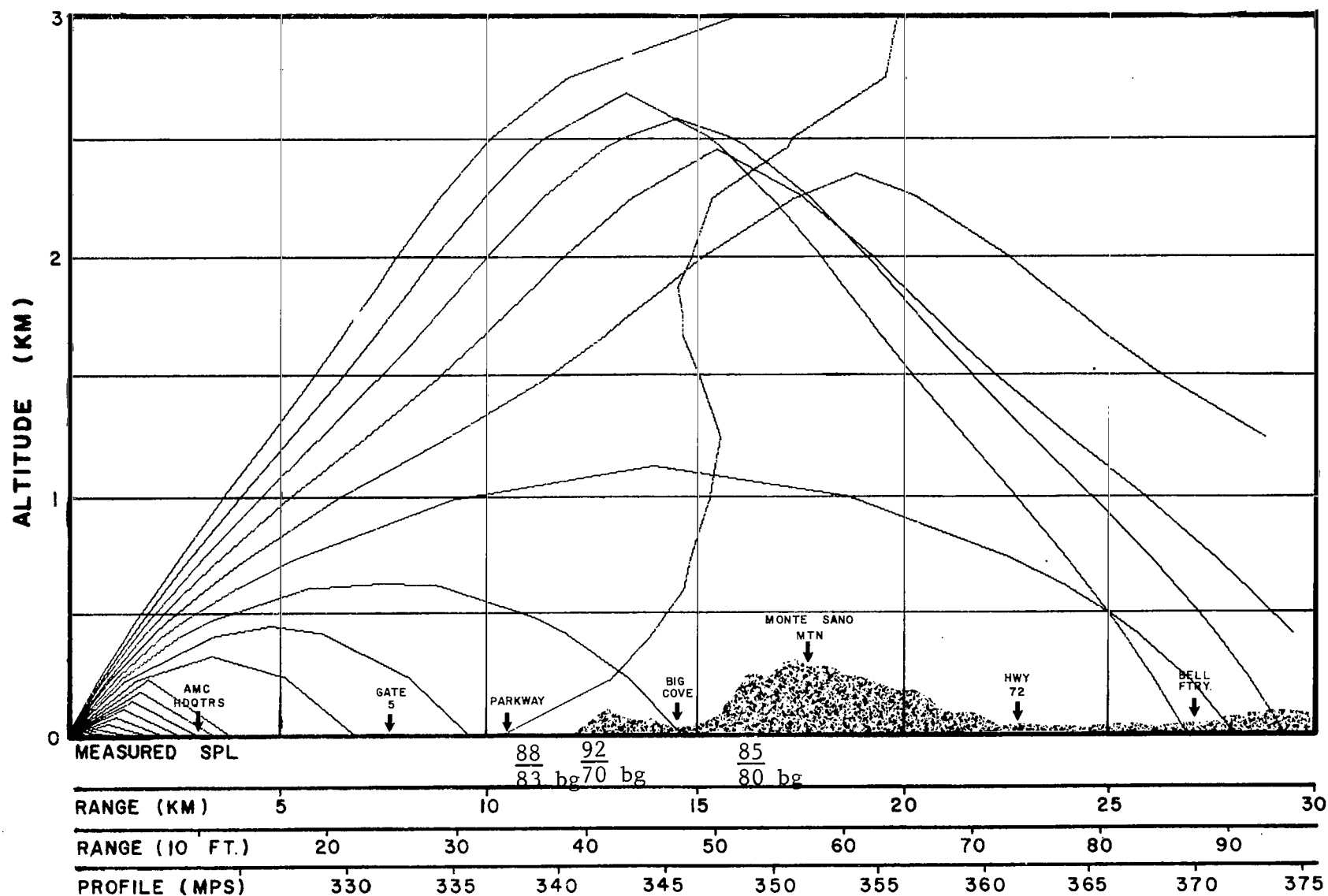


FIG. II CALCULATED ACOUSTIC RAY PATHS
HUNTSVILLE, ALA., 45° AZIMUTH

DATE 3/9/63
TIME 1045C

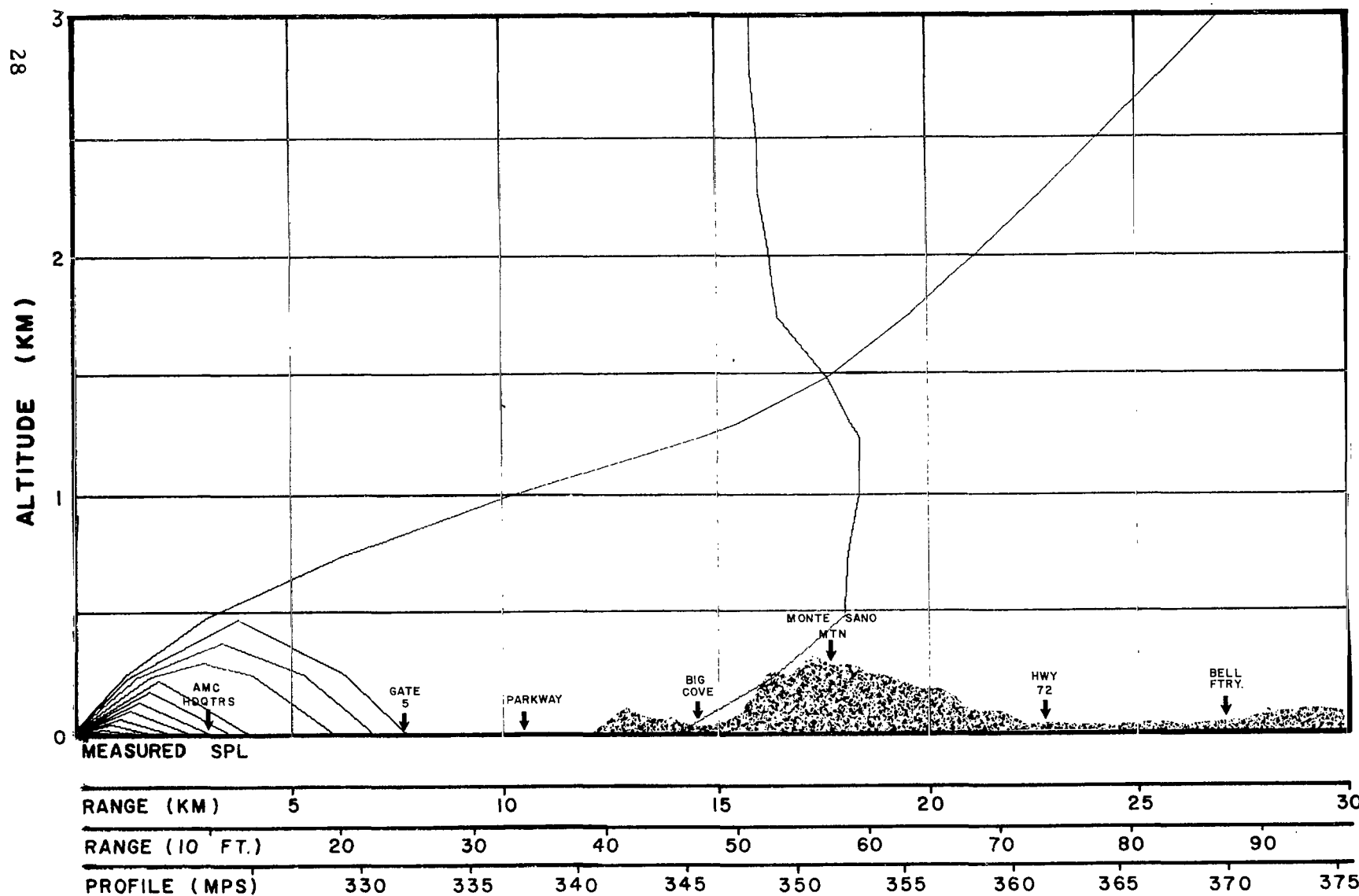


FIG. 12 CALCULATED ACOUSTIC RAY PATHS
HUNTSVILLE, ALA., 45° AZIMUTH

DATE 3/9/63
TIME X-6 Hour Fore-
cast

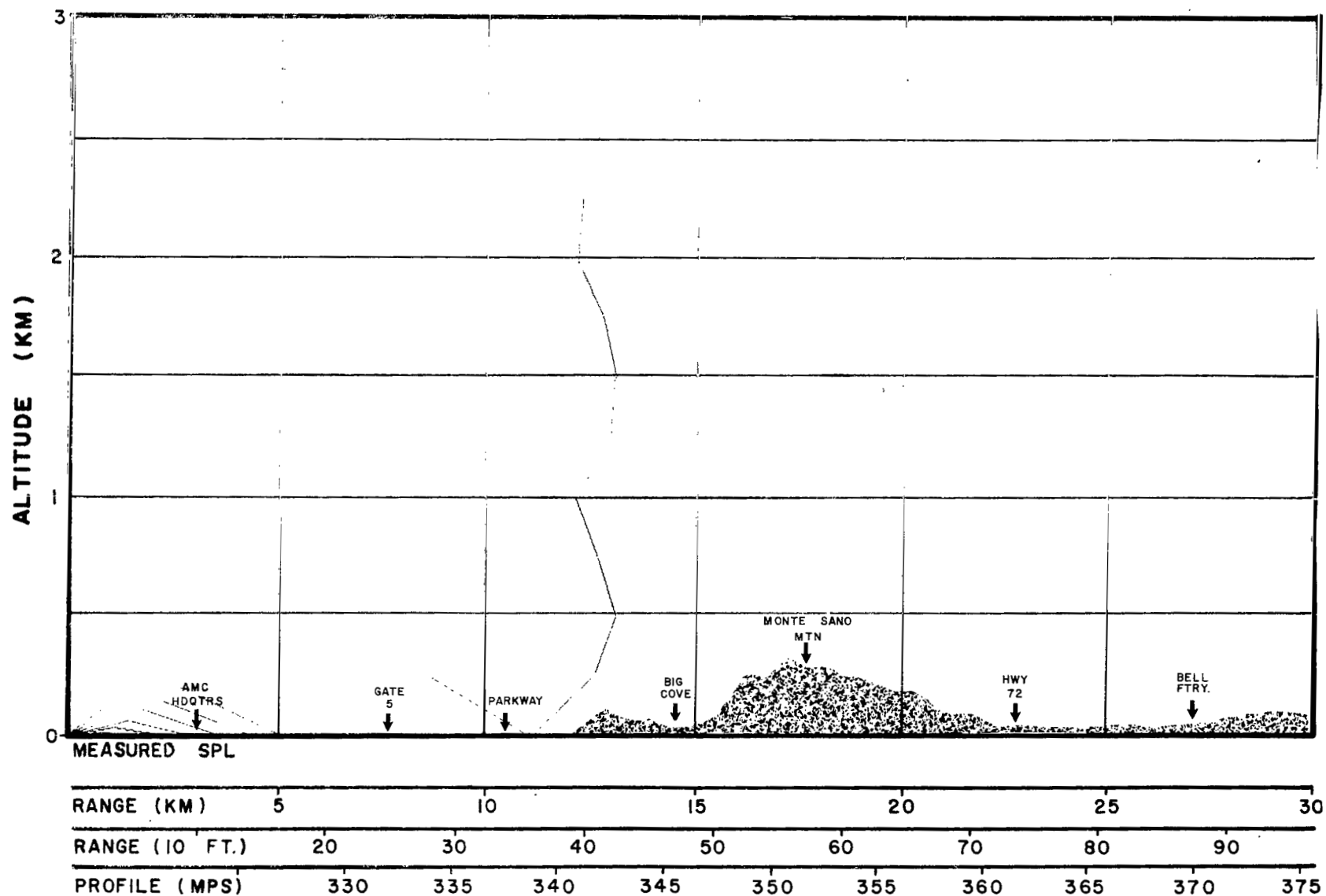


FIG. 13 CALCULATED ACOUSTIC RAY PATHS
HUNTSVILLE, ALA., 45° AZIMUTH

DATE 3/9/63
TIME 1620G

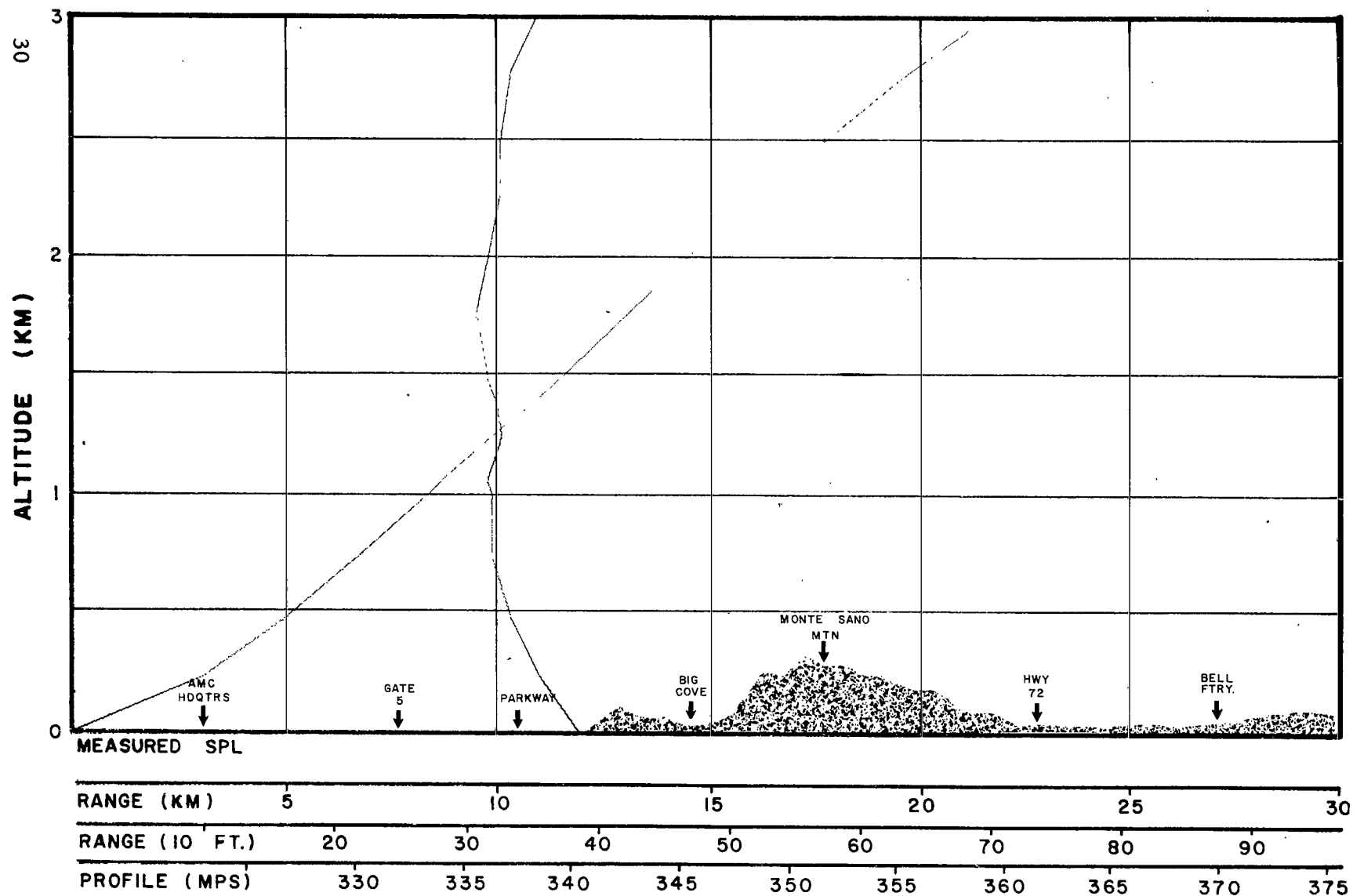


FIG. 14 CALCULATED ACOUSTIC RAY PATHS
HUNTSVILLE, ALA., 45° AZIMUTH

DATE 3/10/63
TIME 1600C

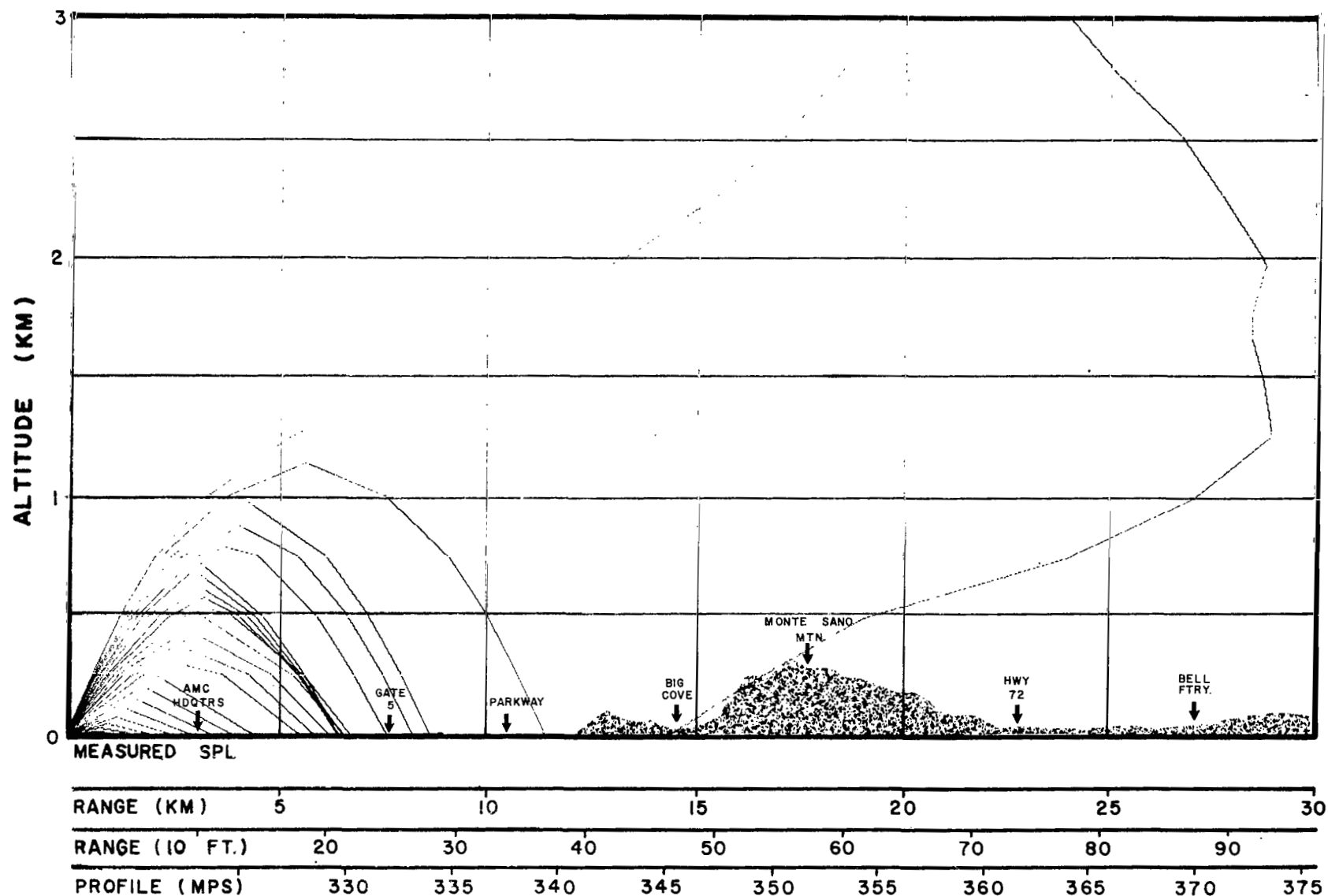


FIG. 15 CALCULATED ACOUSTIC RAY PATHS
HUNTSVILLE, ALA., 45° AZIMUTH

DATE 3/11/63
TIME 0700C

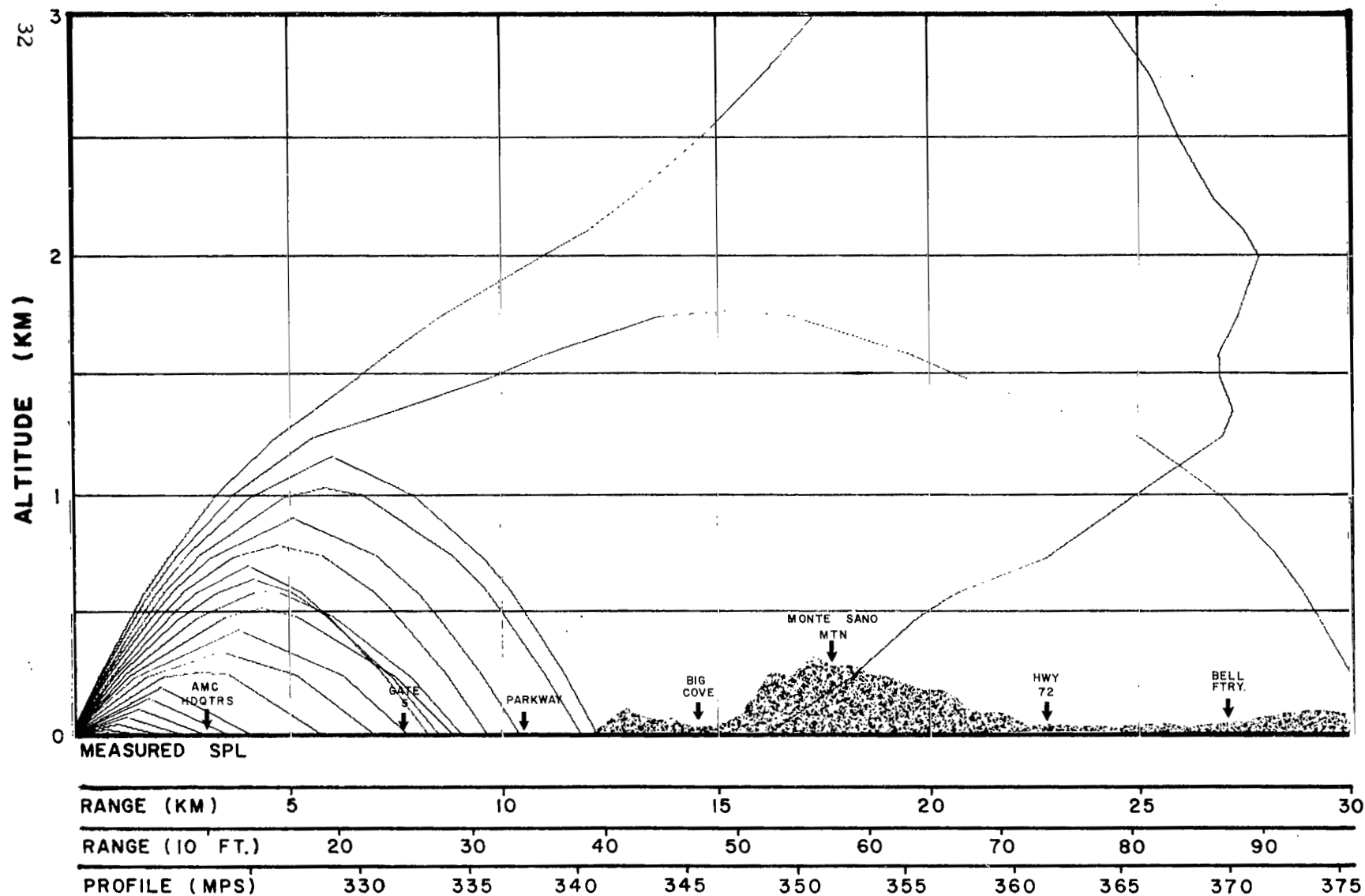


FIG. 16 CALCULATED ACOUSTIC RAY PATHS
HUNTSVILLE, ALA., 45° AZIMUTH

DATE 3/11/63
TIME 0800C

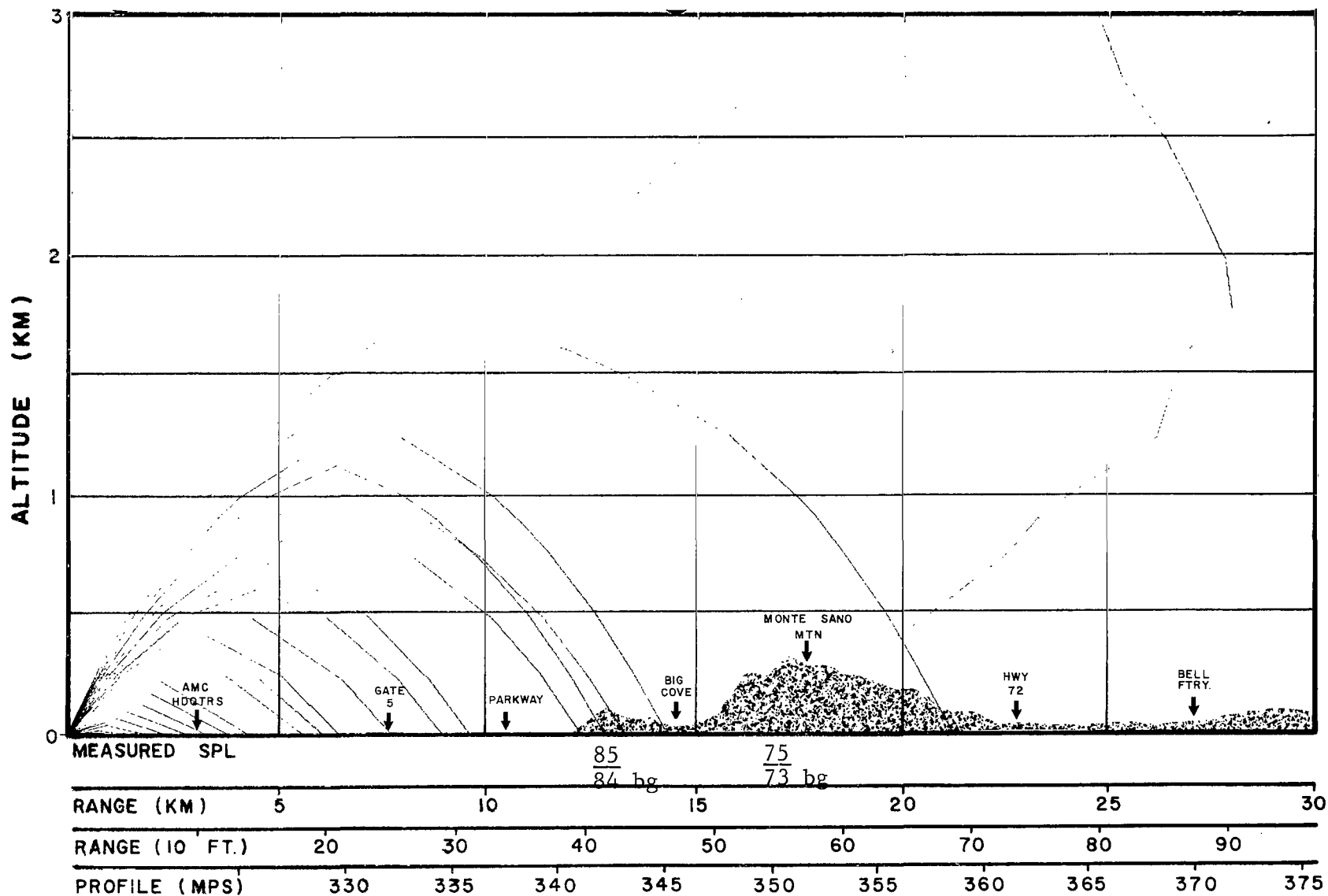


FIG. 17 CALCULATED ACOUSTIC RAY PATHS
HUNTSVILLE, ALA., 45° AZIMUTH

DATE 3/11/63
TIME 1000C

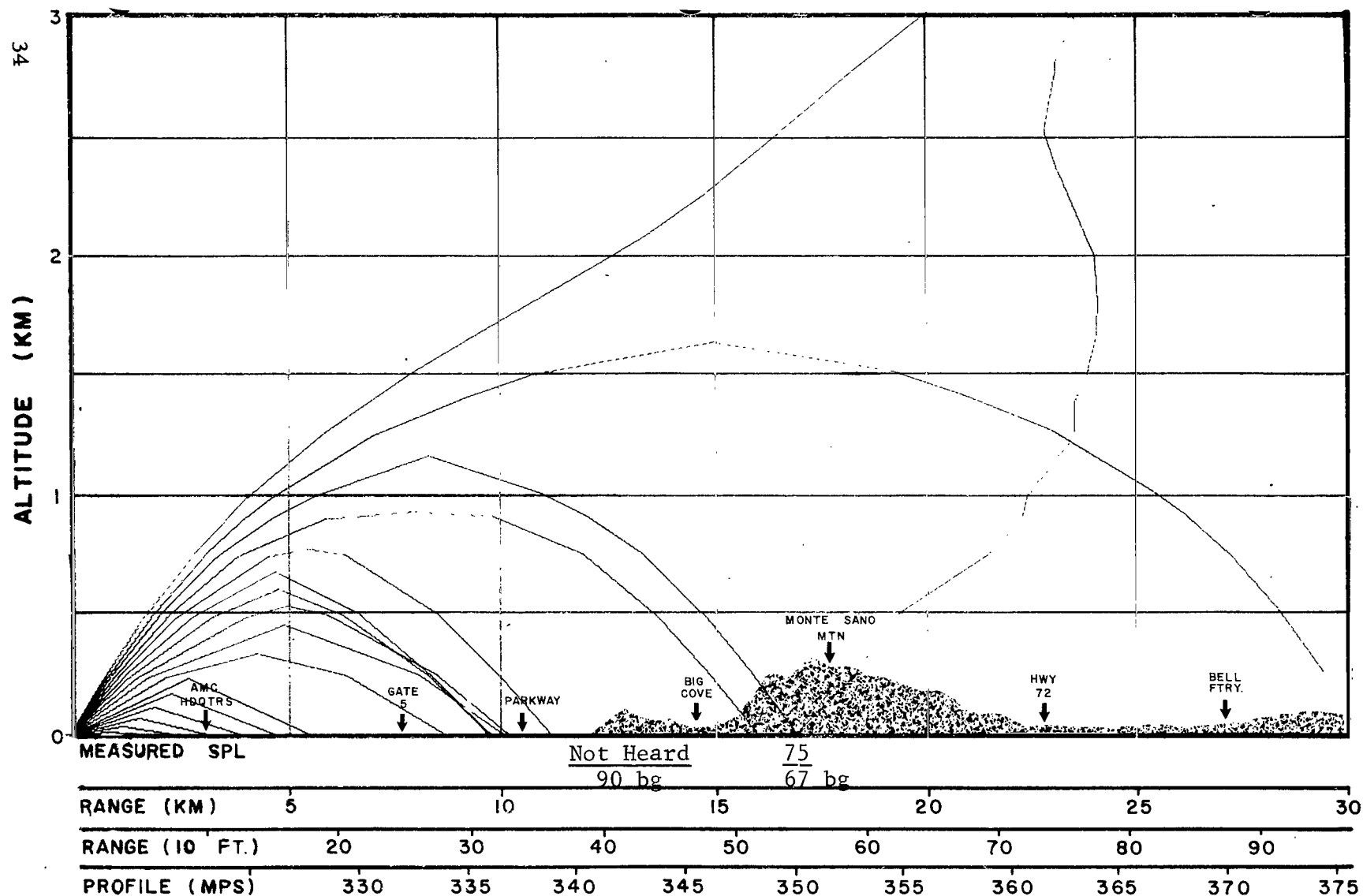


FIG. 18 CALCULATED ACOUSTIC RAY PATHS
HUNTSVILLE, ALA., 45° AZIMUTH

DATE 3/11/63
TIME 1335C

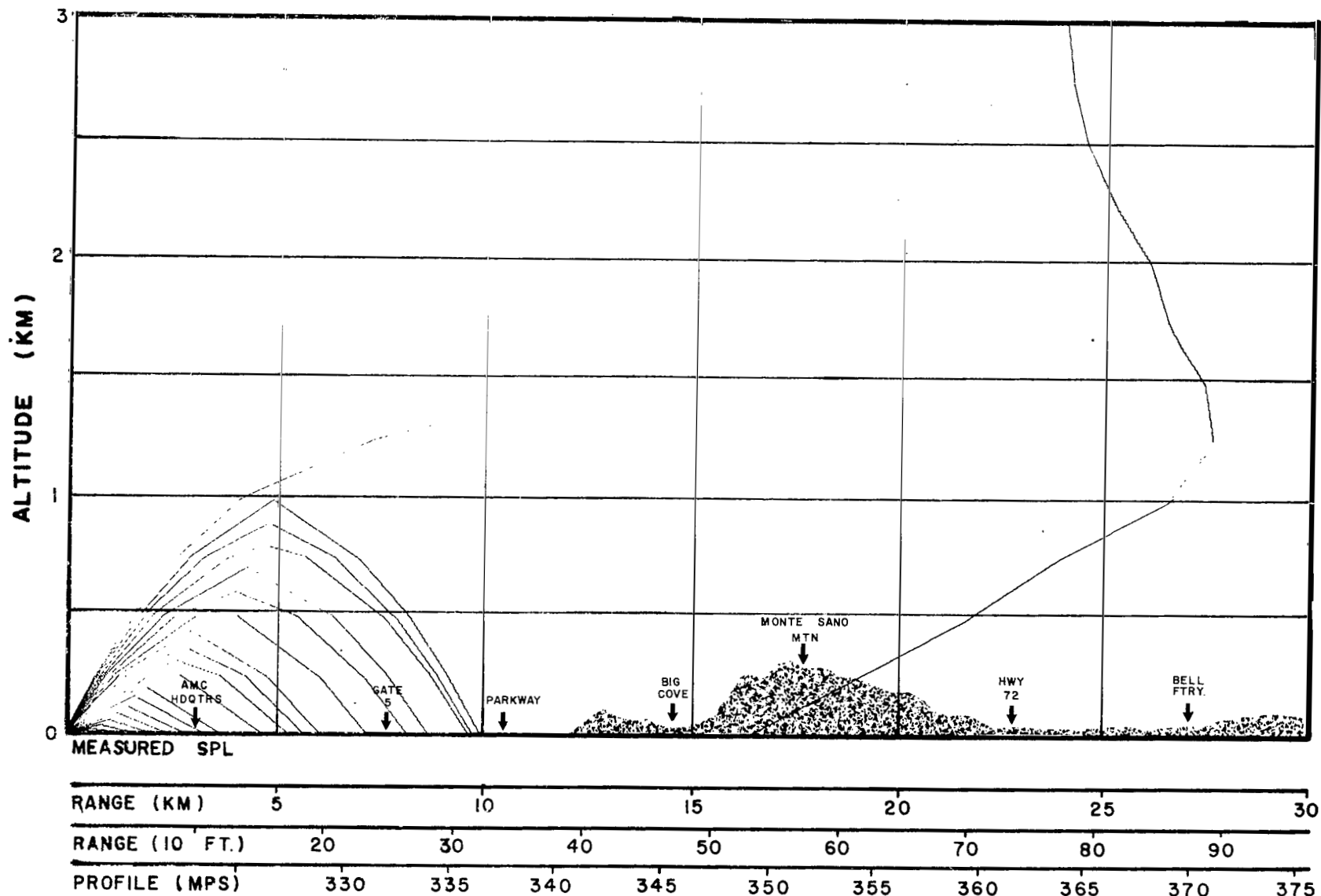


FIG. 19 CALCULATED ACOUSTIC RAY PATHS
HUNTSVILLE, ALA., 45° AZIMUTH

DATE 3/11/63
TIME X-6 Hour Fore-
cast

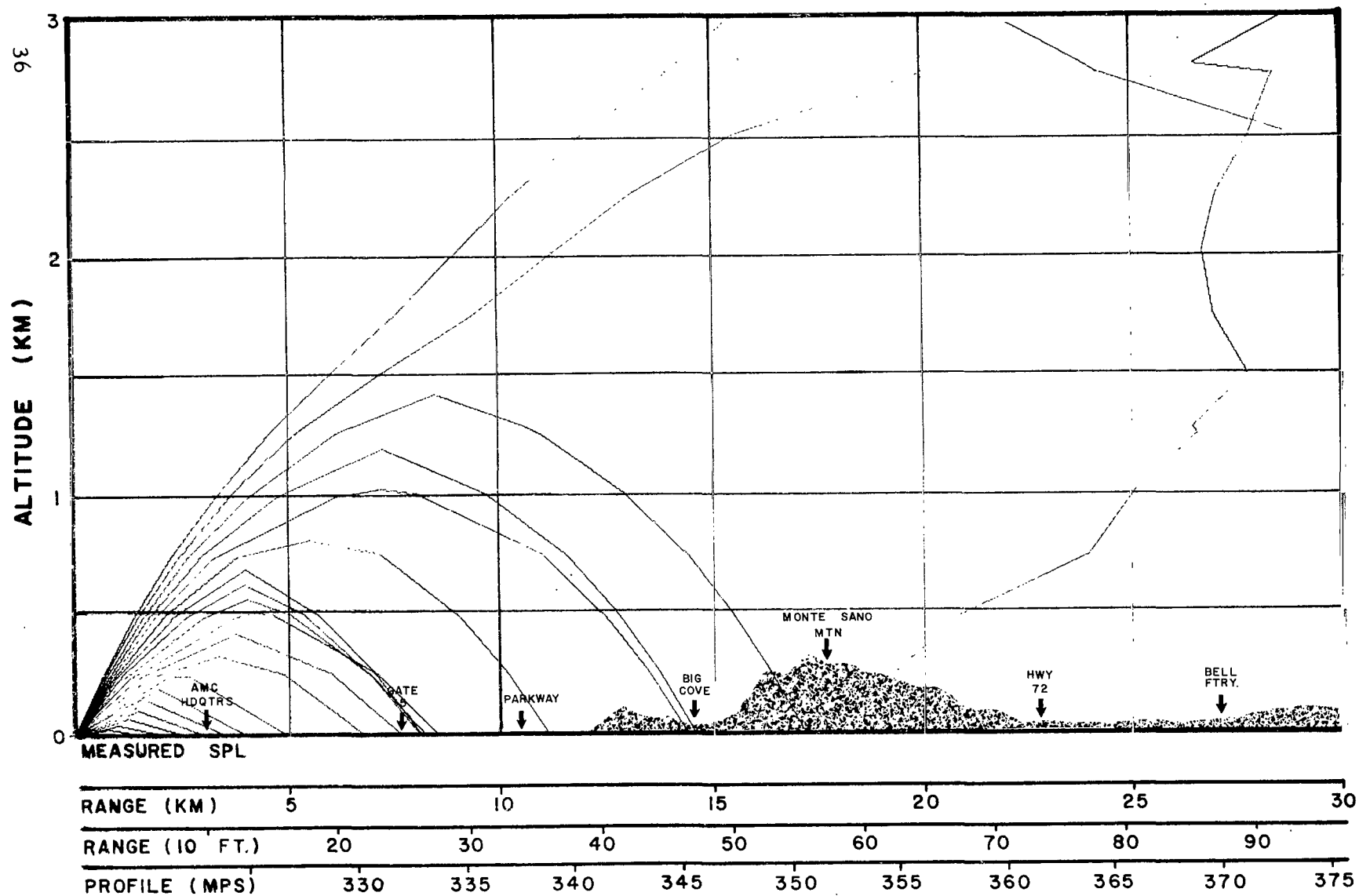


FIG. 20 CALCULATED ACOUSTIC RAY PATHS
HUNTSVILLE, ALA., 45° AZIMUTH

DATE 3/11/63
TIME 1615C

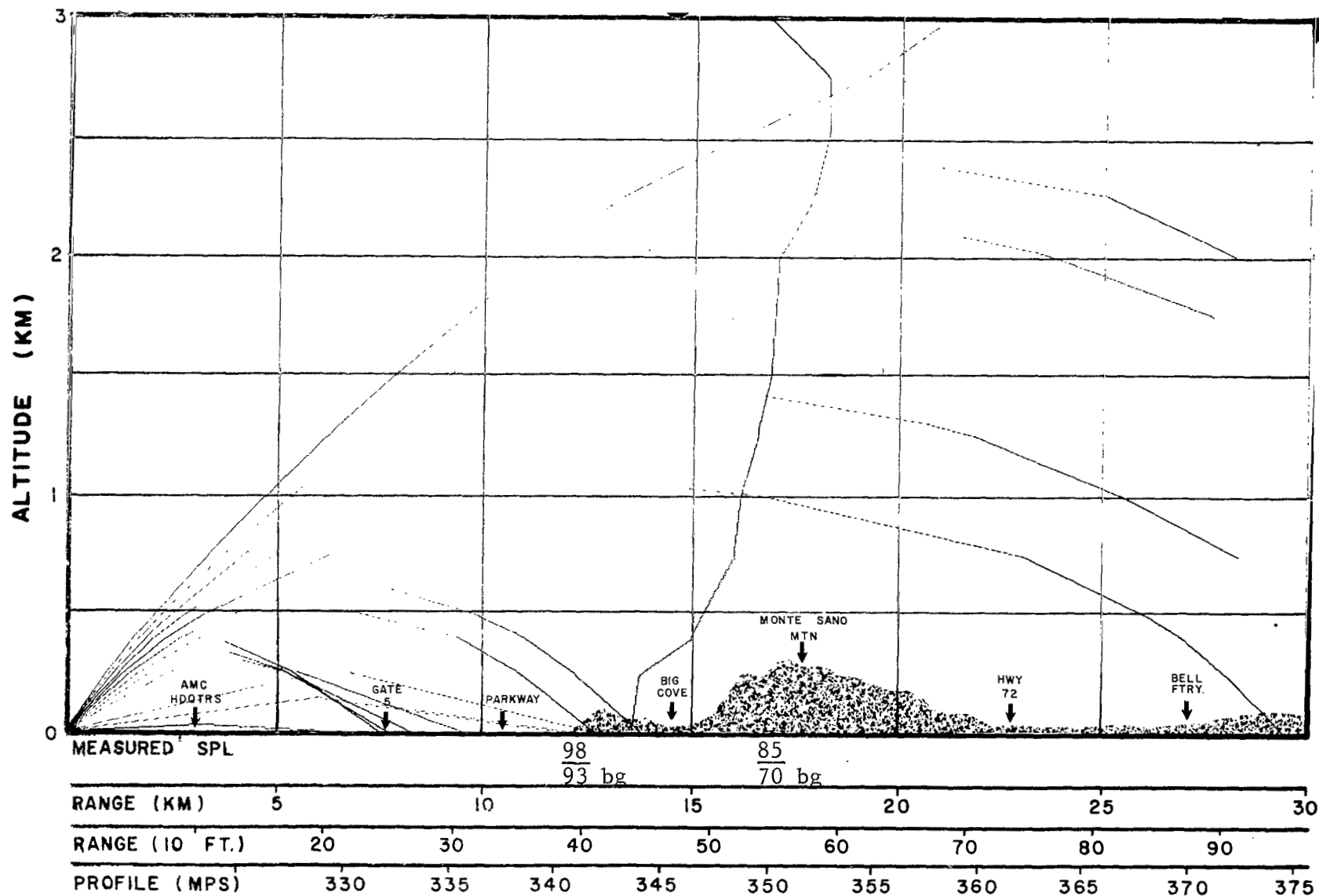


FIG. 21 CALCULATED ACOUSTIC RAY PATHS
HUNTSVILLE, ALA., 45° AZIMUTH

DATE 3/12/63
TIME 1000C

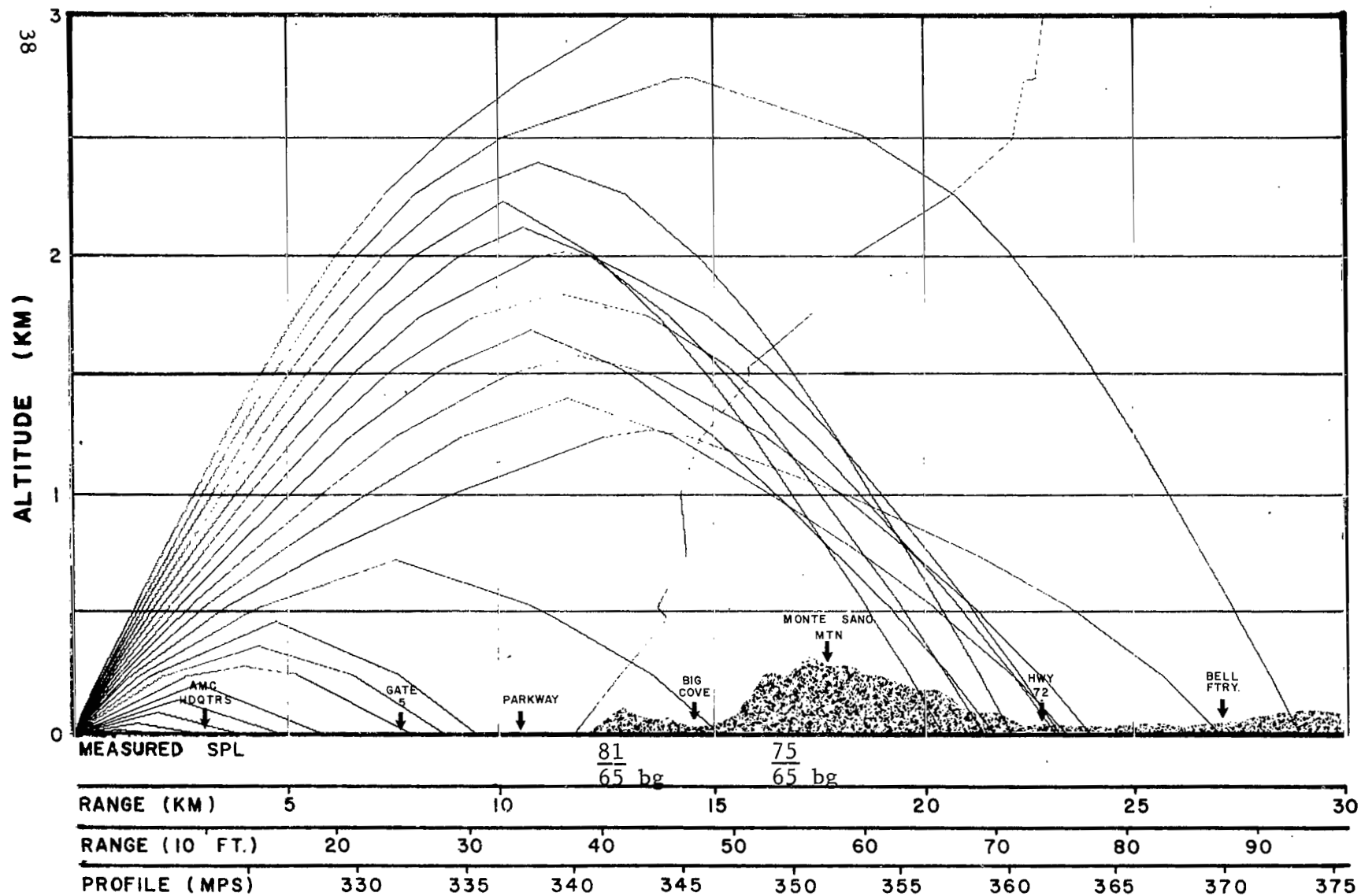


FIG. 22 CALCULATED ACOUSTIC RAY PATHS
HUNTSVILLE, ALA., 45° AZIMUTH

DATE 3/12/63
TIME 1400c

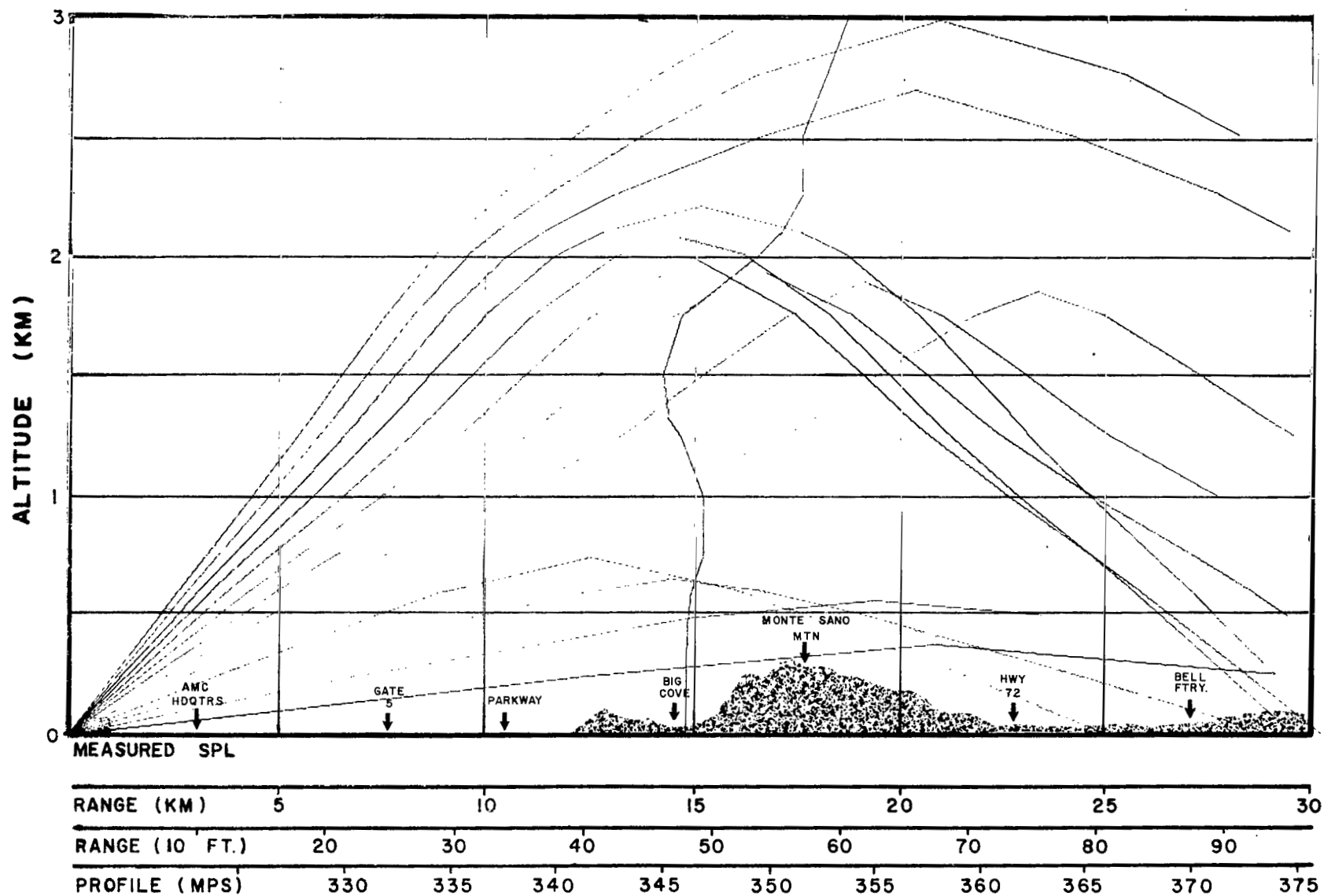


FIG. 23 CALCULATED ACOUSTIC RAY PATHS
HUNTSVILLE, ALA., 45° AZIMUTH

DATE 3/12/63
TIME 1630C

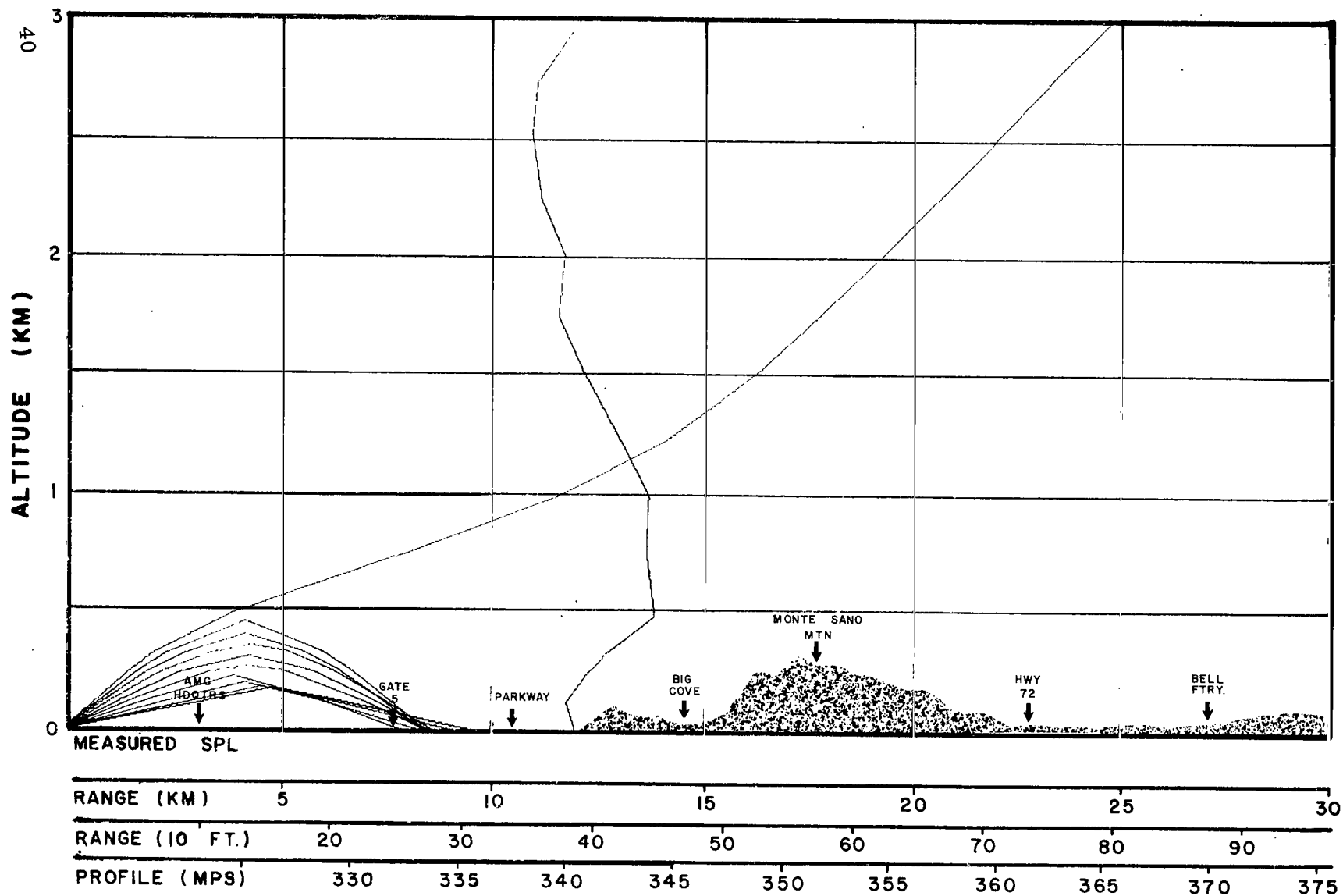


FIG. 24 CALCULATED ACOUSTIC RAY PATHS
HUNTSVILLE, ALA., 45° AZIMUTH

DATE 3/13/63
TIME 0700C

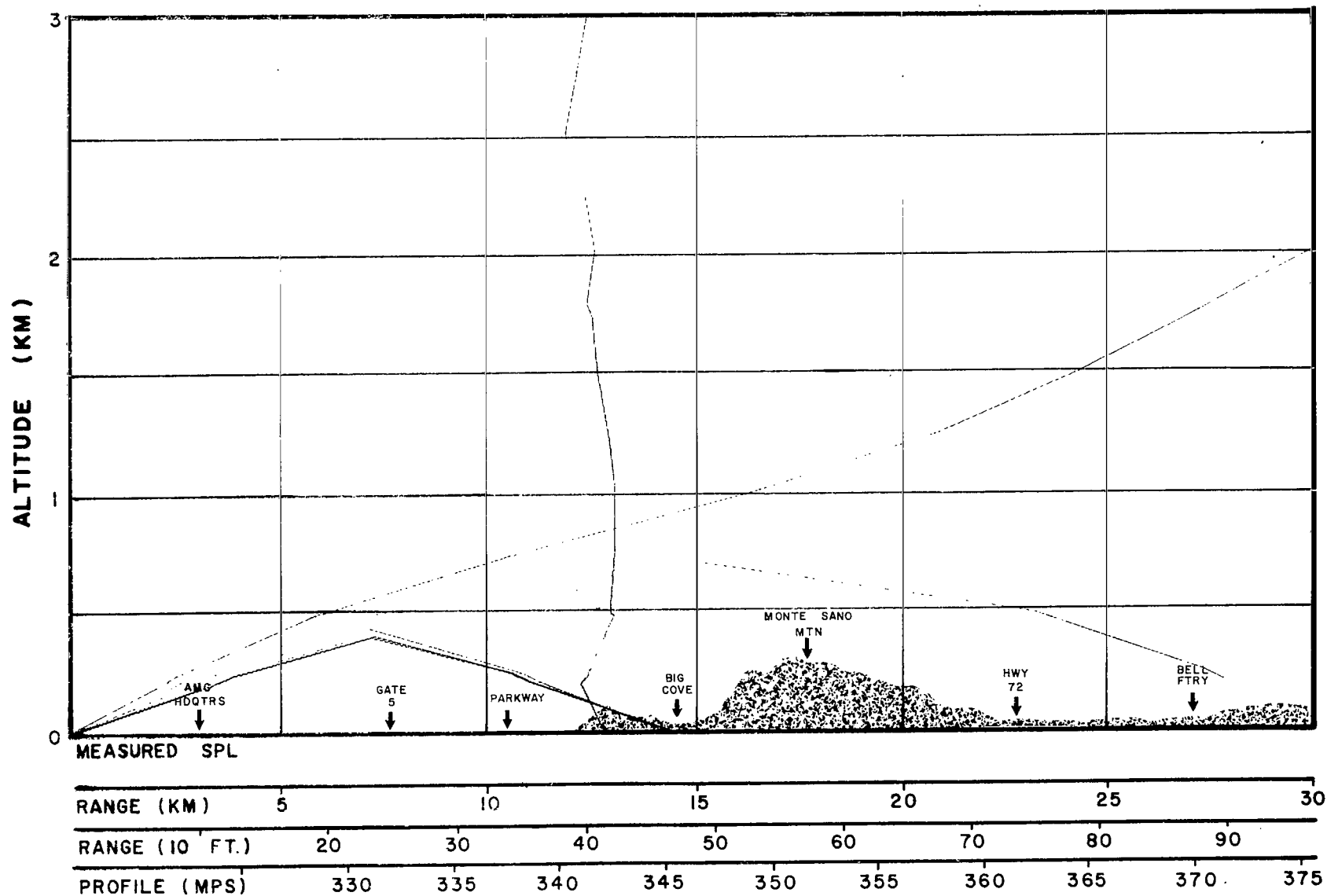


FIG. 25 CALCULATED ACOUSTIC RAY PATHS
HUNTSVILLE, ALA., 45° AZIMUTH

DATE 3/13/63
TIME 0820C

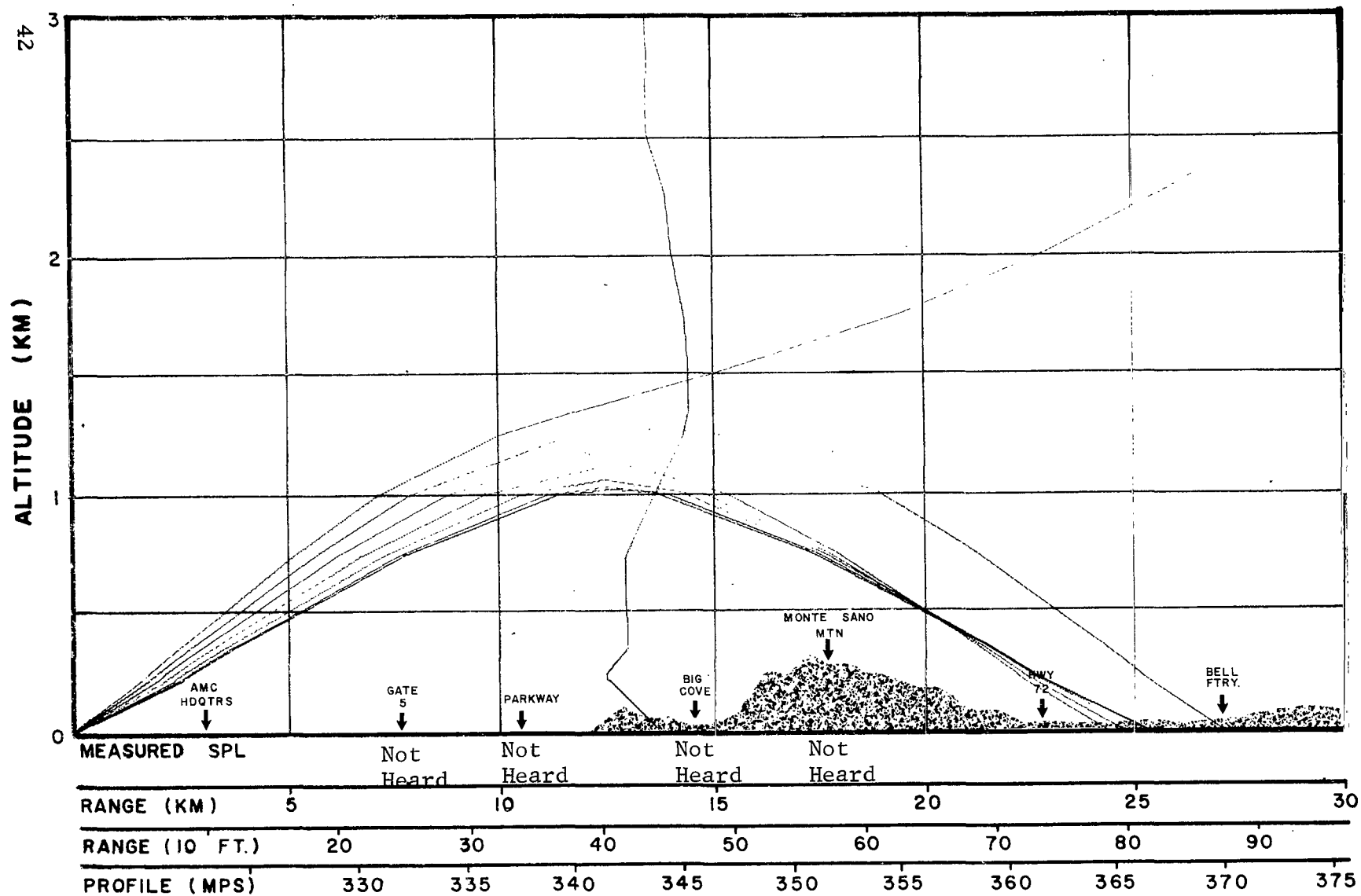


FIG. 26 CALCULATED ACOUSTIC RAY PATHS
HUNTSVILLE, ALA., 45° AZIMUTH

DATE 3/13/63
TIME 1005C

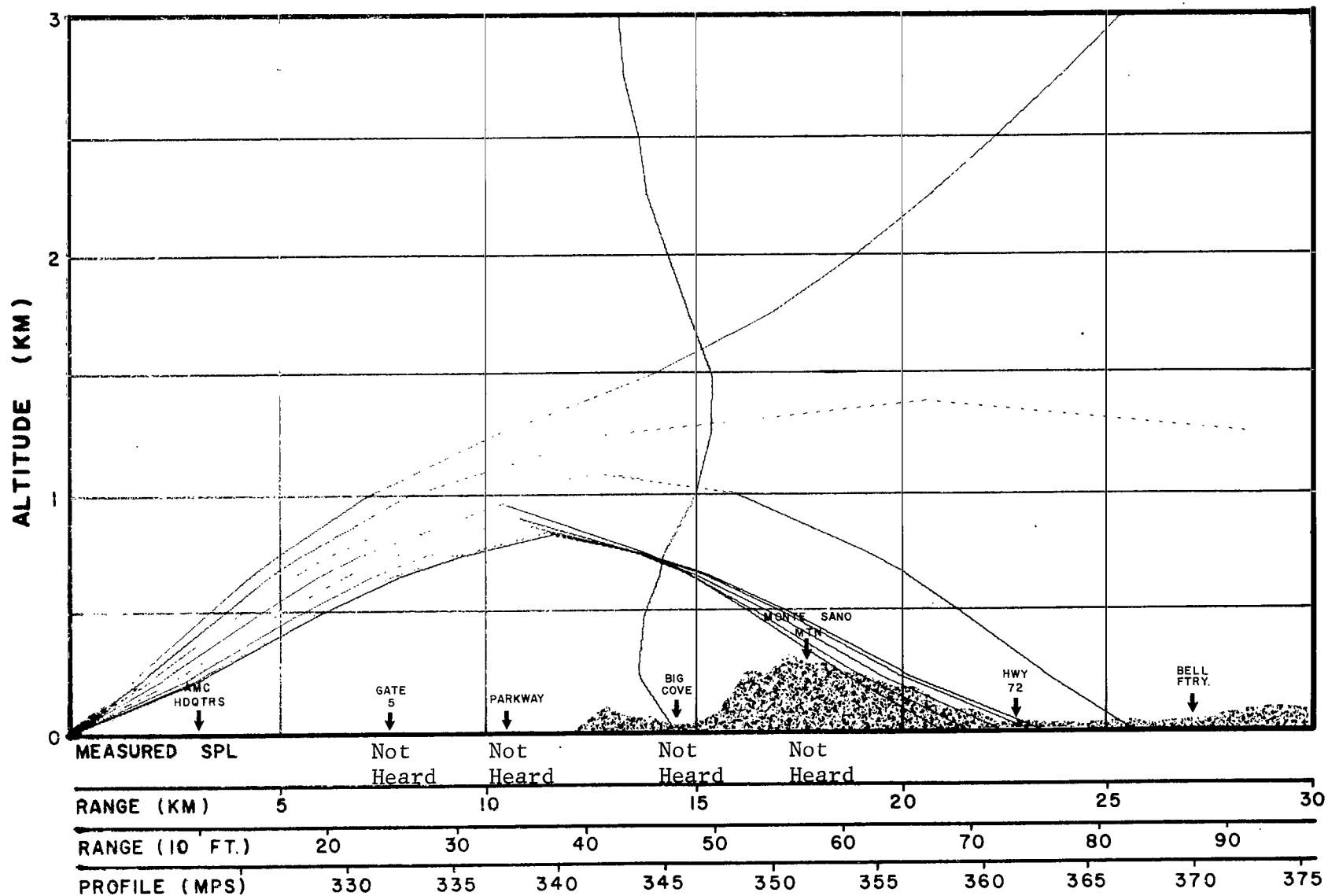


FIG. 27 CALCULATED ACOUSTIC RAY PATHS
HUNTSVILLE, ALA., 45° AZIMUTH

DATE 3/13/63
TIME 1055C

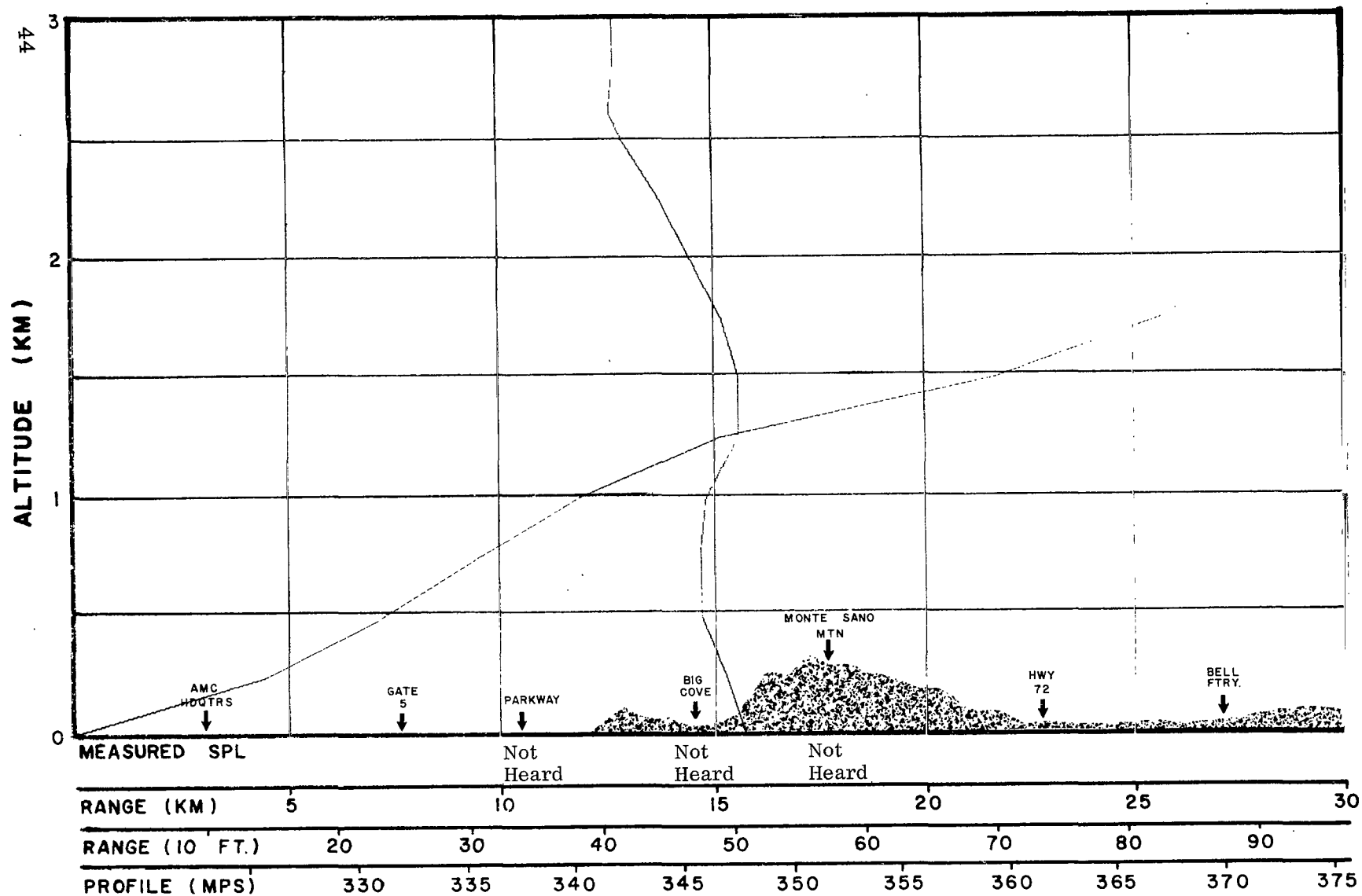


FIG.28 CALCULATED ACOUSTIC RAY PATHS
HUNTSVILLE, ALA., 45° AZIMUTH

DATE 3/13/63
TIME 1400C

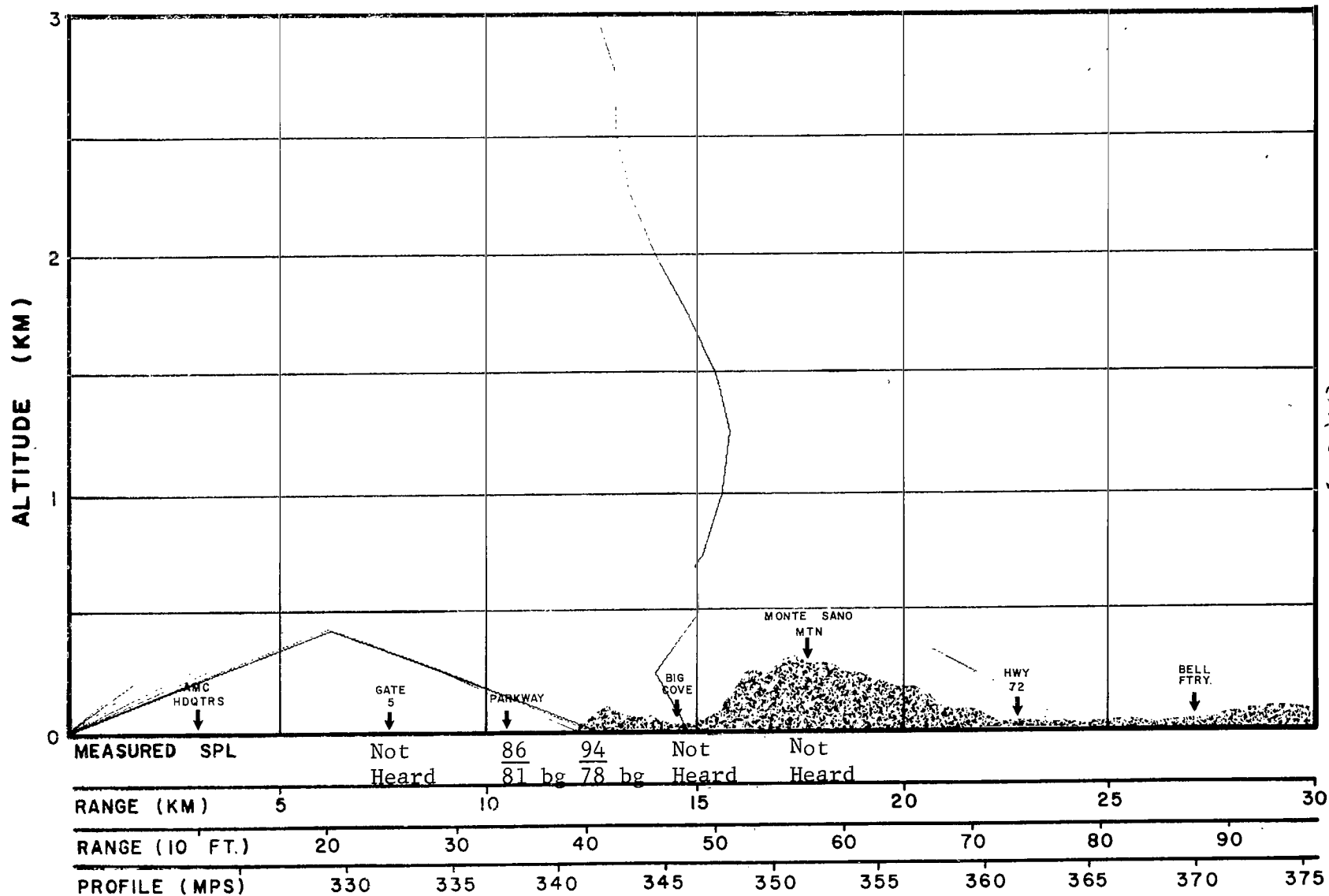


FIG. 29 CALCULATED ACOUSTIC RAY PATHS
HUNTSVILLE, ALA., 45° AZIMUTH

DATE 3/13/63
TIME 1300C

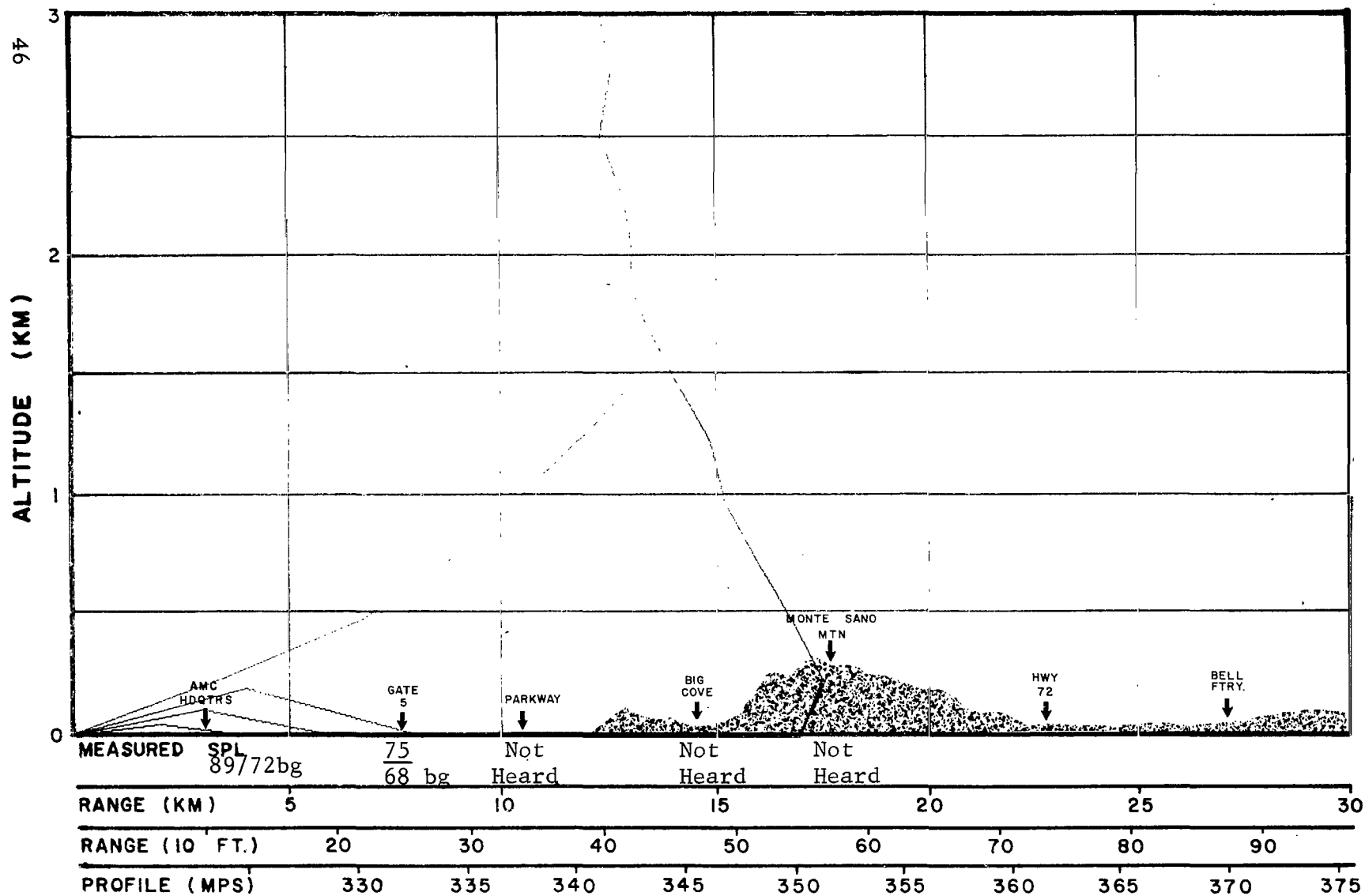


FIG.30 CALCULATED ACOUSTIC RAY PATHS
HUNTSVILLE, ALA., 45° AZIMUTH

DATE 3/13/63
TIME 1500C

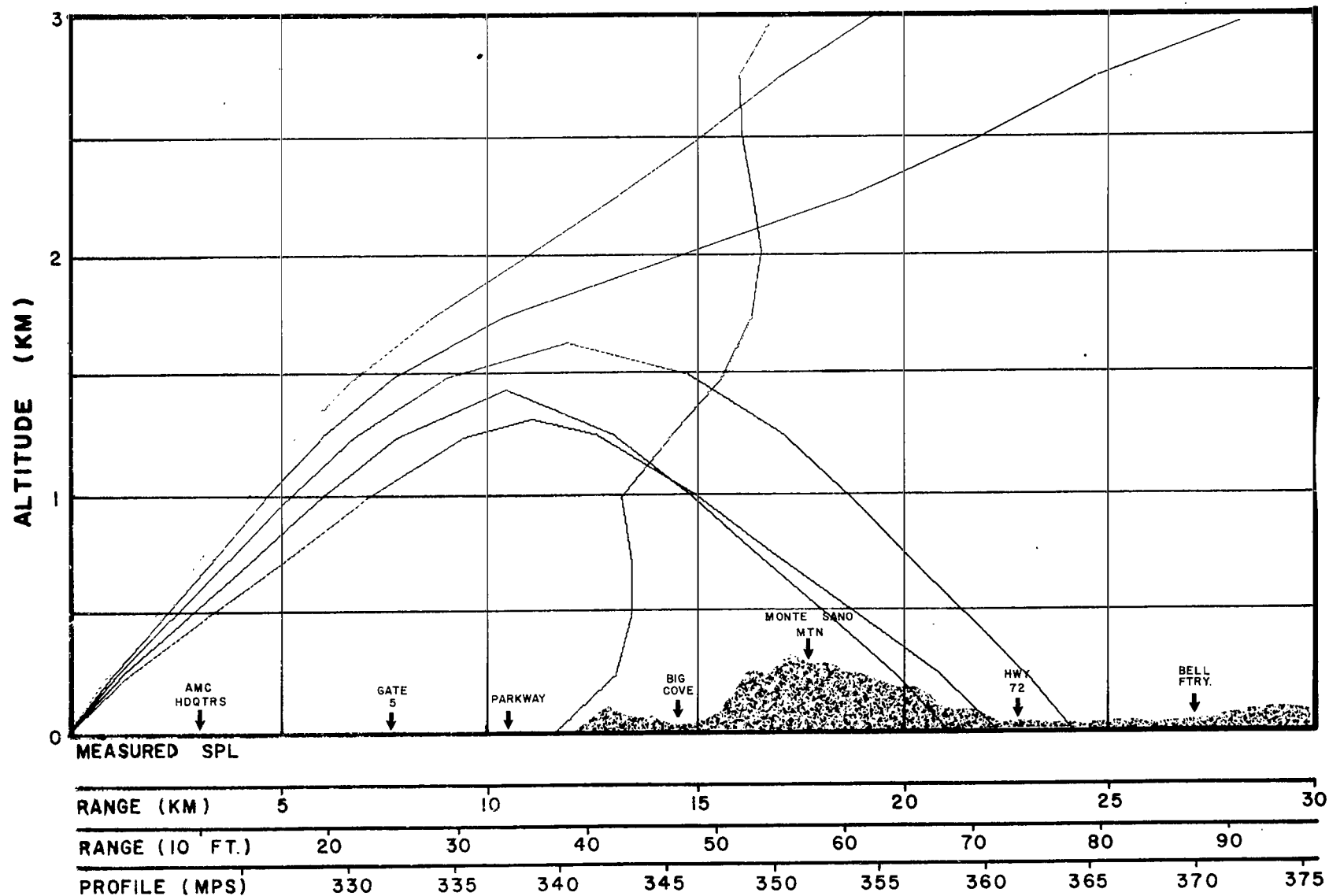


FIG. 31 CALCULATED ACOUSTIC RAY PATHS
HUNTSVILLE, ALA., 45° AZIMUTH

DATE 3/12/63
TIME X-1 Day Fore-
cast

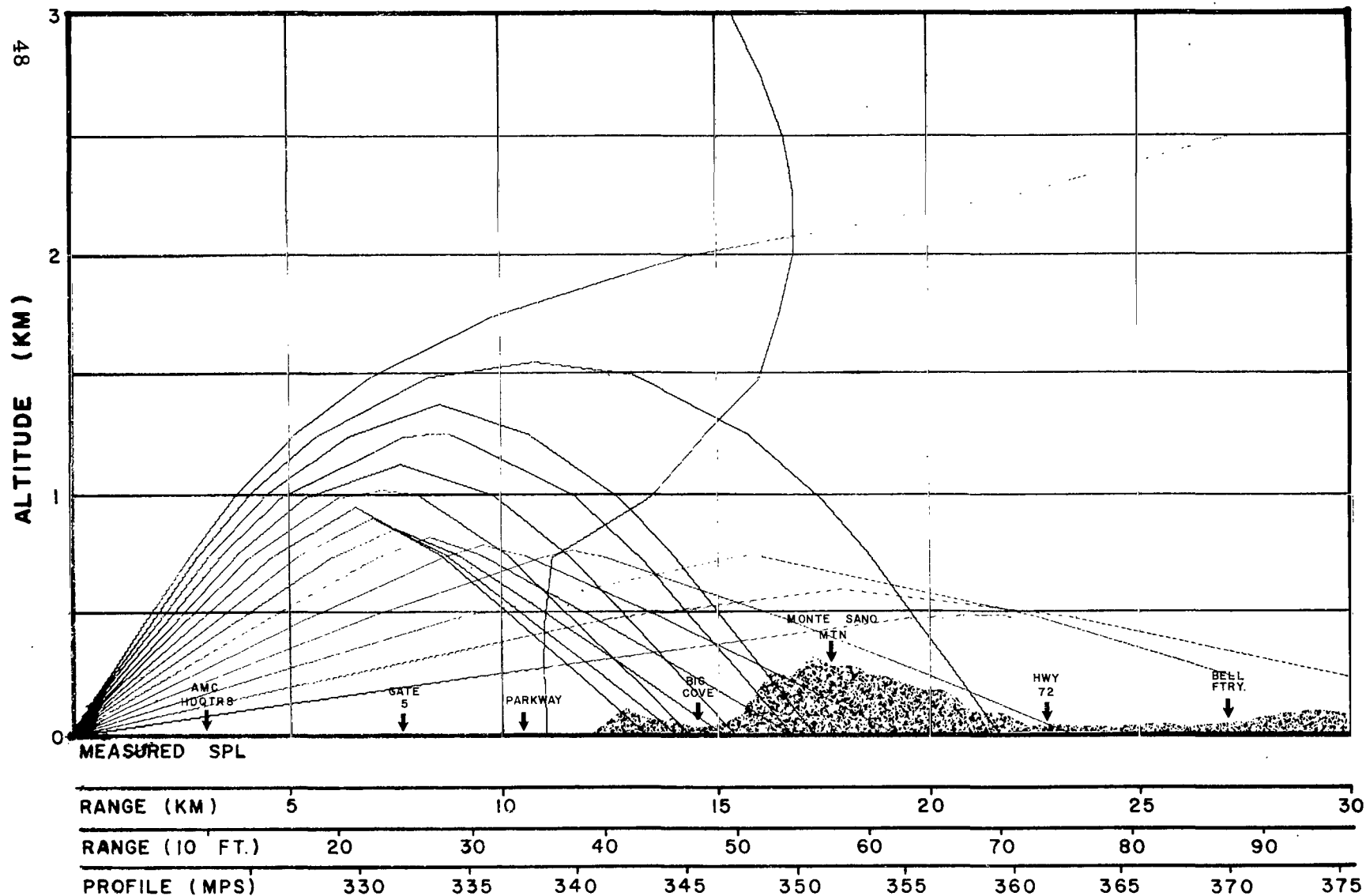


FIG. 32 CALCULATED ACOUSTIC RAY PATHS
HUNTSVILLE, ALA., 45° AZIMUTH

DATE 3/13/63
TIME X-6 Hour Fore-
cast

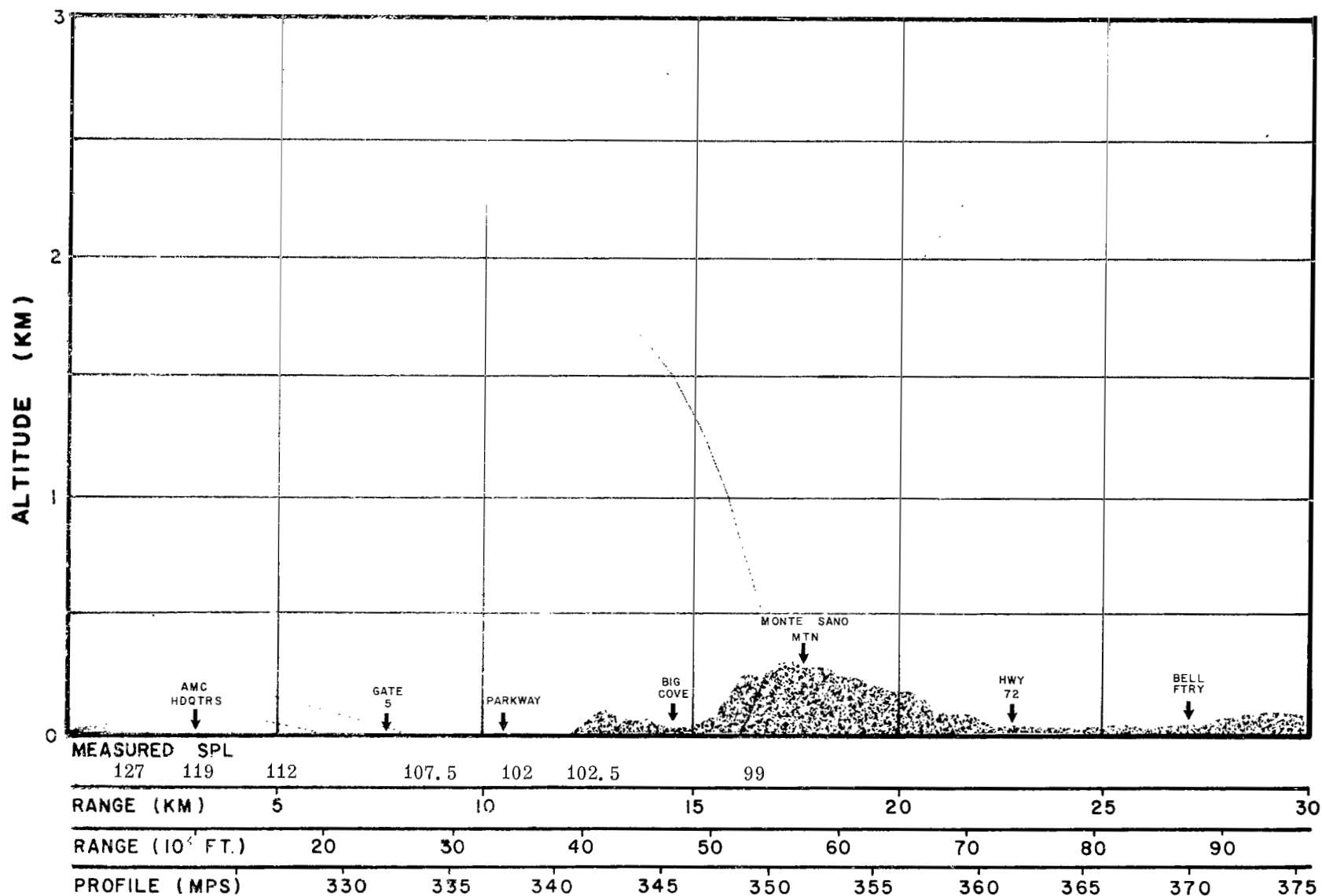


FIG. 33 CALCULATED ACOUSTIC RAY PATHS
HUNTSVILLE, ALA., 45° AZIMUTH

DATE 3/13/63

TIME 1615C

SA-12 Firing Time

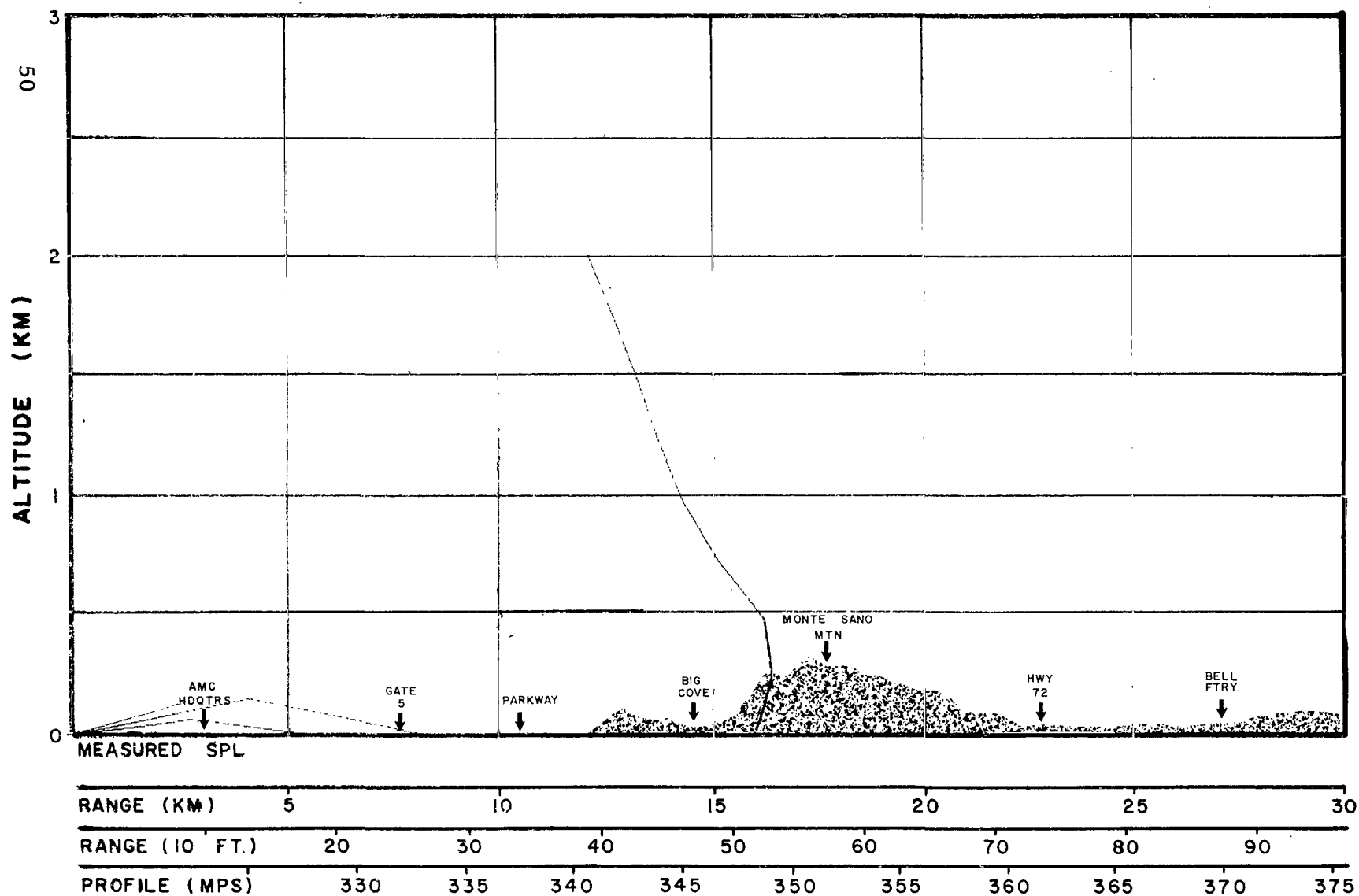


FIG. 34 CALCULATED ACOUSTIC RAY PATHS
HUNTSVILLE, ALA., 45° AZIMUTH

DATE 3/13/63
TIME 1700G

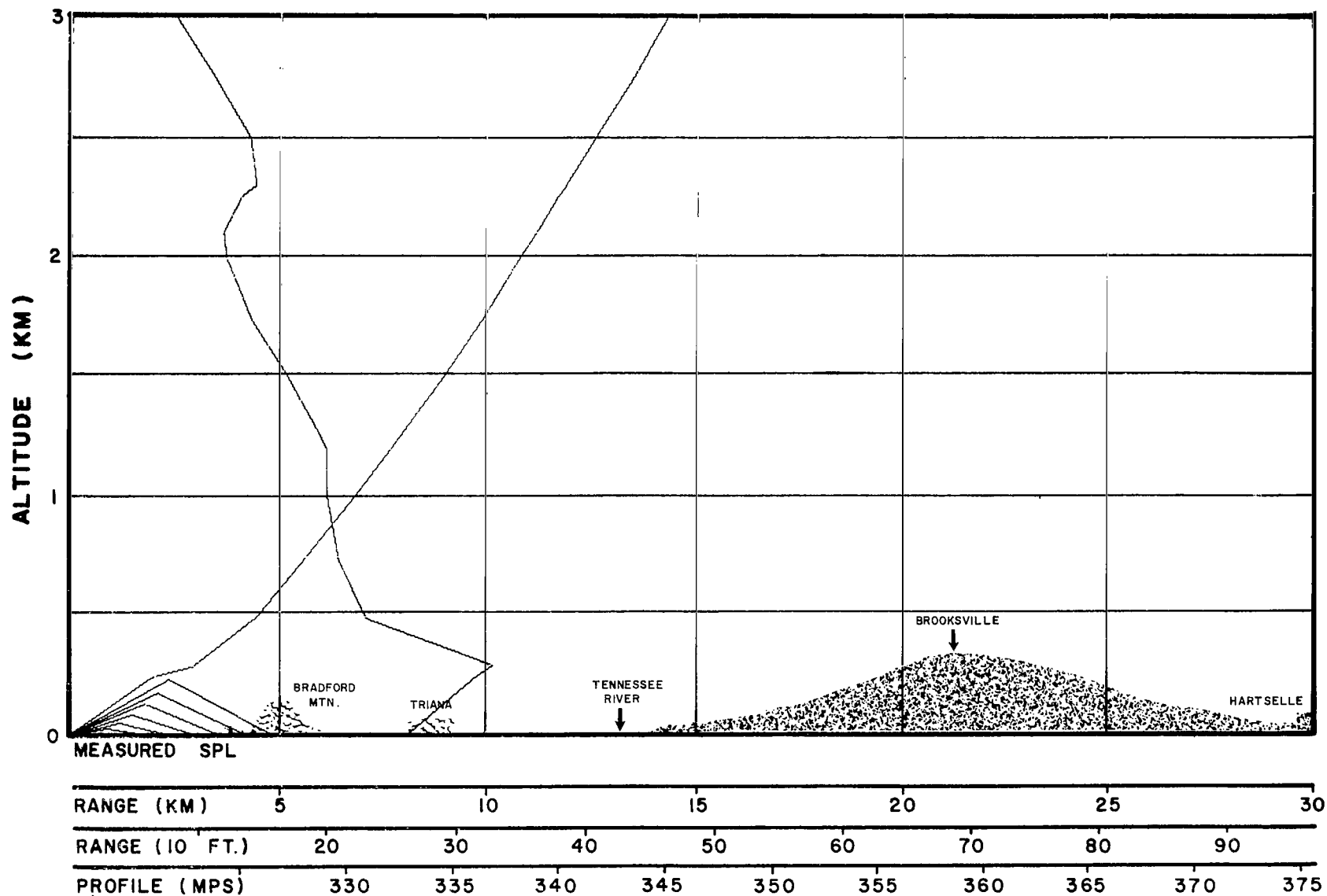


FIG. 35 CALCULATED ACOUSTIC RAY PATHS
 TRIANA, ALA., 222° AZIMUTH

DATE 3/8/63
 TIME 0700C

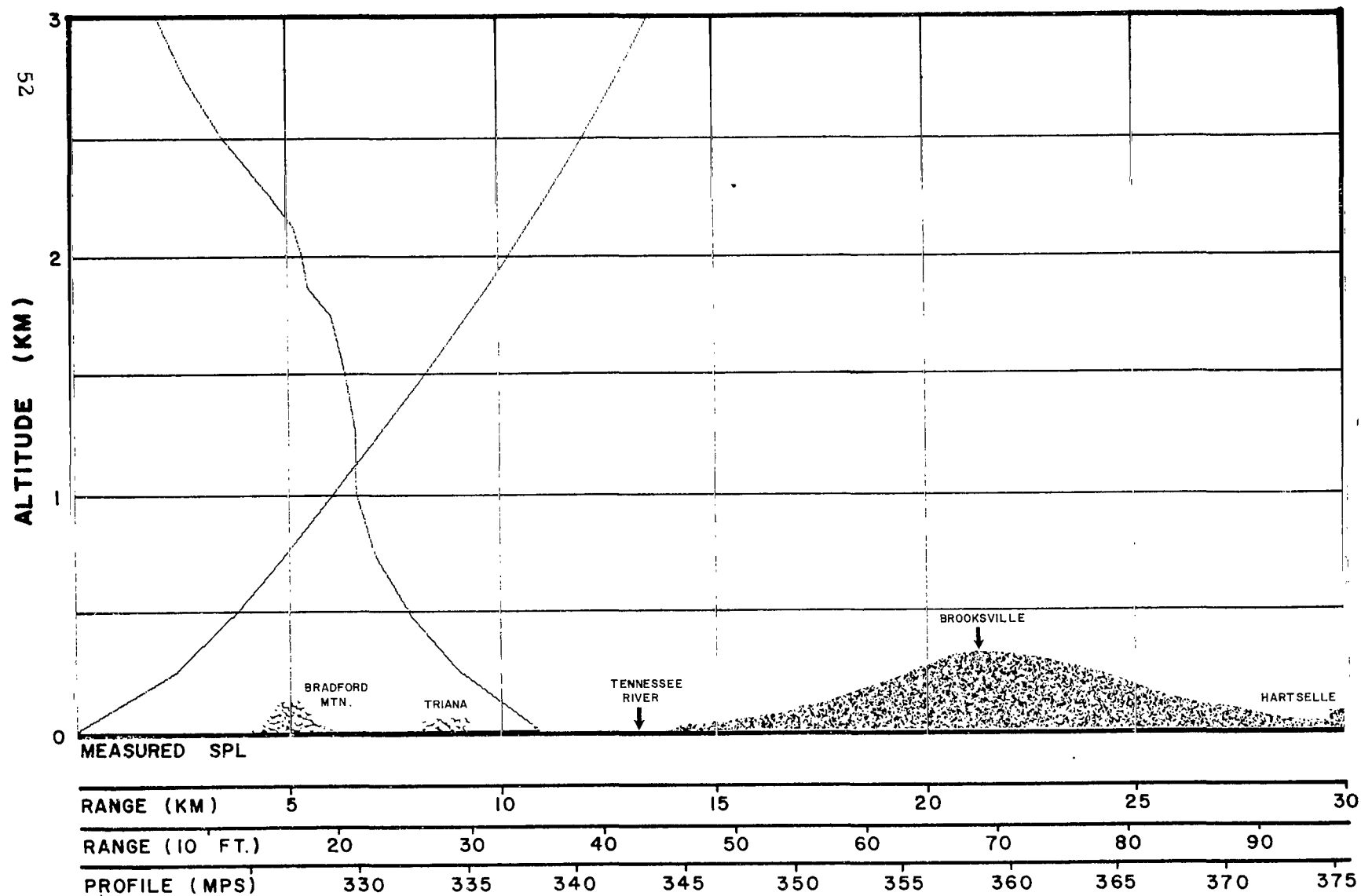


FIG. 36 CALCULATED ACOUSTIC RAY PATHS
 TRIANA, ALA., 22° AZIMUTH

DATE 3/8/63
 TIME 0945G

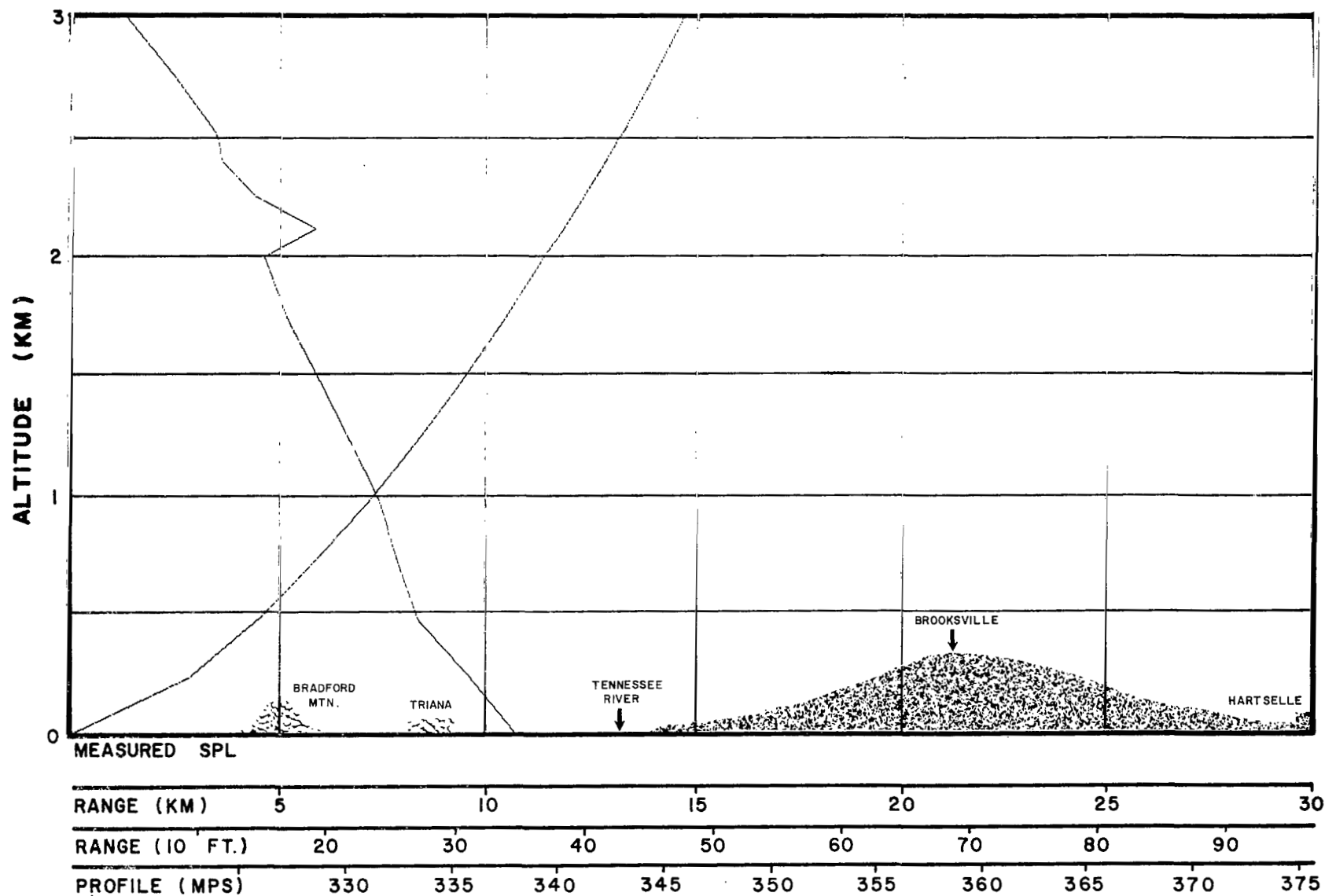


FIG. 37 CALCULATED ACOUSTIC RAY PATHS
 TRIANA, ALA., 222° AZIMUTH

DATE 3/8/63
 TIME 1055C

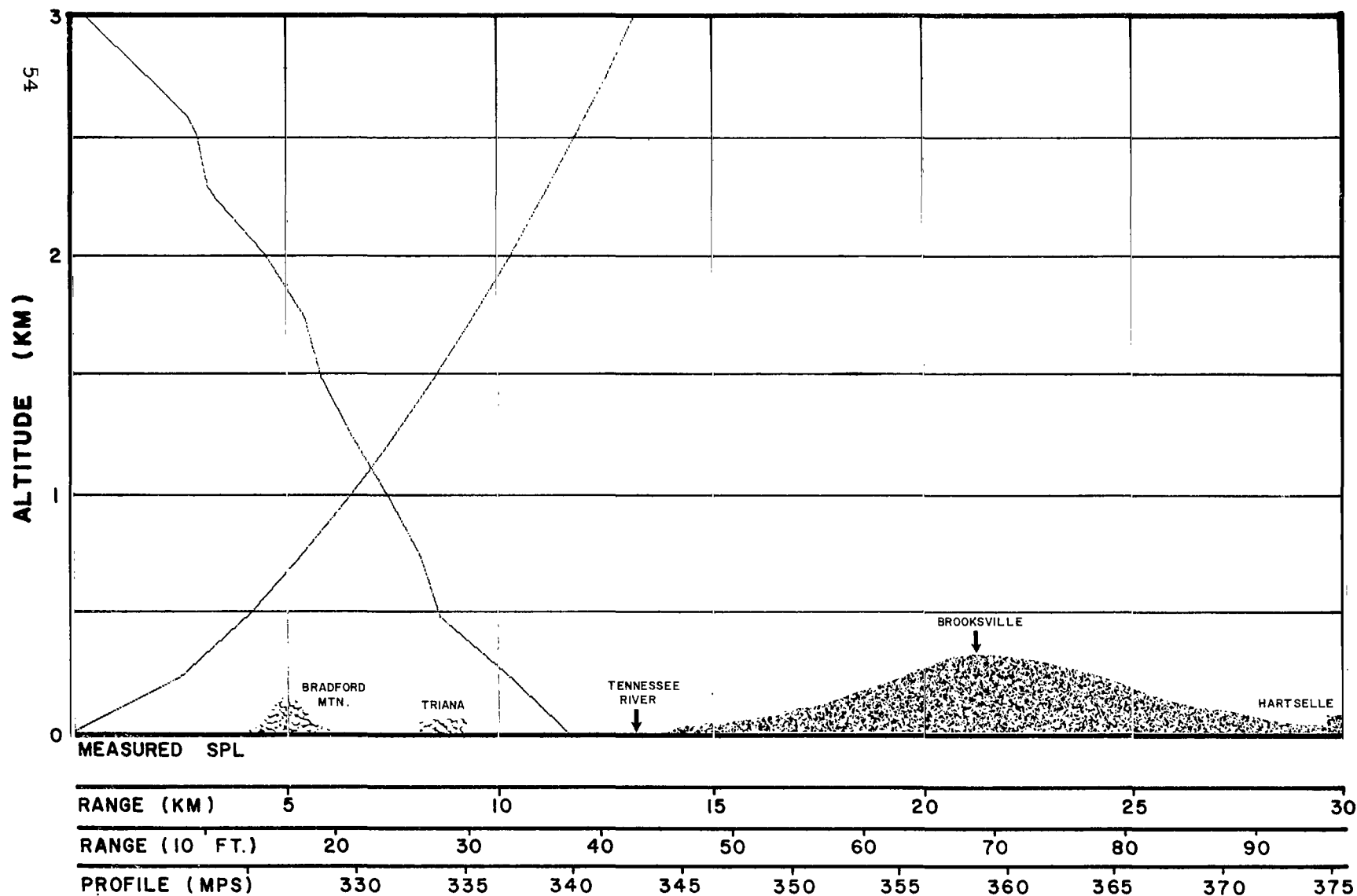


FIG. 38 CALCULATED ACOUSTIC RAY PATHS
 TRIANA, ALA., 222° AZIMUTH

DATE 3/8/63
 TIME 1300C

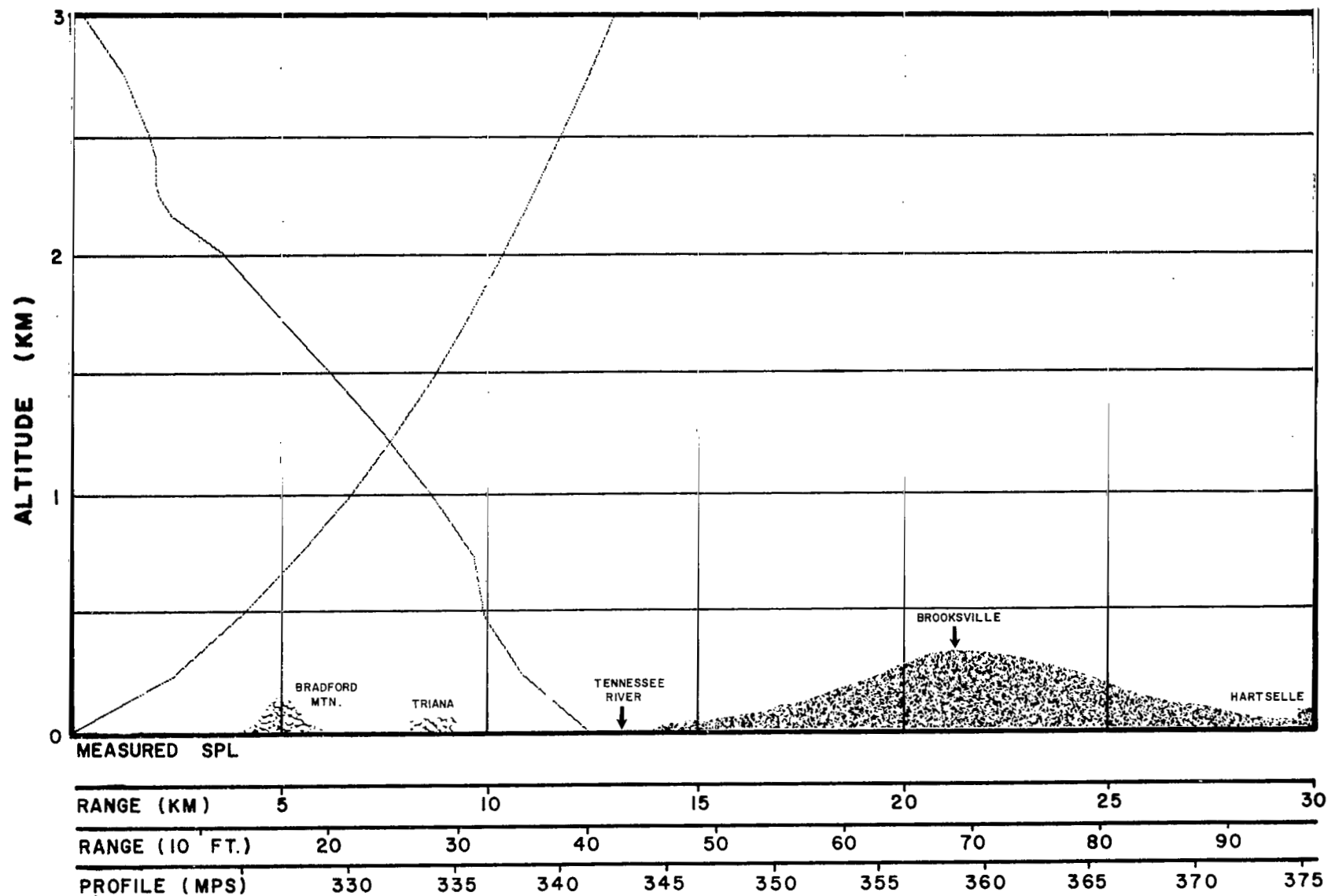


FIG. 39 CALCULATED ACOUSTIC RAY PATHS
 TRIANA, ALA., 222° AZIMUTH

DATE 3/8/63
 TIME 1455C

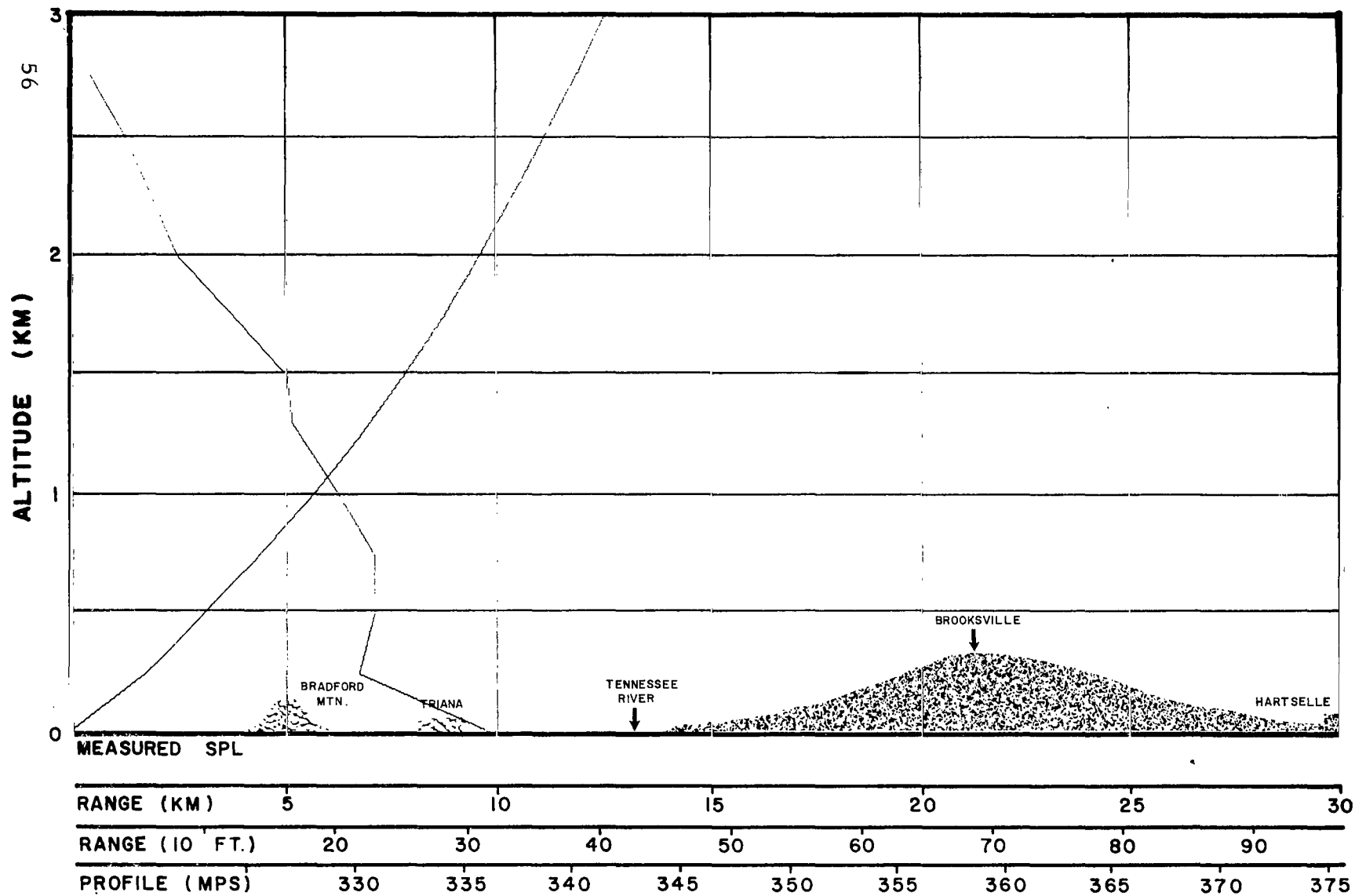


FIG. 40 CALCULATED ACOUSTIC RAY PATHS
 TRIANA, ALA., 222° AZIMUTH

DATE 3/7/63
 TIME X-1 Day Fore-
 cast

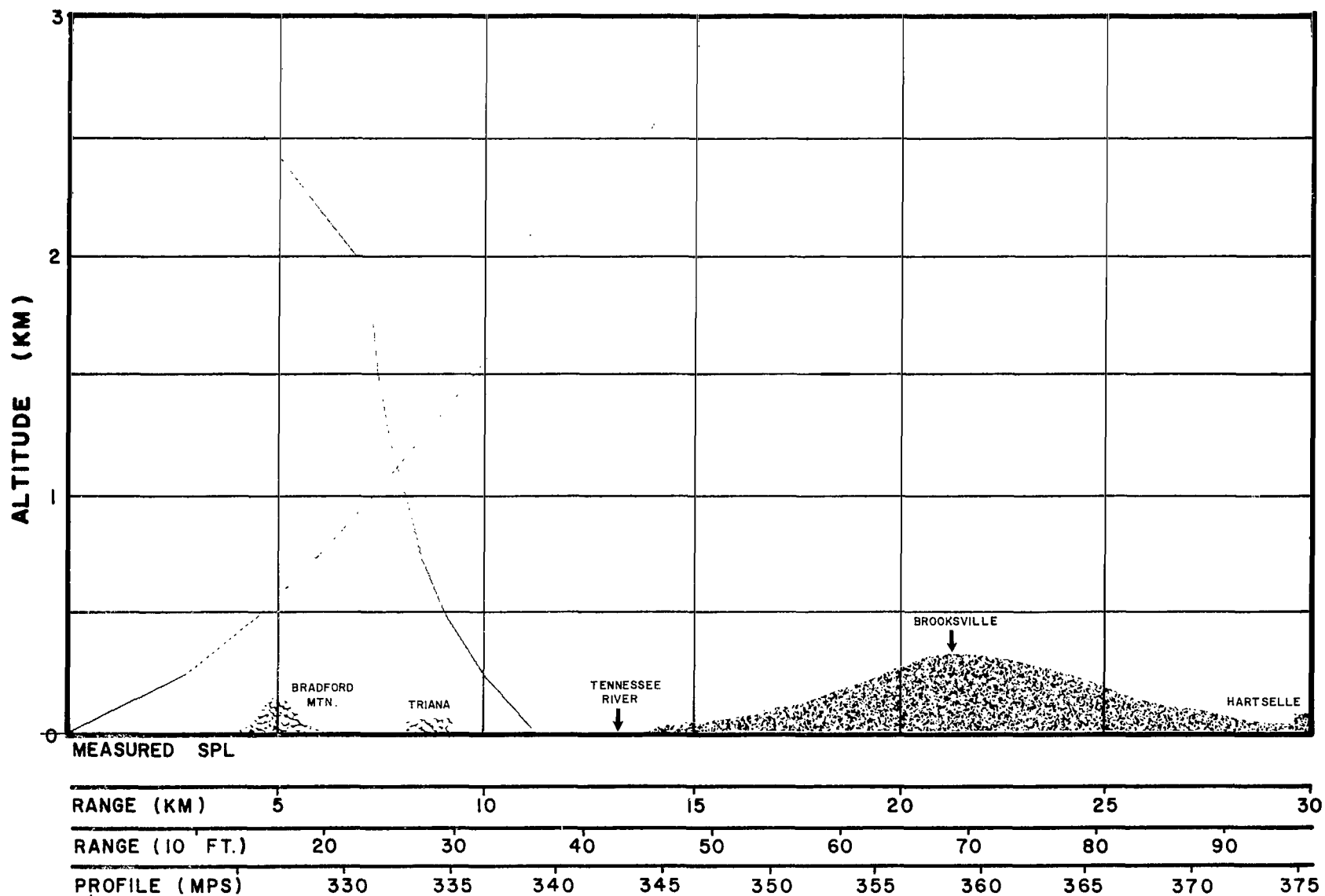


FIG.41 CALCULATED ACOUSTIC RAY PATHS
 TRIANA, ALA., 222° AZIMUTH

DATE 3/8/63
 TIME X-6 Hour Fore-
 cast

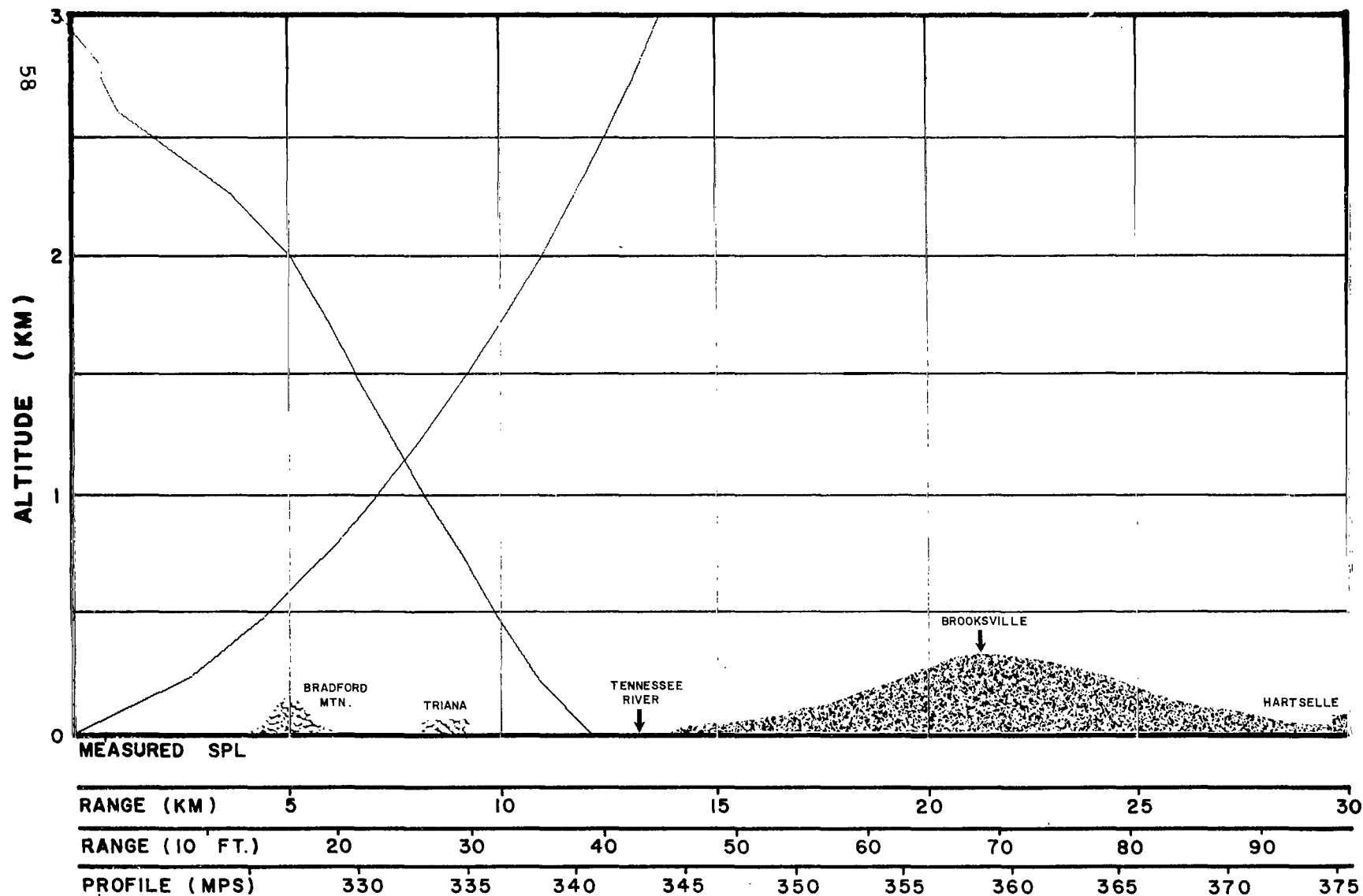


FIG.42 CALCULATED ACOUSTIC RAY PATHS
 TRIANA, ALA., 222° AZIMUTH

DATE 3/8/63
 TIME 1620C

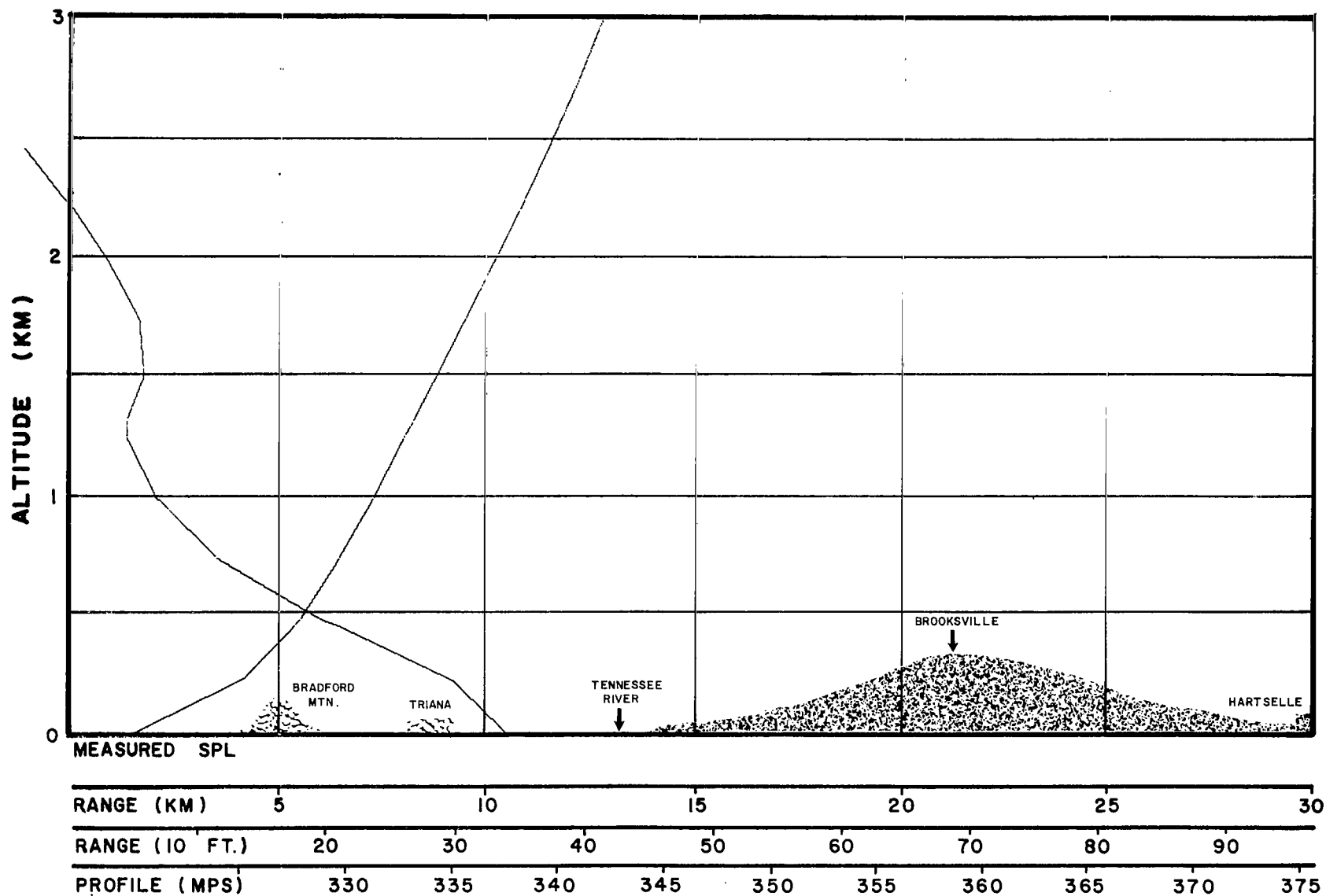


FIG.43 CALCULATED ACOUSTIC RAY PATHS
 TRIANA, ALA., 222° AZIMUTH

DATE 3/9/63
 TIME 0700C

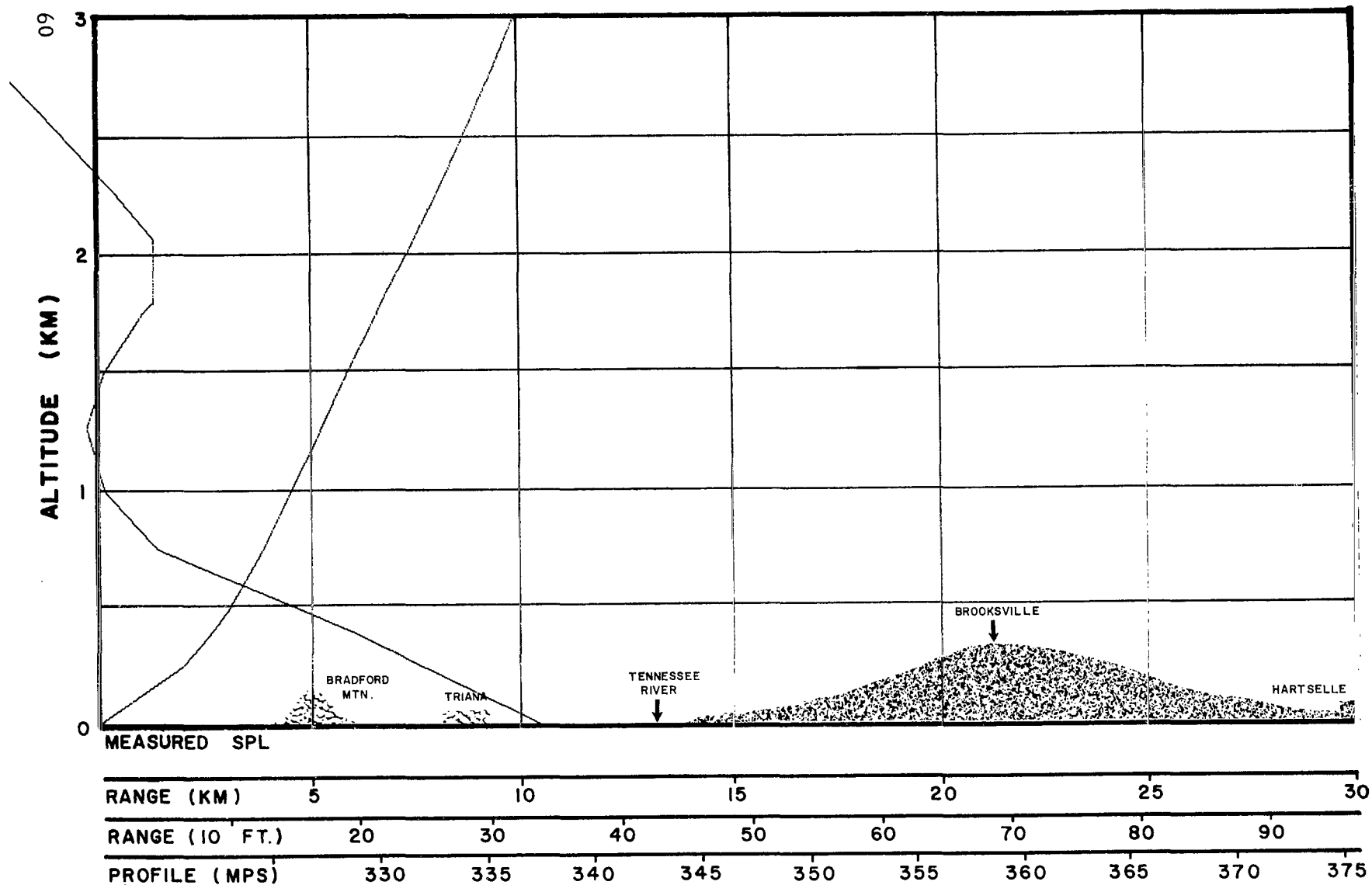


FIG. 44 CALCULATED ACOUSTIC RAY PATHS
 TRIANA, ALA., 222° AZIMUTH

DATE 3/9/63
 TIME 0900C

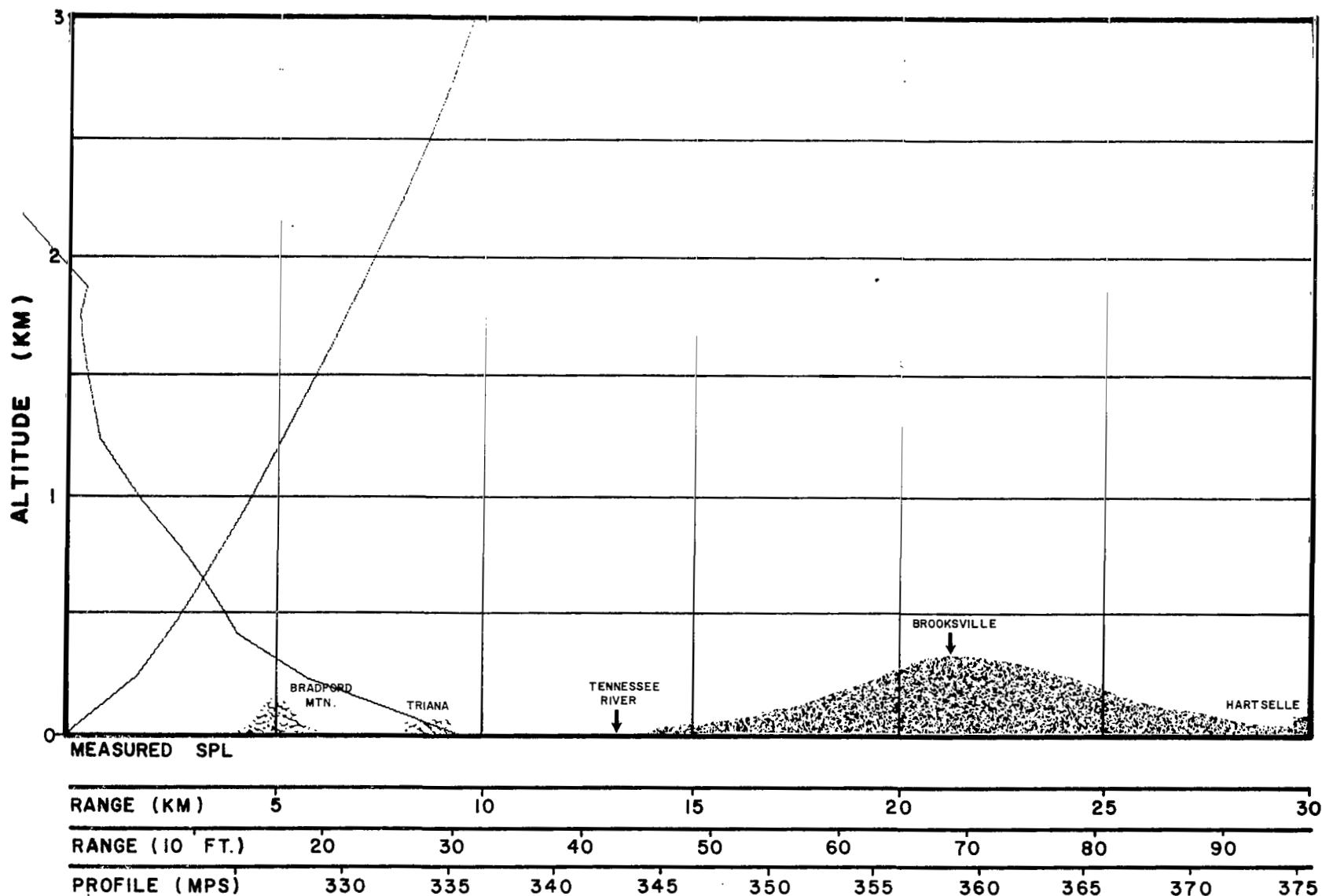


FIG. 45 CALCULATED ACOUSTIC RAY PATHS
 TRIANA, ALA., 222° AZIMUTH

DATE 3/9/63
 TIME 1045C

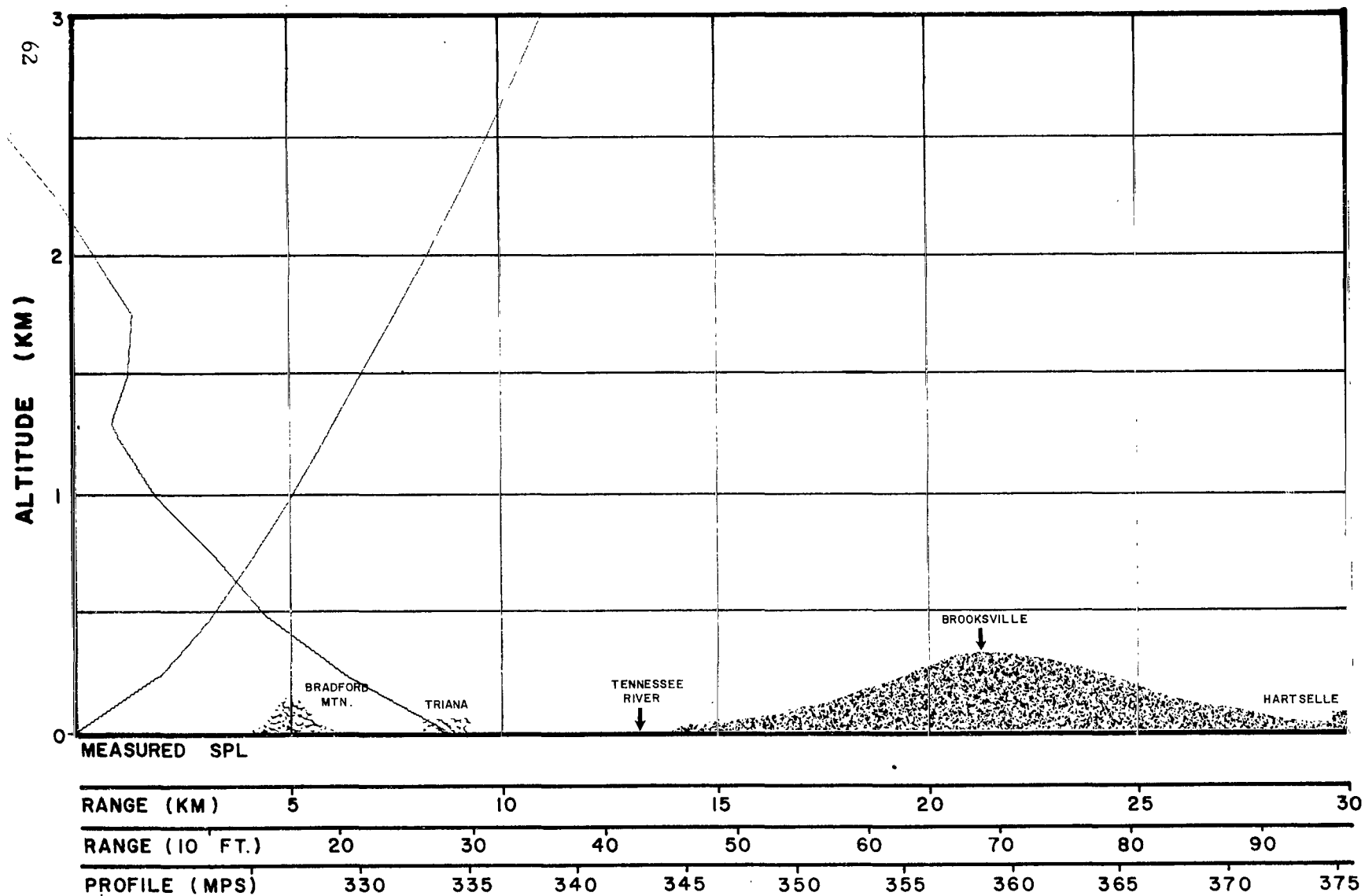


FIG. 46 CALCULATED ACOUSTIC RAY PATHS
 TRIANA, ALA., 222° AZIMUTH

DATE 3/9/63
 TIME X-6 Hour Fore-
 cast

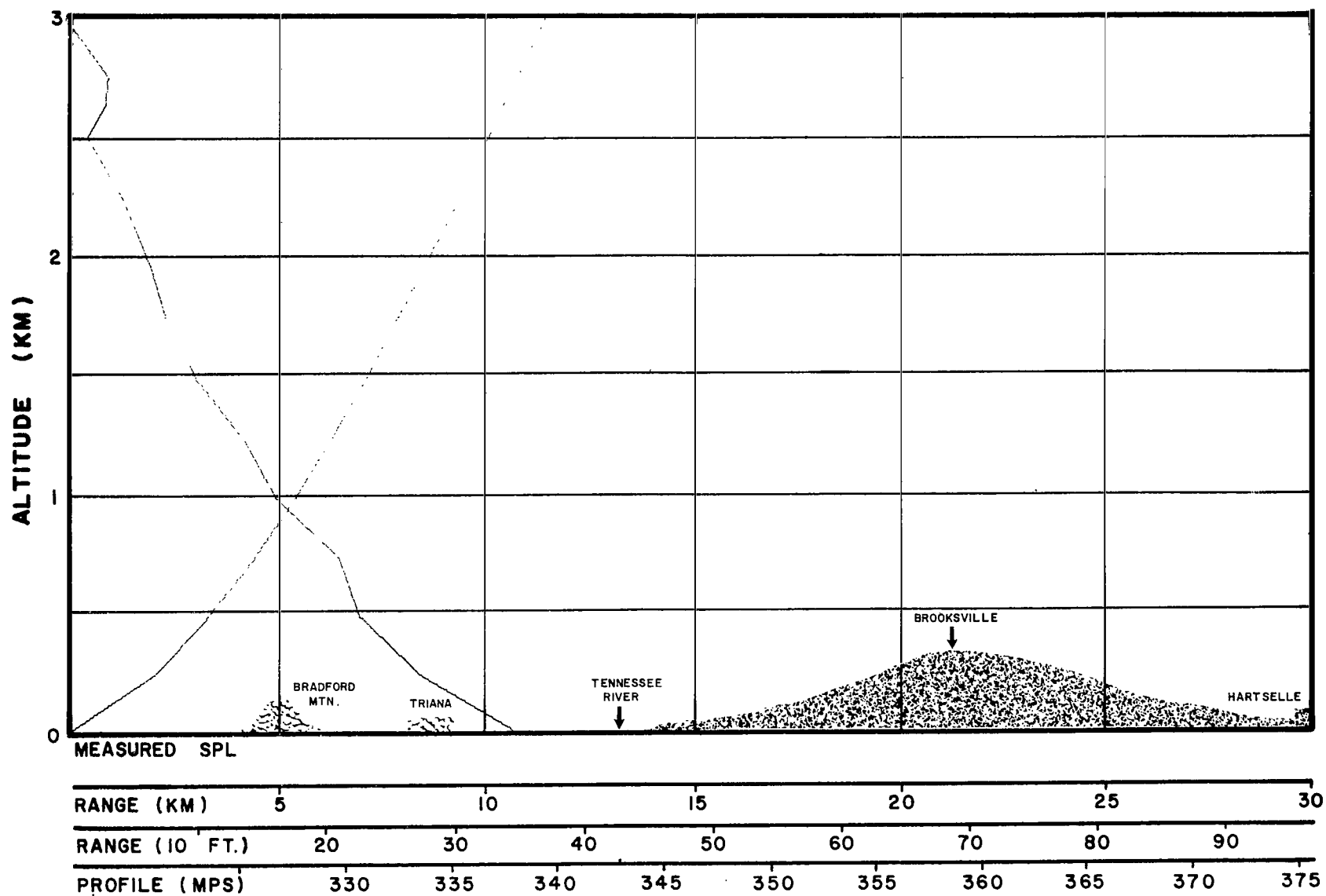


FIG. 47 CALCULATED ACOUSTIC RAY PATHS
 TRIANA, ALA., 222° AZIMUTH

DATE 3/9/63
 TIME 1620C

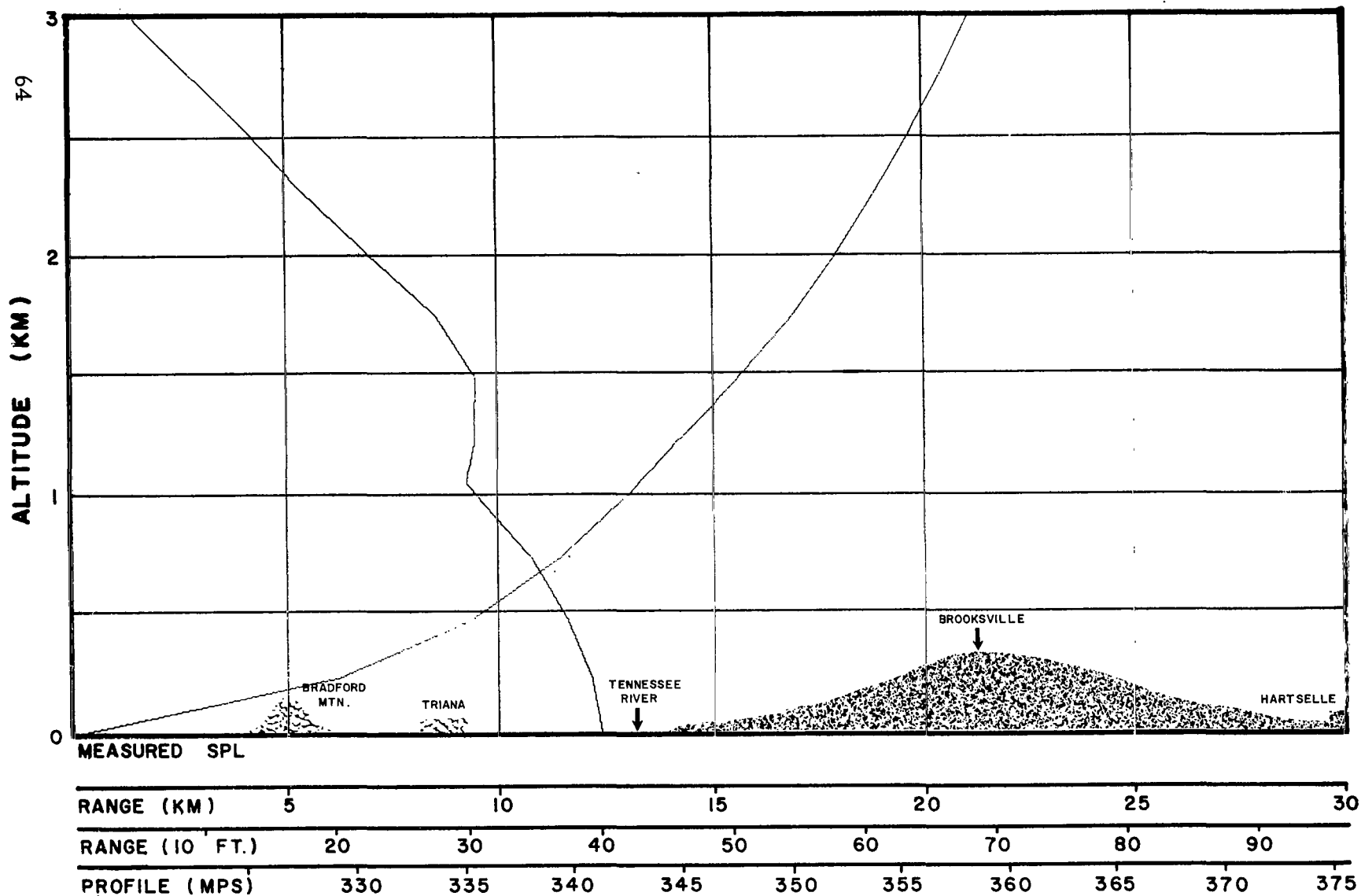


FIG. 48 CALCULATED ACOUSTIC RAY PATHS
 TRIANA, ALA., 222° AZIMUTH

DATE 3/10/63
 TIME 1600C

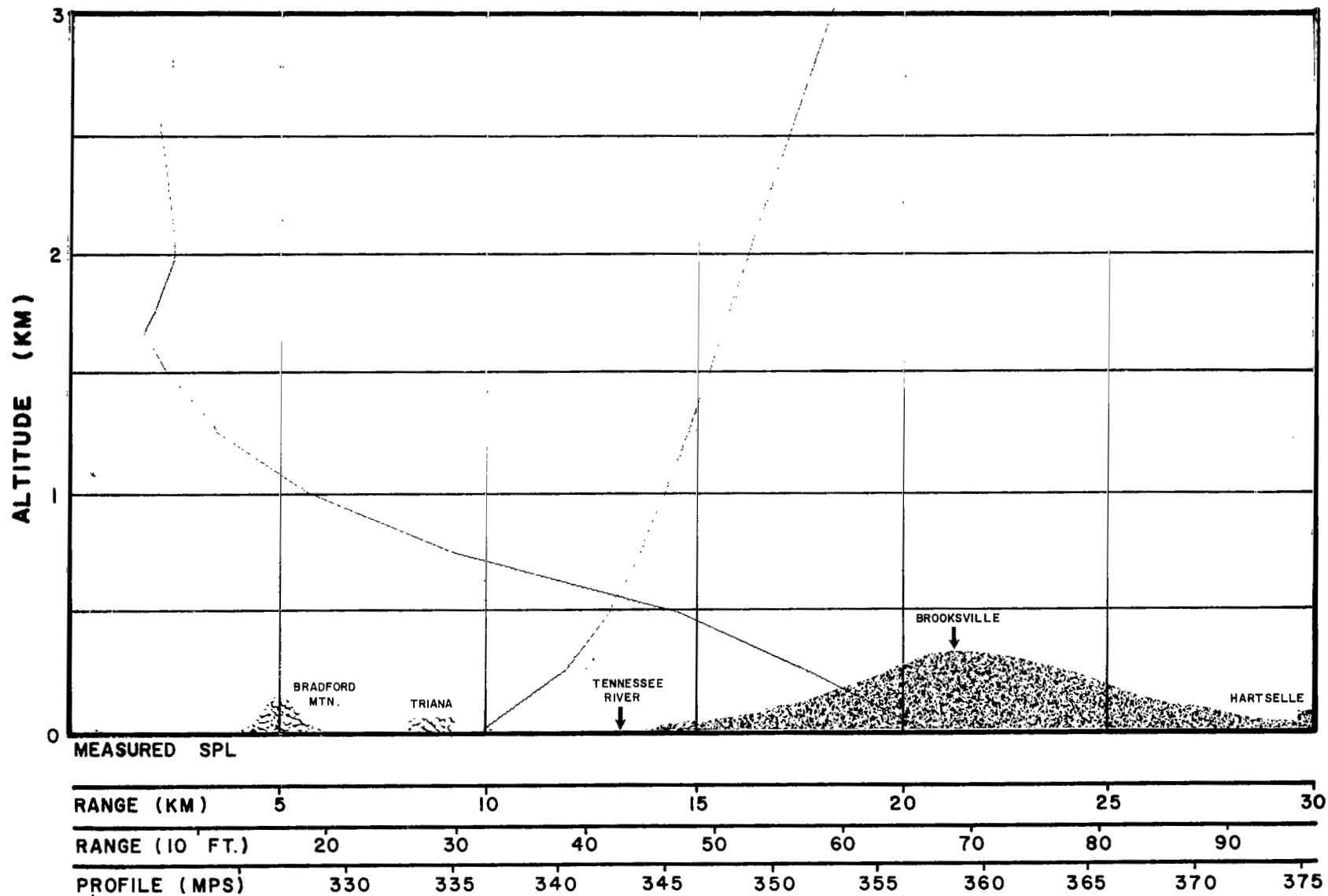


FIG. 49 CALCULATED ACOUSTIC RAY PATHS
 TRIANA, ALA., 222° AZIMUTH

DATE 3/11/63
 TIME 0700C

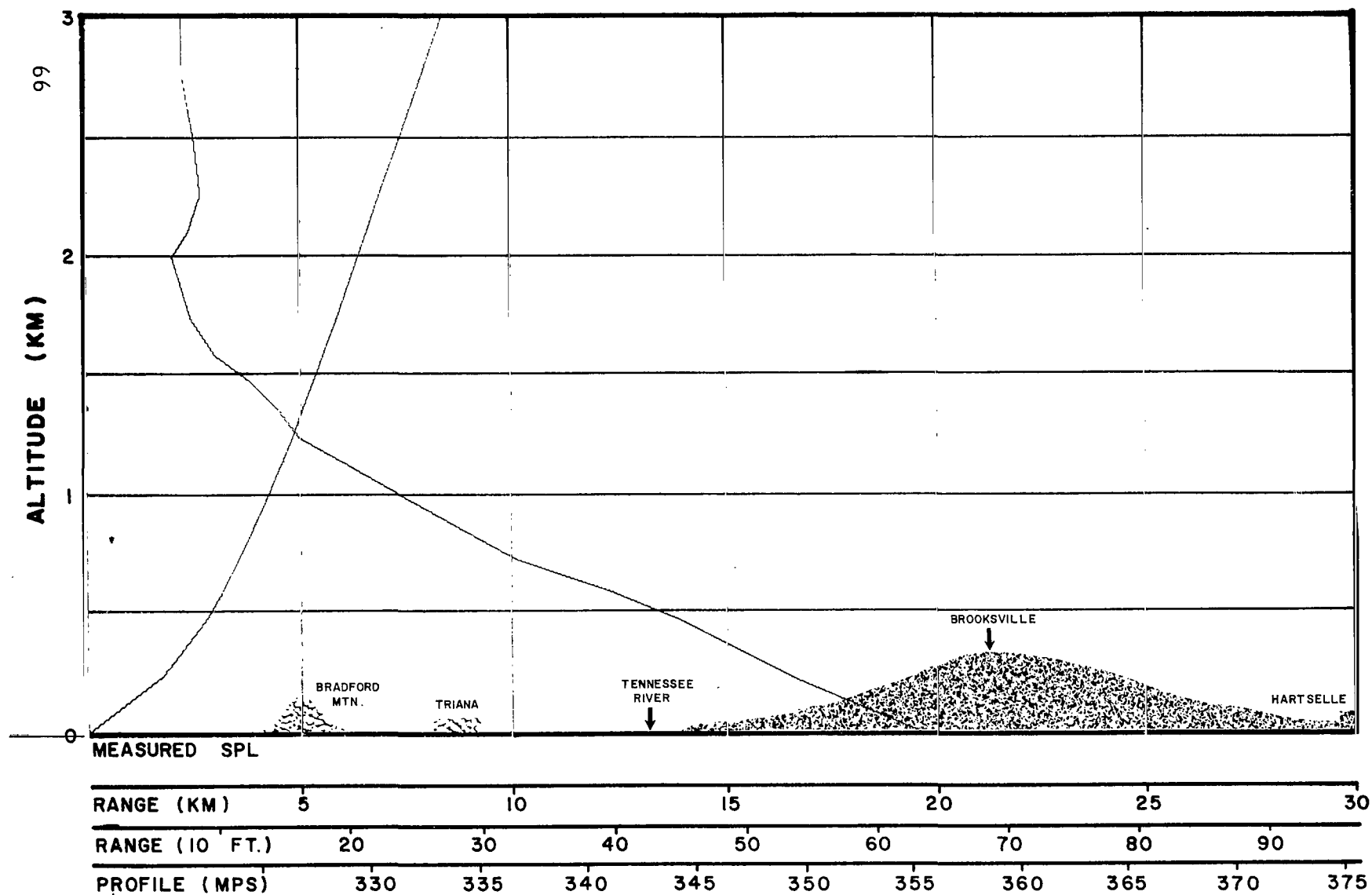


FIG. 50 CALCULATED ACOUSTIC RAY PATHS
 TRIANA, ALA., 222° AZIMUTH

DATE 3/11/63
 TIME 0800C

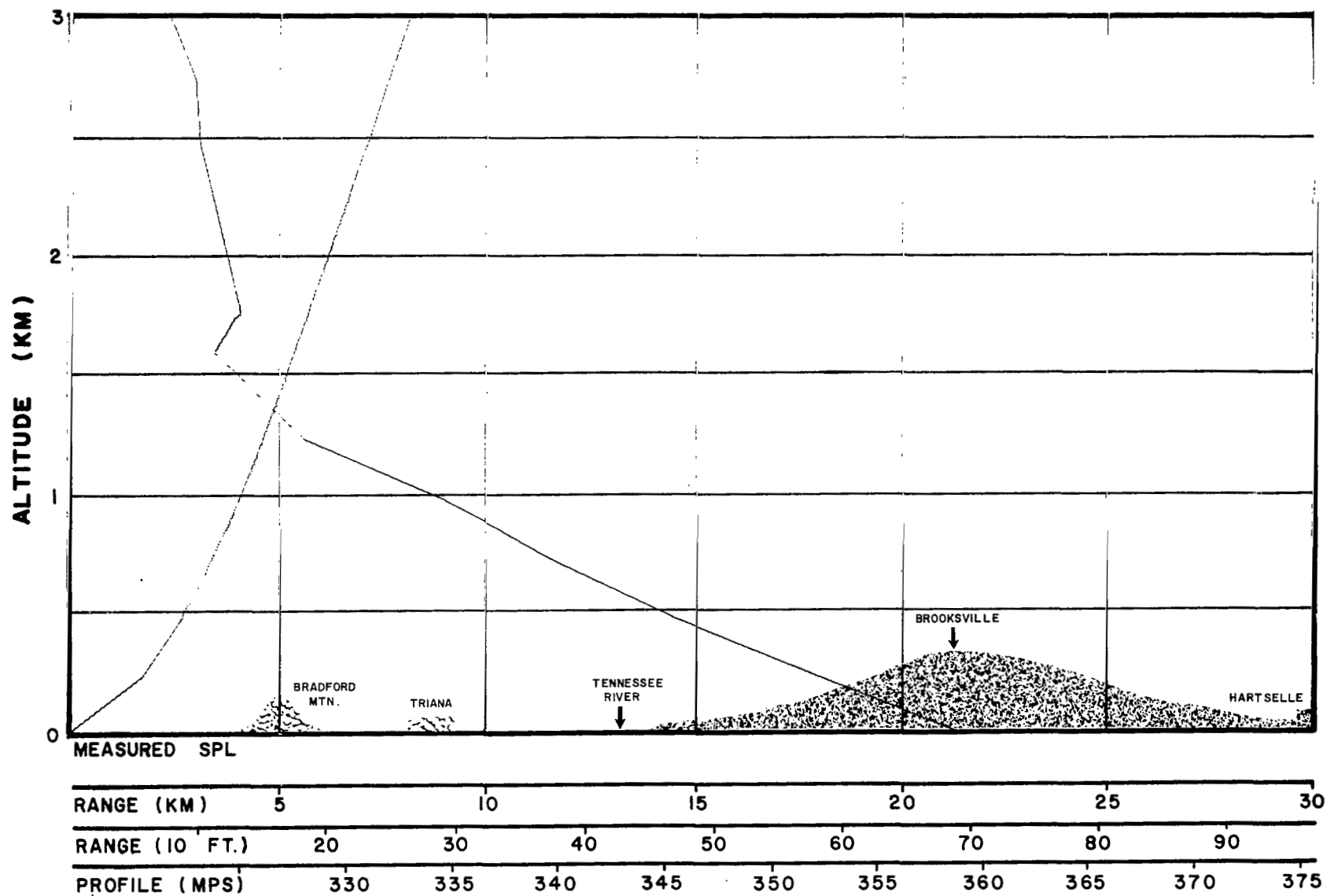


FIG.5I CALCULATED ACOUSTIC RAY PATHS
 TRIANA, ALA., 222° AZIMUTH

DATE 3/11/63
 TIME 1000C

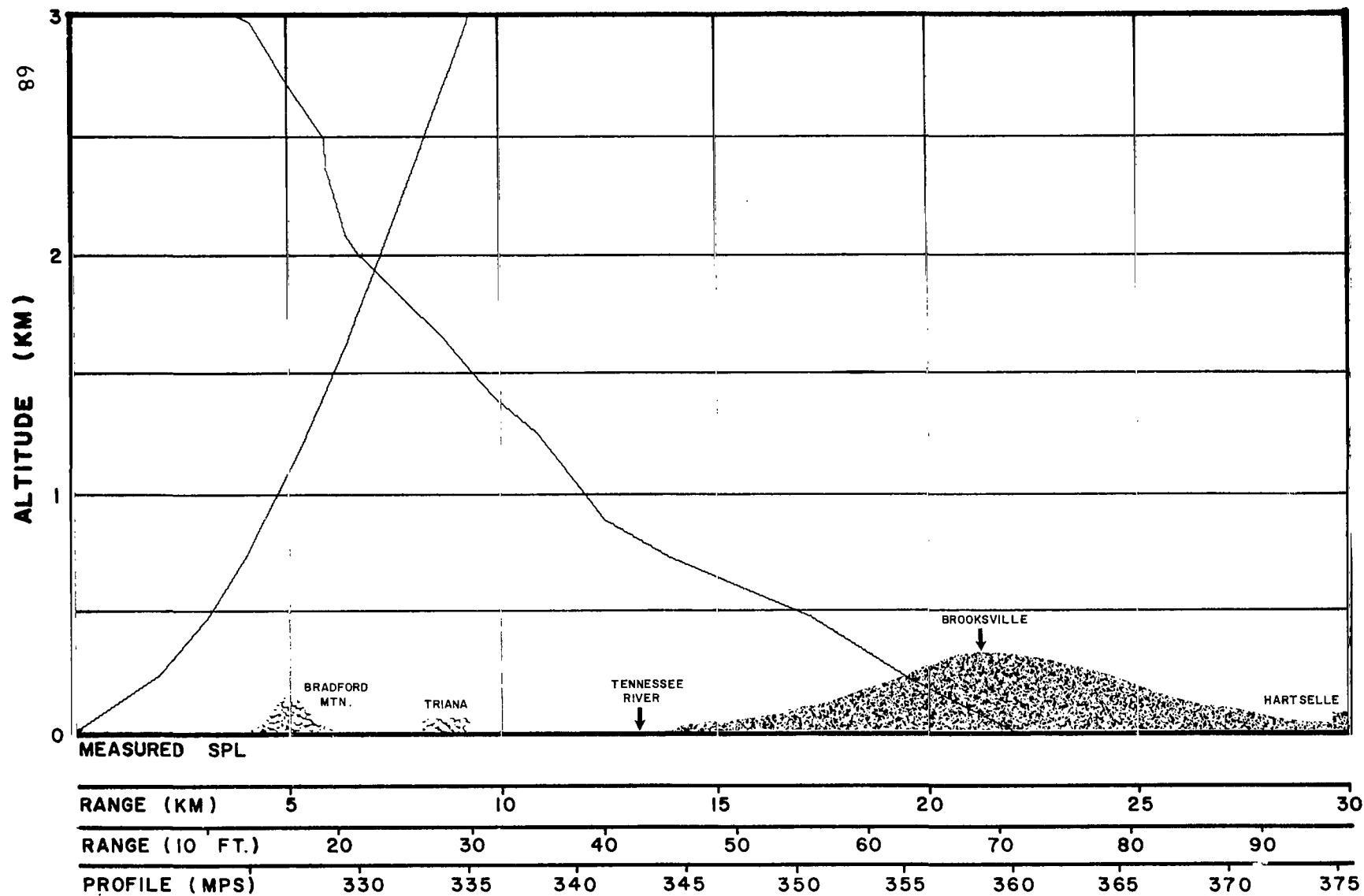


FIG.52 CALCULATED ACOUSTIC RAY PATHS
 TRIANA, ALA., 222° AZIMUTH

DATE 3/11/63
 TIME 1335C

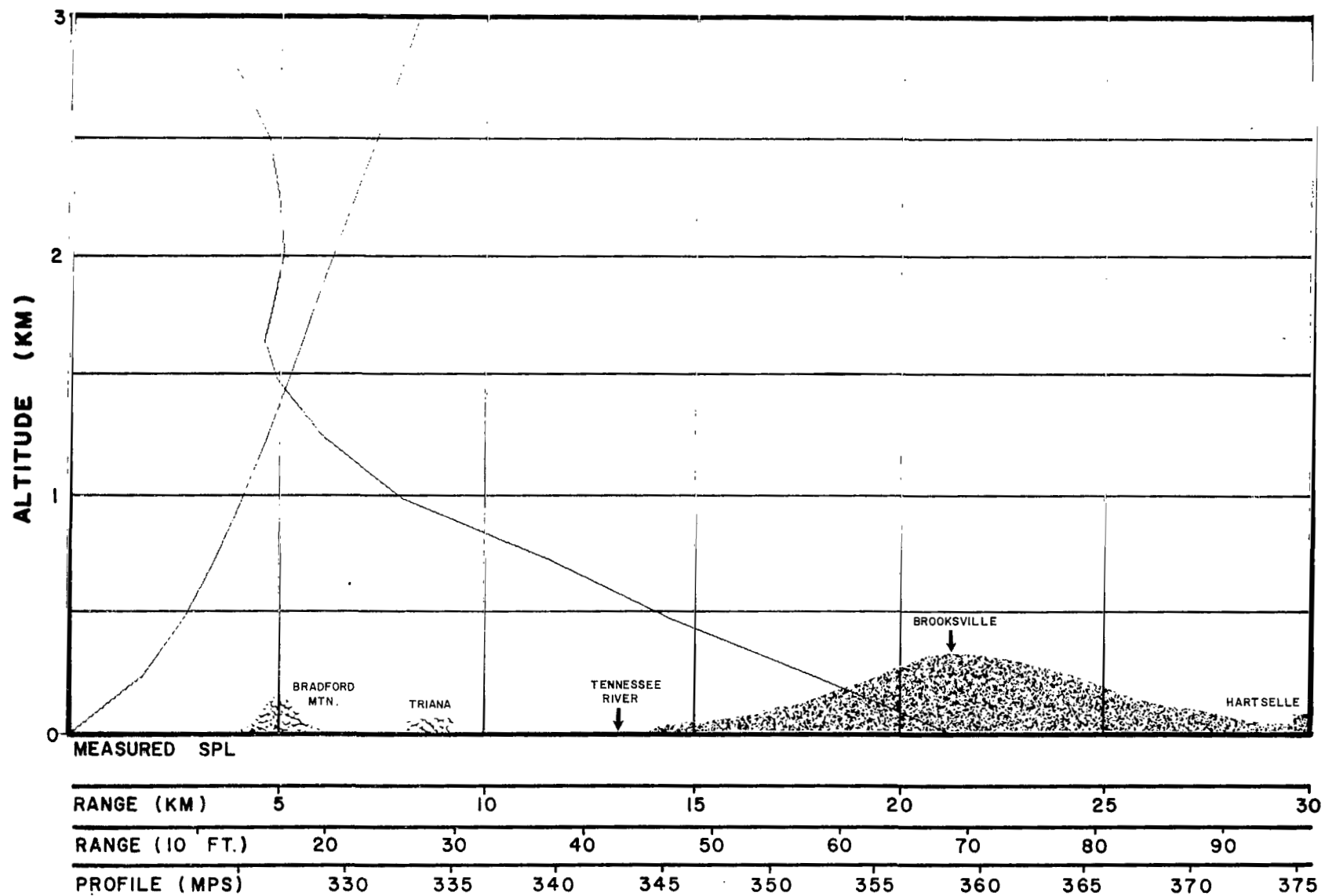


FIG. 53 CALCULATED ACOUSTIC RAY PATHS
 TRIANA, ALA., 222° AZIMUTH

DATE 3/11/63
 TIME X-6 Hour Fore-
 cast

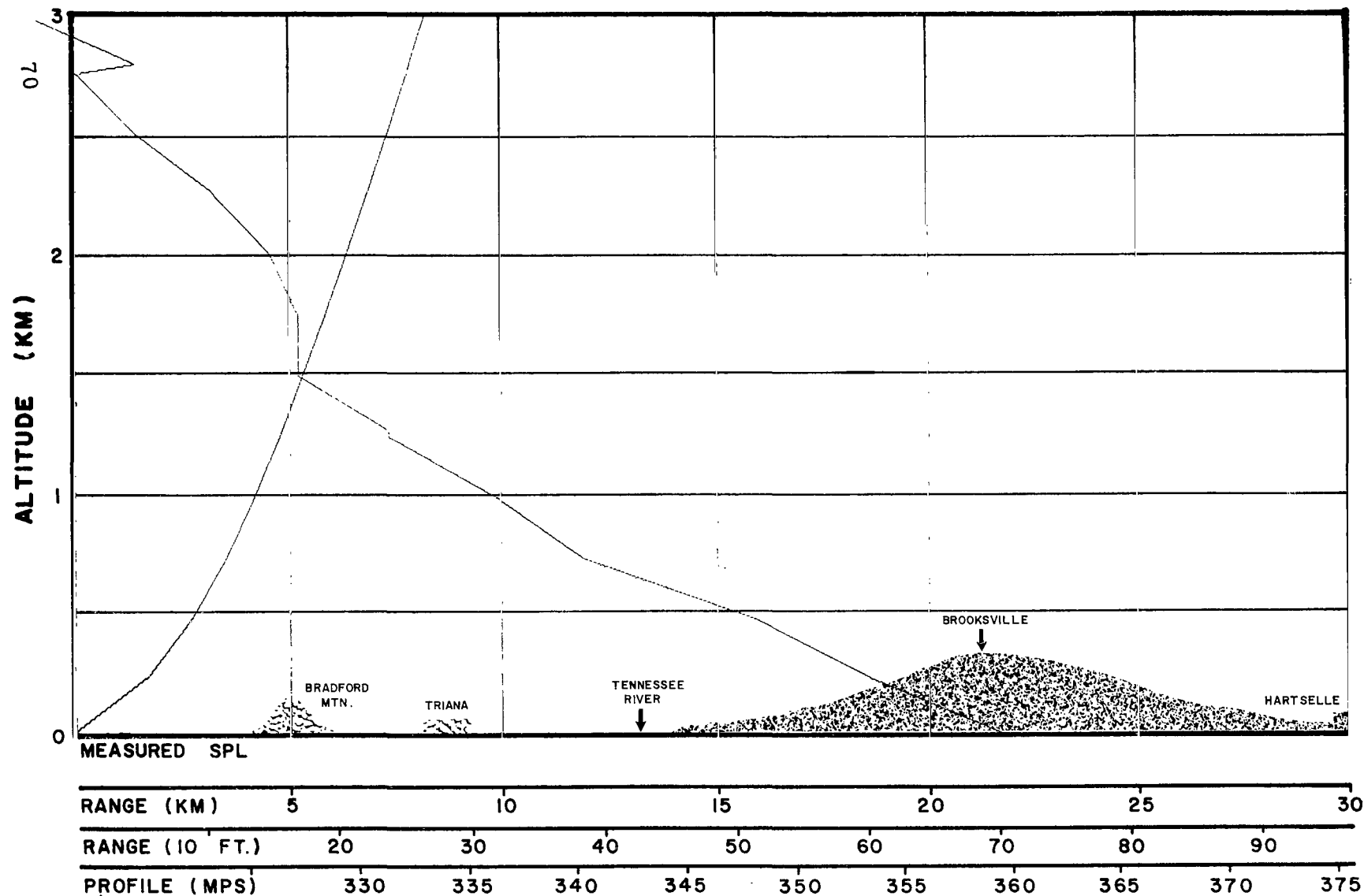


FIG. 54 CALCULATED ACOUSTIC RAY PATHS
 TRIANA, ALA., 222° AZIMUTH

DATE 3/11/63
 TIME 1615G

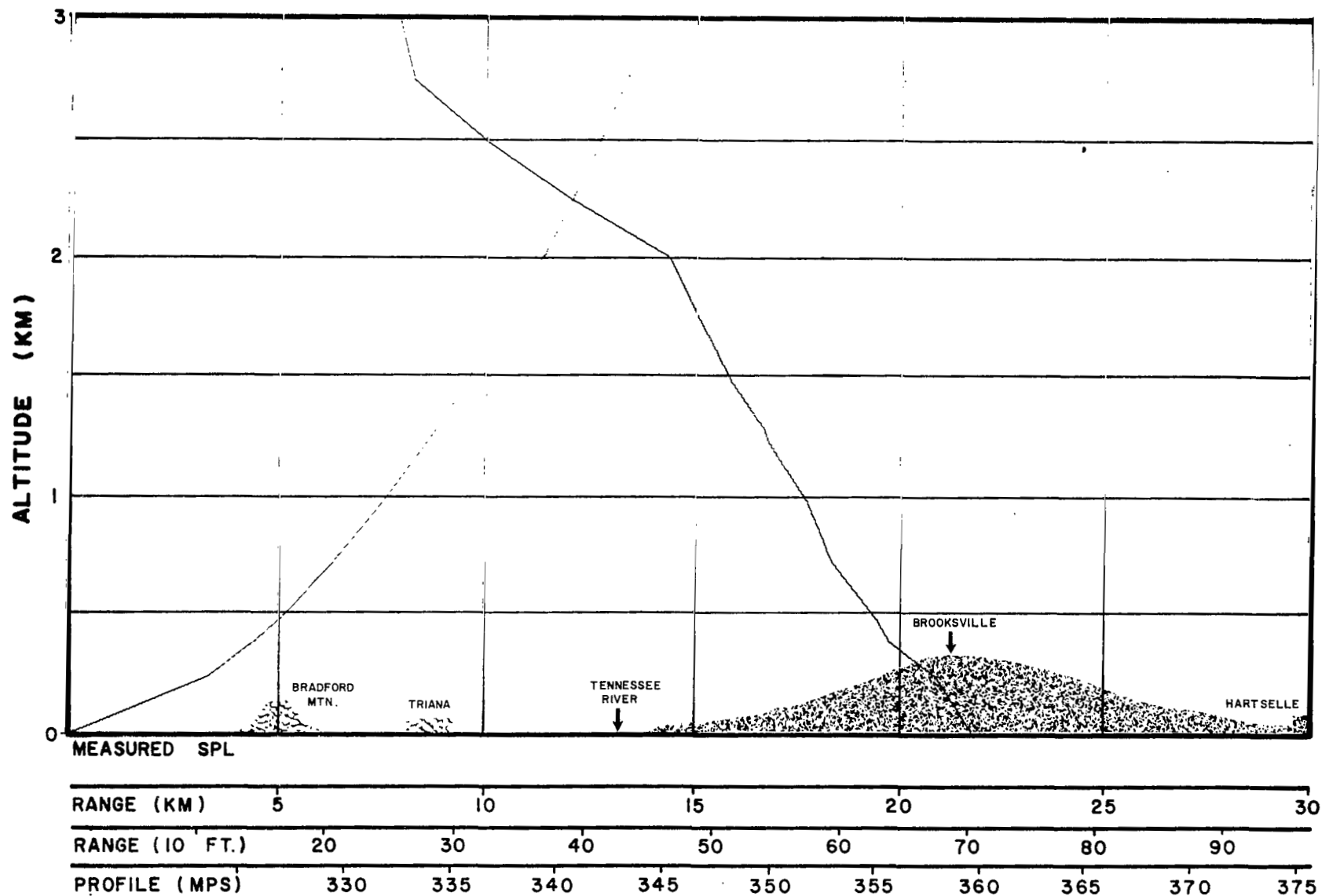


FIG.55 CALCULATED ACOUSTIC RAY PATHS
 TRIANA, ALA., 222° AZIMUTH

DATE 3/12/63
 TIME 1000C

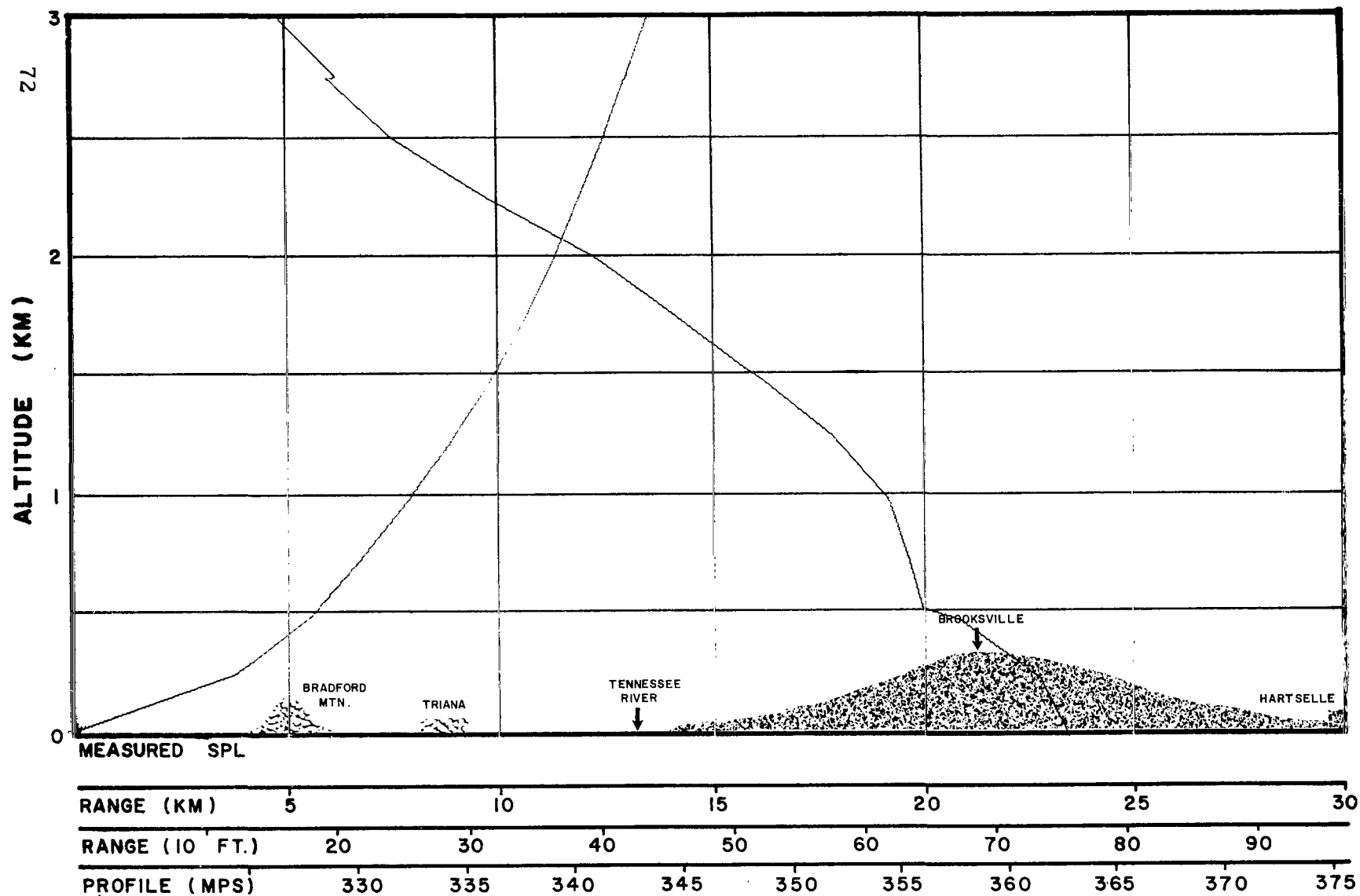


FIG. 56 CALCULATED ACOUSTIC RAY PATHS
 TRIANA, ALA., 222° AZIMUTH

DATE 3/12/63
 TIME 1400C

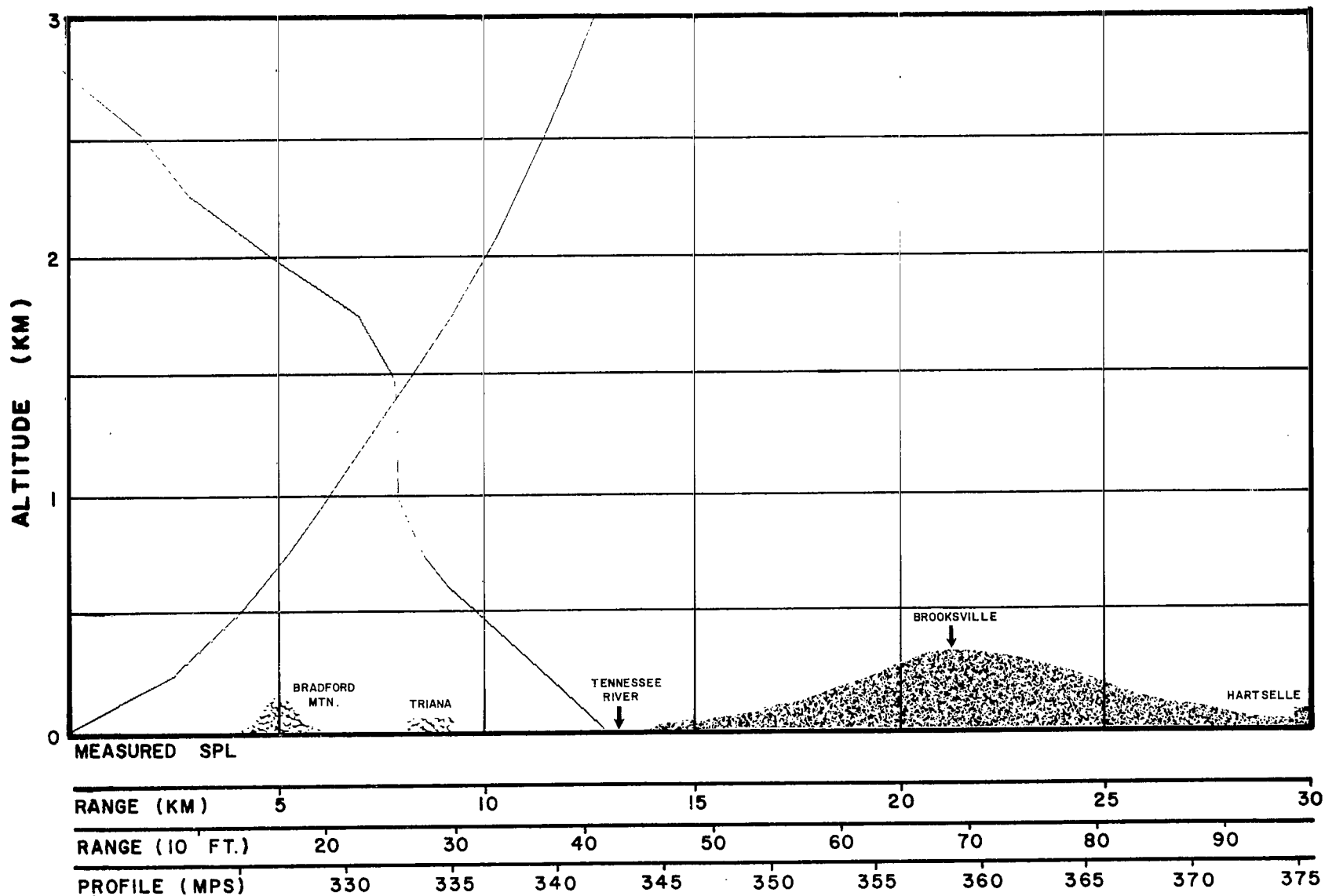


FIG. 57 CALCULATED ACOUSTIC RAY PATHS
 TRIANA, ALA., 222° AZIMUTH

DATE 3/12/63
 TIME 1630C

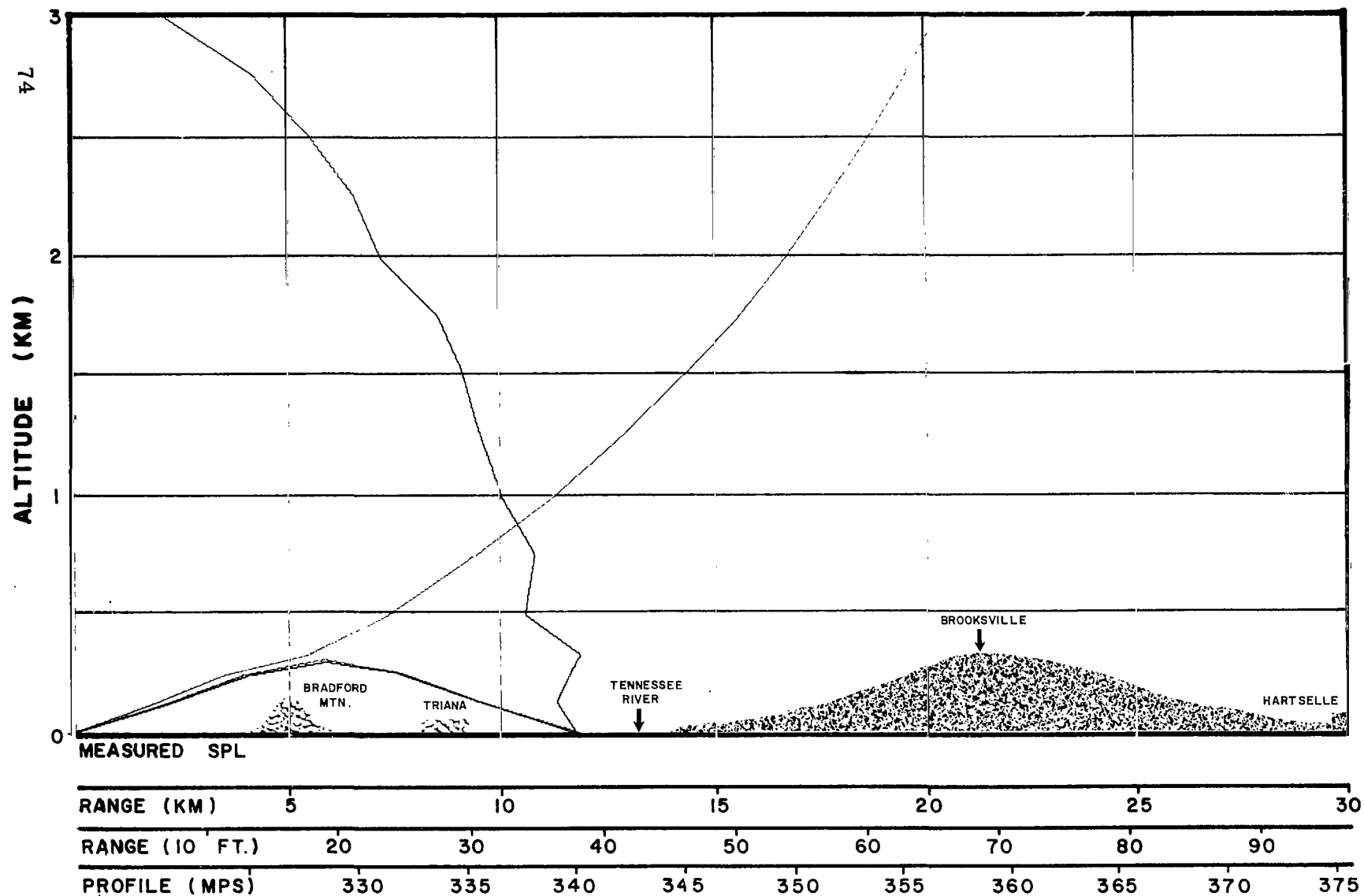


FIG. 58 CALCULATED ACOUSTIC RAY PATHS
 TRIANA, ALA., 222° AZIMUTH

DATE 3/13/63
 TIME 0700C

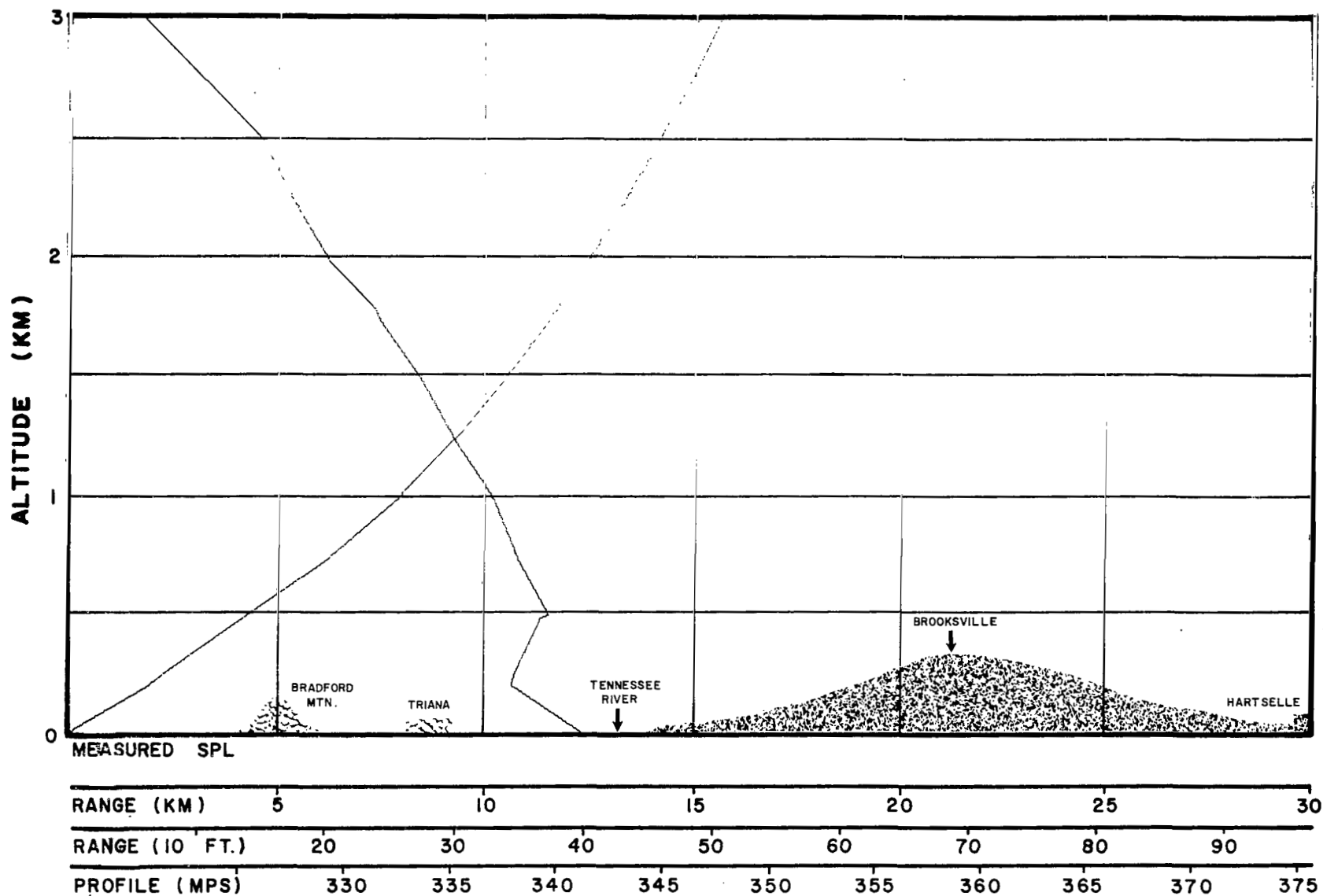


FIG. 59 CALCULATED ACOUSTIC RAY PATHS
 TRIANA, ALA., 222° AZIMUTH

DATE 3/13/63
 TIME 0820C

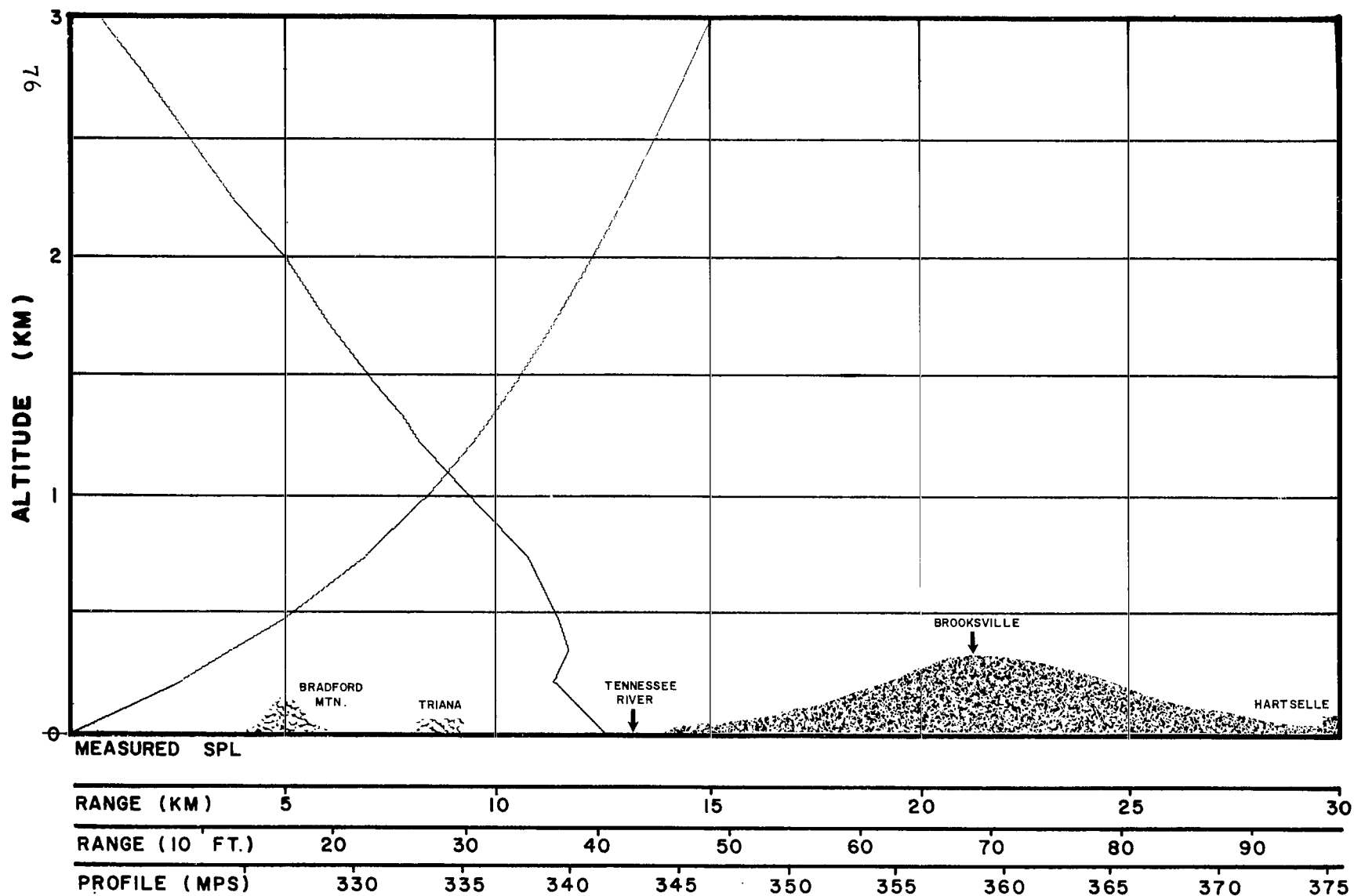


FIG. 60 CALCULATED ACOUSTIC RAY PATHS
 TRIANA, ALA., 222° AZIMUTH

DATE 3/13/63
 TIME 1005G

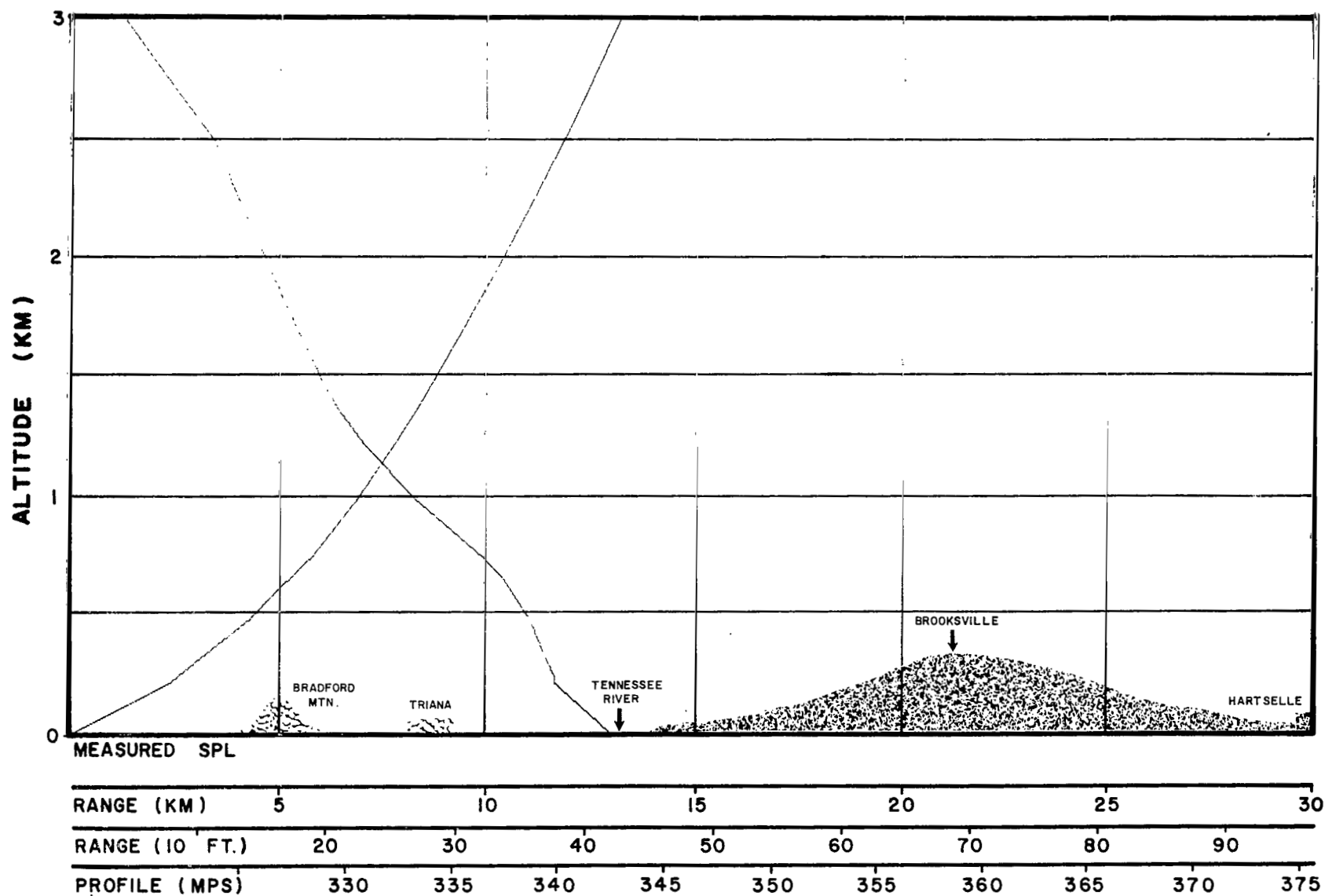


FIG. 61 CALCULATED ACOUSTIC RAY PATHS
 TRIANA, ALA., 222° AZIMUTH

DATE 3/13/63
 TIME 1055C

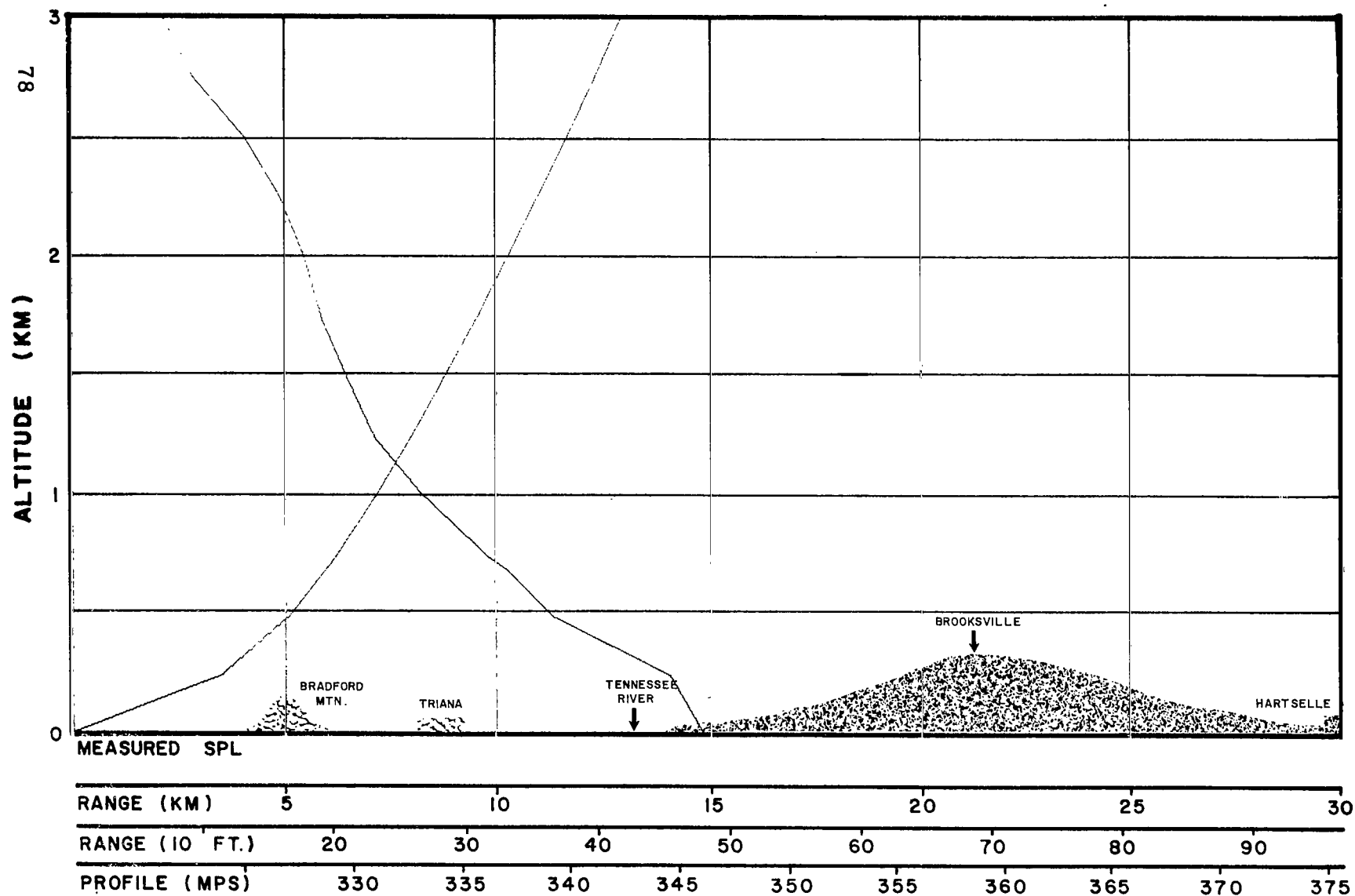


FIG. 62 CALCULATED ACOUSTIC RAY PATHS
 TRIANA, ALA., 222° AZIMUTH

DATE 3/13/63
 TIME 1300C

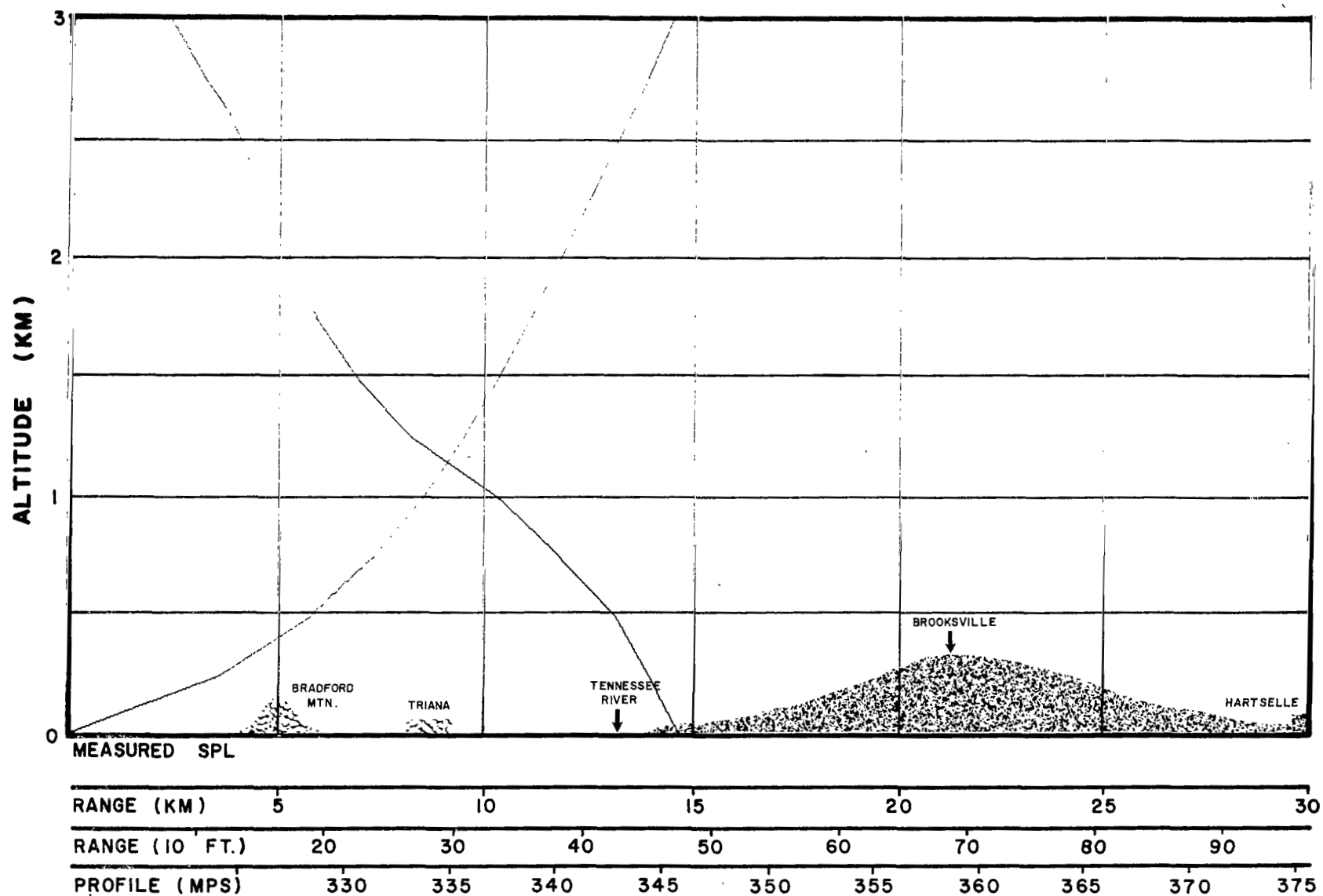


FIG. 63 CALCULATED ACOUSTIC RAY PATHS
 TRIANA, ALA., 222° AZIMUTH

DATE 3/13/63
 TIME 1400C

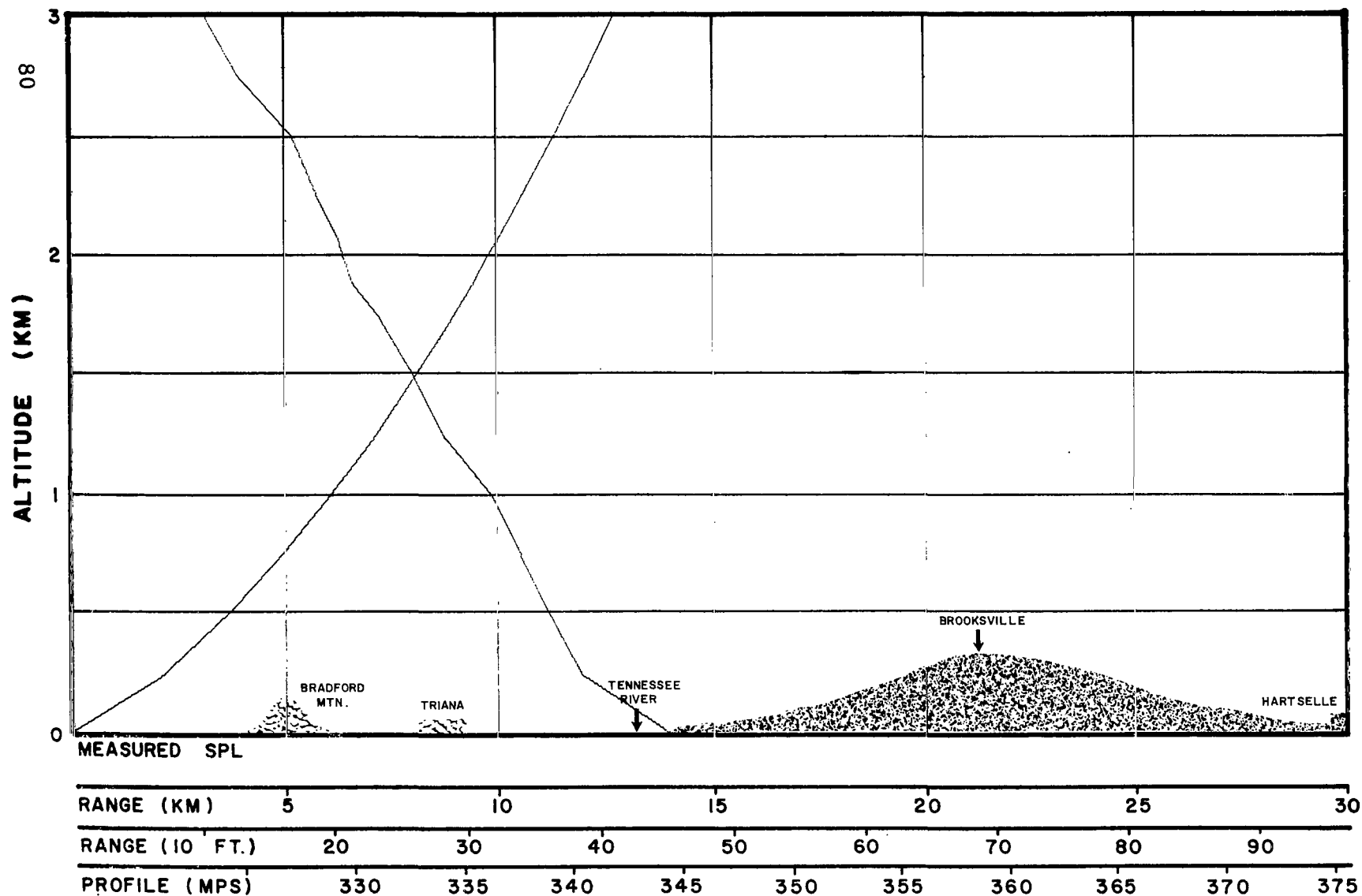


FIG. 64 CALCULATED ACOUSTIC RAY PATHS
 TRIANA, ALA., 222° AZIMUTH

DATE 3/13/63
 TIME 1500C

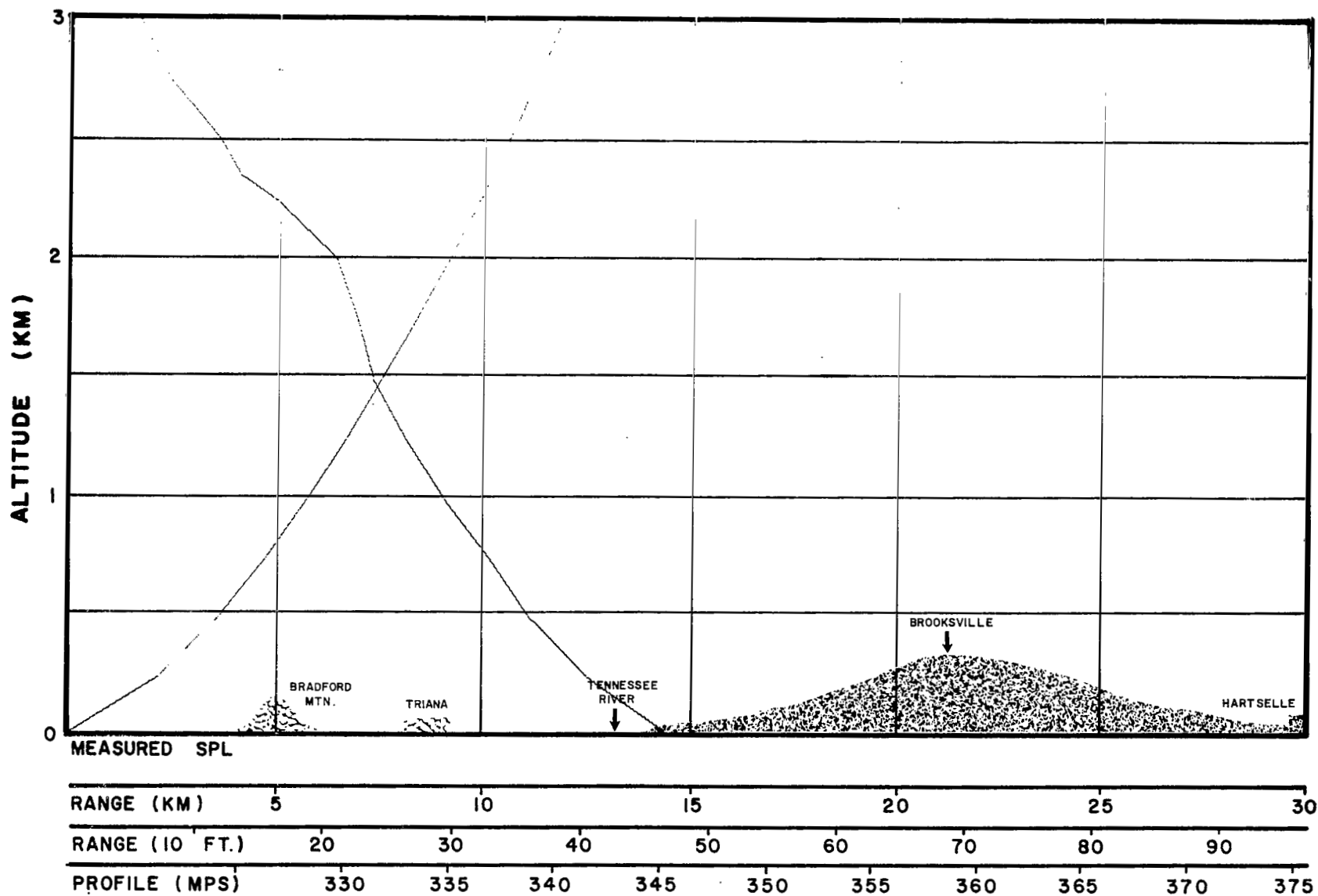


FIG.65 CALCULATED ACOUSTIC RAY PATHS
 TRIANA, ALA., 222° AZIMUTH

DATE 3/13/63
 TIME 1615C

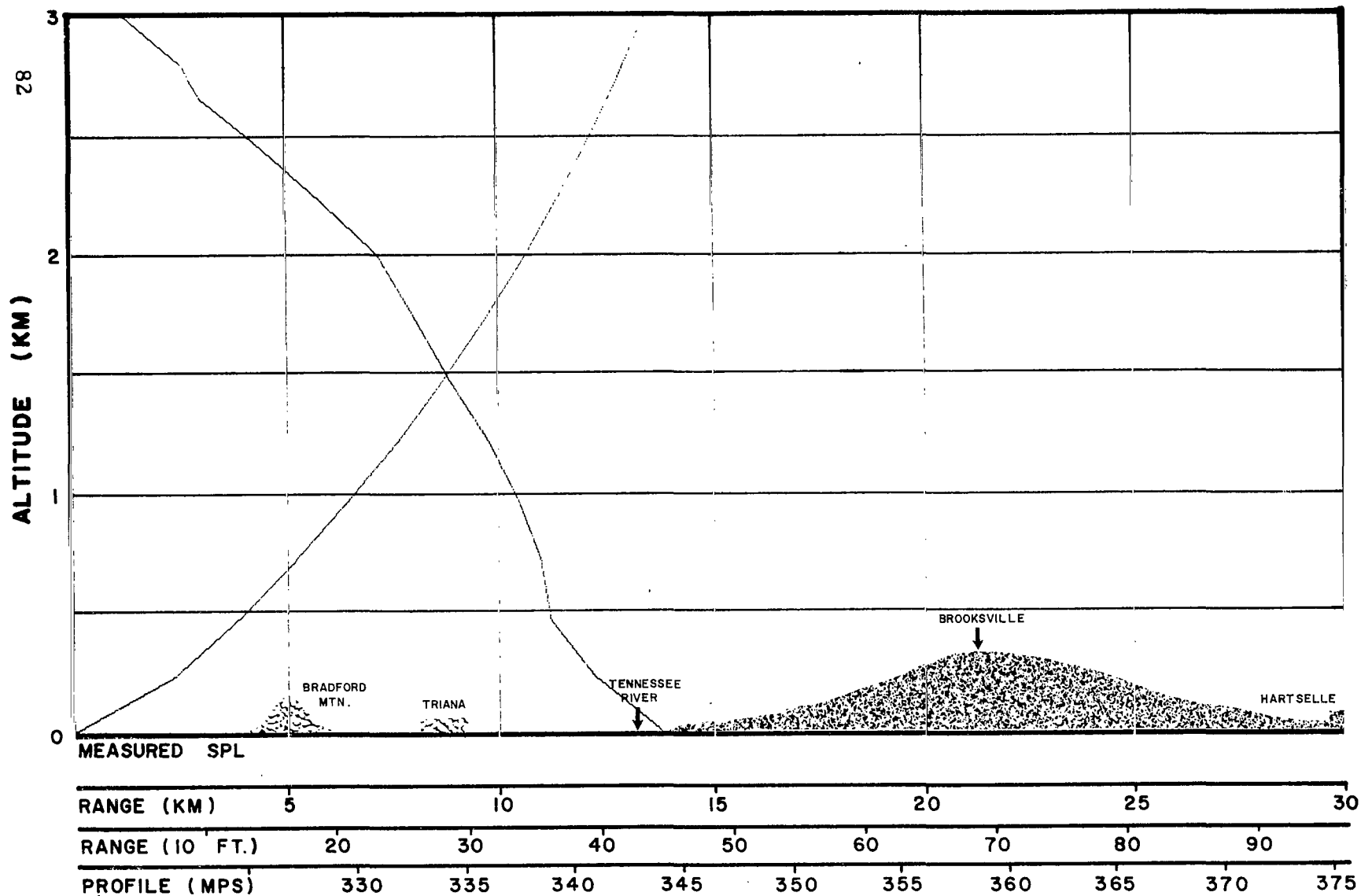


FIG.66 CALCULATED ACOUSTIC RAY PATHS
 TRIANA, ALA., 222° AZIMUTH

DATE 3/13/63
 TIME 1700C

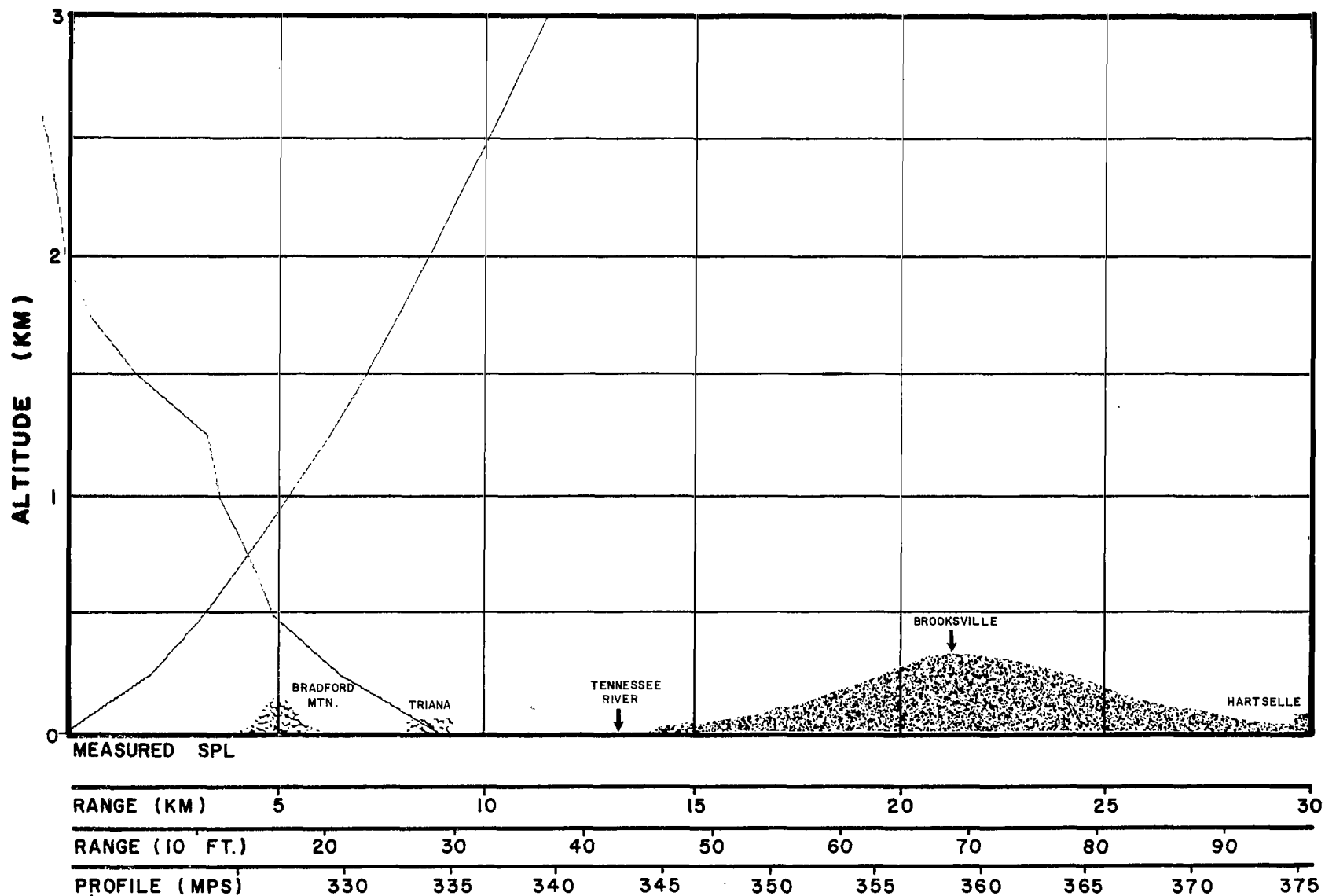


FIG.67 CALCULATED ACOUSTIC RAY PATHS
 TRIANA, ALA., 222° AZIMUTH

DATE 3/12/63
 TIME X-1 Day Fore-
 cast

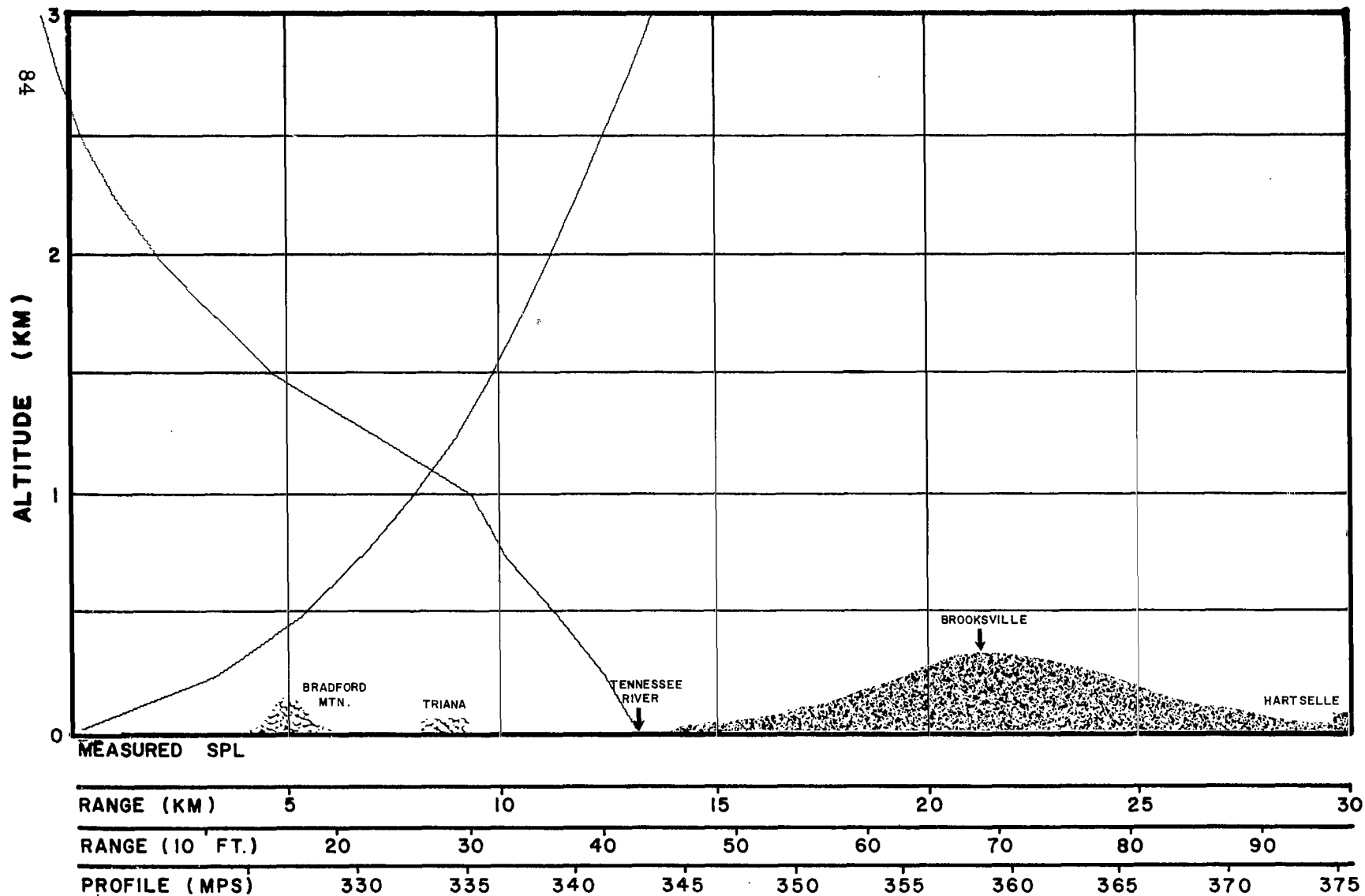


FIG.68 CALCULATED ACOUSTIC RAY PATHS
 TRIANA, ALA., 222° AZIMUTH

DATE 3/13/63
 TIME X-6 Hour Fore-
 cast

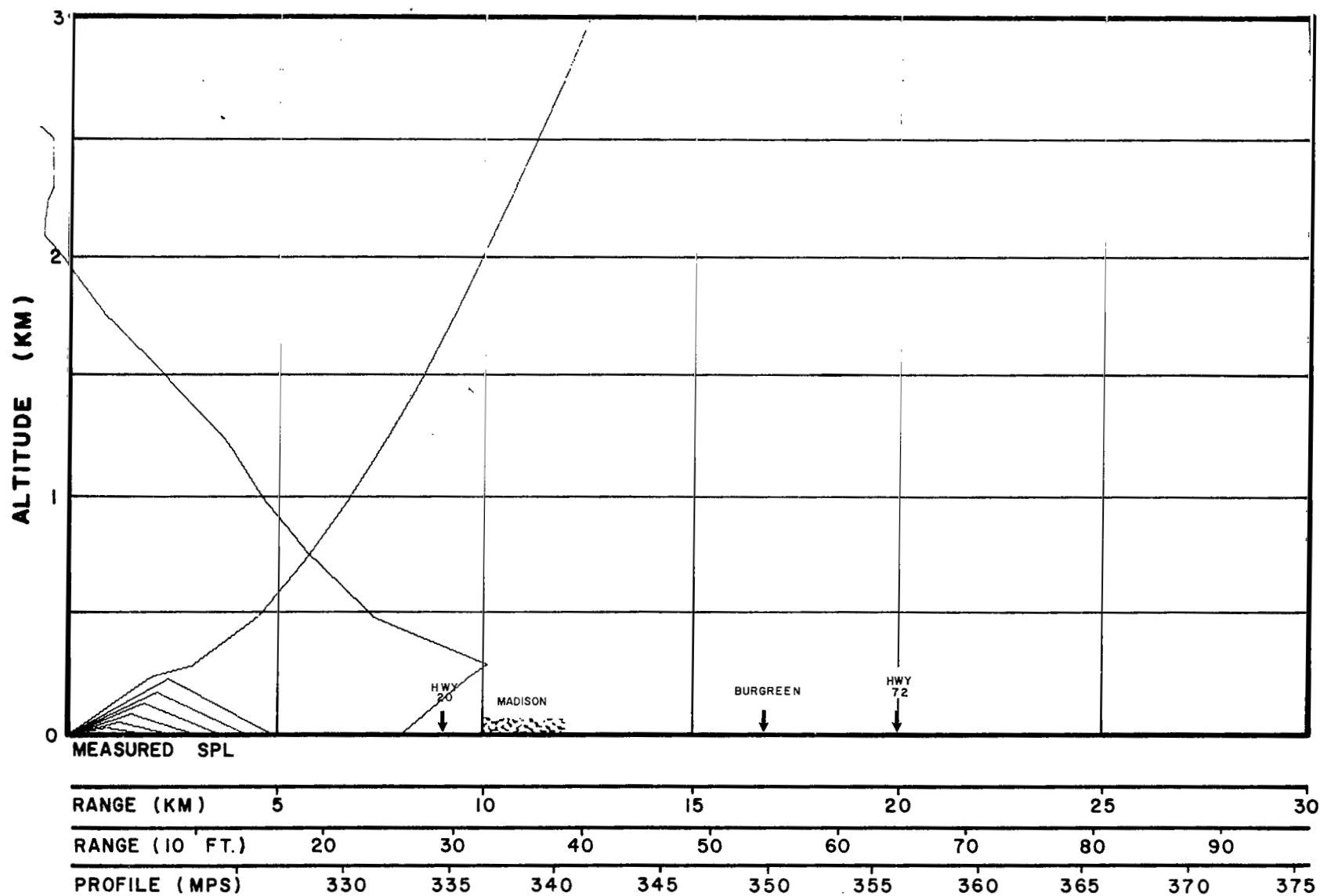


FIG.69 CALCULATED ACOUSTIC RAY PATHS
MADISON, ALA., 315° AZIMUTH

DATE 3/8/63
TIME 0700C

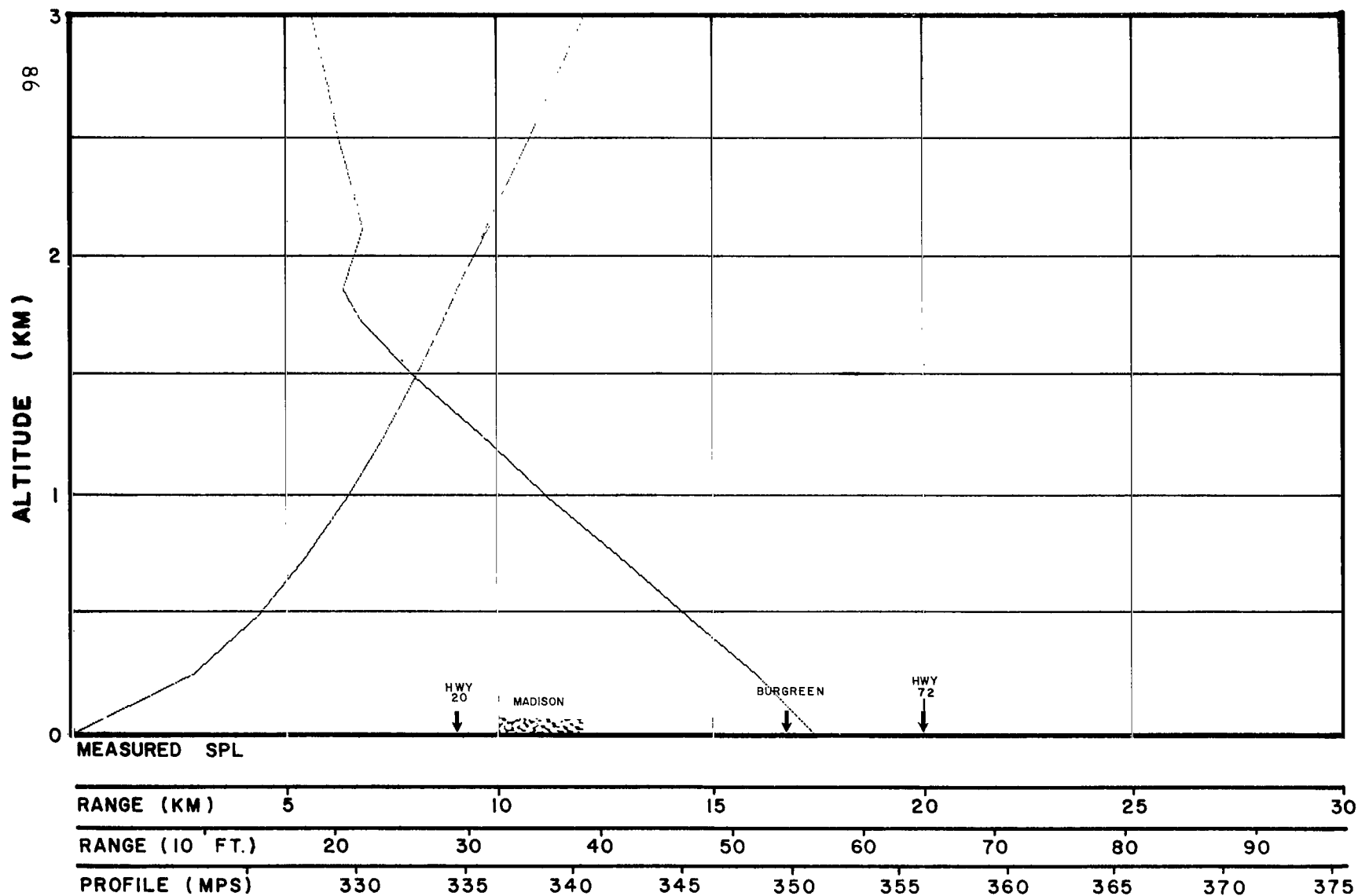


FIG. 70 CALCULATED ACOUSTIC RAY PATHS
MADISON, ALA., 315° AZIMUTH

DATE 3/8/63
TIME 0945C

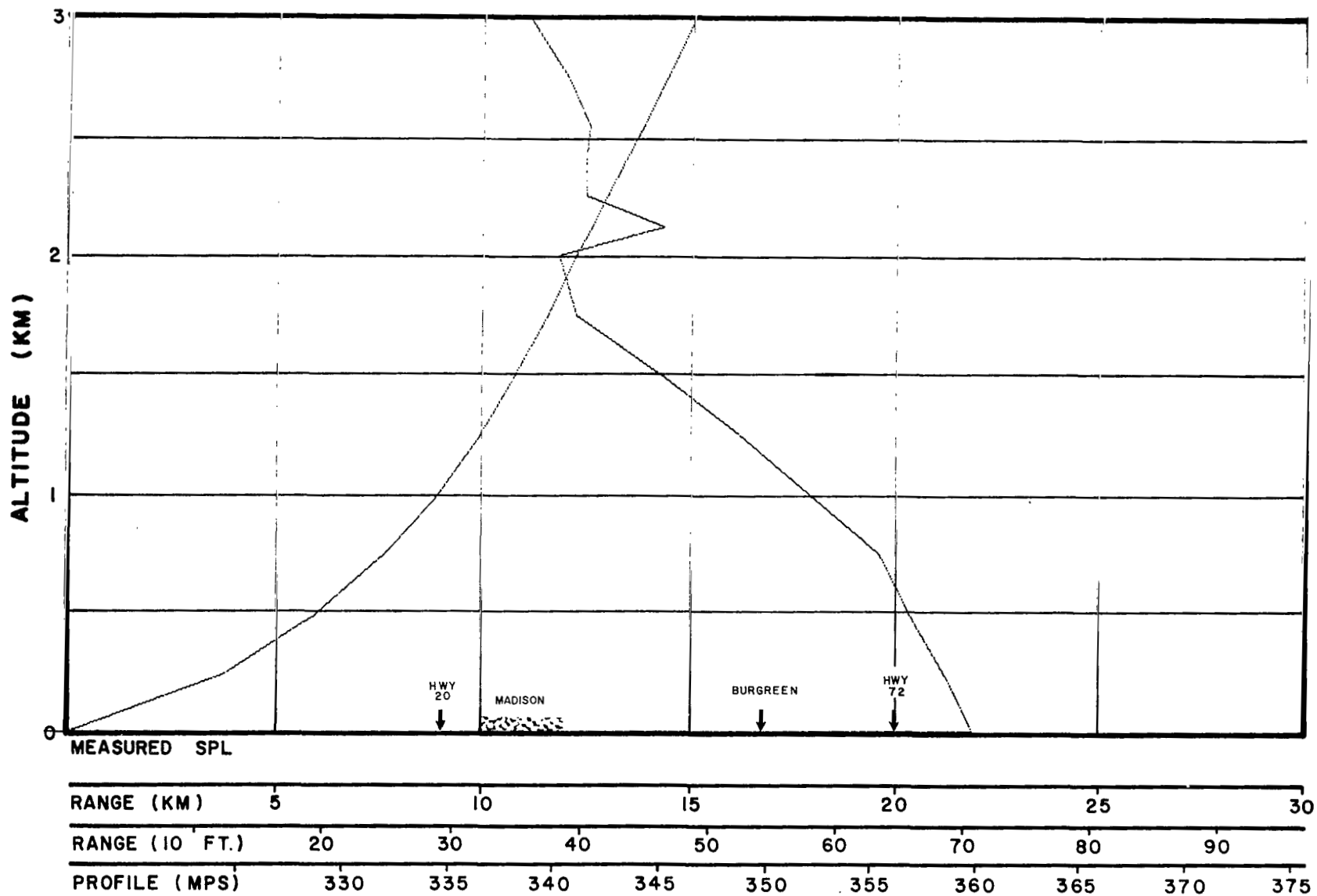


FIG.71 CALCULATED ACOUSTIC RAY PATHS
MADISON, ALA., 315° AZIMUTH

DATE 3/8/63
TIME 1055C

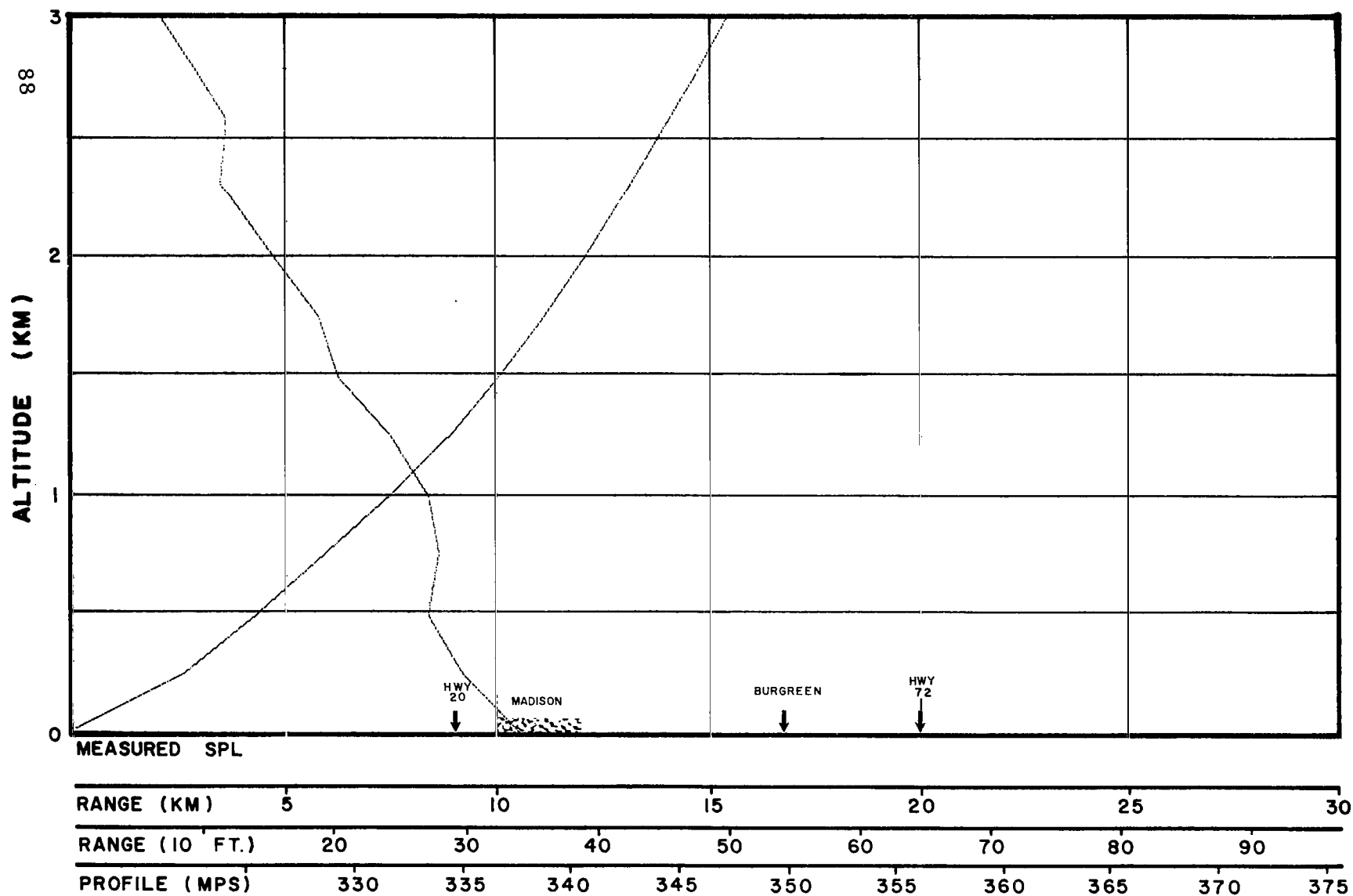


FIG.72 CALCULATED ACOUSTIC RAY PATHS
MADISON, ALA., 315° AZIMUTH

DATE 3/8/63
TIME 1300C

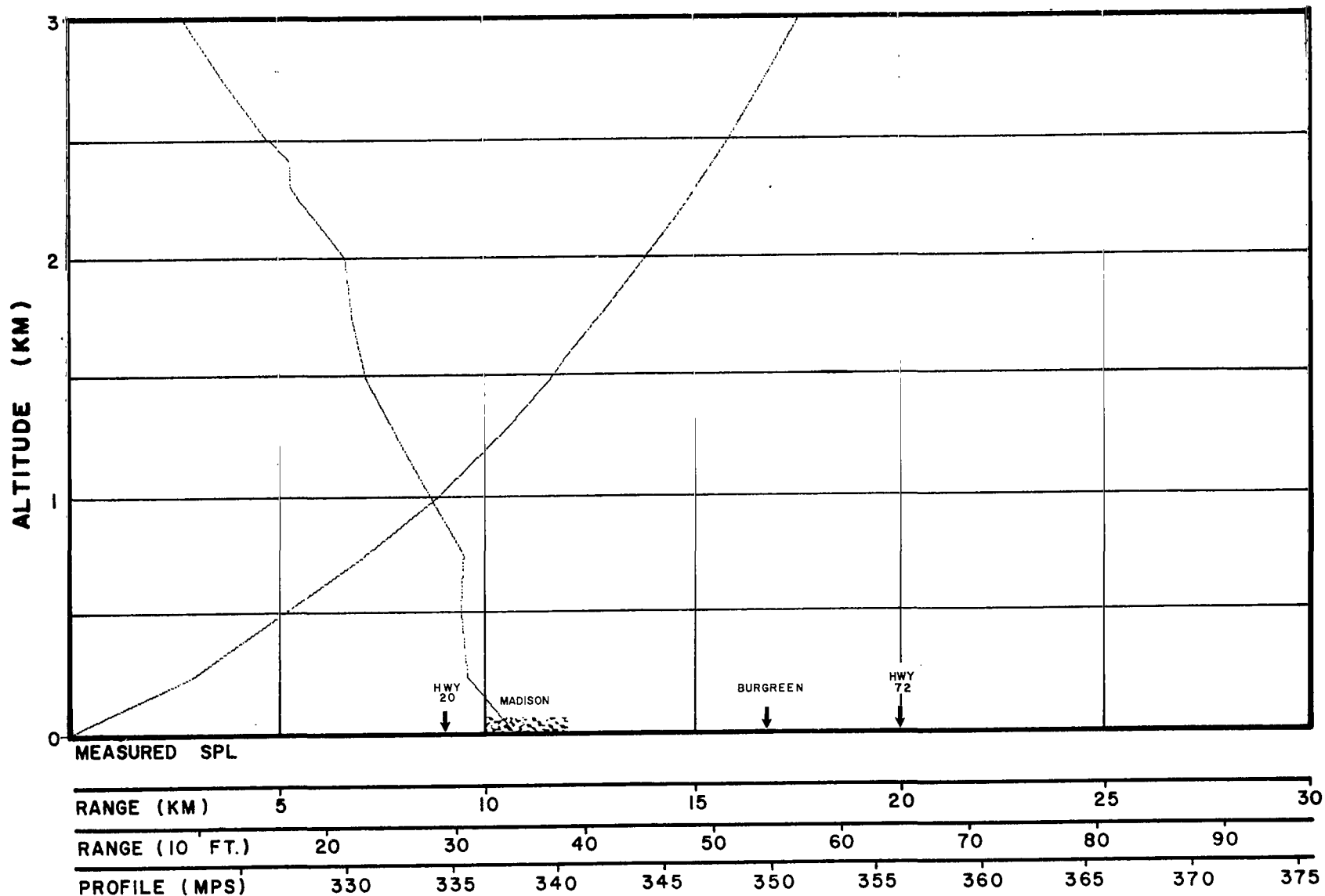


FIG.73 CALCULATED ACOUSTIC RAY PATHS
MADISON, ALA., 315° AZIMUTH

DATE 3/8/63
TIME 1455C

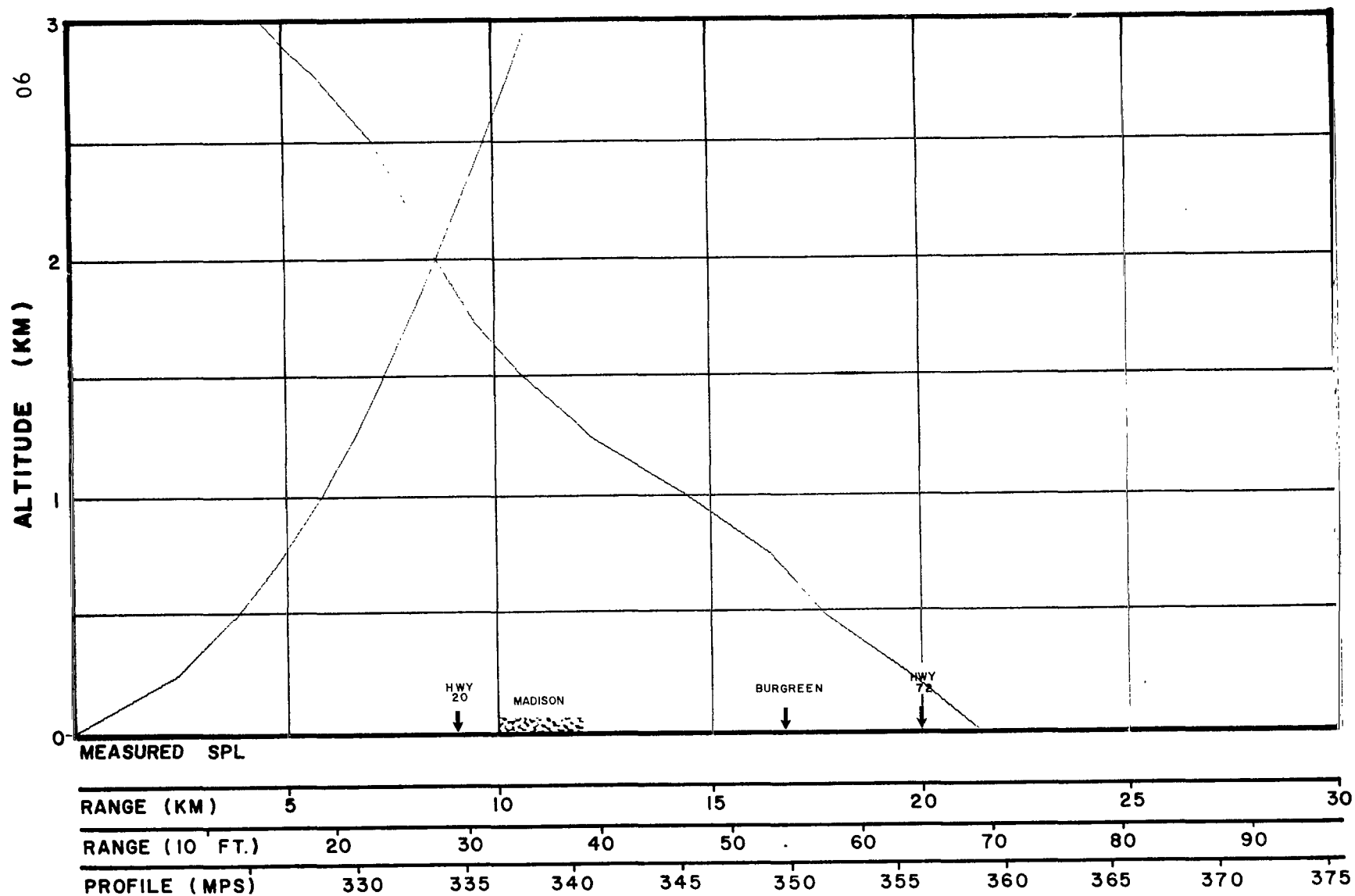


FIG. 74 CALCULATED ACOUSTIC RAY PATHS
MADISON, ALA., 315° AZIMUTH

DATE 3/7/63
TIME X-1 Day Fore-
cast

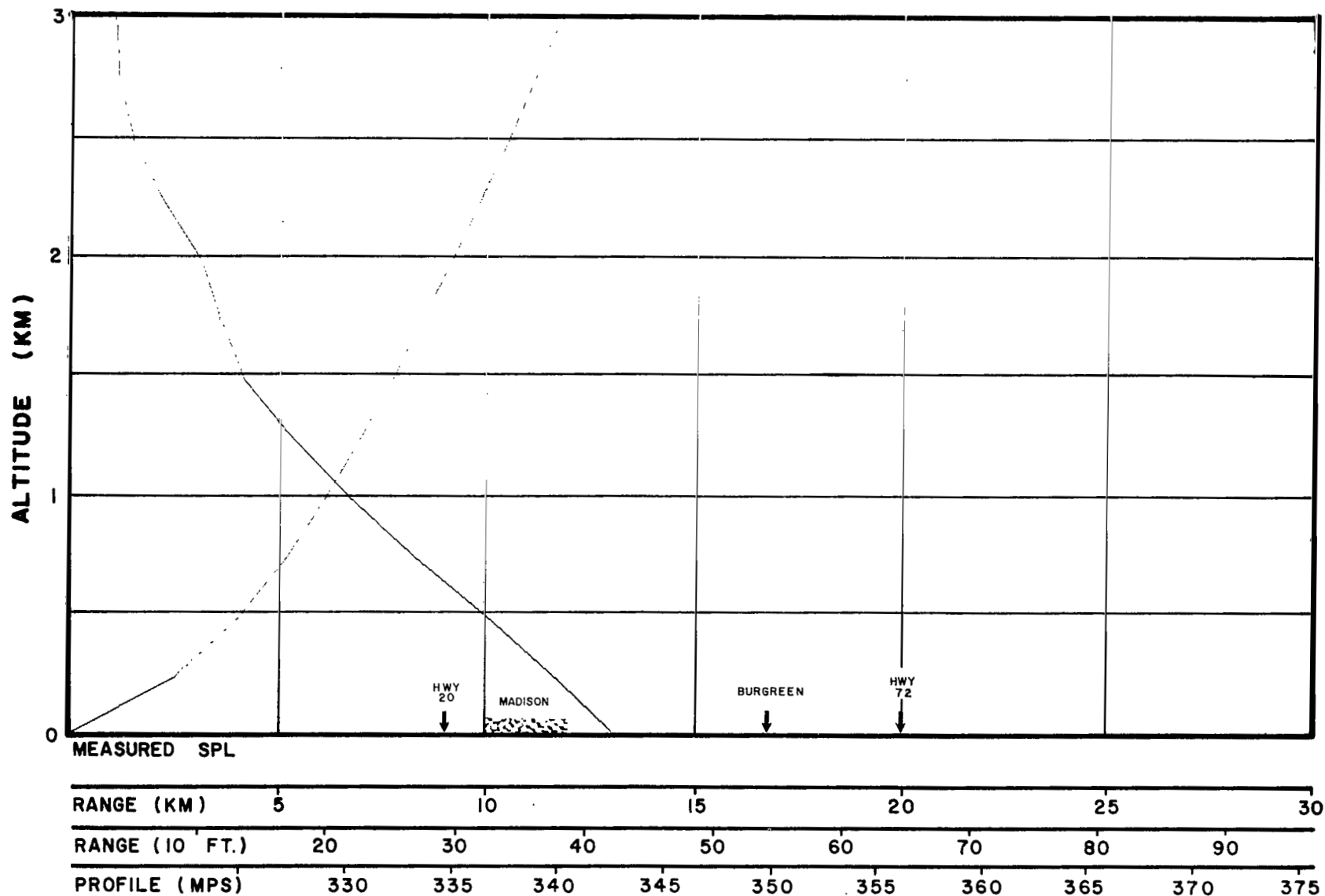


FIG. 75 CALCULATED ACOUSTIC RAY PATHS
MADISON, ALA., 315° AZIMUTH

DATE 3/8/63
TIME X-6 Hour Fore-
cast

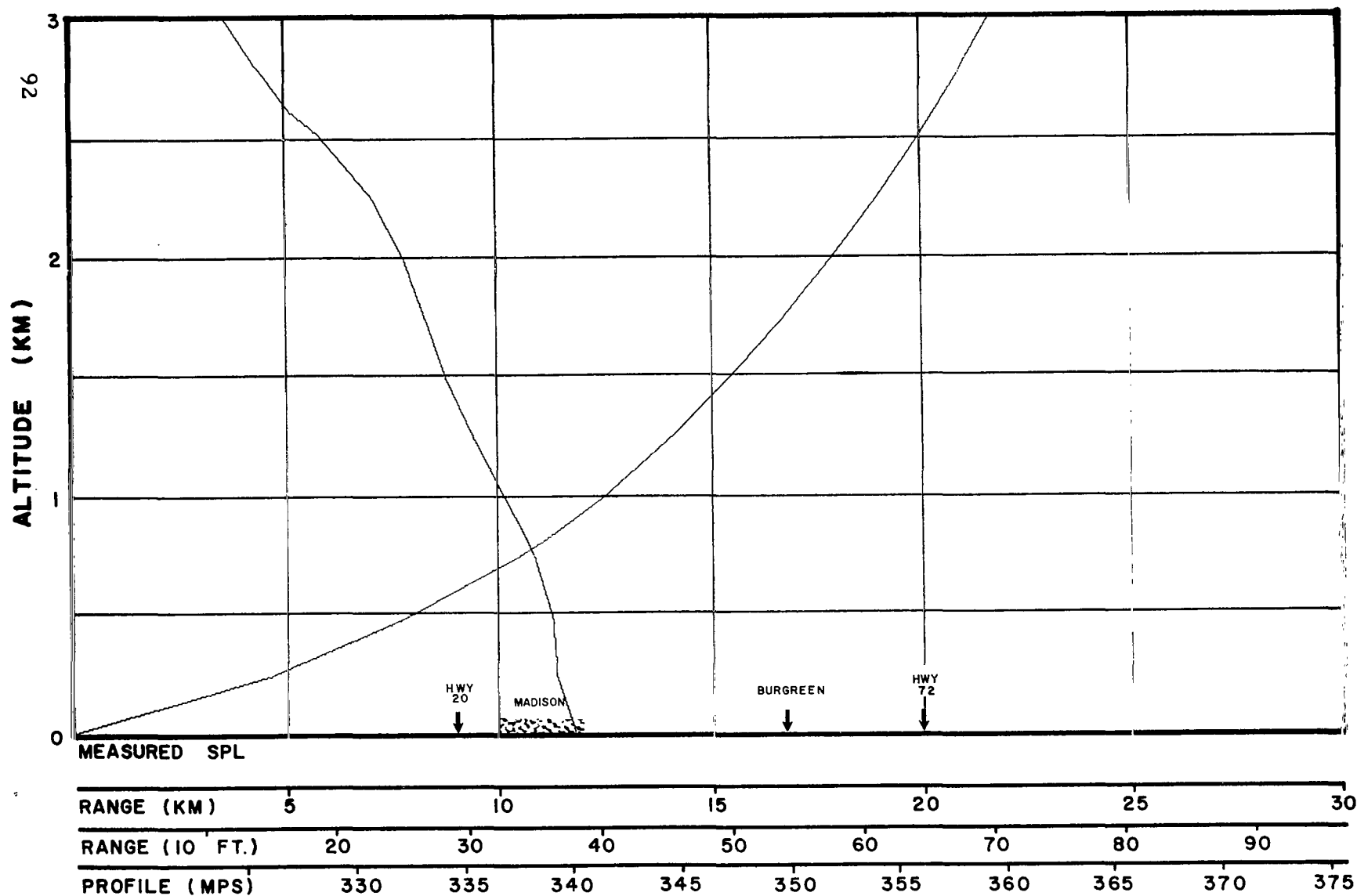


FIG. 76 CALCULATED ACOUSTIC RAY PATHS
MADISON, ALA., 315° AZIMUTH

DATE 3/8/63
TIME 1620G

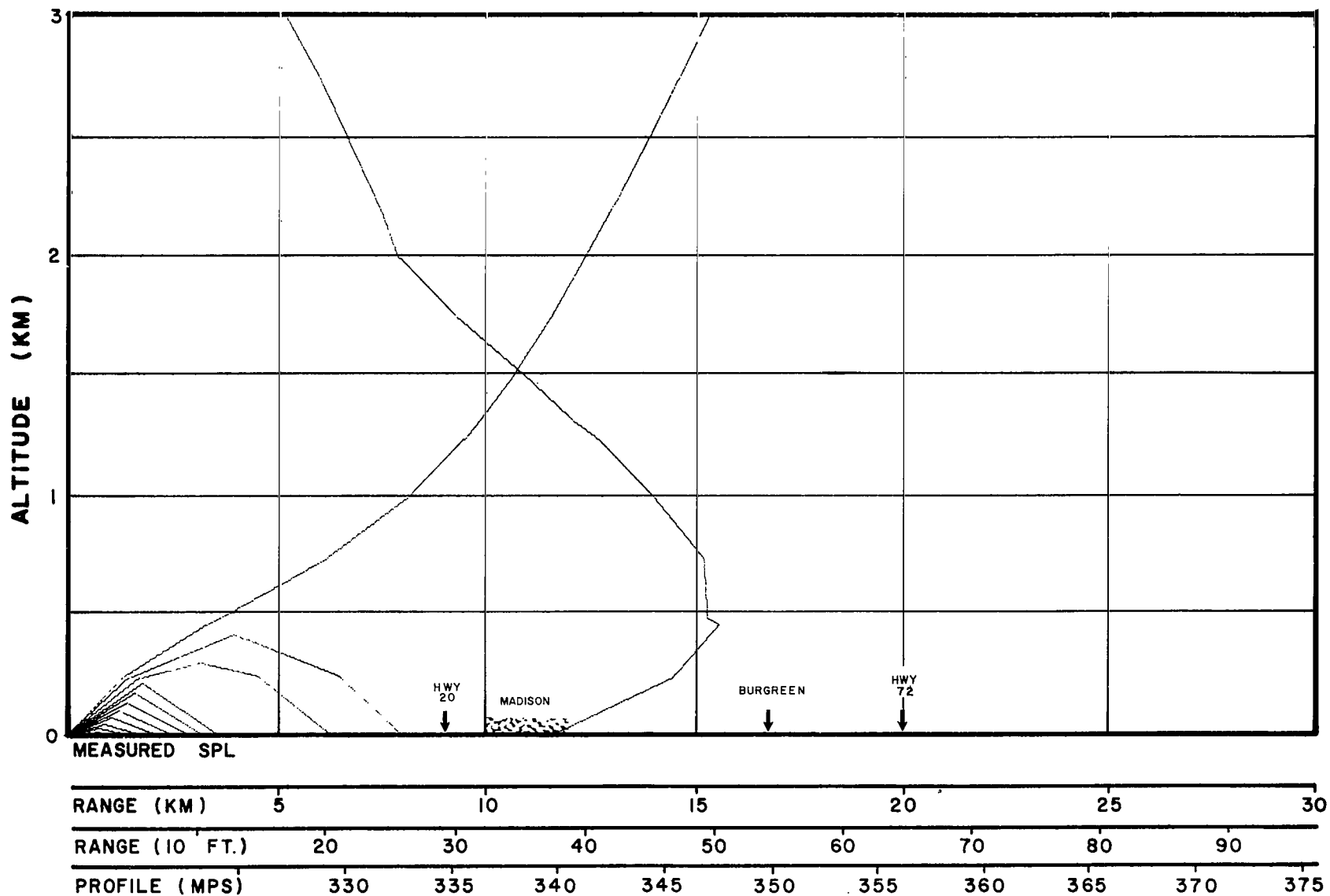


FIG.77 CALCULATED ACOUSTIC RAY PATHS
MADISON, ALA., 315° AZIMUTH

DATE 3/9/63
TIME 0700C

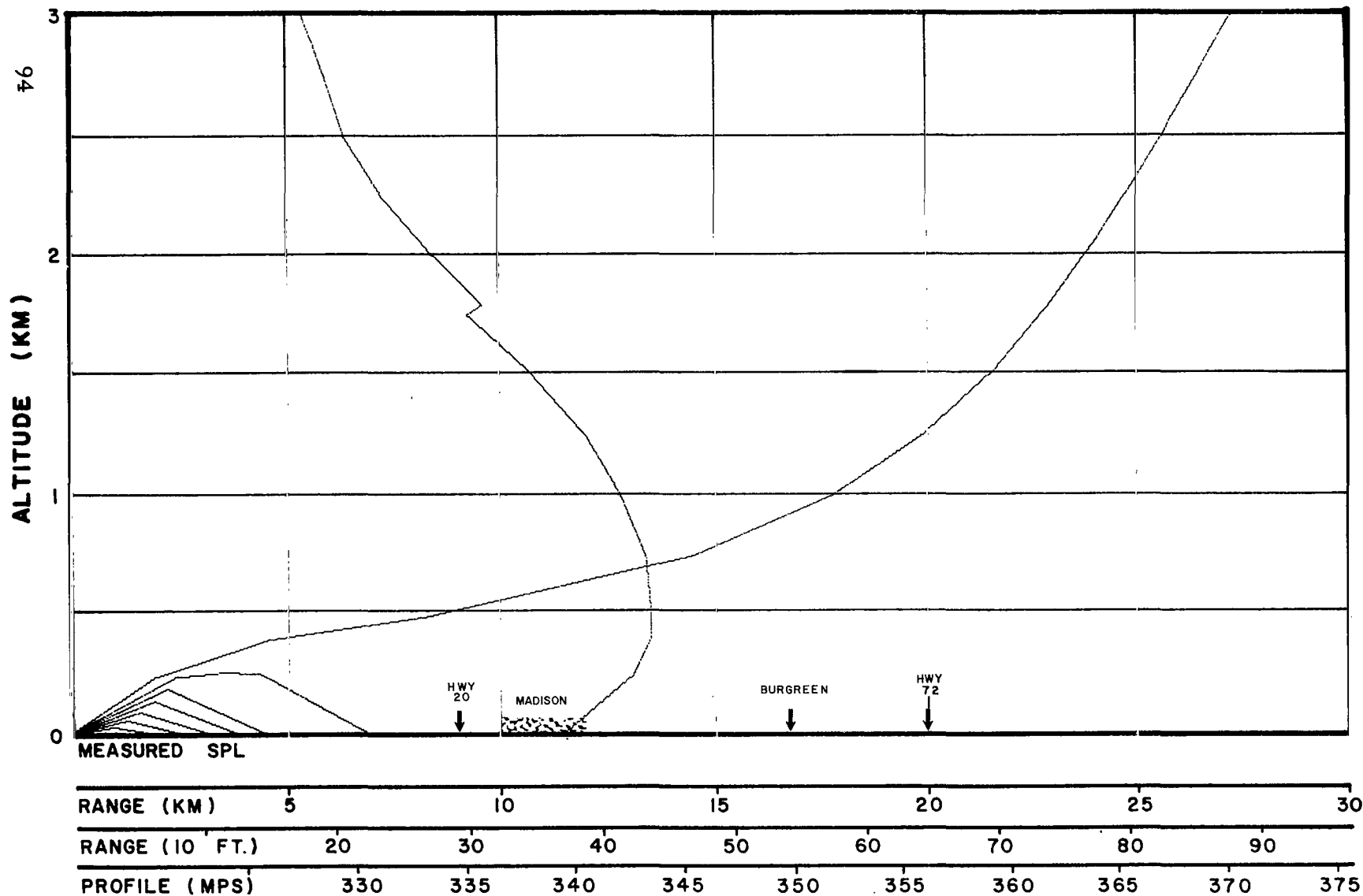


FIG. 78 CALCULATED ACOUSTIC RAY PATHS
MADISON, ALA., 315° AZIMUTH

DATE 3/9/63
TIME 0900C

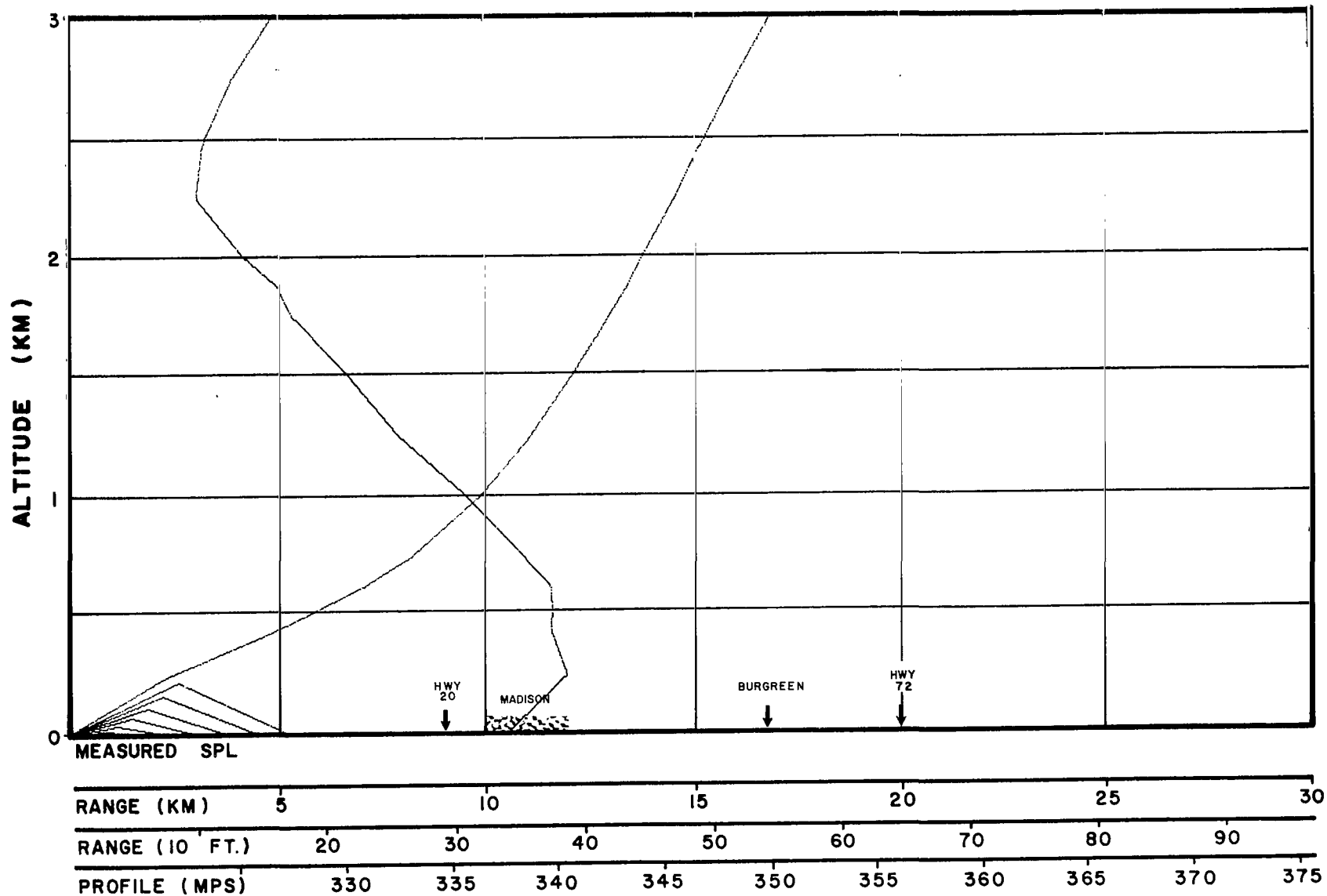


FIG. 79 CALCULATED ACOUSTIC RAY PATHS
MADISON, ALA., 315° AZIMUTH

DATE 3/9/63
TIME 1045C

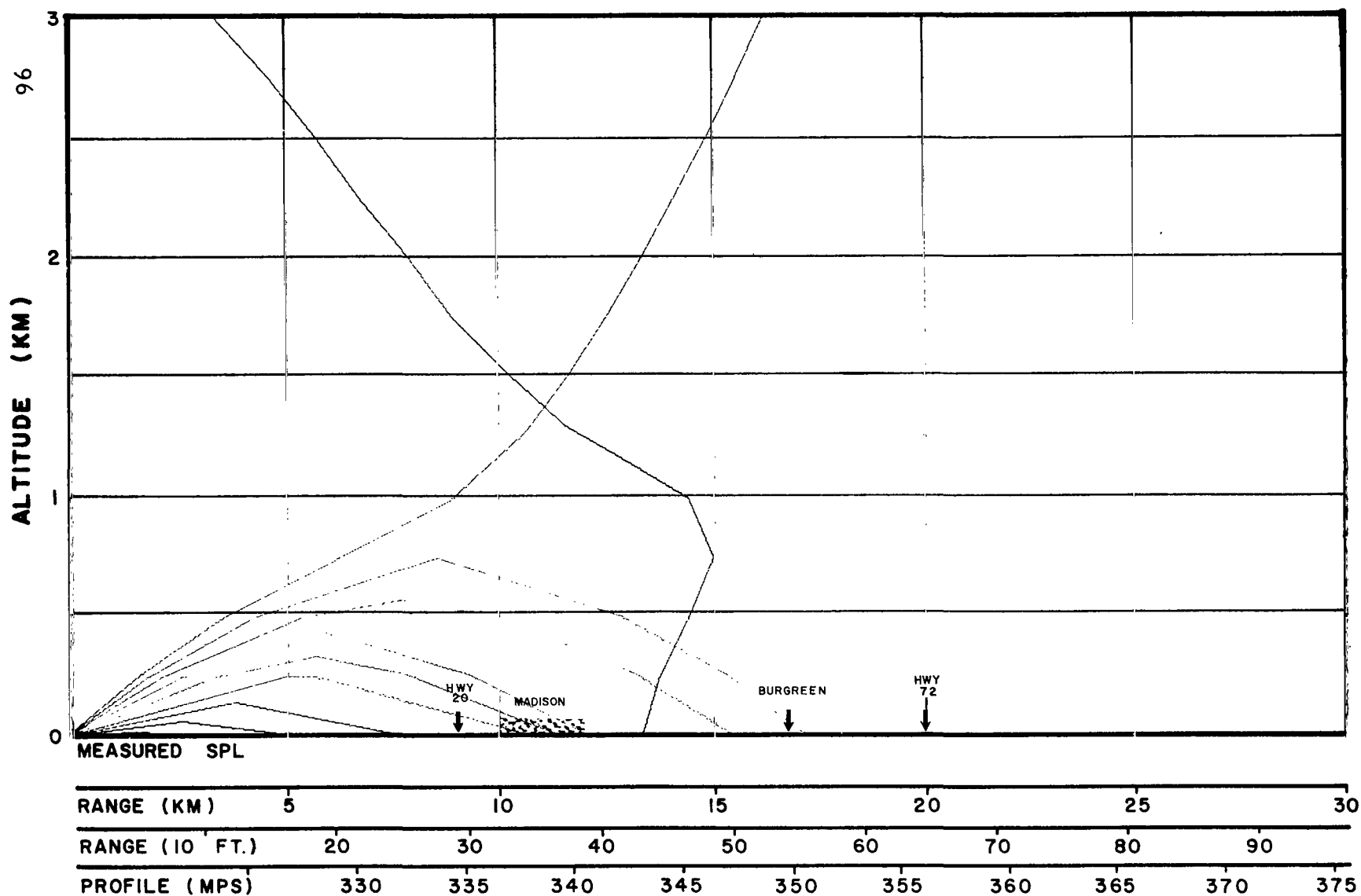


FIG. 80 CALCULATED ACOUSTIC RAY PATHS
MADISON, ALA., 315° AZIMUTH

DATE 3/9/63
TIME X-6 Hour Fore-
cast

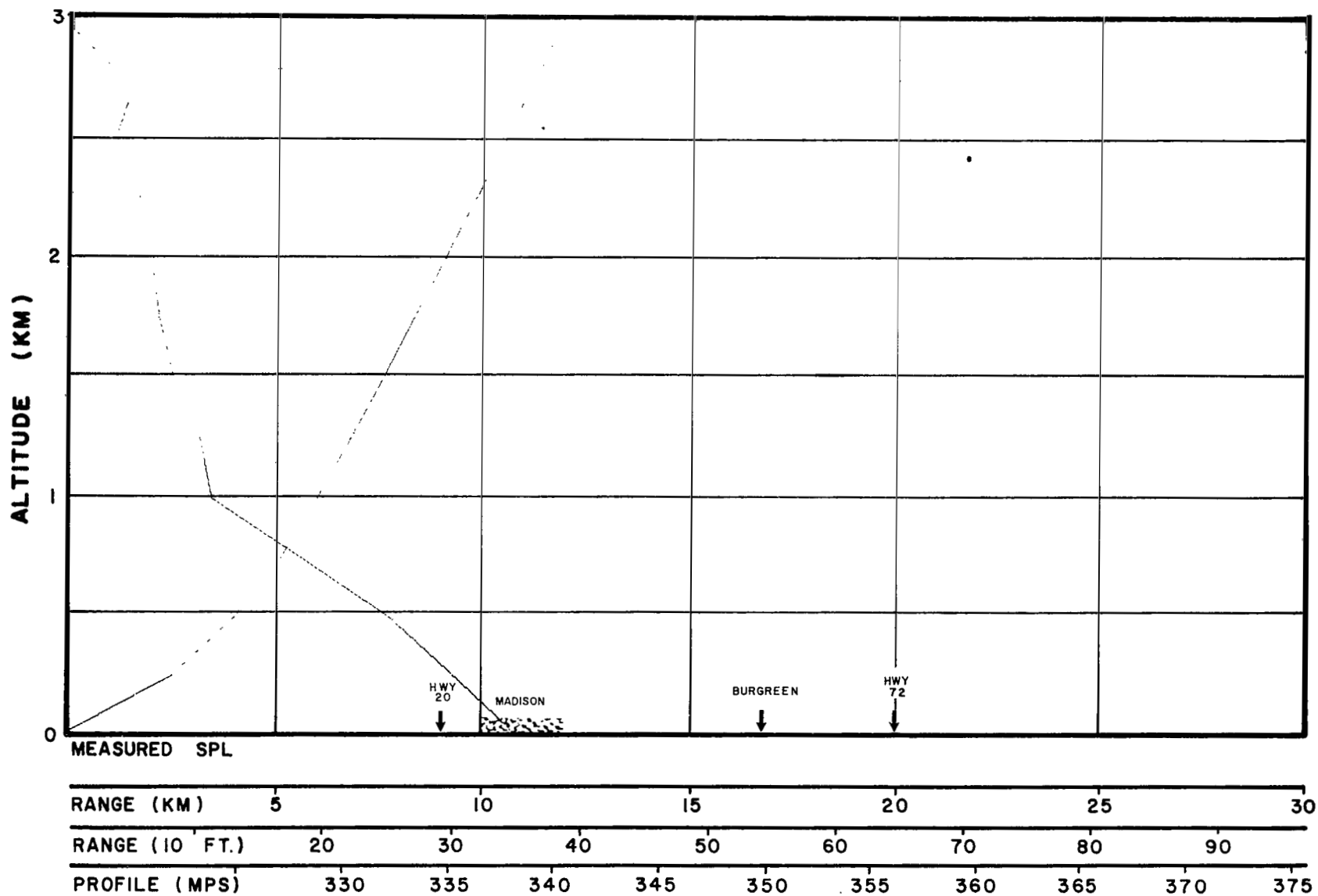


FIG.8I CALCULATED ACOUSTIC RAY PATHS
MADISON, ALA., 315° AZIMUTH

DATE 3/9/63
TIME 1620C

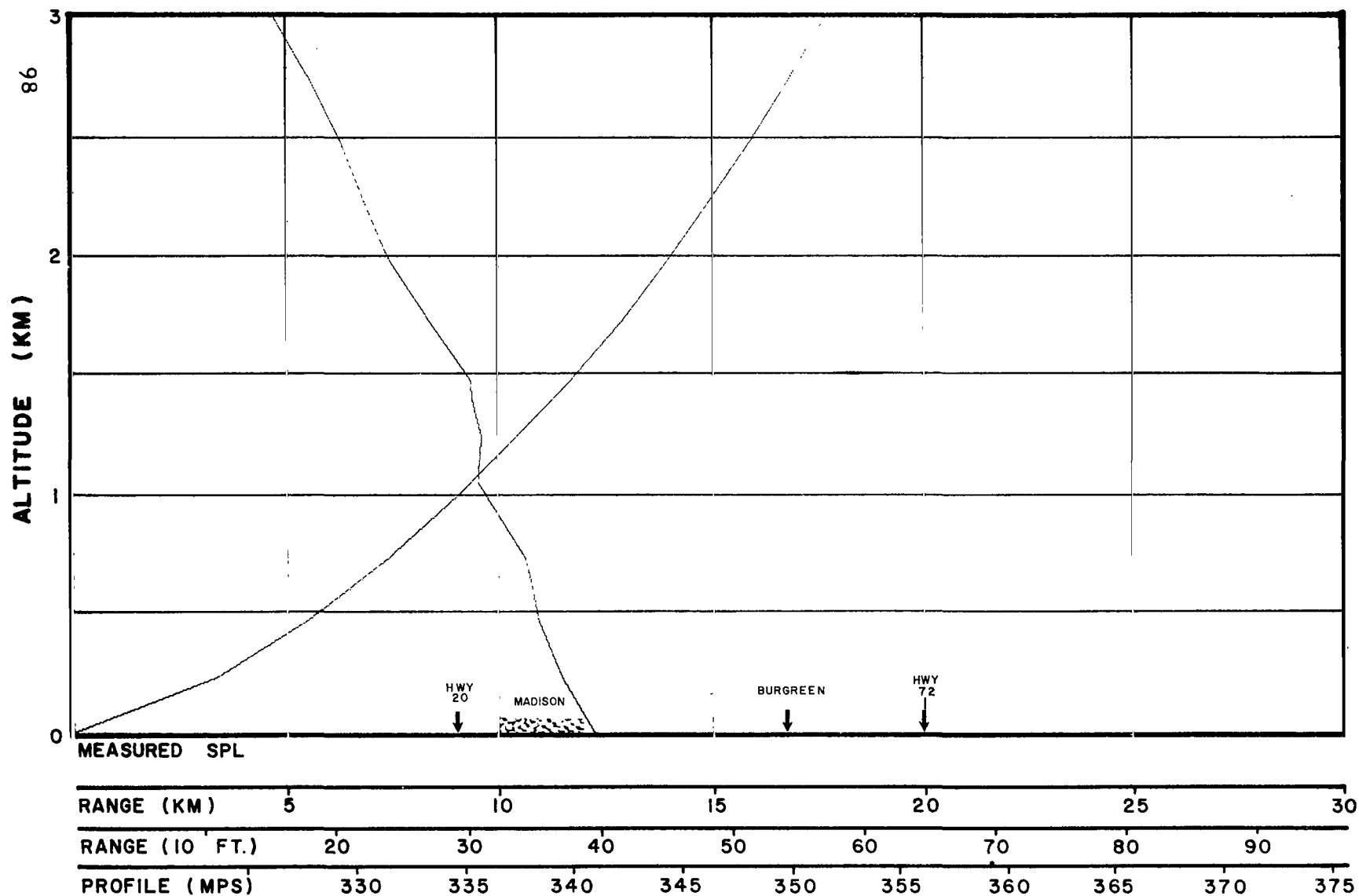


FIG.82 CALCULATED ACOUSTIC RAY PATHS
MADISON, ALA., 315° AZIMUTH

DATE 3/10/63
TIME 1600C

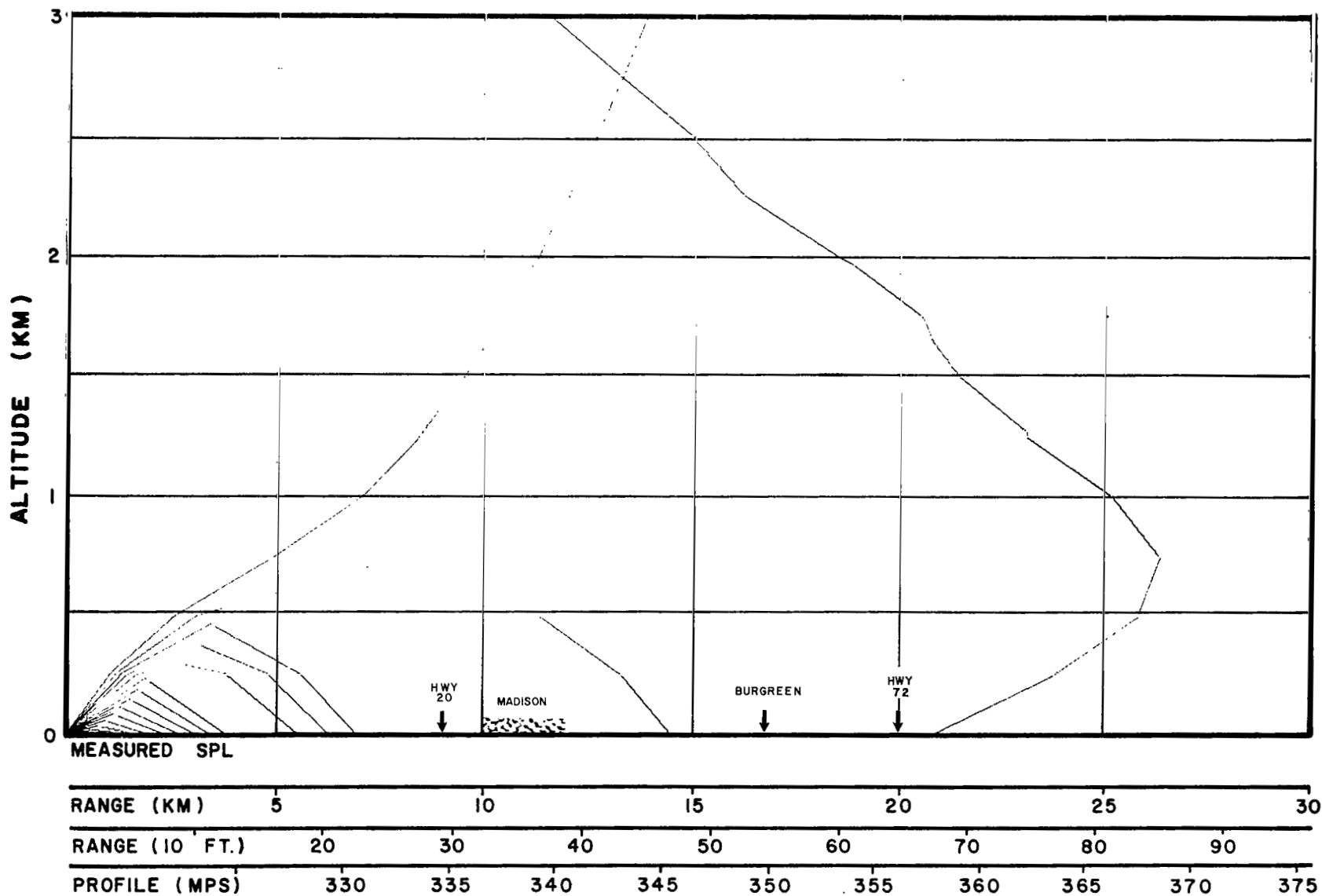


FIG 83 CALCULATED ACOUSTIC RAY PATHS
MADISON, ALA., 315° AZIMUTH

DATE 3/11/63
TIME 0700C

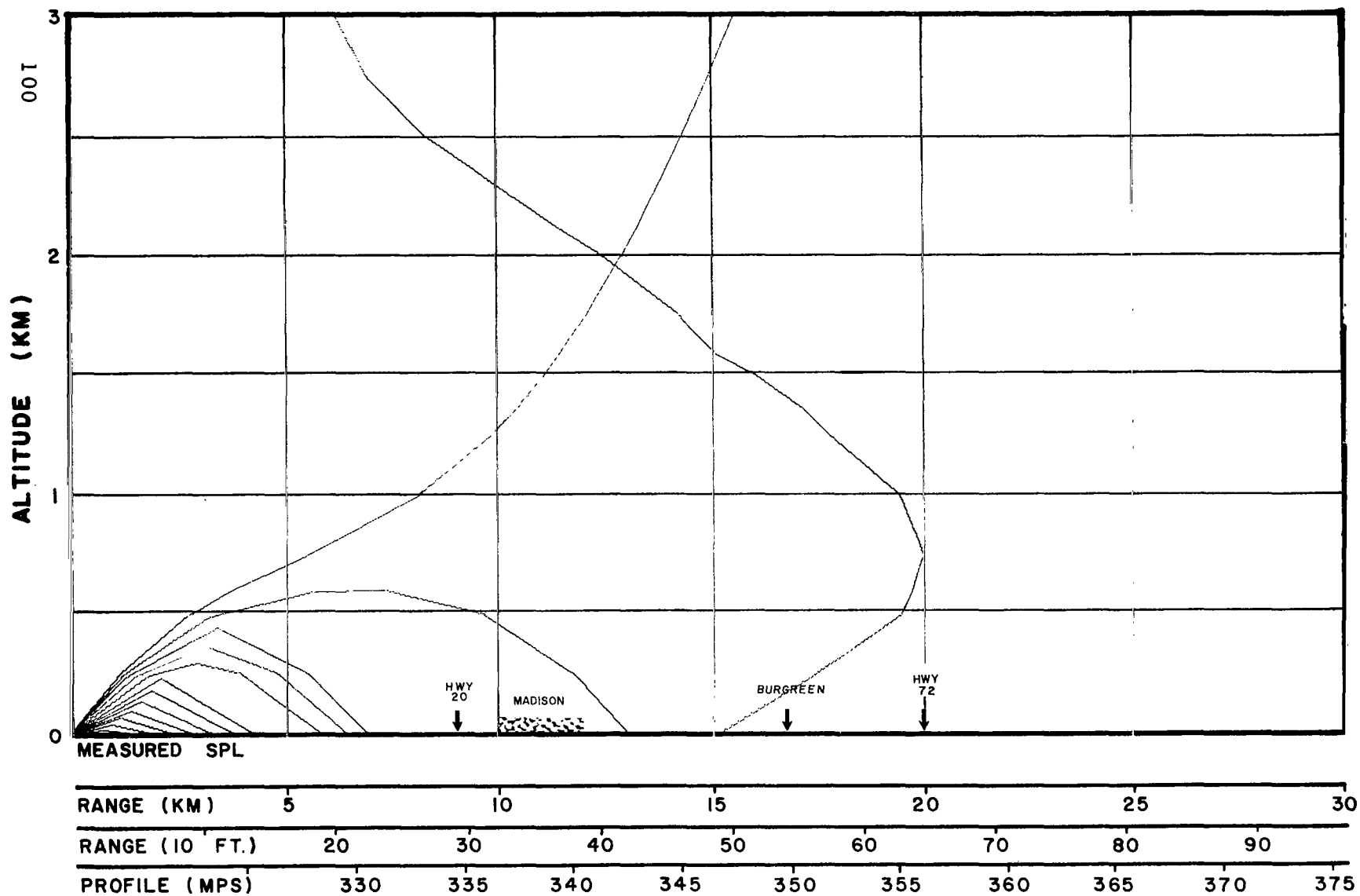


FIG. 84 CALCULATED ACOUSTIC RAY PATHS
MADISON, ALA., 315° AZIMUTH

DATE 3/11/63
TIME 0800C

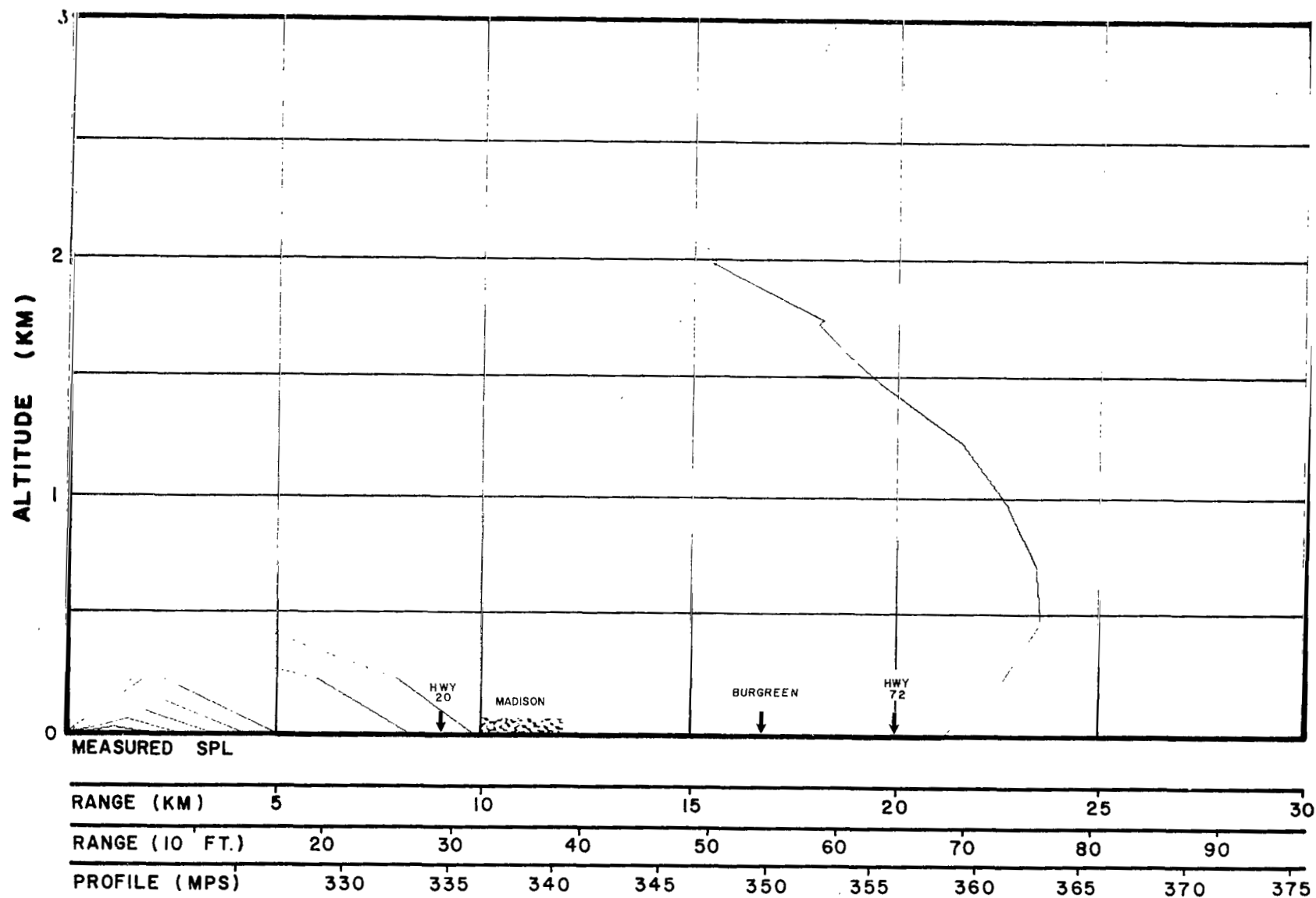


FIG.85 CALCULATED ACOUSTIC RAY PATHS
MADISON, ALA., 315° AZIMUTH

DATE 3/11/63
TIME 1000G

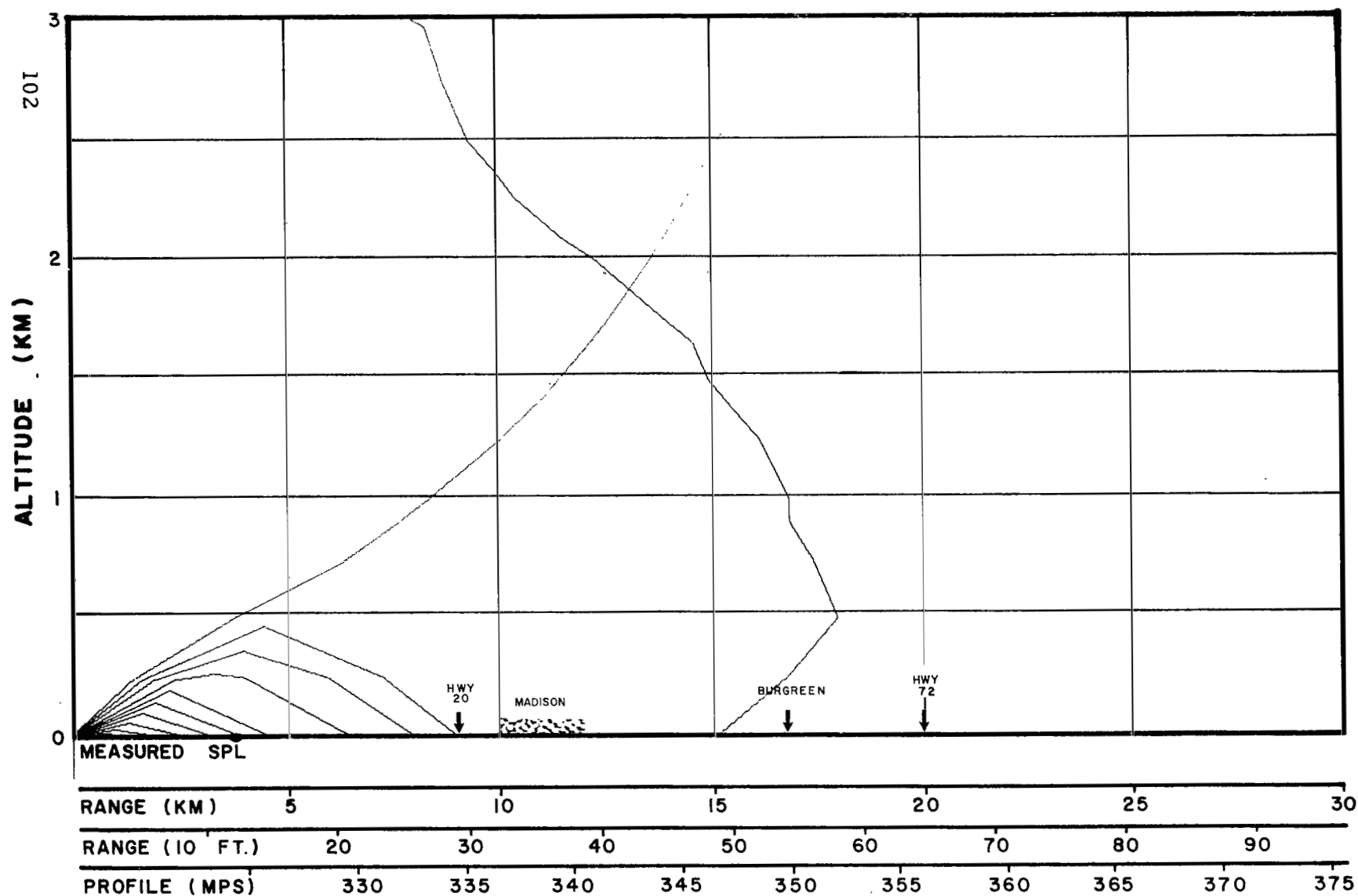


FIG. 86 CALCULATED ACOUSTIC RAY PATHS
MADISON, ALA., 315° AZIMUTH

DATE 3/11/63
TIME 1335C

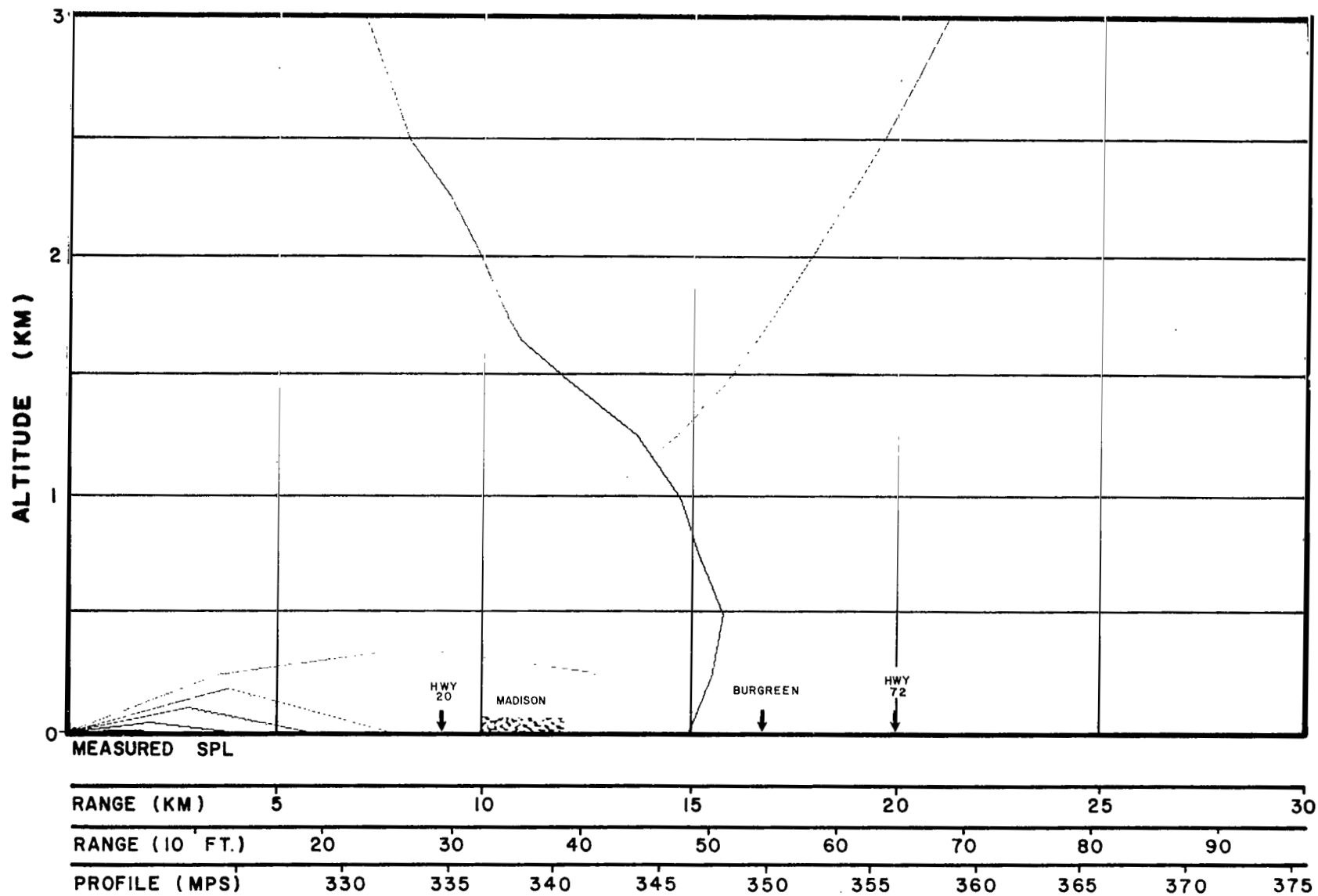


FIG.87 CALCULATED ACOUSTIC RAY PATHS
MADISON, ALA., 315° AZIMUTH

DATE 3/11/63
TIME X-6 Hour Fore-
cast

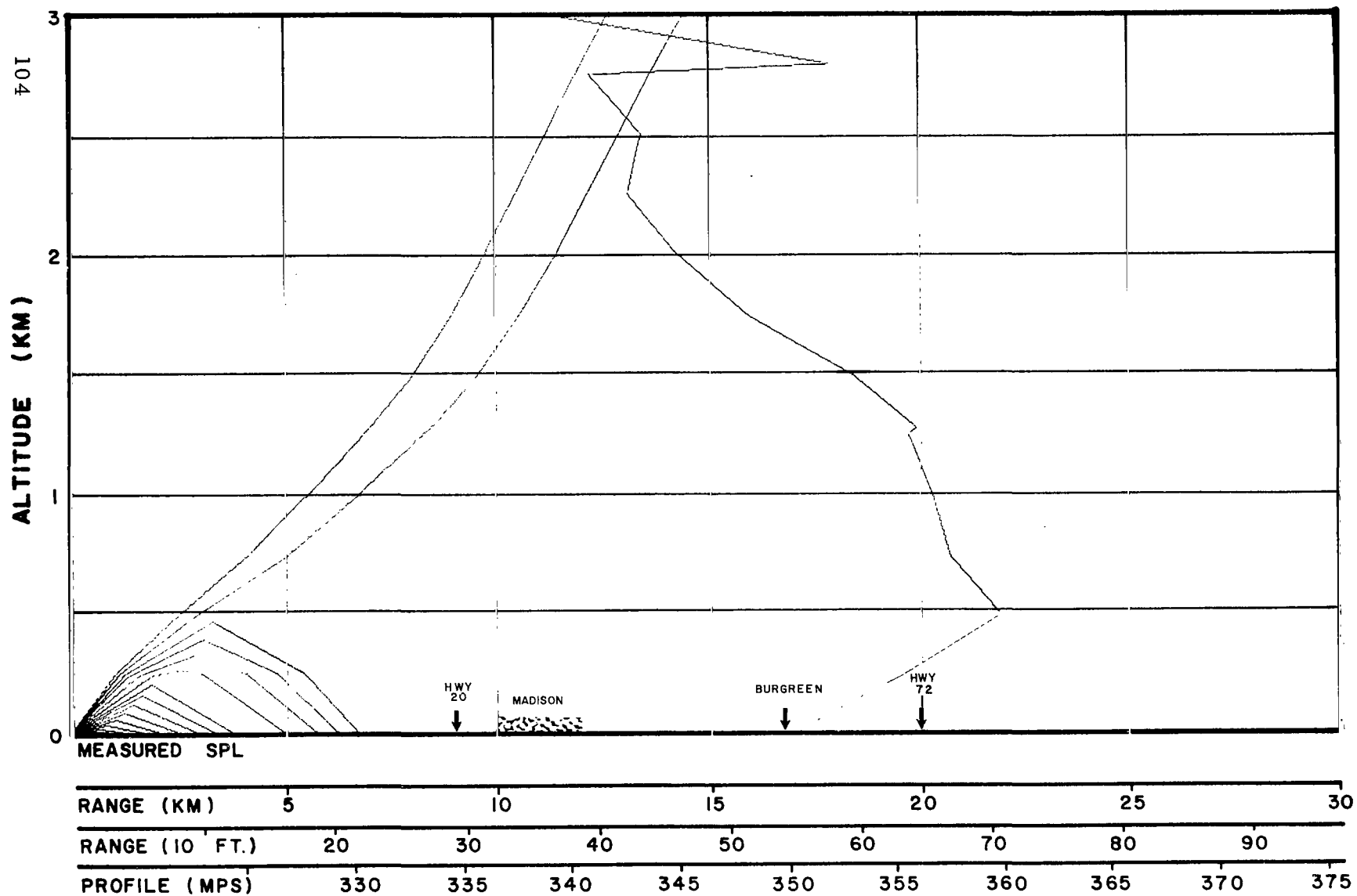


FIG. 88 CALCULATED ACOUSTIC RAY PATHS
MADISON, ALA., 315° AZIMUTH

DATE 3/11/63
TIME 1615C

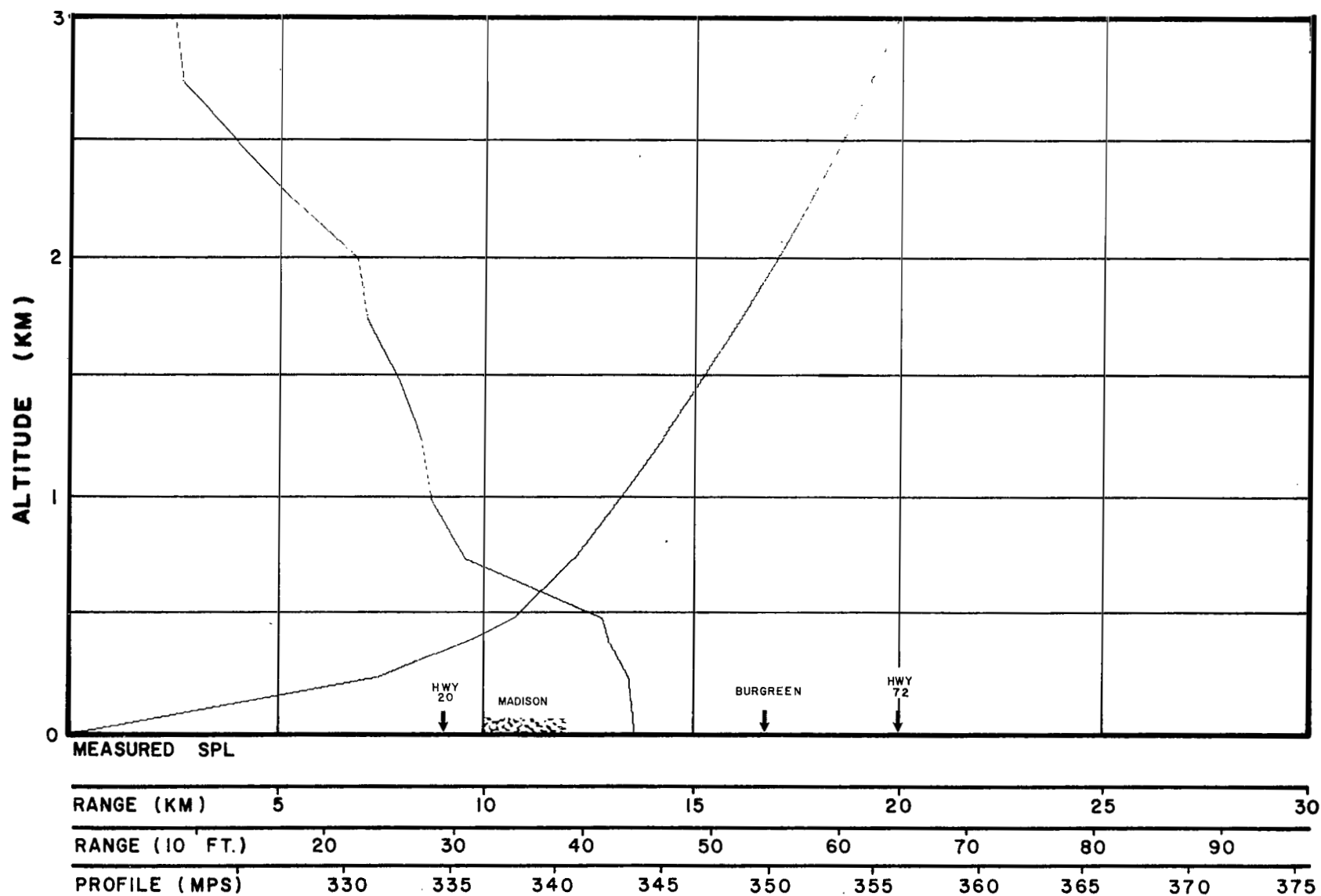


FIG. 89 CALCULATED ACOUSTIC RAY PATHS
MADISON, ALA., 315° AZIMUTH

DATE 3/12/63
TIME 1000C

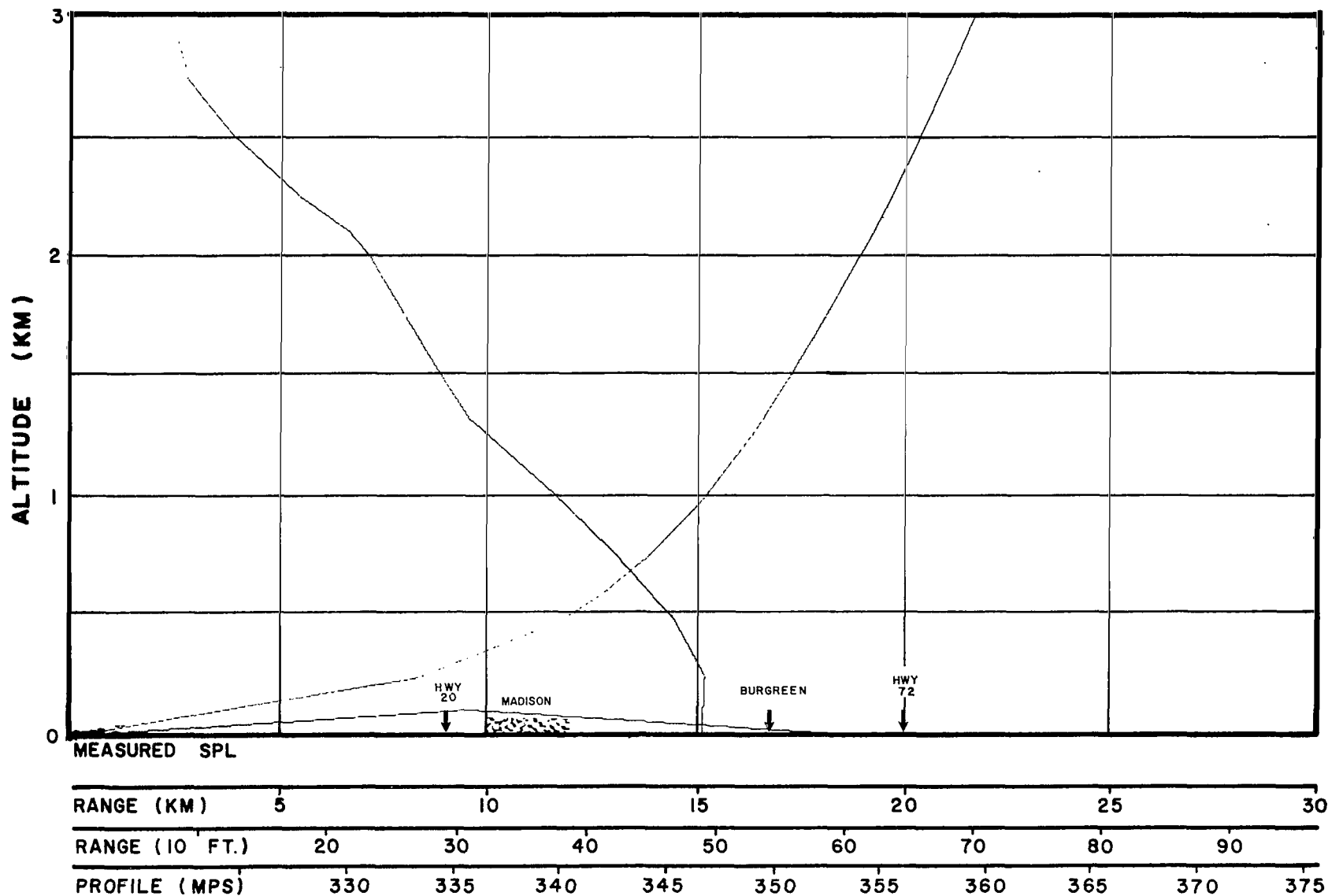


FIG.9I CALCULATED ACOUSTIC RAY PATHS
MADISON, ALA., 315° AZIMUTH

DATE 3/12/63
TIME 1630C

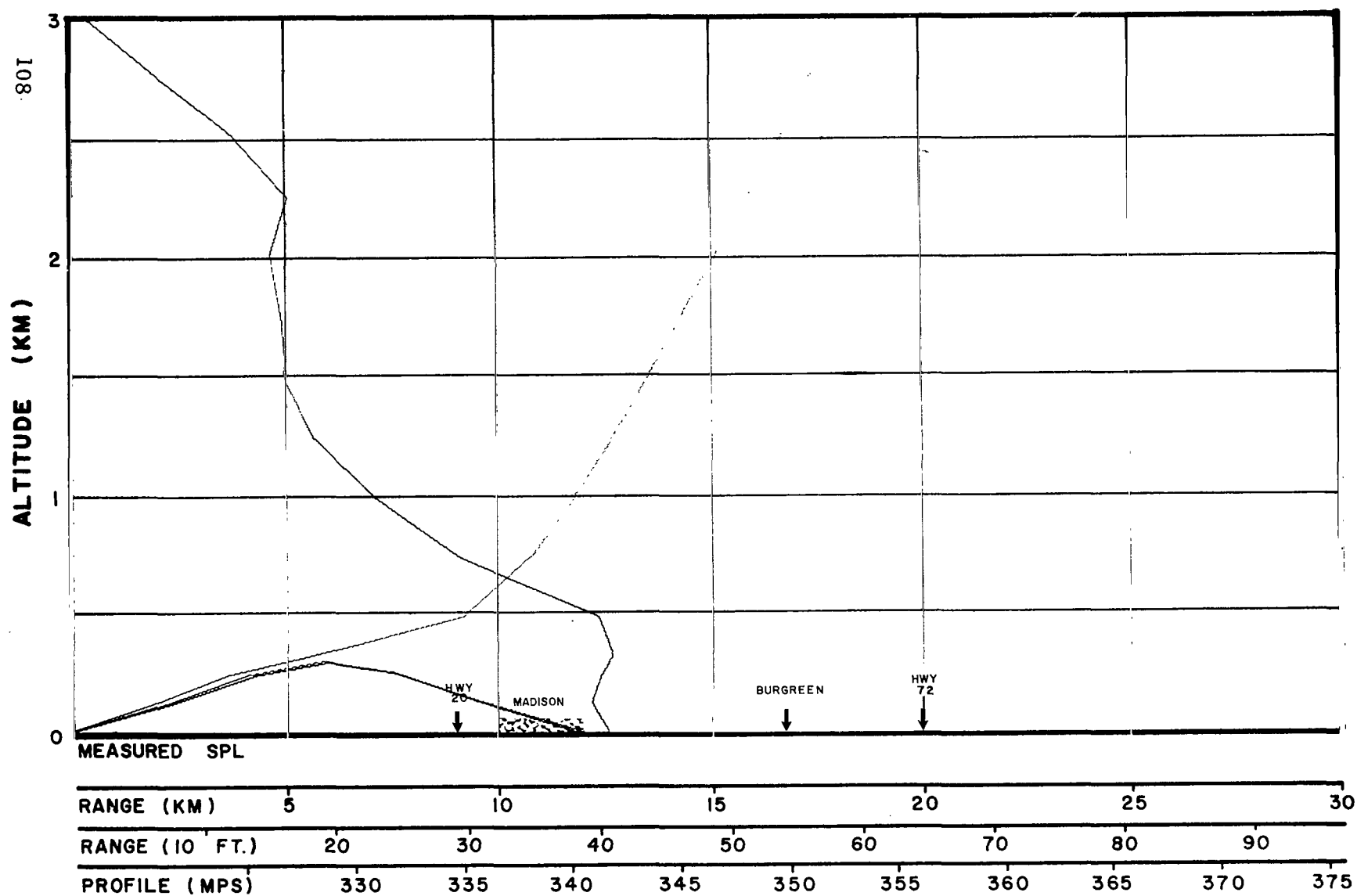


FIG.92 CALCULATED ACOUSTIC RAY PATHS
MADISON, ALA., 315° AZIMUTH

DATE 3/13/63
TIME 0700C

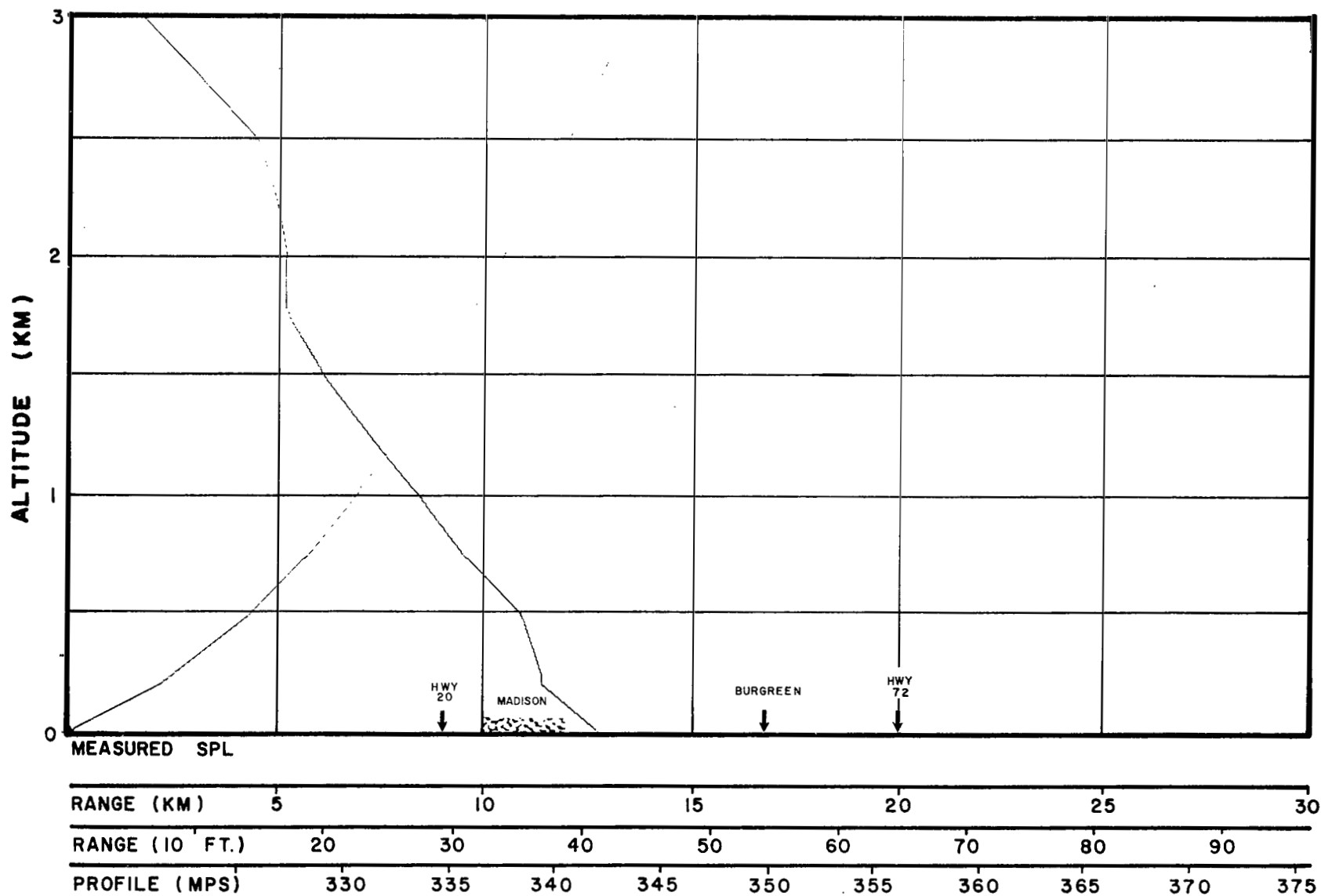


FIG.93 CALCULATED ACOUSTIC RAY PATHS
MADISON, ALA., 315° AZIMUTH

DATE 3/13/63
TIME 0820C

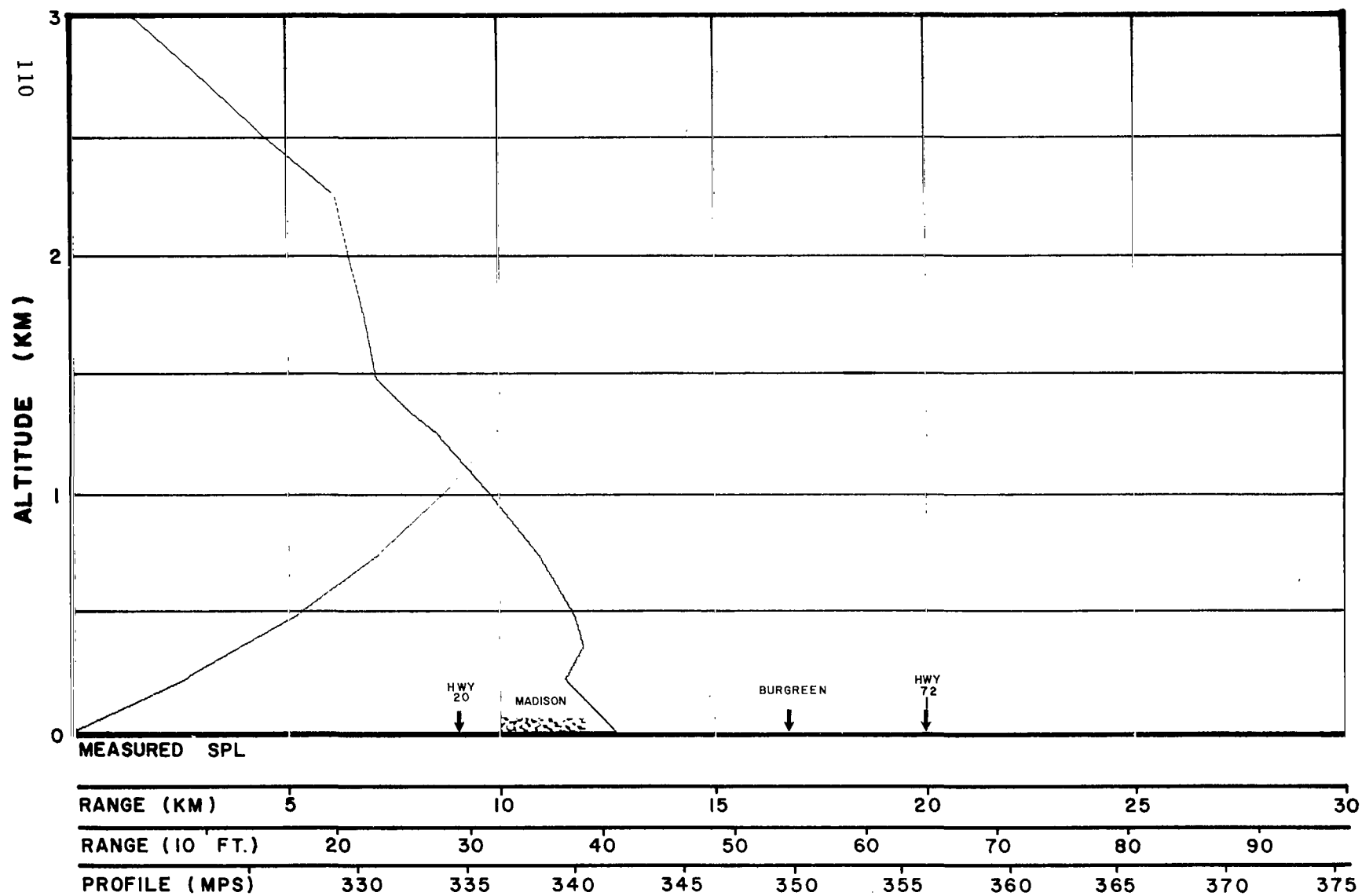


FIG.94 CALCULATED ACOUSTIC RAY PATHS
MADISON, ALA., 315° AZIMUTH

DATE 3/13/63
TIME 1005C

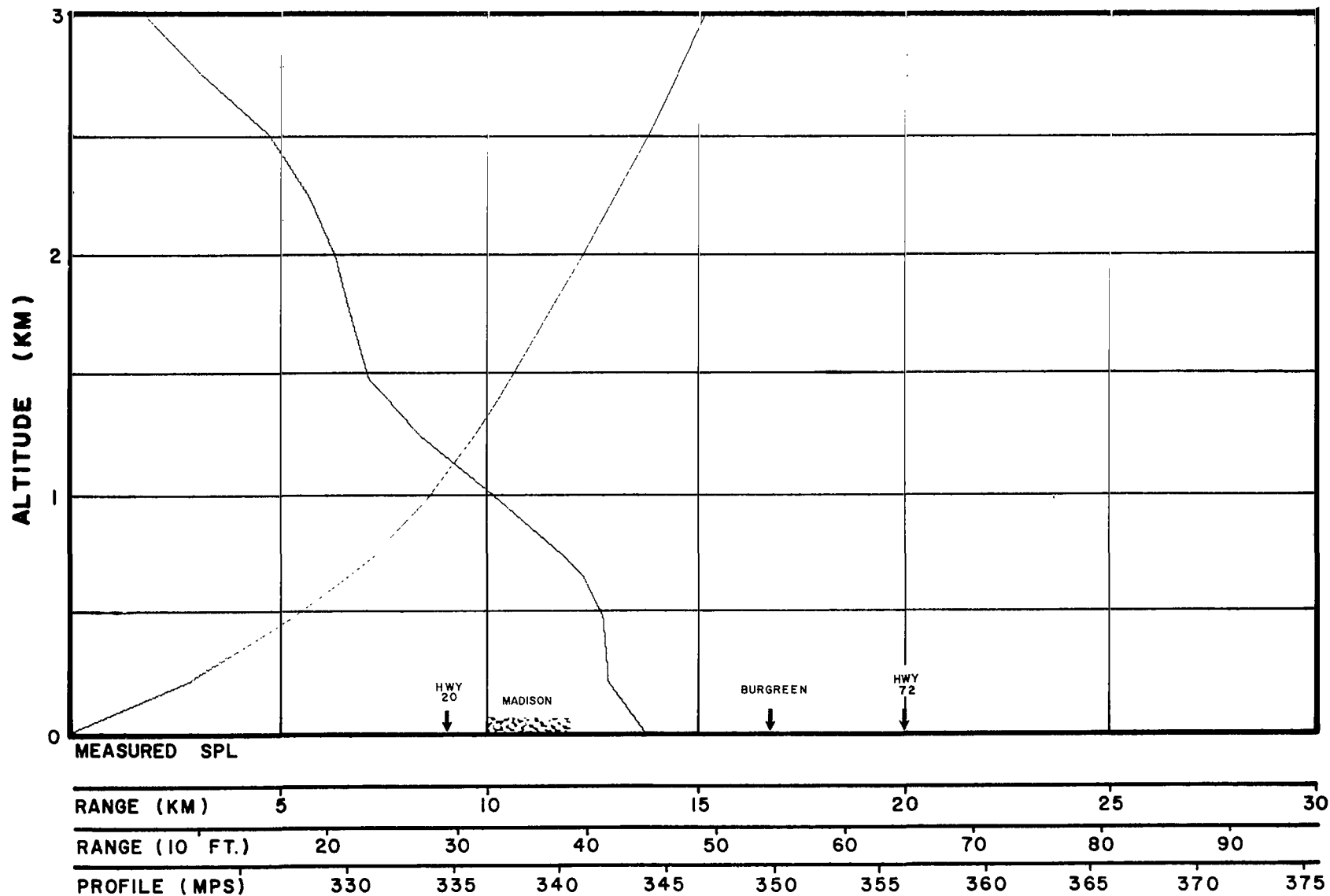


FIG. 95 CALCULATED ACOUSTIC RAY PATHS
MADISON, ALA., 315° AZIMUTH

DATE 3/13/63
TIME 1055C

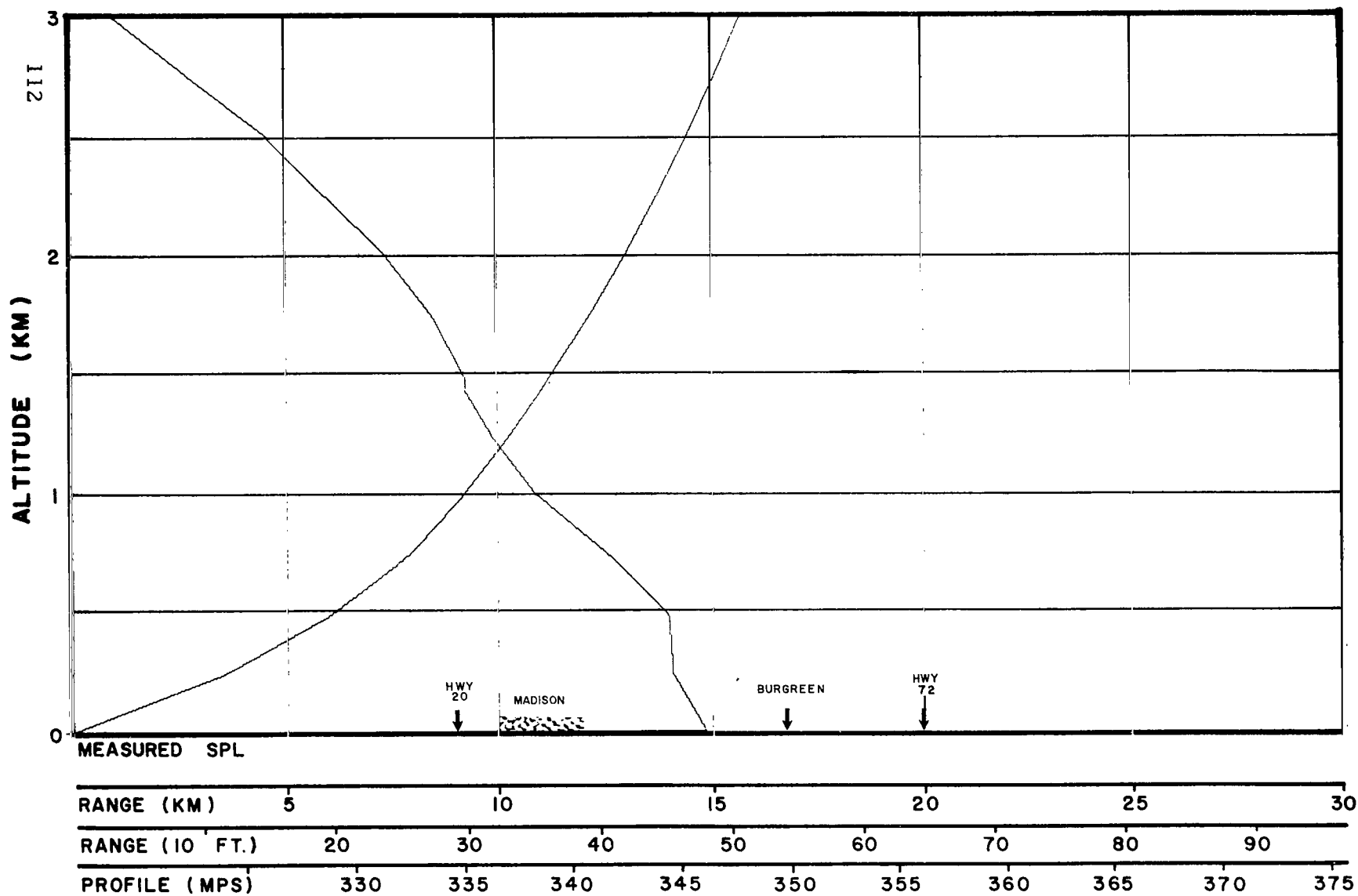


FIG. 96 CALCULATED ACOUSTIC RAY PATHS
MADISON, ALA., 315° AZIMUTH

DATE 3/13/63
TIME 1300C

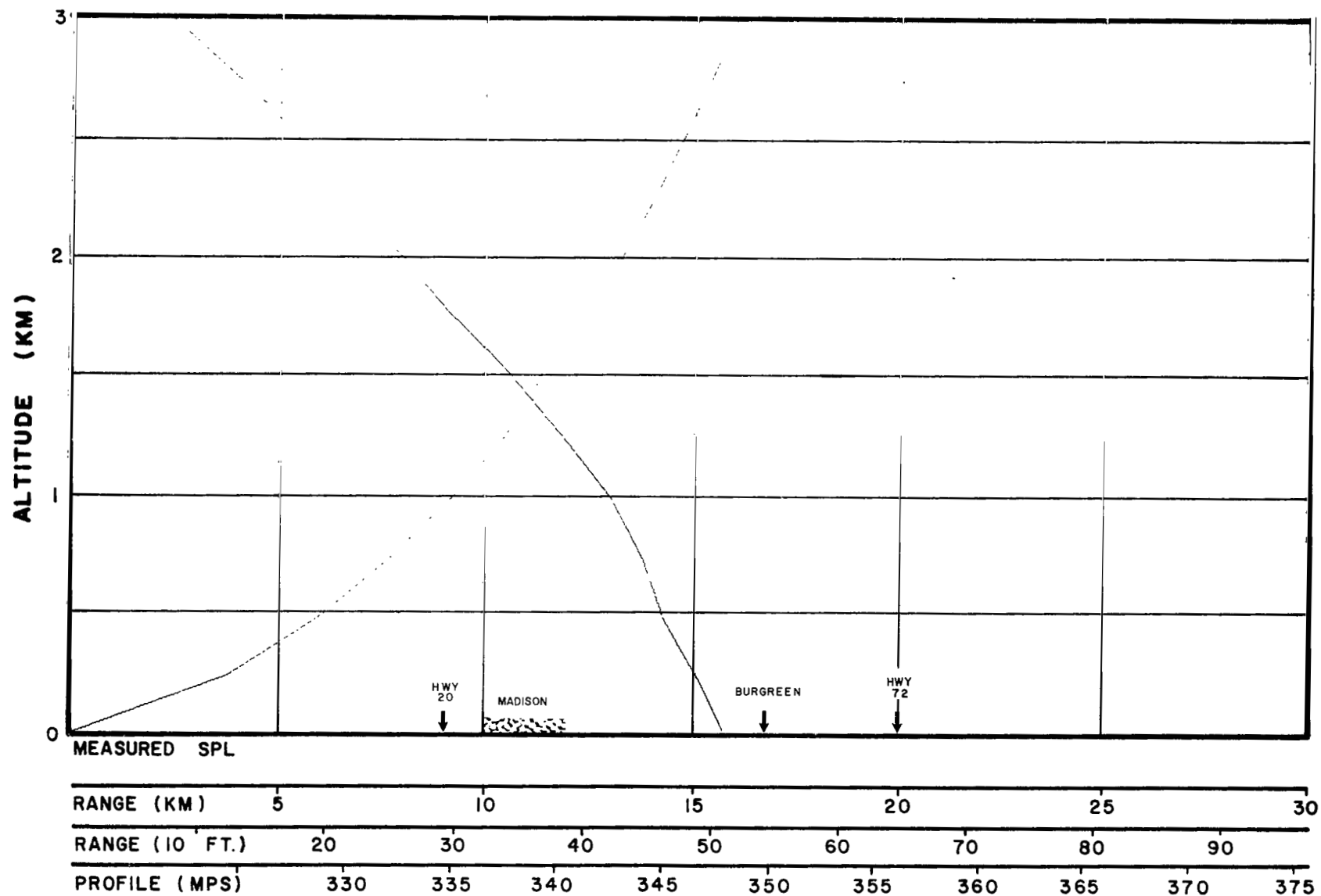


FIG. 97 CALCULATED ACOUSTIC RAY PATHS
MADISON, ALA., 315° AZIMUTH

DATE 3/13/63
TIME 1400C

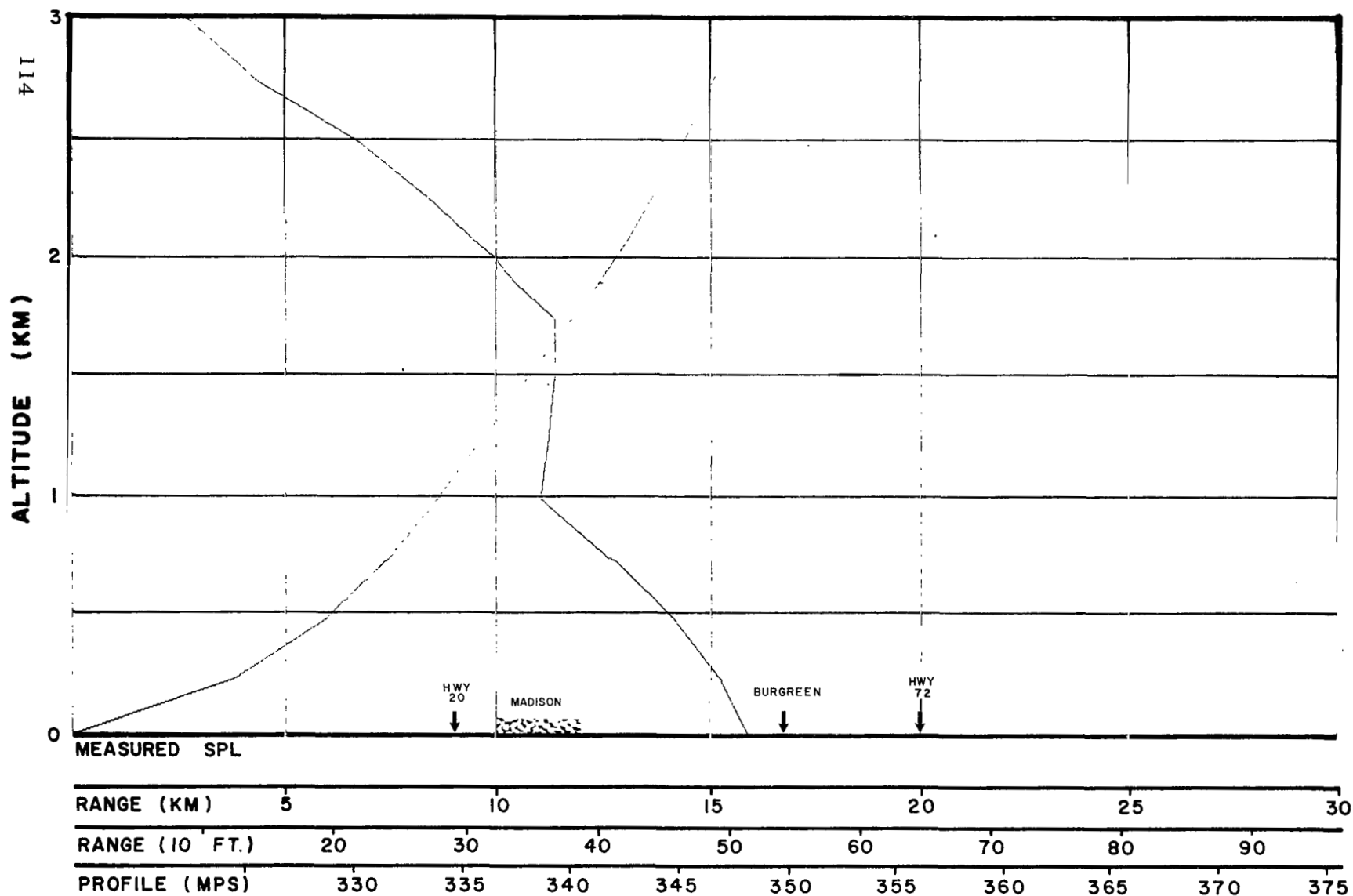


FIG. 98 CALCULATED ACOUSTIC RAY PATHS
MADISON, ALA., 315° AZIMUTH

DATE 3/13/63
TIME 1500C

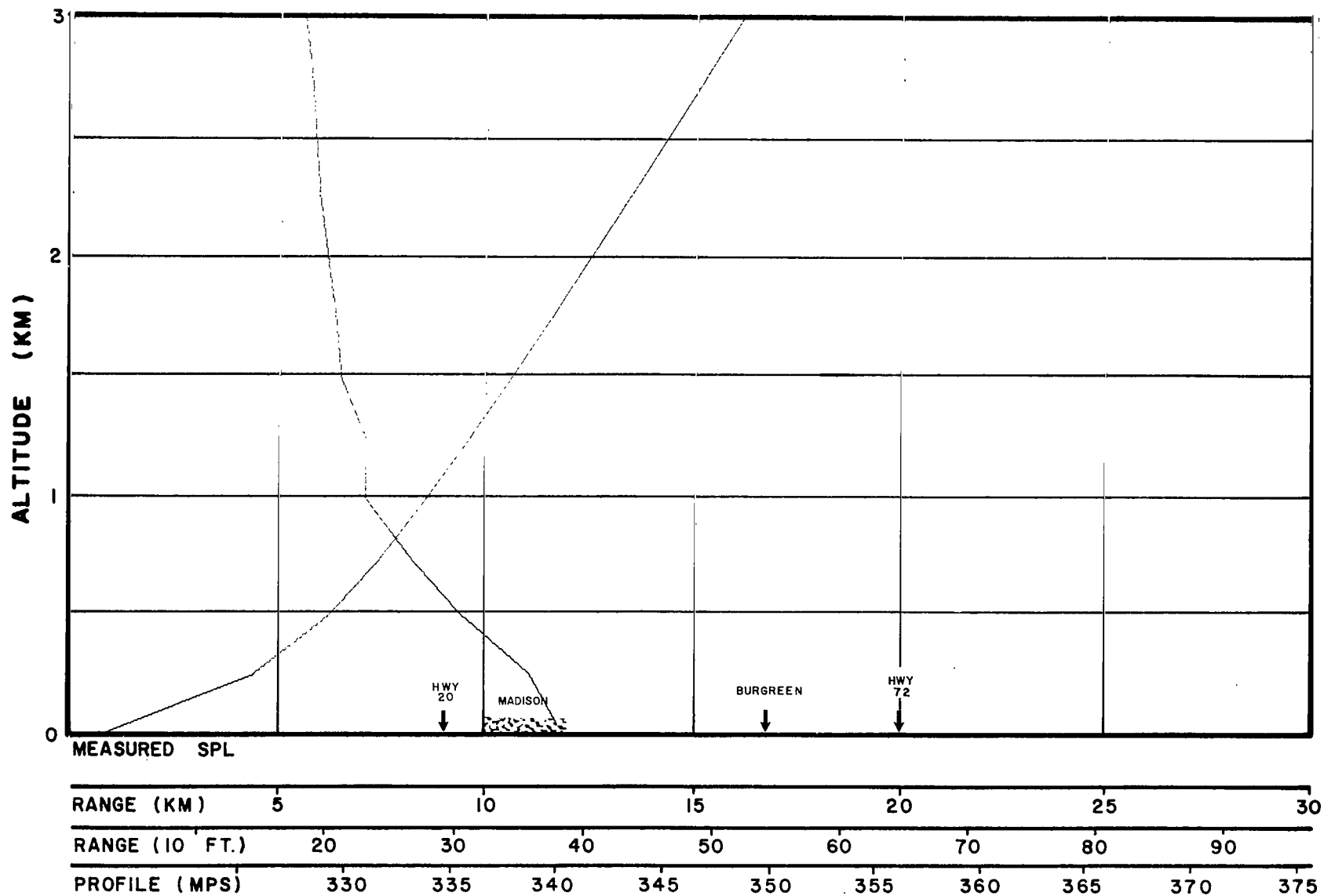


FIG. 99 CALCULATED ACOUSTIC RAY PATHS
MADISON, ALA., 315° AZIMUTH

DATE 3/12/63
TIME X-1 Day Fore-
cast

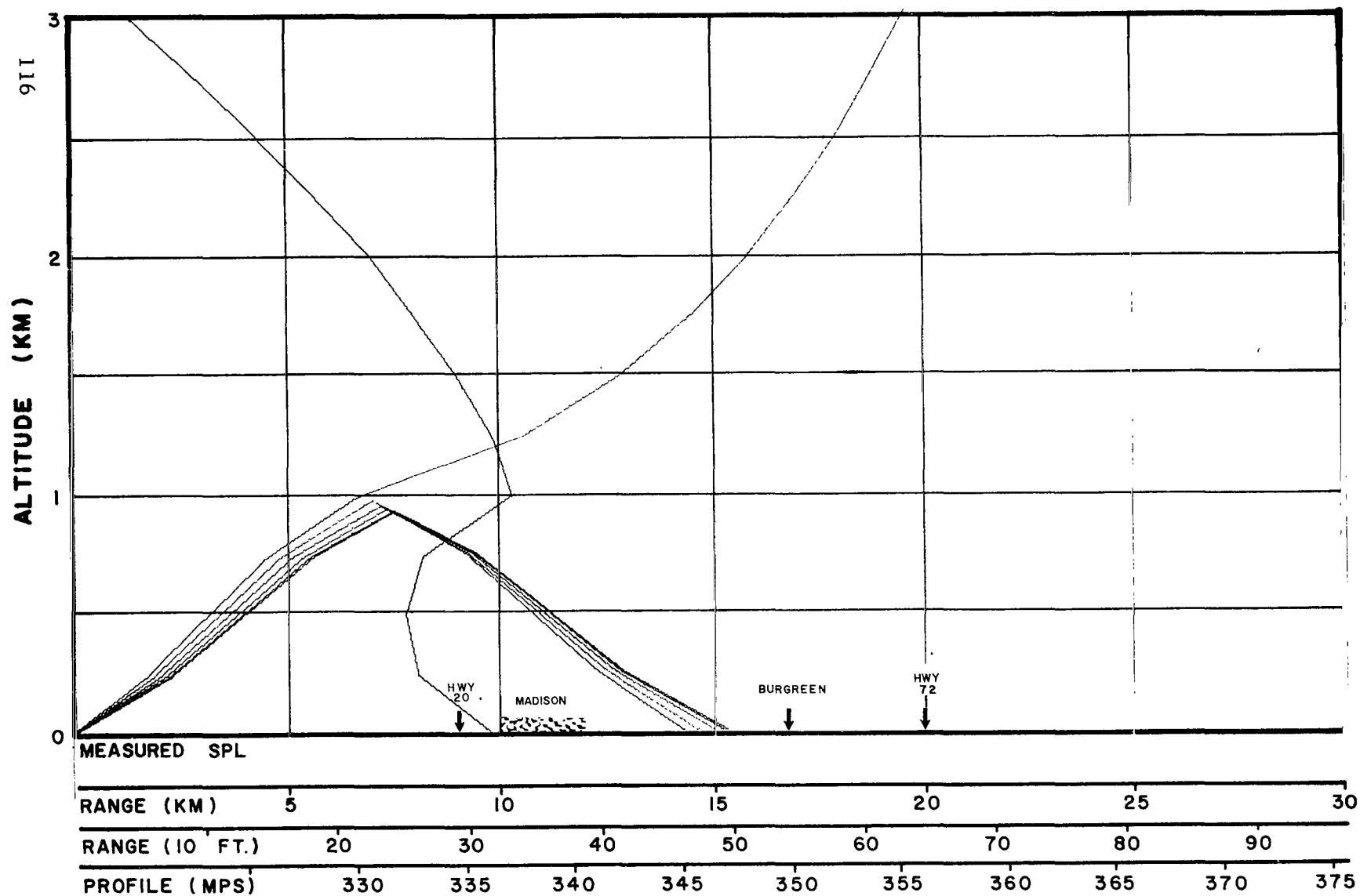


FIG. 100 CALCULATED ACOUSTIC RAY PATHS
MADISON, ALA., 315° AZIMUTH

DATE 3/13/63
TIME X-6 Hour Fore-
cast

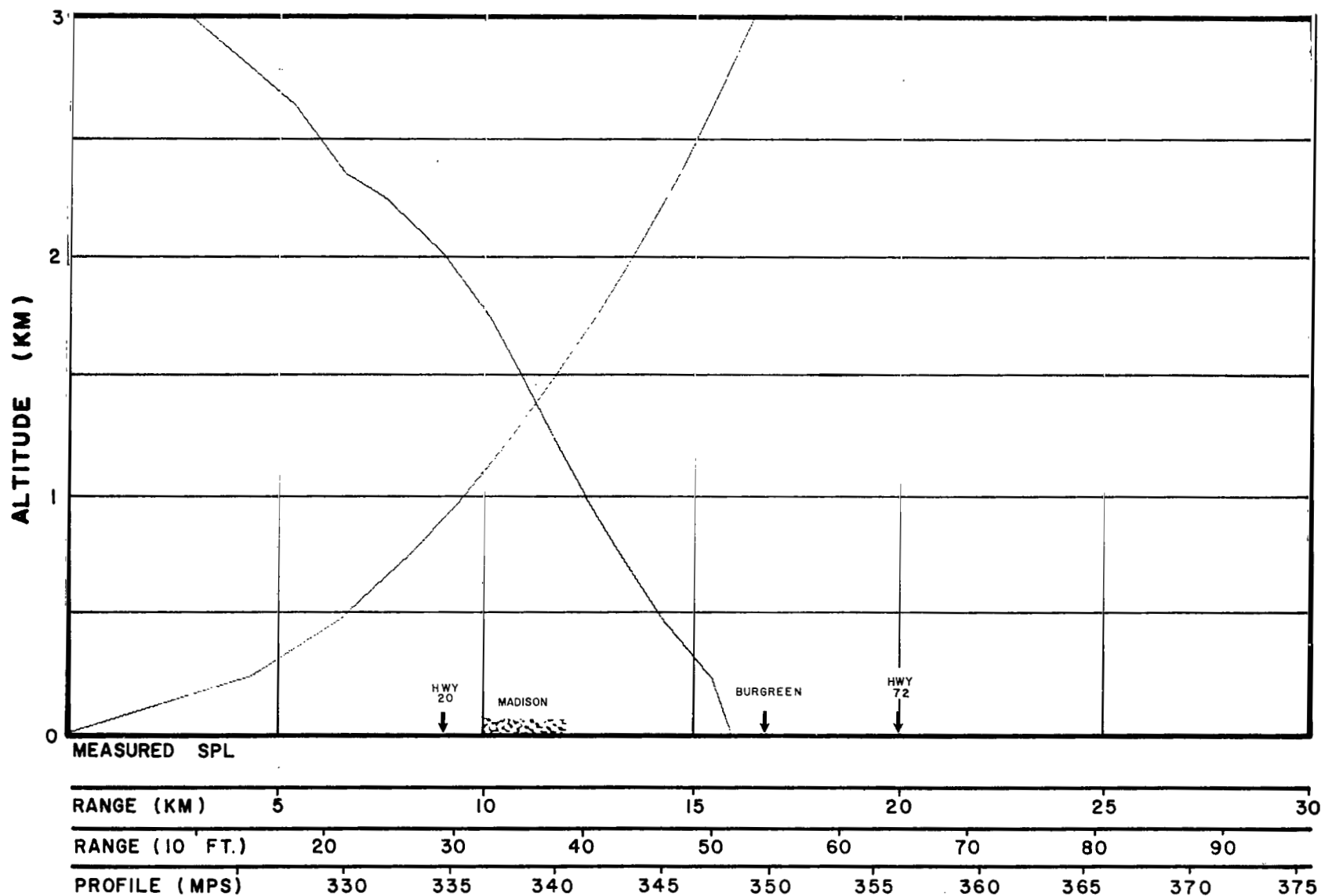


FIG.101 CALCULATED ACOUSTIC RAY PATHS
MADISON, ALA., 315° AZIMUTH

DATE 3/13/63
TIME 1615C

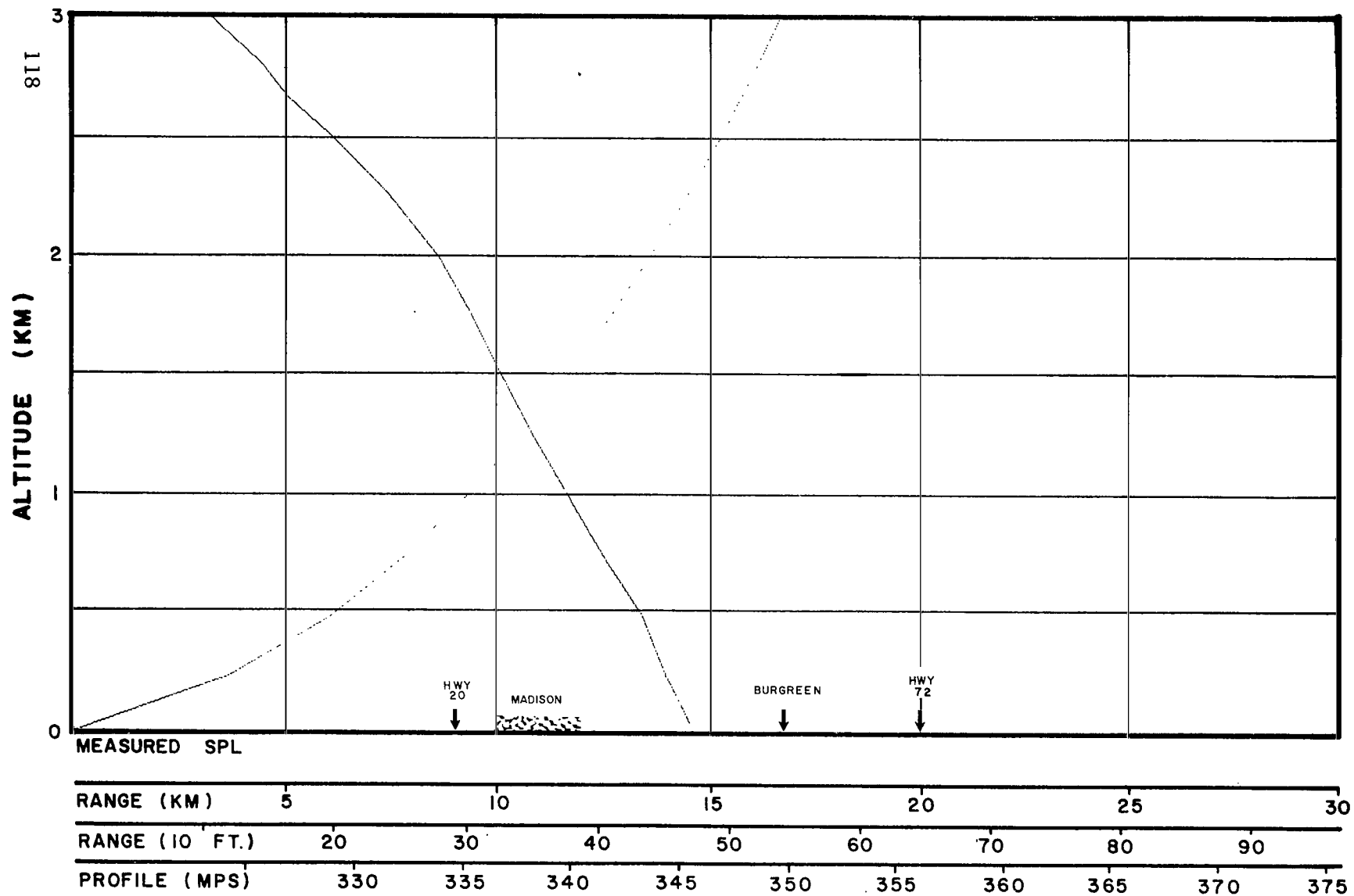


FIG.102 CALCULATED ACOUSTIC RAY PATHS
MADISON, ALA., 315° AZIMUTH

DATE 3/13/63
TIME 1700C

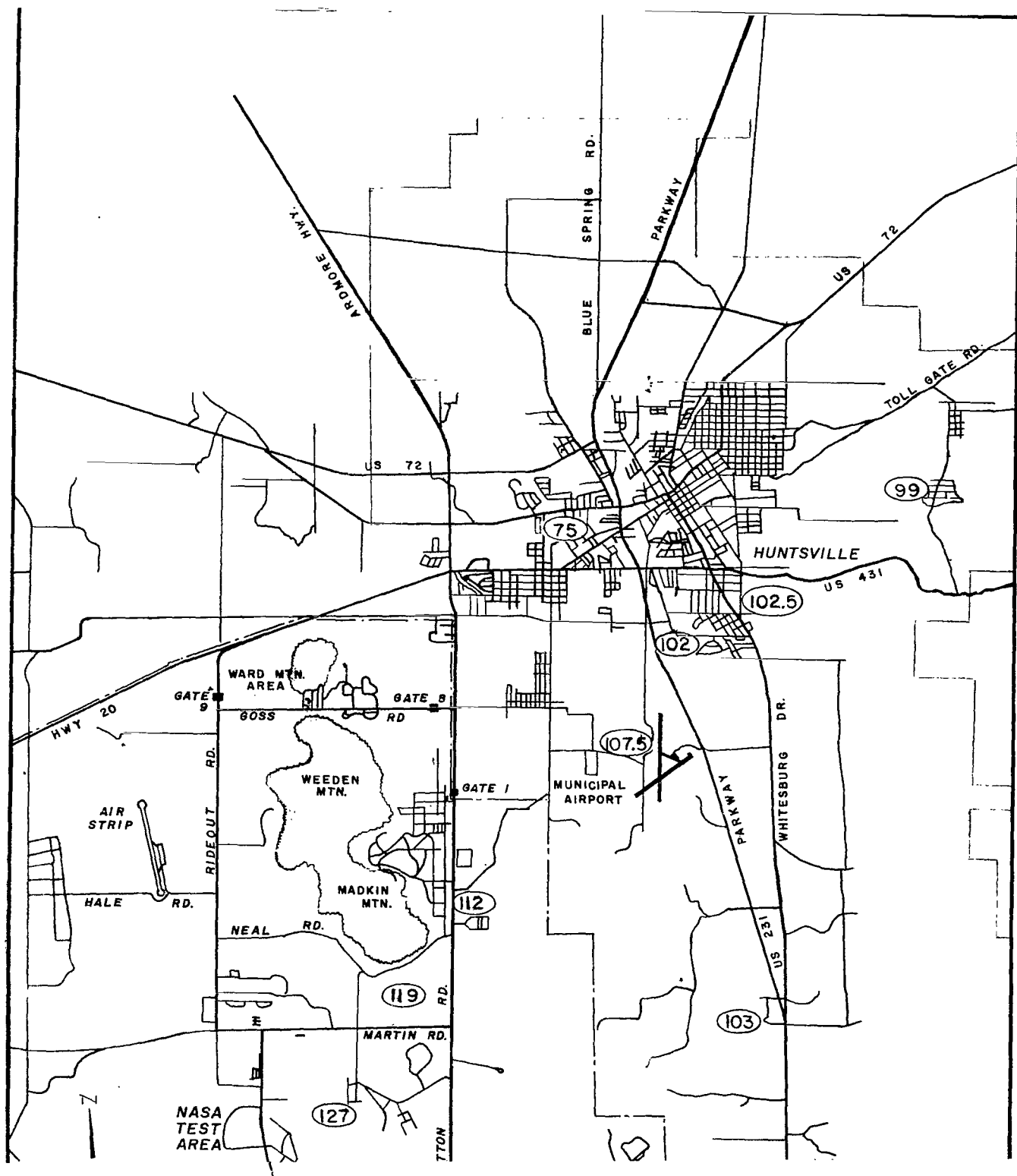


FIG. 103 SOUND PRESSURE LEVELS MEASURED DURING SATURN TEST SA-12 MARCH 13, 1963, 1615 CST

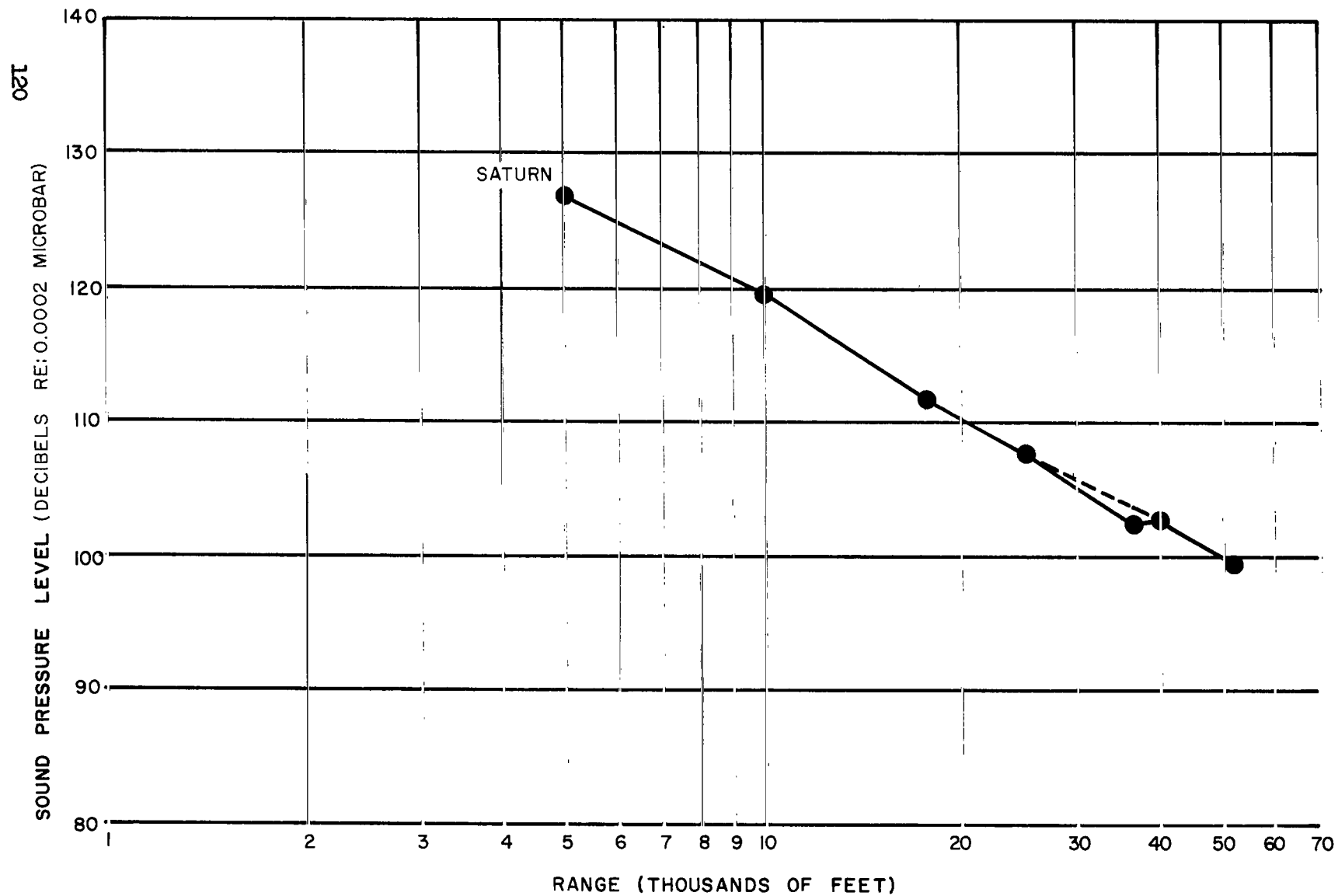
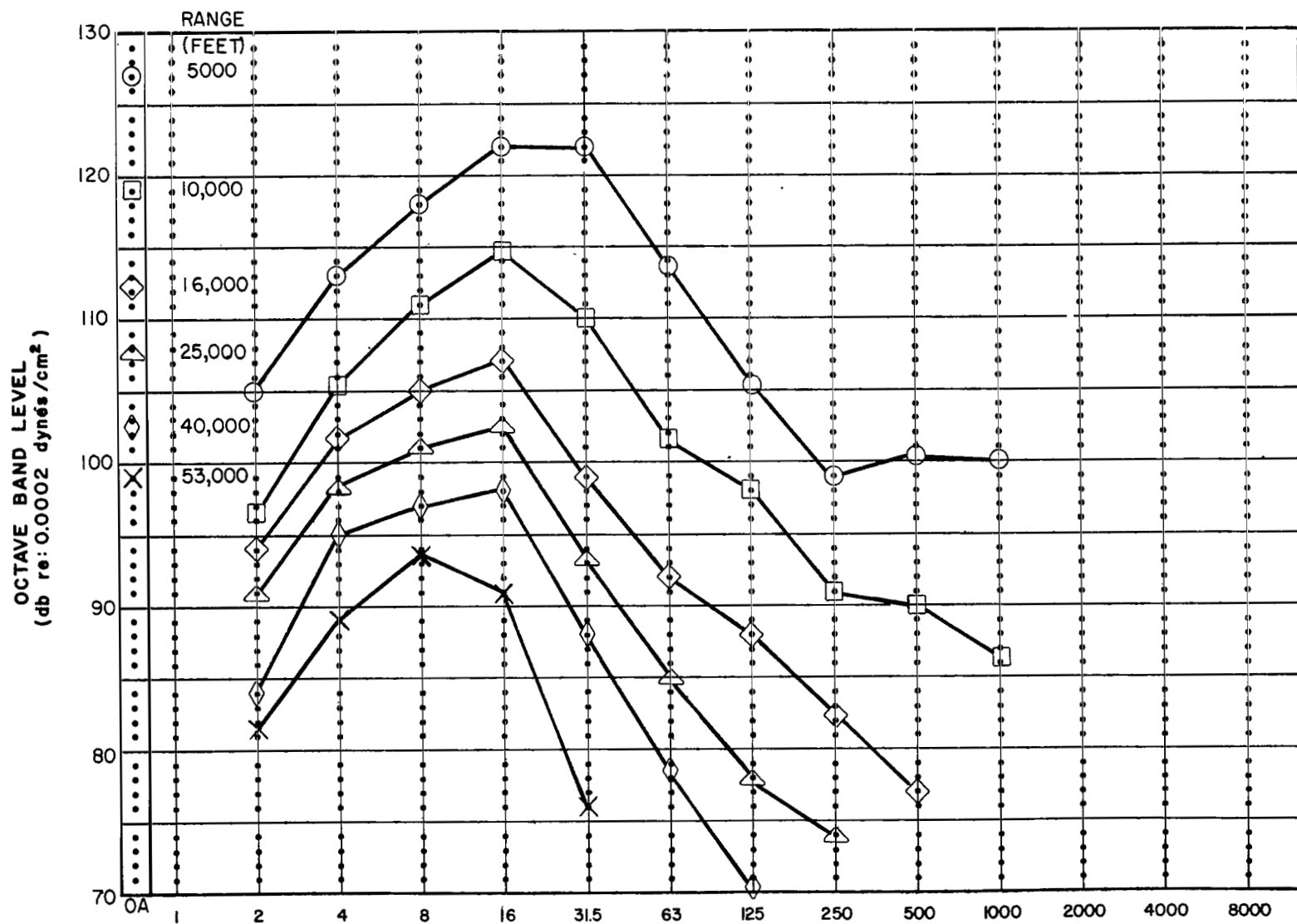
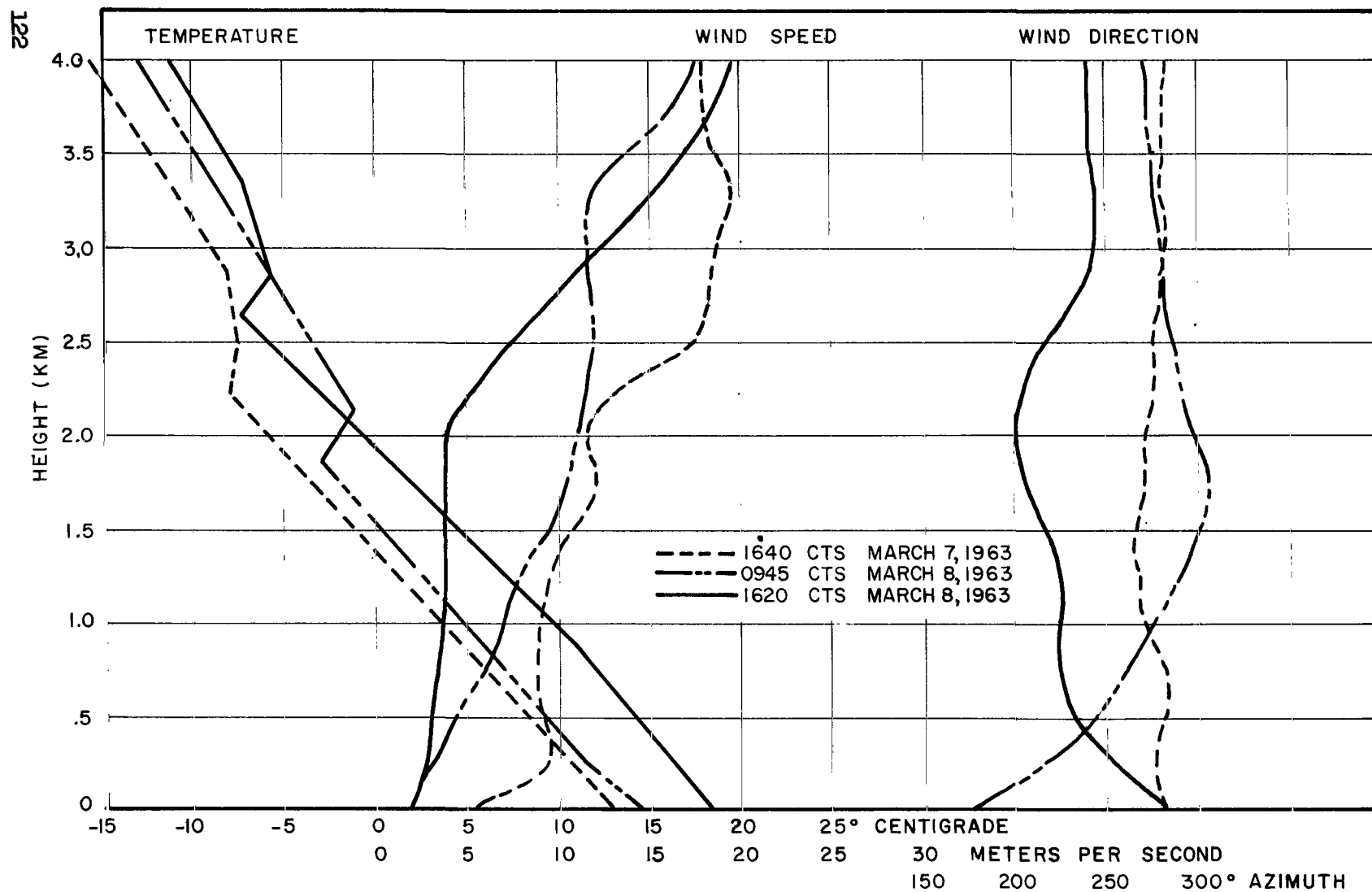


FIG. 104 MEASURED SPL_s FROM SATURN AND HORN, MARCH 13, 1963



**FIG. 105 MID-FREQUENCIES OF OCTAVE BANDS (cps)
FREQUENCY SPECTRA AT VARIOUS RANGES FROM TEST**



**FIG. A-1 VIRTUAL TEMPERATURE, WIND SPEED, & WIND DIRECTION PROFILES
MARSHALL SPACE FLIGHT CENTER**

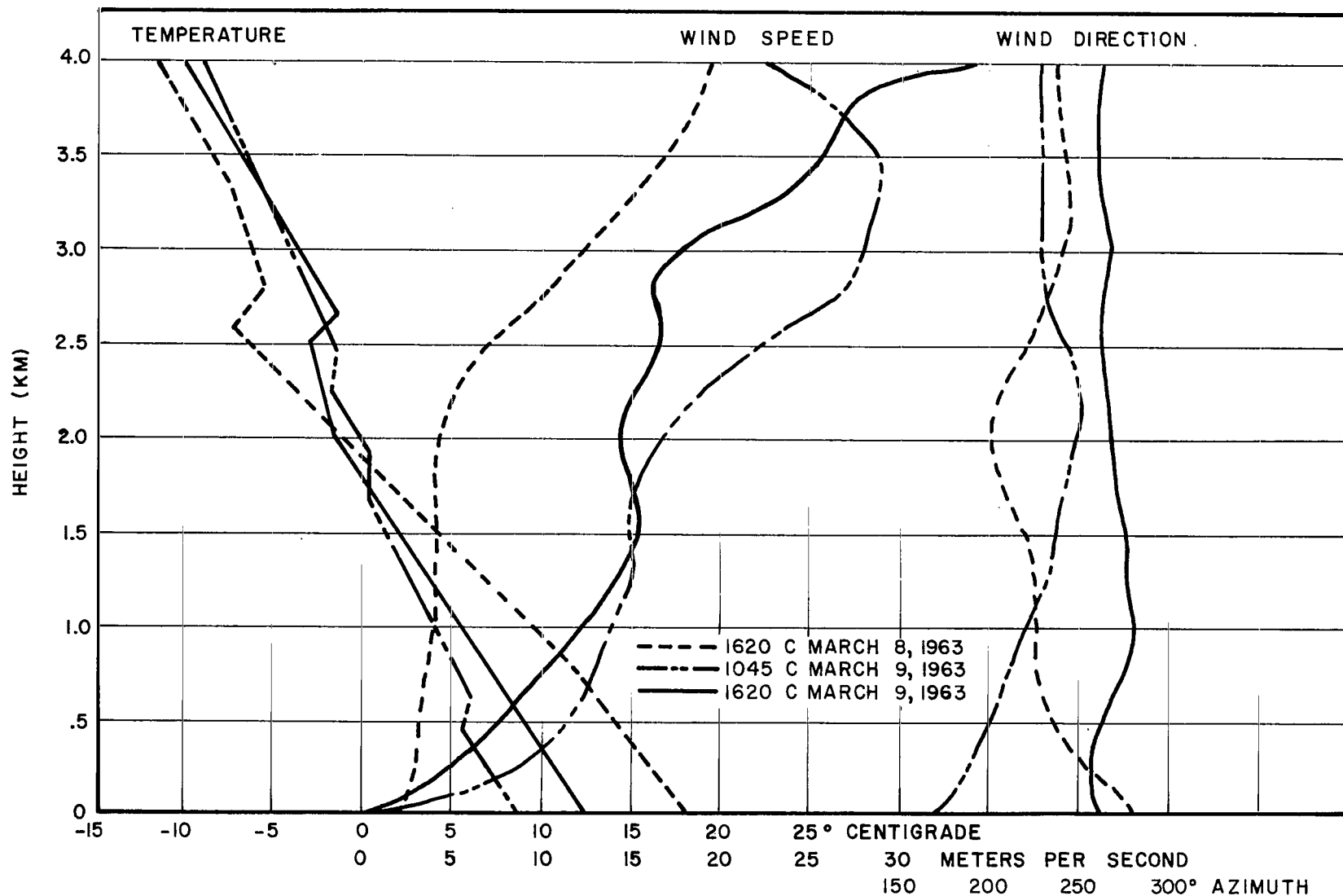


FIG. A-2 VIRTUAL TEMPERATURE, WIND SPEED, & WIND DIRECTION PROFILES
MARSHALL SPACE FLIGHT CENTER

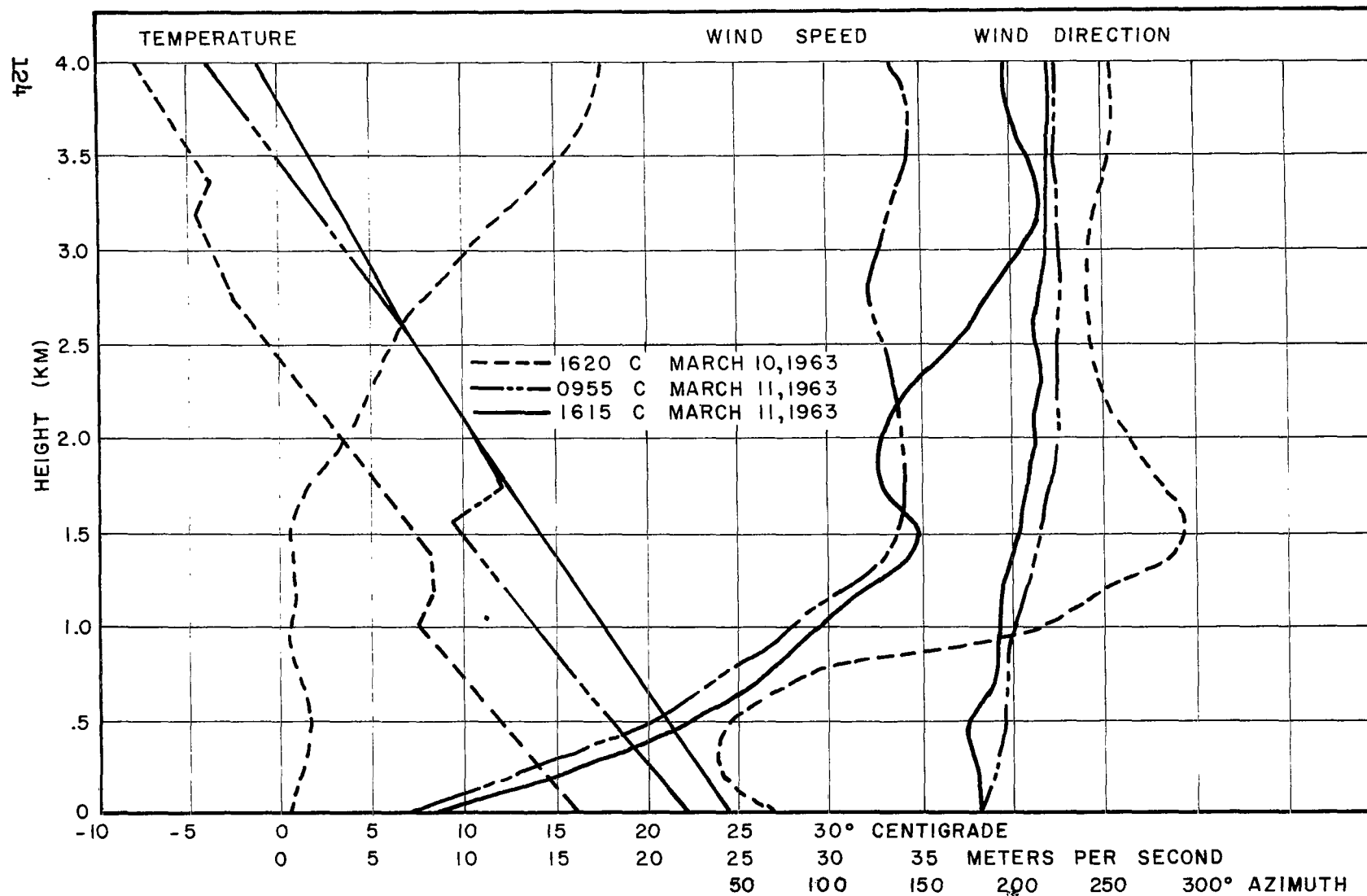


FIG. A-3 VIRTUAL TEMPERATURE, WIND SPEED, & WIND DIRECTION PROFILES
MARSHALL SPACE FLIGHT CENTER



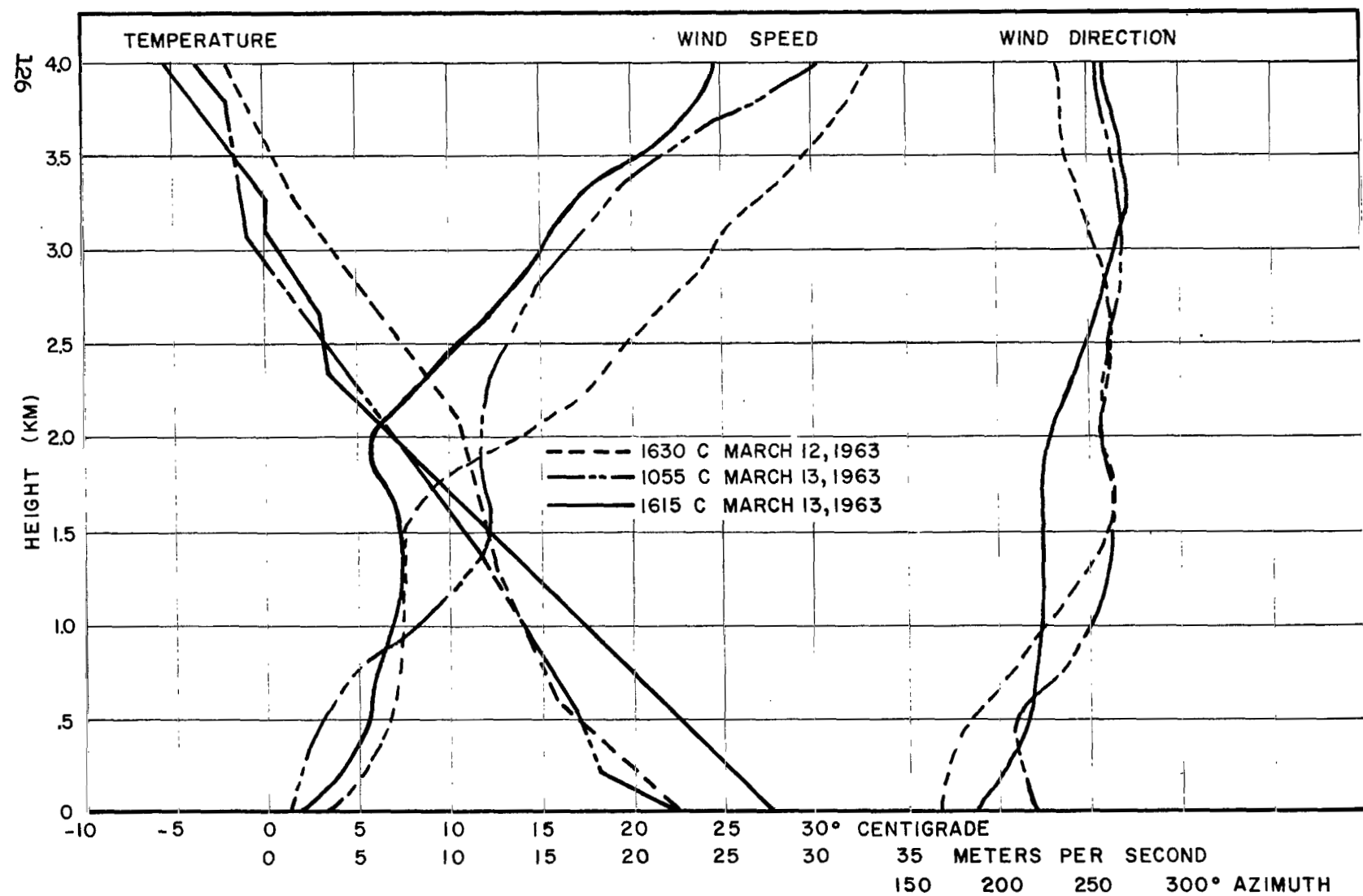


FIG. A-5 VIRTUAL TEMPERATURE, WIND SPEED, & WIND DIRECTION PROFILES
MARSHALL SPACE FLIGHT CENTER

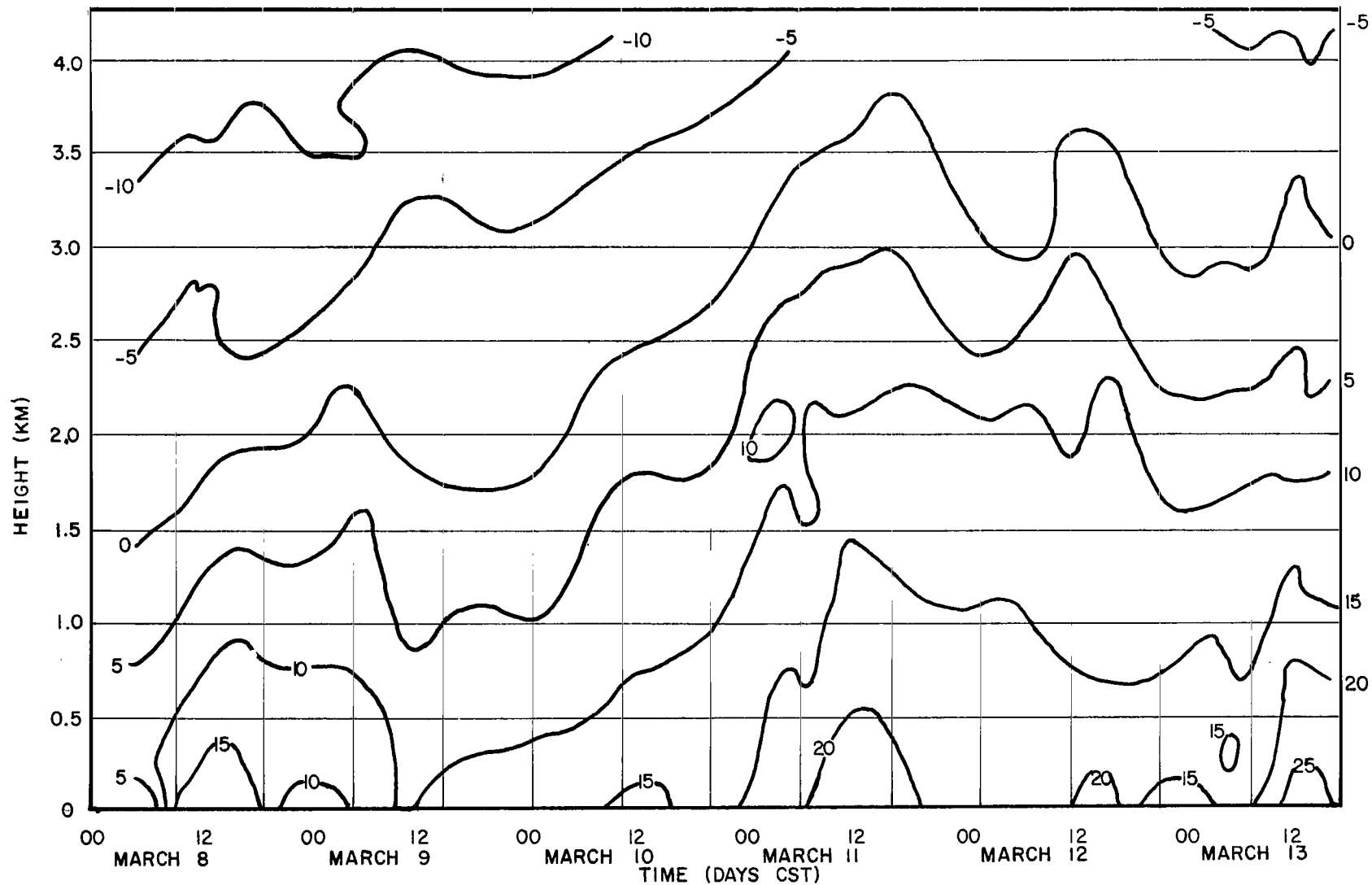
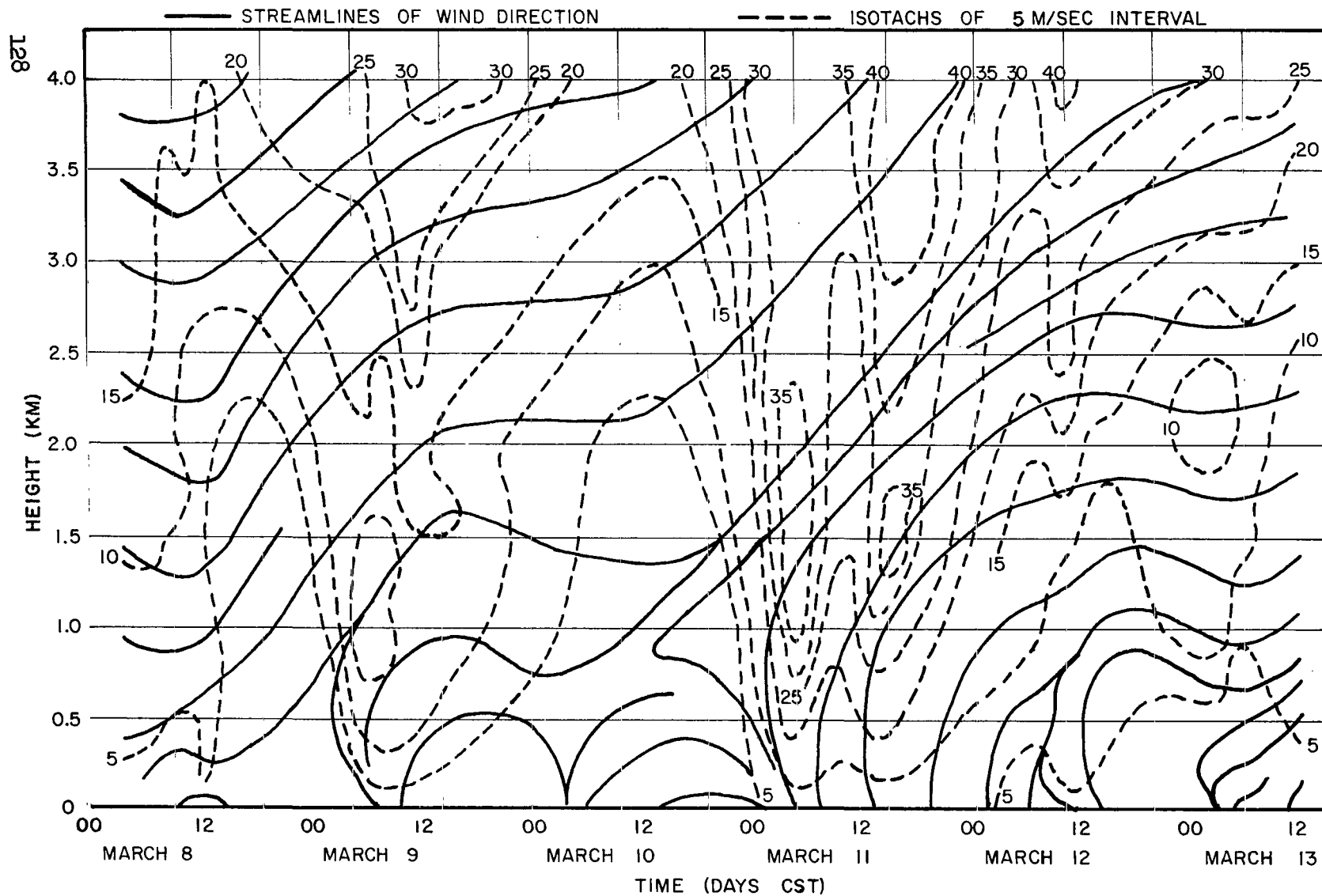


FIG. A-6 TIME CROSS-SECTION TEMPERATURE (DEGREES C°)
MARSHALL SPACE FLIGHT CENTER



**FIG. A-7 TIME CROSS-SECTION WINDS
MARSHALL SPACE FLIGHT CENTER**

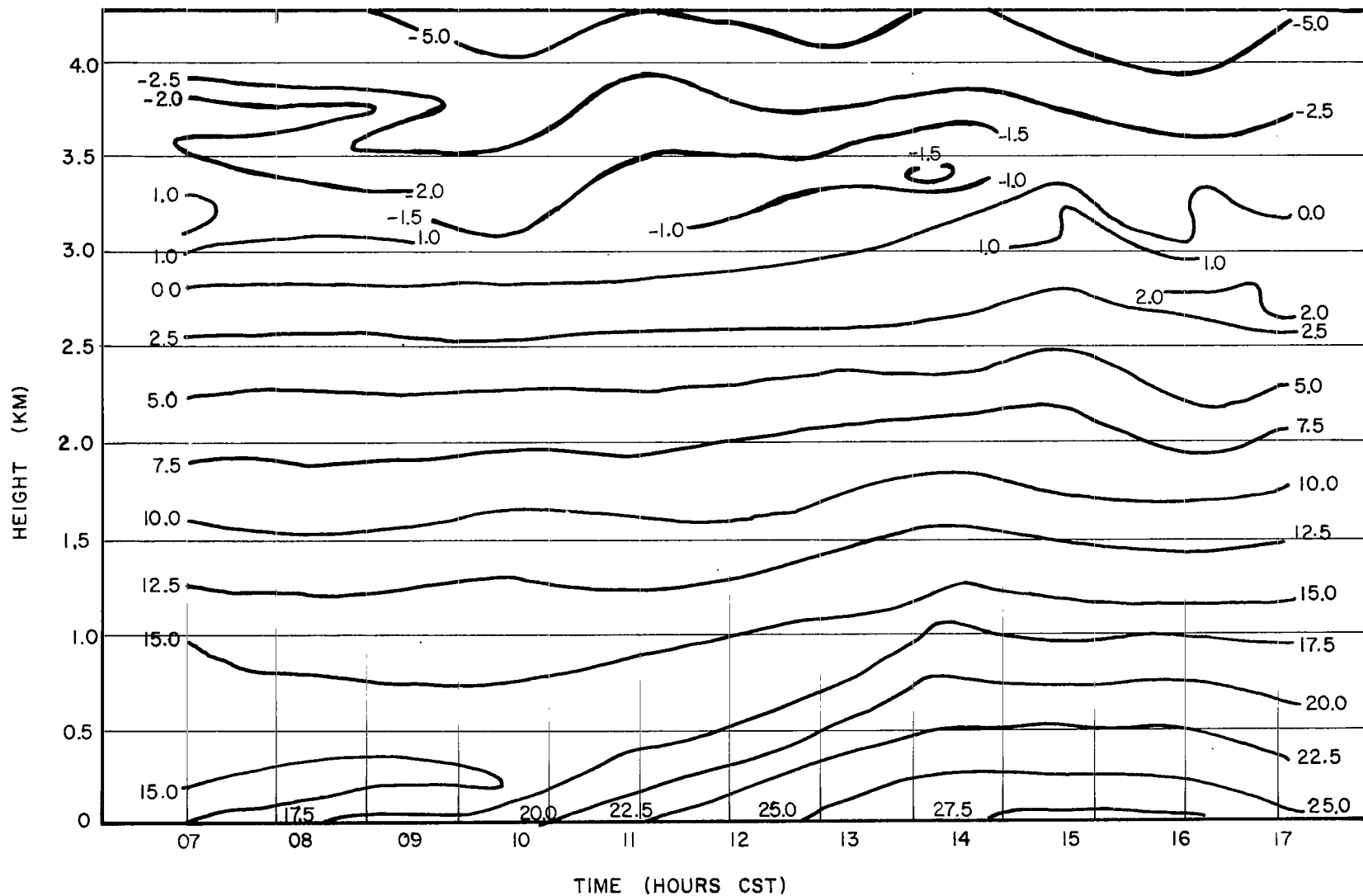
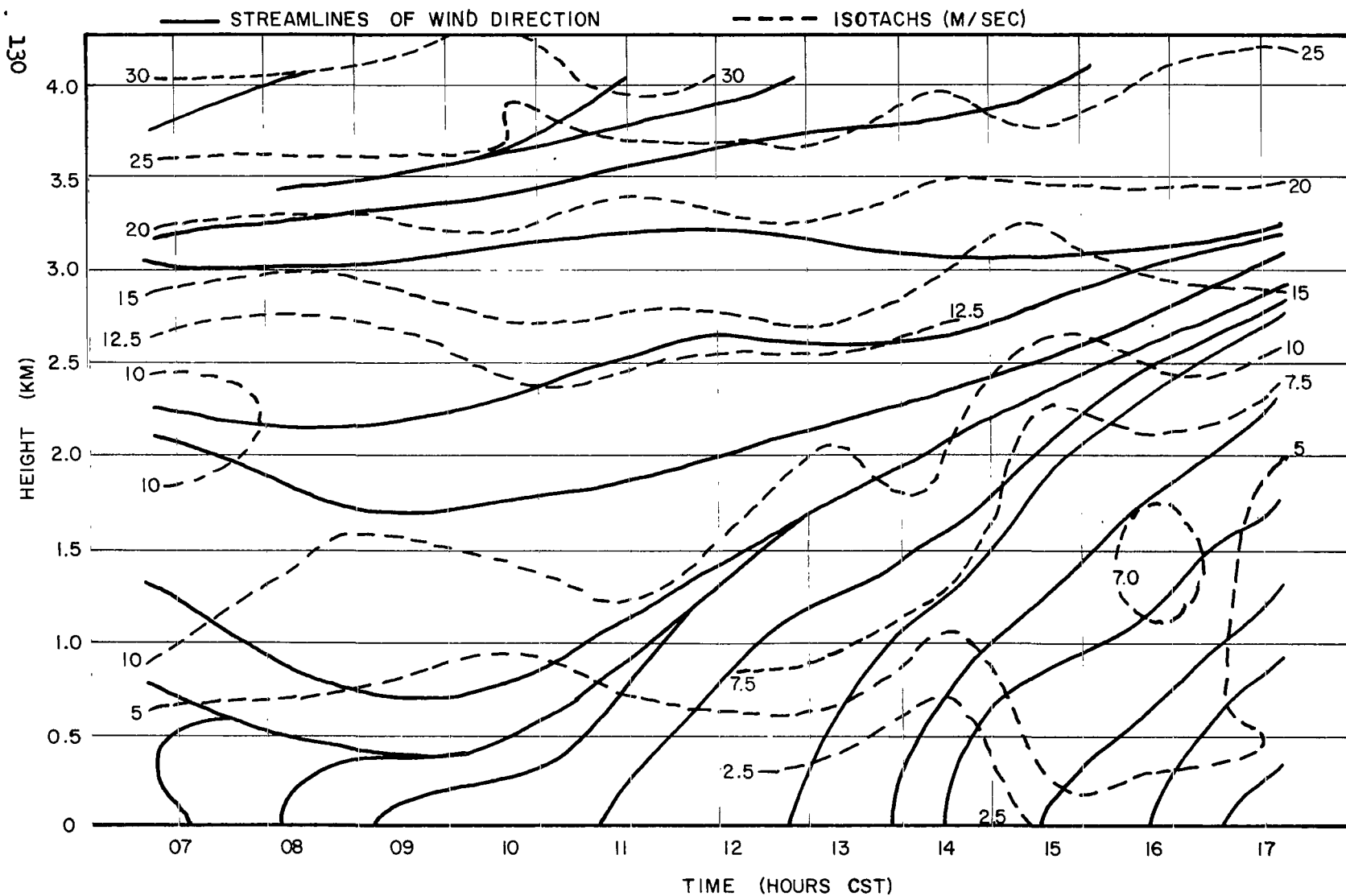


FIG. A-8 TIME CROSS-SECTION TEMPERATURE (DEGREES C°)
MARCH 13, 1963
MARSHALL SPACE FLIGHT CENTER



**FIG. A-9 TIME CROSS-SECTION WINDS
MARCH 13, 1963
MARSHALL SPACE FLIGHT CENTER**

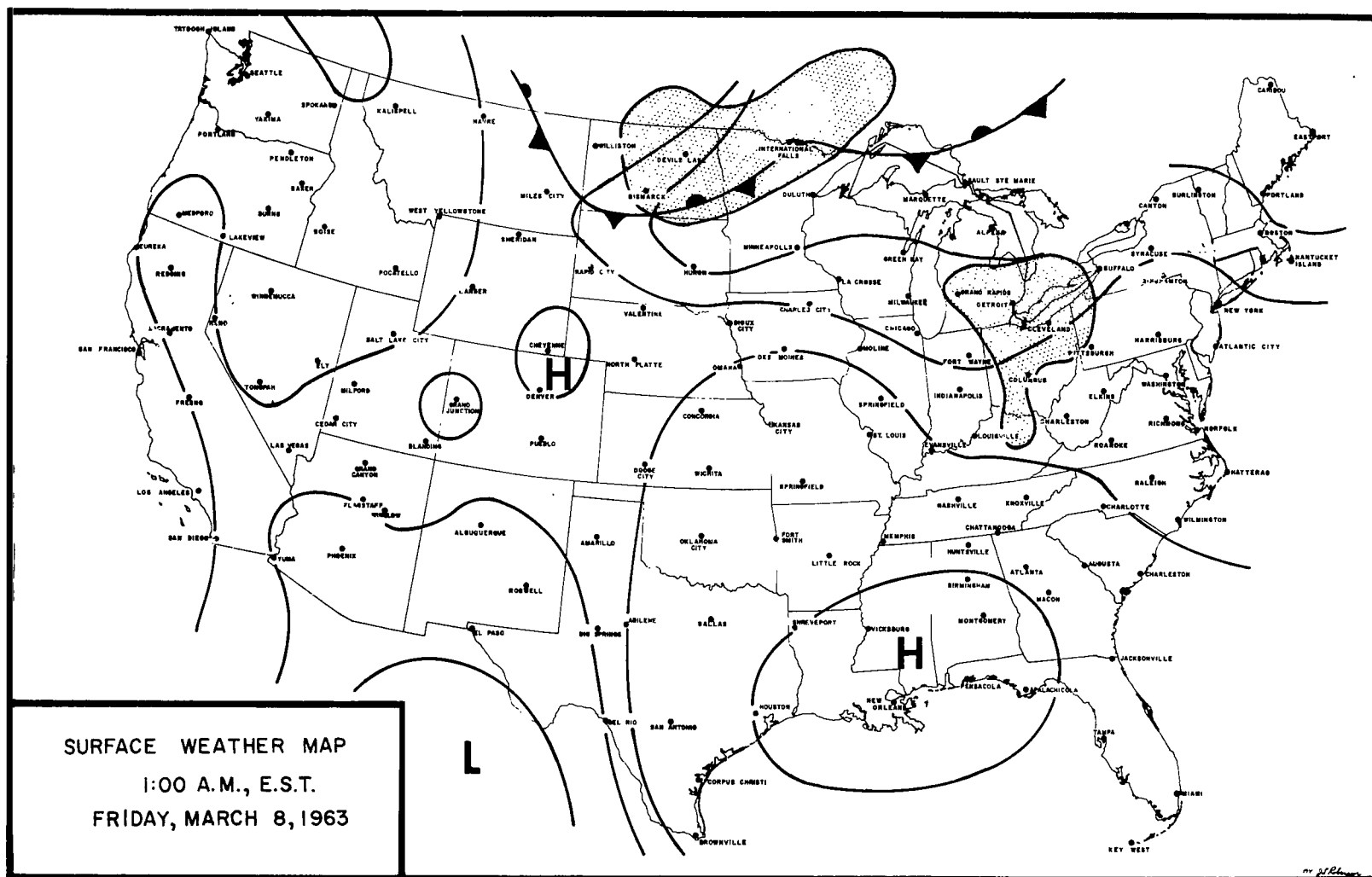


FIG. A-10 SURFACE WEATHER MAP

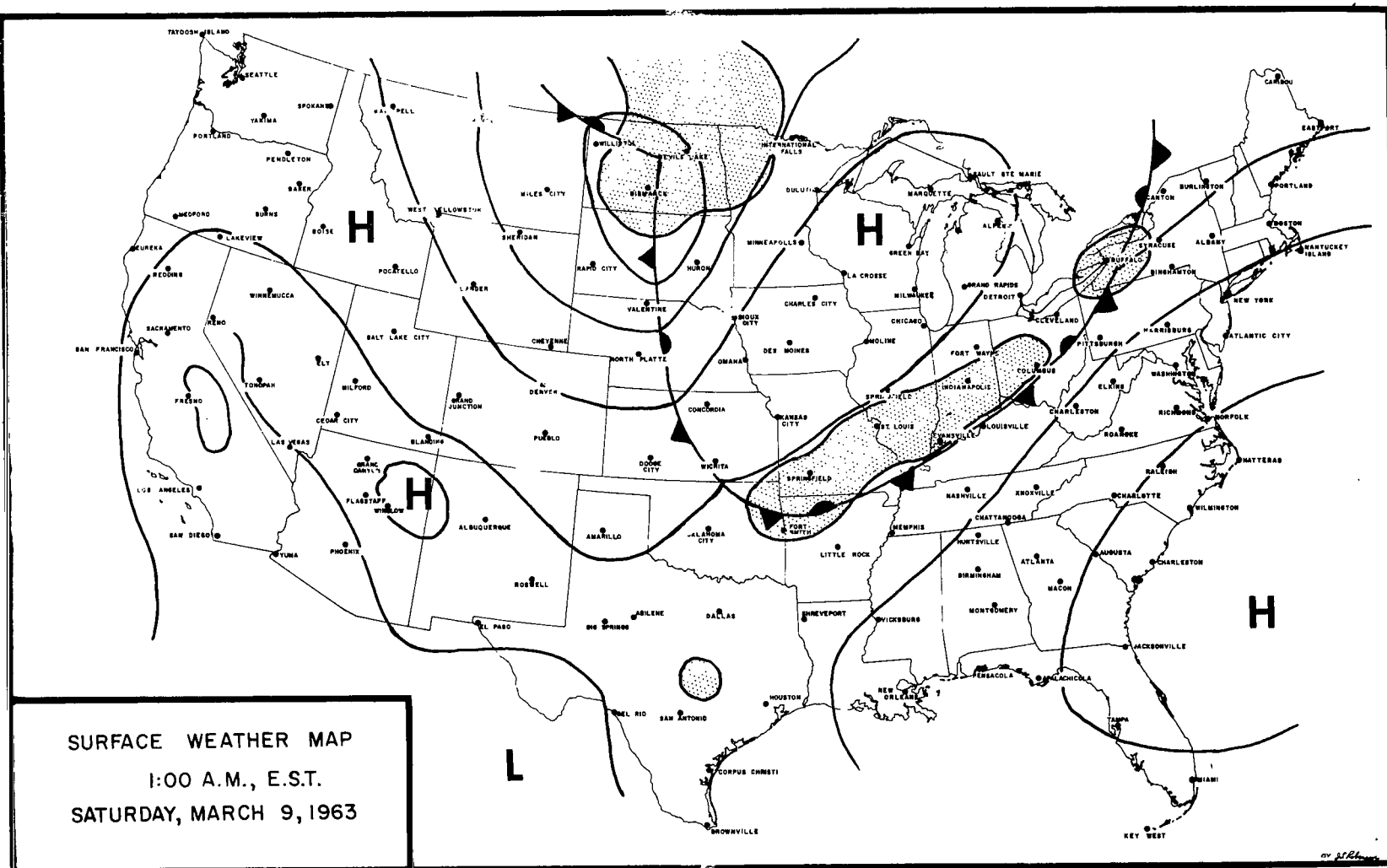


FIG. A-II SURFACE WEATHER MAP

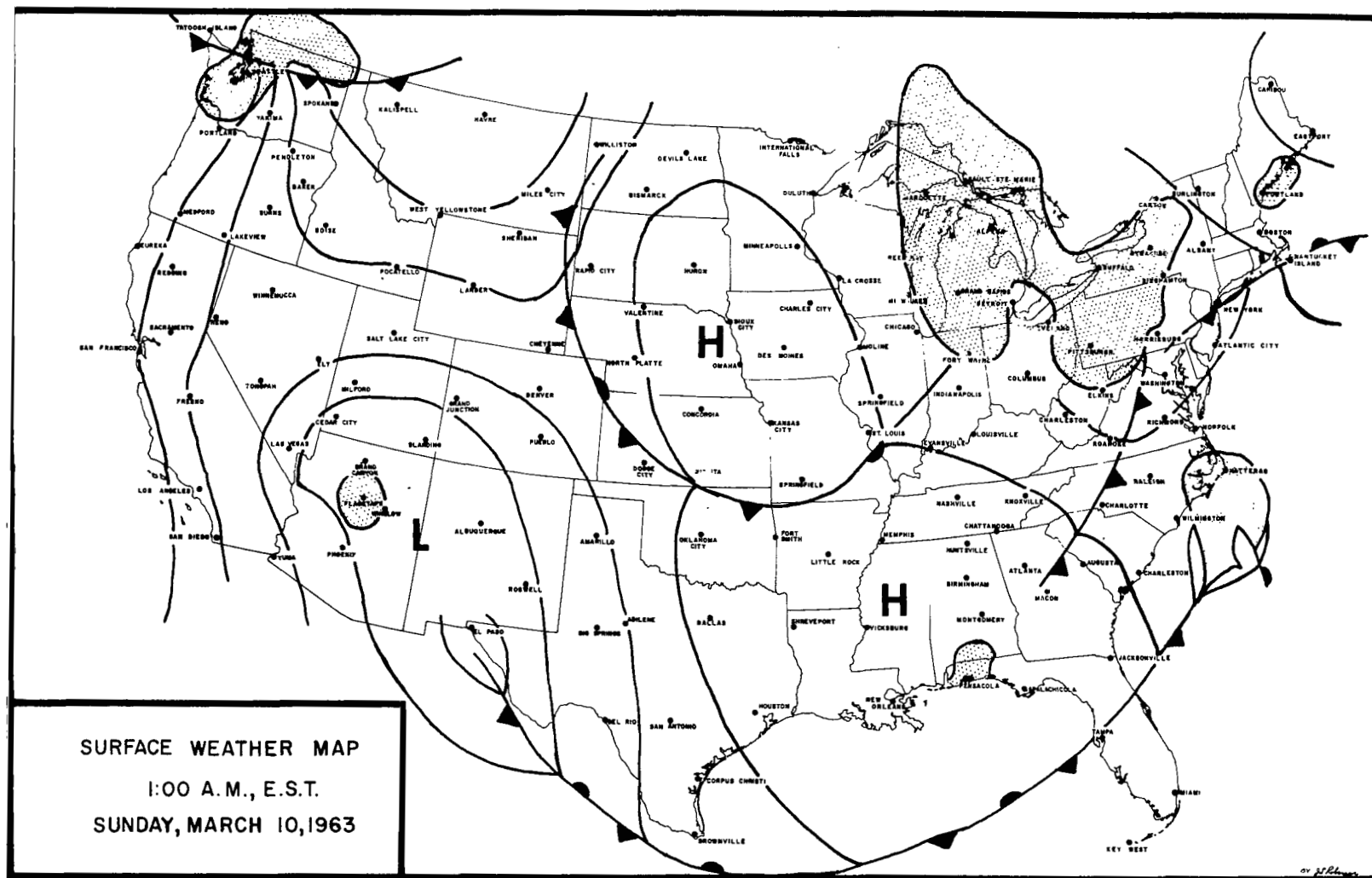


FIG. A-12 SURFACE WEATHER MAP

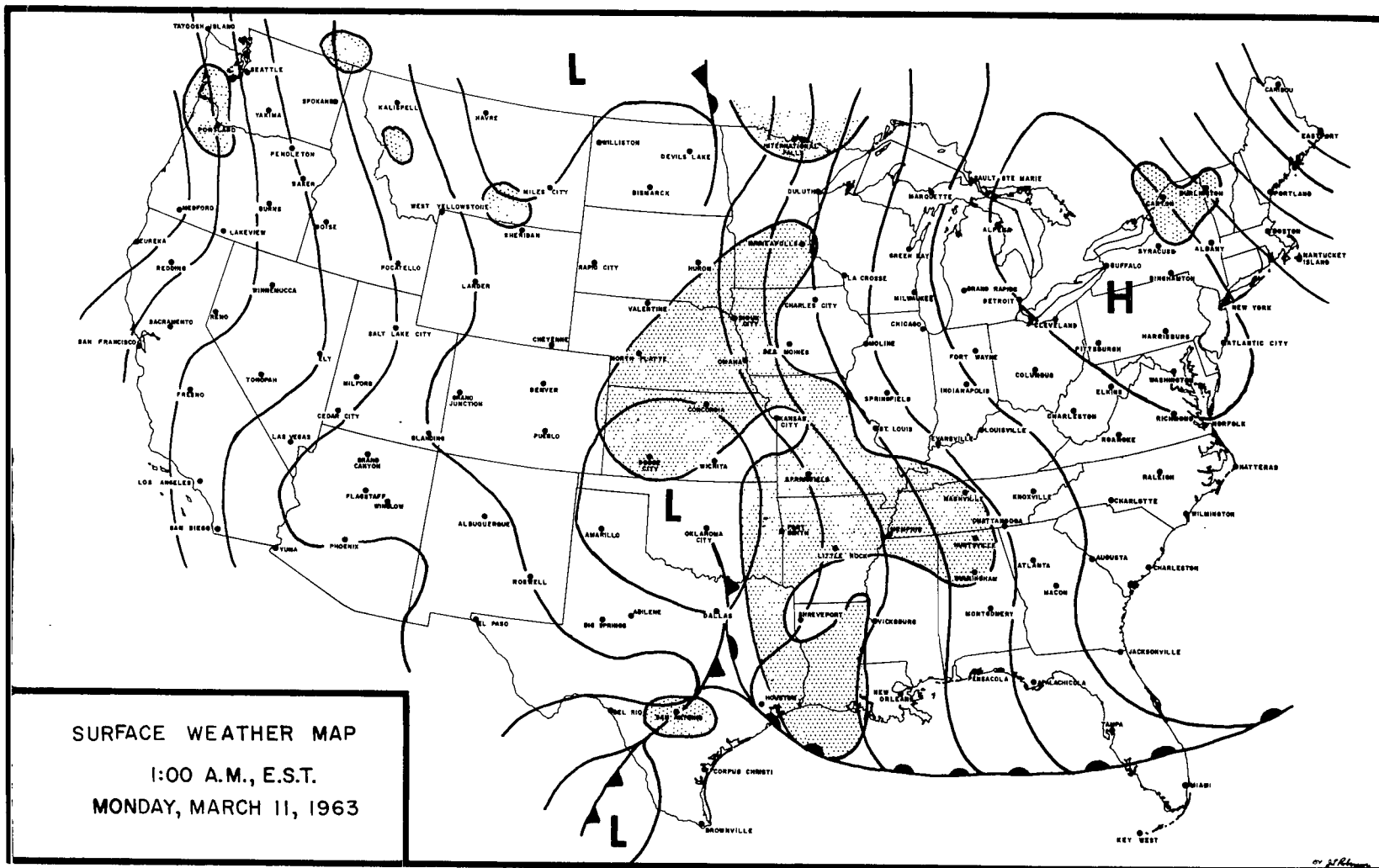


FIG. A-13 SURFACE WEATHER MAP

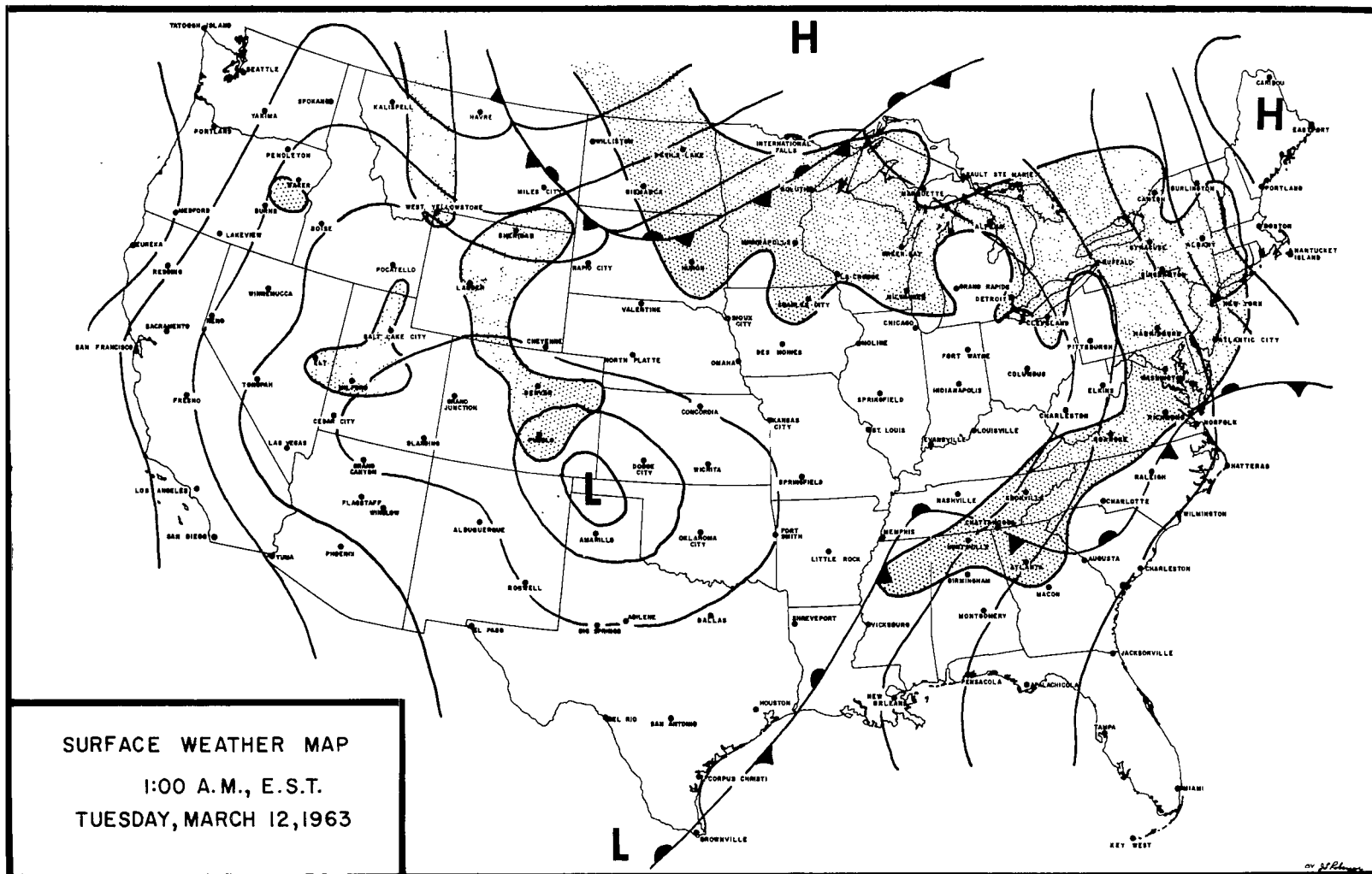


FIG. A-14 SURFACE WEATHER MAP

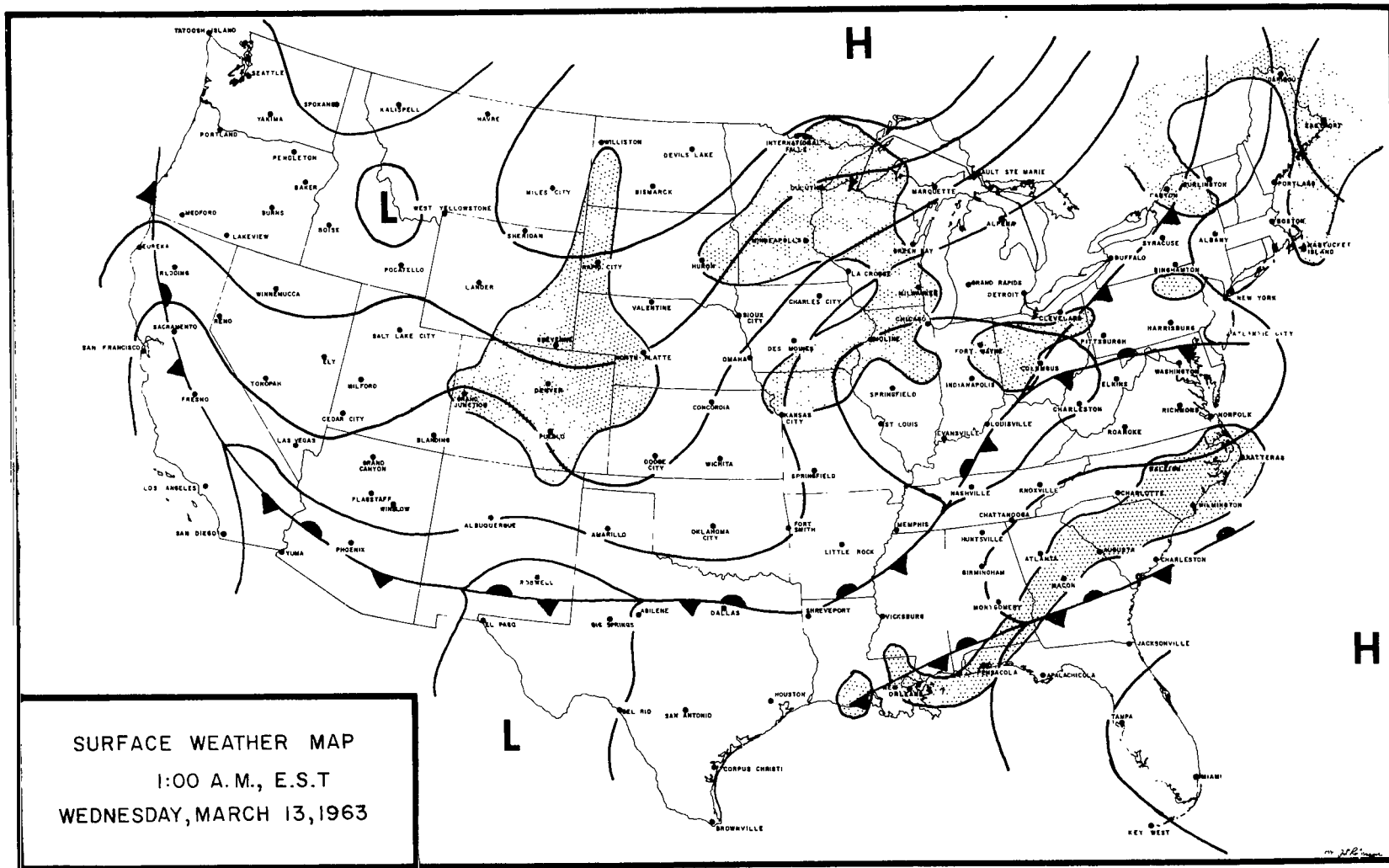


FIG. A-15 SURFACE WEATHER MAP

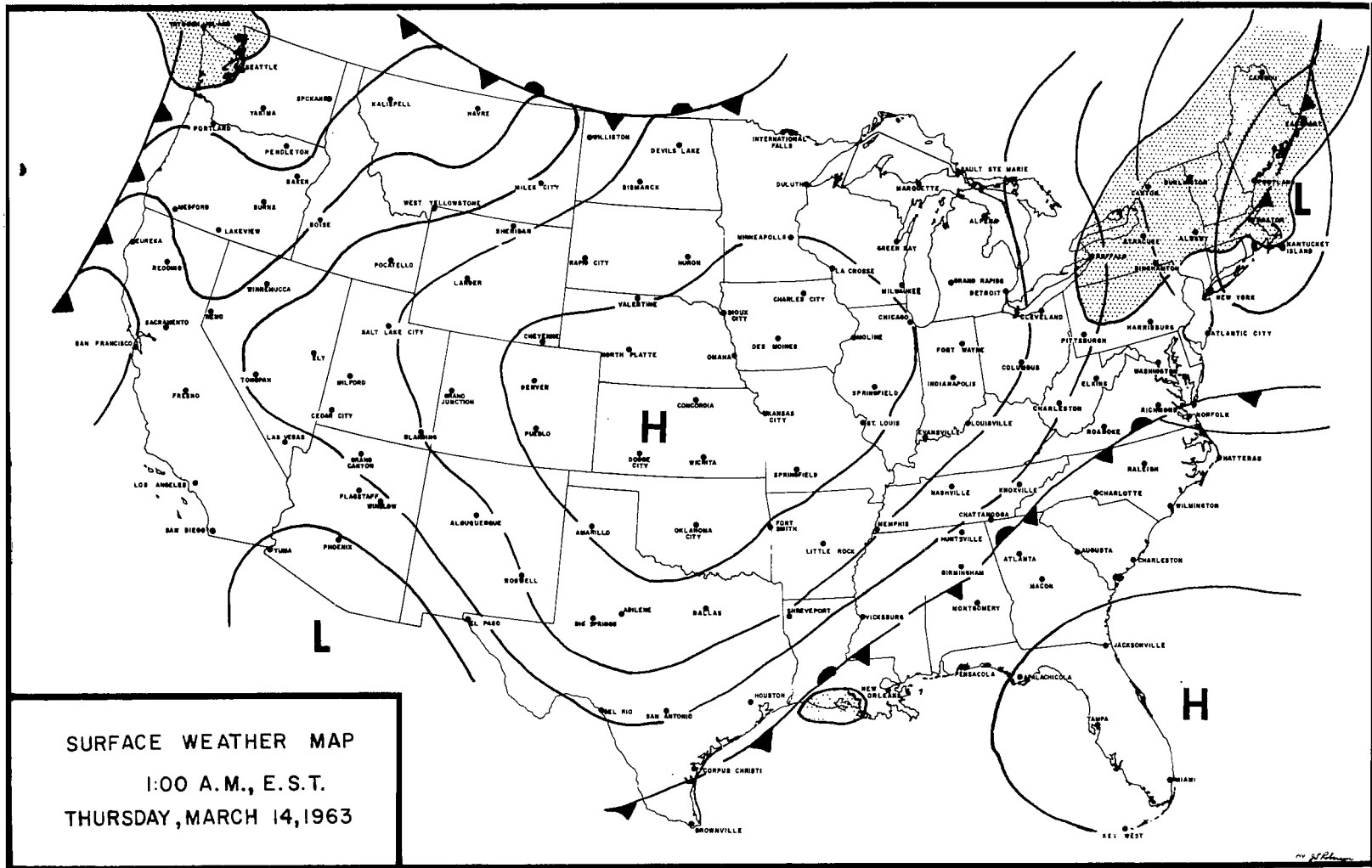


FIG. A-16 SURFACE WEATHER MAP

REFERENCES

1. Polly, R. C. and Tedrick, R. N. , "Far-Field Propagation Characteristics At The Marshall Space Flight Center, December 1962", M-TEST-MC, 1963.
2. Polly, R. C. and Tedrick, R. N. , "Far-Field Propagation Characteristics At The Marshall Space Flight Center, January 1963", M-TEST-MC, 1963.
3. Dorland, W. D. , "Far-Field Noise Characteristics at Saturn Static Tests", NASA TN-D-611, August 1961.
4. Cox, E. F. et al, "Meteorology Directs Where Blast Will Strike," AMS Bulletin 35: 95-103, 1954.
5. Nyborg, W. L. and Mintzer, D. , "Review of Sound Propagation in the Lower Atmosphere", WADC Tech. Report 57-354, 1957.
6. Tedrick, R. N. "Performance Characteristics of a Large Free-Field Exponential Horn," MTP-TEST-63-4, 1963.

217125
58

"The aeronautical and space activities of the United States shall be conducted so as to contribute . . . to the expansion of human knowledge of phenomena in the atmosphere and space. The Administration shall provide for the widest practicable and appropriate dissemination of information concerning its activities and the results thereof."

—NATIONAL AERONAUTICS AND SPACE ACT OF 1958

NASA SCIENTIFIC AND TECHNICAL PUBLICATIONS

TECHNICAL REPORTS: Scientific and technical information considered important, complete, and a lasting contribution to existing knowledge.

TECHNICAL NOTES: Information less broad in scope but nevertheless of importance as a contribution to existing knowledge.

TECHNICAL MEMORANDUMS: Information receiving limited distribution because of preliminary data, security classification, or other reasons.

CONTRACTOR REPORTS: Technical information generated in connection with a NASA contract or grant and released under NASA auspices.

TECHNICAL TRANSLATIONS: Information published in a foreign language considered to merit NASA distribution in English.

TECHNICAL REPRINTS: Information derived from NASA activities and initially published in the form of journal articles.

SPECIAL PUBLICATIONS: Information derived from or of value to NASA activities but not necessarily reporting the results of individual NASA-programmed scientific efforts. Publications include conference proceedings, monographs, data compilations, handbooks, sourcebooks, and special bibliographies.

Details on the availability of these publications may be obtained from:

SCIENTIFIC AND TECHNICAL INFORMATION DIVISION
NATIONAL AERONAUTICS AND SPACE ADMINISTRATION
Washington, D.C. 20546